National Research Council Canada

Conseil national de recherches Canada

NRC·CNRC

Canadian Journal of Fisheries and Aquatic Sciences

Journal canadien des sciences halieutiques et aquatiques

http://cjfas.nrc.ca

http://jcsha.cnrc.ca

ISSN 0706-652X / CJFSDX 60(12) 1433–1575 (2003)

The *Canadian Journal of Fisheries and Aquatic Sciences*, previously published as *Contributions to Canadian Biology* 1901–1925, *Contributions to Canadian Biology and Fisheries* 1926–1934, *Journal of the Biological Board of Canada* 1934–1937, and *Journal of the Fisheries Research Board of Canada* 1938–1979, is issued monthly to form annual volumes of 12 numbers plus supplements.

Editorial policy. The Journal publishes original research articles, perspectives (syntheses, critiques, re-evaluations), discussions (comment and reply), and rapid communications. Manuscripts may concern cells, organisms, populations, communities, ecosystems, or processes that affect aquatic systems. They may cover a range of disciplines including biology and ecology of marine and freshwater organisms, limnology, oceanography, physiology, toxicology, genetics, economics, disease, and management. Preference will be given to manuscripts that emphasize understanding of observed phenomena and interpretation of experimental results. The Journal encourages papers that lead from clearly stated purpose or rationale and from testable hypotheses, concepts, or questions to identifiable conclusions or syntheses. Such papers may amplify, modify, question, or redirect accumulated knowledge embodied in contemporary perceptions of a particular state of aquatic sciences. The Journal discourages papers that are essentially descriptive, except in emerging disciplines; have only site-specific or local applications (a certain year, place, taxon, chemical compound, etc.); only confirm previously established principles; or apply standard techniques without breaking new methodological ground.

Manuscripts for publication should be submitted to the Senior Editor, *Canadian Journal of Fisheries and Aquatic Sciences*, Department of Zoology, University of Guelph, Guelph, ON N1G 2W1, Canada (519-824-4120 ext. 52646; fax: 519-767-9798; e-mail: cjfas@uoguelph.ca).

Submissions in either English or French are acceptable. The information must be original, that is, not copyrighted, published, or submitted elsewhere except in abstract form or unless by written consent of the Editor.

Correspondence concerning accepted manuscripts and corrected proofs should be sent to NRC Research Press, National Research Council of Canada, Ottawa, ON K1A 0R6, Canada (fax: 613-952-7656; e-mail: pubs@nrc-crnc.gc.ca).

Instructions to Authors are published once a year in the first issue of each volume. Copies are available from NRC Research Press or at http://cjfas.nrc.ca. The **Publication Policy** of NRC Research Press is available at http://pubs.nrc-crnc.gc.ca.

Microfilm. Issues from 1934 through the current volume can be purchased on 16- or 35-mm microfilm. Photocopies of individual articles or issues can be purchased from University Microfilms International, 330 North Zeeb Road, Ann Arbor, MI 48106, U.S.A.

U.S. periodical postage paid at Champlain, N.Y., and at additional mailing offices. Attention U.S. POSTMASTER: Send address changes to **Canadian Journal of Fisheries and Aquatic Sciences**, c/o USACAN Media Distribution Center, P.O. Box 2888, Plattsburg, NY 12901, U.S.A.

Publié sans interruption depuis 1901, le *Journal canadien des sciences halieutiques et aquatiques* a paru sous plusieurs titres : *Contributions to Canadian Biology* 1901–1925, *Contributions to Canadian Biology and Fisheries* 1926–1934, *Journal of the Biological Board of Canada* 1934–1937, et *Journal of the Fisheries Research Board of Canada* 1938–1979. Le Journal paraît tous les mois, formant ainsi un volume de 12 numéros, et offre en plus jusqu'à deux suppléments par année.

Politique éditoriale. On publie, dans le Journal, des articles rendant compte de recherche originale, des perspectives (synthèses, critiques et réévaluations), des discussions (commentaires et réponses) et des communications rapides. Les documents peuvent porter sur les cellules, organismes, populations, communautés, écosystèmes ou processus qui affectent les systèmes aquatiques. Ils peuvent relever de divers domaines y compris la biologie et l'écologie des organismes marins et d'eau douce, la limnologie, l'océanographie, la physiologie, la toxicologie, la génétique, l'économie, la pathologie et la gestion. On accorde la préséance aux articles qui contribuent à la compréhension de phénomènes observés et à l'interprétation de résultats expérimentaux. On invite les auteurs à soumettre des articles ayant des objectifs précis ou relevant d'hypothèses, de concepts ou de questions vérifiables et se terminant par de solides conclusions ou d'utiles synthèses. Ces articles enrichissent, changent, mettent en question ou réorientent les connaissances acquises sur divers aspects des sciences aquatiques. On décourage toutefois la soumission d'articles simplement descriptifs (à moins qu'il ne s'agisse de nouvelles disciplines), d'application très limitée (applicables à une seule année, une seule région ou un seul taxon, portant sur un unique composé chimique, etc.); d'articles qui ne font que reprendre les principes énoncés dans des articles précédents; et d'articles rendant compte de l'application de normes sans gain de méthodologie.

Les auteurs voudront adresser leurs **manuscrits** à la directrice scientifique principale, *Journal canadien des sciences halieutiques et aquatiques*, Department of Zoology, University of Guelph, Guelph, ON N1G 2W1, Canada (519-824-4120 poste 52646; télécopieur : 519-767-9798; courriel : cjfas@uoguelph.ca).

Les contributions peuvent être en anglais ou en français. Elles doivent être originales, c.-à.-d. qu'elles ne doivent pas avoir fait l'objet d'un copyright, avoir été publiées ou soumises ailleurs, sauf sous forme abrégée ou avec le consentement du rédacteur. Le CNRC ne se tient en aucune façon responsable des opinions exprimées par un collaborateur ou des déclarations qui pourrait faire ce dernier.

La correspondance ayant trait aux manuscrits acceptés et les **épreuves corrigés** doivent être envoyées aux Presses scientifiques du CNRC, Conseil national de recherches du Canada, Ottawa, ON K1A 0R6, Canada (télécopieur : 613-952-7656; courriel : pubs@nrc-crnc.gc.ca).

Les Recommandations aux auteurs sont publiées une fois par année dans le premier numéro de chaque volume. Des copies sont disponibles auprès du Bureau de la rédaction aux Presses scientifiques du CNRC ou au http://jcsha.cnrc.ca. **La Politique de publication** est disponible auprès des Presses scientifiques du CNRC ou au http://pubs.nrc-crnc.gc.ca.

Microfilms. On peut acheter sur microfilms de 16 ou 35 mm tous les numéros depuis 1934. Des photocopies d'articles ou de numéros individuels sont aussi en vente auprès de University Microfilms International, 330 North Zeeb Road, Ann Arbor, MI 48106, É.-U.

This Journal is indexed or abstracted in / Cette revue est signalée ou résumée dans
ABSEARCH, Aquatic Sciences and Fisheries Abstracts, Biological Abstracts, Biological & Agricultural Index, CAB Abstracts, Chemical Abstracts, Current Contents, Elsevier BIOBASE, Environmental Abstracts, Environmental Periodicals Bibliography, GEOBASE, GeoRef, Internationale Bibliographie der Zeitschriftenliteratur, Life Sciences Collection, Meteorological and Geoastrophysical Abstracts, Oceanic Abstracts, PASCAL Database, and Science Citation Index.

Volume 60, Number 12, December 2003

Canadian Journal of Fisheries and Aquatic Sciences

Published by the National Research Council of Canada

Volume 60, numéro 12, décembre 2003

Journal canadien des sciences halieutiques et aquatiques

Publié par le Conseil national de recherches du Canada

Senior Editor / Directrice scientifique principale **Moira M. Ferguson**

Editors / Directeurs

Jeffrey A. Hutchings, *Dalhousie University, Halifax*
Pierre Pepin, *Northwest Atlantic Fisheries Centre, DFO/MPO, St. John's, Newfoundland*
W. Gary Sprules, *University of Toronto at Mississauga*
Assistant to the Editors / Adjointe aux directeurs scientifiques **Holly Foster**

Associate Editors / Directeurs scientifiques associés

M.T. Arts, *Environment Canada, Burlington*
D. Boisclair, *Université de Montréal*
U. Borgmann, *Environment Canada, Burlington*
S.E. Campana, *DFO/MPO, Dartmouth*
R. Carignan, *Université de Montréal*
J.J. Dodson, *Université Laval*
G.T. Evans, *DFO/MPO, St. John's, Newfoundland*
K.T. Frank, *DFO/MPO, Dartmouth*
M.M. Hansen, *Danish Institute for Fisheries Research, Silkeborg, Denmark*
R. Hilborn, *University of Washington*
A. Hontela, *Université du Québec à Montréal*
D.F. Houlihan, *University of Aberdeen*
F.A. Huntingford, *University of Glasgow*
G.S. Jamieson, *DFO/MPO, Nanaimo*
B. Jonsson, *Norwegian Institute for Nature Research, Oslo, Norway*
P. Magnan, *Université du Québec à Trois Rivières*
C.T. Marshall, *University of Aberdeen*
R.B. Millar, *University of Auckland, New Zealand*
Y.T. Prairie, *Université du Québec à Montréal*
T.J. Quinn II, *University of Alaska–Fairbanks, Juneau, Alaska*
T.P. Quinn, *University of Washington*
R.D. Robarts, *Environment Canada, Saskatoon*
B. Sainte-Marie, *DFO/MPO, Mont-Joli*
D.W. Schindler, *University of Alberta*
R.E.H. Smith, *University of Waterloo*
S.J. Smith, *DFO/MPO, Dartmouth*
W.F. Vincent, *Université Laval*
R.D. Vinebrooke, *University of Alberta*
C.J. Walters, *University of British Columbia*
R.D. Ward, *CSIRO Marine Research, Australia*
B. de Young, *Memorial University of Newfoundland*

NRC Research Press / Presses scientifiques du CNRC

Editor-in-Chief / Directeur général **Bruce P. Dancik**
Assistant Editor-in-Chief / Directeur général adjoint **Iain E.P. Taylor**

Journals Program / Programme des revues

Fax / Télécopieur : 613-952-7656; e-mail / courriel : pubs@nrc-cnrc.gc.ca; URL / URL : http://pubs.nrc-cnrc.gc.ca
Acting Director / Directeur par intérim **Cameron D. Macdonald**
Business Manager / Gestionnaire des affaires **Paul McClymont**
Manager, Journals Program / Gestionnaire, Programme des revues **Carolyn Brown**
Managing Editor / Rédactrice administrative **Cecily M. Pearson** (613-993-9099)
Publication Officers / Agentes de publication **Jennifer McColl**
Advertising / Annonces publicitaires **Judy Gorman** (613-993-0151)
Reprints / Tirés à part **Roxanne Landriault** (613-990-2254)
Subscriptions / Abonnements **Eileen Evans-Nantais** (613-990-7873)

The National Research Council of Canada accepts no responsibility for statements or opinions expressed by a contributor. Acceptance of an advertisement, announcement, or other material does not imply endorsement by either the Journal's Senior Editor or the National Research Council.

© National Research Council of Canada 2003. All rights reserved.

No part of this publication may be reproduced, stored, or transmitted in any form or by any means, without the written permission of the publisher, except as stated below.

The National Research Council of Canada grants **permission*** to individuals to make single copies of articles for personal use. Any person may reproduce short excerpts from articles in the journal for any purpose that respects the moral rights of authors, provided that the source is fully acknowledged. As a courtesy, the consent of authors of such material should be obtained directly from the author.

Authorization to reproduce items for other than personal use, as stated above, is granted by the National Research Council of Canada provided that the copyright fee of $7.00 per copy is paid directly to CANCOPY, One Yonge Street, Suite 1900, Toronto, ON M5E 1E5, Canada.

*The above permission does not extend to other kinds of copying, such as copying for general distribution, for advertising, or promotional purposes, for creating new collective works, or for resale. For such copying, arrangements must be made with the publisher, National Research Council of Canada, Ottawa, ON K1A 0R6, Canada.

Subscription information

The *Canadian Journal of Fisheries and Aquatic Sciences* (ISSN 0706-652X) is published monthly by the National Research Council of Canada. The 2003 annual subscription rates (second class postage) for Canada are $830CAN institutional and $257CAN personal, for US & foreign $830US institutional and $257US personal. For air mail add $175US to foreign rate. Canadian customers please include 7% GST (business no. 12149 1807 RT 0275). Subscriptions are entered for the calendar year. Remittances should be made payable to the Receiver General for Canada credit NRC. Price for regular single issues: institutional, $105.00; personal, $35.00. Supplements will be priced separately. Special rates apply to members of Canadian scientific and engineering societies if they subscribe through their respective societies.

There are no refunds on cancelled subscriptions once delivery has begun. Claims for missing issues should be made within four months (N. America) or six months (outside N. America) following the date of publication. The publisher expects to supply missing issues only when losses have occurred in transit and when the reserve stock will permit. For change of address and subscription enquiries: Subscription Office, NRC Research Press, National Research Council of Canada, Ottawa, ON K1A 0R6, Canada; tel.: 613-993-9084; fax: 613-952-7656; e-mail: pubs@nrc-crnc.gc.ca.

Microform backfiles are available from UMI, P.O. Box 1346, Ann Arbor, MI 48106-1346, U.S.A., and Micromedia Ltd., 20 Victoria St., Toronto, ON M5C 2N8, Canada.

All issues of the *Canadian Journal of Fisheries and Aquatic Sciences* since 1996 are available on the Web. Pricing information can be found at http://pubs.nrc-crnc.gc.ca.

Le Conseil national de recherches du Canada ne se tient en aucune façon responsable des opinions exprimées par un collaborateur ou des déclarations que pourrait faire ce dernier. La publication d'annonces publicitaires, d'avis et autres n'implique pas l'endossement de leur contenu par la directrice principale de la Revue ou le CNRC.

© Conseil national de recherches du Canada 2003. Tous droits réservés.

Il est interdit de reproduire, de sauvegarder ou de transmettre quelque partie de la présente publication dans quelque format ou de quelque façon sans le consentement écrit de l'éditeur, à l'exception des conditions suivantes.

Le Conseil national de recherches du Canada accorde aux particuliers le droit de faire des copies individuelles pour leur usage personnel. Toute personne peut reproduire de courts extraits des articles de la Revue pour autant que les droits moraux de l'auteur soient respectés et que la mention de provenance soit clairement indiquée. Il est de convenance de demander le consentement de l'auteur avant de faire mention de son travail.

On obtiendra l'autorisation de reproduire des articles à d'autres fins que l'usage personnel (tel qu'on l'a décrit ci-dessus) auprès du Conseil national de recherches du Canada pour autant que des redevances de droits d'auteurs de 7,00 $/copie soient versées au CANCOPY, 1, rue Yonge, bureau 1900, Toronto, ON M5E 1E5, Canada.

*La permission ci-dessus ne s'applique pas à la reproduction à grande échelle, telle que la reproduction aux fins de distribution générale, publicitaire ou promotionnelle, de compilation de nouveaux ouvrages collectifs ou de revente. Dans de tels cas, il faudra ratifier une entente particulière avec l'éditeur, le Conseil national de recherches du Canada, Ottawa, ON K1A 0R6, Canada.

Renseignements sur l'abonnement

Journal canadien des sciences halieutiques et aquatiques (ISSN 0706-652X) est une publication mensuelle du Conseil national de recherches du Canada. Le prix de l'abonnement annuel au Canada (courrier de deuxième classe) est de 830 $CAN pour les organismes et de 257 $CAN pour les particuliers. À l'étranger (y compris les É.-U.), le prix de l'abonnement est de 830 $US pour les organismes et de 257 $US pour les particuliers. L'expédition par avion exige des frais de 175 $US en sus du prix d'abonnement à l'étranger. Les clients du Canada doivent ajouter la TPS de 7% (numéro d'entreprise 12149 1807 RT 0275). Les abonnements sont pour l'année civile. Tout paiement doit être adressé au Receveur général du Canada, crédit du CNRC. Le prix par numéro est de 105 $ pour les organismes et de 35 $ pour les particuliers. Le prix des hors-série varie. Les membres des sociétés canadiennes de sciences et de génie bénéficient de taux préférentiels en s'abonnant via leurs sociétés respectives.

Aucun remboursement ne sera accordé ni aucune annulation acceptée une fois que les livraisons auront commencé. Les réclamations de numéros manquants devront être soumises dans les quatre mois (Amérique du Nord) ou dans les six mois (à l'extérieur de l'Amérique du Nord) suivant la date de publication. L'éditeur ne fournira de numéros manquants que si le document a été perdu pendant l'expédition et que si le stock le permet. Adressez tout changement d'adresse ou toute question quant à l'abonnement au : Bureau des abonnements, Presses scientifiques du CNRC, Conseil national de recherches Canada, Ottawa, ON K1A 0R6, Canada; téléphone : 613-993-9084; télécopieur : 613-952-7656; courriel : pubs@nrc-crnc.gc.ca.

On peut obtenir les fichiers rétrospectifs sur **microforme** auprès de UMI, P.O. Box 1346, Ann Arbor, MI 48106-1346, É.-U., et auprès de Micromedia Ltée, 20, rue Victoria, Toronto, ON M5C 2N8, Canada.

À partir de 1996, tous les numéros de *Journal canadien des sciences halieutiques et aquatiques* sont accessibles sur le Web. On trouvera des renseignements sur les tarifs à http://pubs.nrc-crnc.gc.ca.

RAPID COMMUNICATION / COMMUNICATION RAPIDE

Folly and fantasy in the analysis of spatial catch rate data

Carl Walters

Abstract: Spatial catch per effort data can provide useful indices of population trends provided that they are averaged so as to correct for effects of changes in the distribution of fishing activity. Simple, nonspatial ratio estimates should not be used in such analyses. The averaging for any time period must necessarily make some assumptions about what catch rates would have been in spatial strata that had not yet, or were no longer, being fished. Ignoring the unfished strata (averaging only over the areas that were fished) amounts to assuming that they behaved the same as the fished strata and can lead to severe hyperdepletion in abundance indices for fisheries that developed progressively over large regions.

Résumé : Les données spatiales de captures par unité d'effort fournissent des indices utiles des tendances démographiques à la condition qu'elles soient transformées en moyennes de manière à tenir compte des effets des changements dans la répartition des activités de pêche. Des estimations simples et non spatiales de rapports ne doivent pas être utilisés dans de telles analyses. Le calcul des moyennes pour chaque période de temps doit nécessairement établir des présuppositions sur ce qu'auraient été les taux de capture dans les strates spatiales dans lesquelles on n'a pas encore pêché ou dans lesquelles la pêche a cessé. Si on ne tient pas compte des strates où il ne se fait pas de pêche (en calculant les moyennes seulement à partir des zones de pêche), on assume que toutes les strates réagissent de la même façon, qu'il y ait ou non de la pêche; cela peut mener à une sévère hyperdéplétion dans les indices d'abondance pour les pêches commerciales qui ont évolué progressivement sur de grands espaces.

[Traduit par la Rédaction]

Introduction

Information on trends in relative abundance is critical for most long-term stock assessments, and we typically must use commercial catch rate (catch per unit effort, CPUE) data to estimate such trends. In many cases, detailed logbook records allow spatial analysis of catch rate data, typically by spatial grid cells viewed as sampling strata, so as to hopefully remove the obvious biases that would be expected from nonrandom search behavior by fishers.

Unfortunately, two very serious mistakes have commonly been made in the analysis of spatial catch rate data. The first involves the incorrect use of ratio (catch/effort) estimators, and the second involves failure to recognize hidden assumptions about abundance trends in spatial cells that were not fished at all early or late in fishery development. Both of these mistakes are liable to produce exaggerated trend indices, i.e., "hyperdepletion" (Hilborn and Walters 1992), the appearance that stock size has declined much more than it actually has. The second of these is by far the most serious. This paper reviews both and offers suggestions for dealing with the second.

Received 28 October 2003. Accepted 26 November 2003. Published on the NRC Research Press Web site at http://cjfas.nrc.ca on 8 December 2003.
J17795

C. Walters. Fisheries Centre, The University of British Columbia, Vancouver, BC V6T1Z4, Canada (e-mail: c.walters@fisheries.ubc.ca).

Folly: incorrect use of ratio estimators

Because catch per effort is obviously a ratio of catch to effort, it has been usual to use ratio estimators for it, i.e., to sum up catches over some units of time and space and then divide the sum by total effort over these units. This calculation should be done only for small enough units (spatial cells, time periods) to have had effectively random sampling within each unit. However, in some cases, e.g., Myers and Worm (2003), catches and efforts have been summed over spatial cells (strata) to produce a single, overall ratio estimate of catch per effort. This method in effect places much more "weight" on data from those cells that were heavily fished than on cells for which catches and efforts were low, whether or not the heavily fished cells were representative in any way of relative abundance in lightly fished or unfished cells. Texts on statistical sampling theory (e.g., Cochran 1963, pp. 167–172) present better estimators for ratios in stratified random sampling, and those estimators are of the form $\bar{c} = \Sigma_h w_h r_h$, where h is the cell or sampling stratum, w_h is the physical stratum size divided by the physical sampling universe size, and r_h is the ratio estimator for cell h. That is, stratified sampling estimators for ratios consist of weighted averages of ratios for individual cells or strata, where the

 doi: 10.1139/F03-152 © 2003 NRC Canada

weights do not depend in any way on the number of observations made in the individual strata.

In fisheries where effort was initially concentrated in a few cells then later spread widely, as in the Japanese pelagic long-line fishery examined by Myers and Worm (2003; see maps at http://fish.dal.ca/~myers/Myers_Supplementary2.pdf), catch rates have typically dropped dramatically in the initial fishing areas before fishers were willing to spread their efforts more widely (for obvious risk-management reasons). The catch-rate declines in such areas are not in any way representative of overall (over all cells) stock change, and to pretend that the overall ratio estimator of catch rate was in fact representative of overall stock change amounts to the folly of pretending that the whole system was declining at the same rate as it did in the initial fishing area.

Fantasy: ignoring unfished cells/strata

The ratio estimation mistake above is simply a failure to apply well-known statistical methods for analysis of stratified sampling data. A much more subtle but ultimately more important mistake has been to apply the correct formulae for stratified sampling (separate ratio estimator for each cell, take average of these weighted by cell sizes), but to do so only for those cells that were actually fished in a given time period. After all, how can we justify trying to make any claim about what was going on in those cells that were not even visited or sampled by fishers?

The construction of an overall trend index for change in a spatially structured stock is the same as constructing a very large table, with a row for each time period (typically year or month) and a column for each spatial cell or stratum that might have been occupied at each time (i.e., each cell for which there was ever any fishing, whether or not the cell was fished in all time periods). For standard theorems from stratified sampling to apply to the calculation of the index for each time period (as an average across a row of the table), we would need to have catch-rate data for every cell, in every period. This almost never happens, especially early in fishery development. Faced with a table that has many missing entries, we have three choices: (*i*) we can refuse to construct any overall stock trend index and instead restrict statistical analysis and inference to only those cells that were fished each year (in which case the index is meaningless as an input for overall stock assessment); (*ii*) we can assume that the mean catch rate over those cells that were fished in any period is somehow representative of what would have been seen in the cells that were not fished, i.e., that cells were chosen for fishing at random or that it would be acceptable to fill all empty table cells in each row with the mean of the cells that were fished in that row; or (*iii*) we can somehow fill the empty table cells with our best estimates of what would have been seen in those cells had they been fished, which almost certainly would not be the mean of the cells that were fished in each period.

Notice that there is an element of fantasy in either of approaches (*ii*) or (*iii*). For fisheries that have moved progressively across large grounds, like pelagic long-liners crossing the Pacific during the 1950s (see Myers and Worm 2003), it would be unwise to use (*ii*) and assert that catch rates obtained in the western Pacific as the fishery first started to spread were representative of what stock abundances were doing in the (unfished) eastern Pacific at that time (as witness high catch rates obtained later, when the fishery did reach further afield). A far more credible estimate of the catch rate that would have been obtained in such unfished cells would be the catch rates that were obtained later when the fishery actually reached those cells, but even these "best estimates" require the fantasy that stock size in each cell was stable over time (at the level first seen by fishing) before fishing arrived at it.

So to analyze the long-term data without making some bad assumption (e.g., that unfished areas were behaving the same as fished ones), we are forced to think very carefully about how best to "fill in" the gaps in space–time tables of catch rates. Just as we cannot analyze even crude catch and effort data without making some dangerous assumptions (e.g., that local catch rate is in fact proportional to local abundance), the table filling has to involve some strong judgmental decisions about what assumptions to use. The important point is that once we recognize that the table has to be filled in somehow, we can at least elect to make reasonable assumptions rather than unwise ones based on the mistaken notion that statistical rigor or scientific objectivity (the main bases for averaging only over the fished cells) can somehow substitute for judgment.

When we deliberately and consciously ask the question "what is our best estimate of the catch rate for any particular space–time table entry for which we do not have direct observations", several alternatives become apparent (besides the unwise one of just using the average over row elements that were actually fished). First, we can look forward and backward in time (up and down the table column) for catch rate information that may be representative of what would have been observed, essentially performing some sort of trend analysis and interpolation (extrapolation) from the time series that is available for the cell. Second, if there are data for the same time period from spatially "nearby" cells and if we can show that there is spatial correlation structure in catch rates, we can use spatial statistics methods to interpolate (extrapolate) across the spatial grid. Third, we can use data on spatial covariates of distribution (e.g., water temperature) to improve both the spatial and temporal trend estimates, or to at least provide estimates of changing range boundaries (which cells likely had zero abundance). Fourth, we can use estimators based on spatial models of dispersal–migration and local renewal dynamics, essentially fitting the time–space data to a much larger model than would typically be used for overall stock assessment.

Figure 1 illustrates just how big a difference the catch rate averaging method can make, using the Japanese long-line data for albacore (*Thunnus alalunga*) and yellowfin (*Thunnus albacares*) tuna in the Pacific. Three time trend patterns are shown: (1) the ratio estimator (total catch)/(total effort) reported by Myers and Worm (2003); (2) spatial average catch rate, only over those cells that were actually fished each year; and (3) catch rate averaged over all cells that were ever fished, with two filling conventions. First, the catch rate before first fishing in each cell was set to the average of the catch rates observed for the cell in the first 3 years after fishing reached it (i.e., abundance stable before fishing). Second, for cells that were "abandoned" by the fishery, the

© 2003 NRC Canada

Fig. 1. Catch per unit effort (CPUE) trends for large tuna and billfish (total number of fish per hook) from the 5 × 5 degree cell Japanese long-line database (Myers and Worm 2003), estimated by three alternative methods for (*a*) Atlantic, (*b*) Pacific, and (*c*) Indian oceans. Full spatial (solid line) assigns mean of first three observed catch rates to each cell for years before it was first fished and the last observed catch rate for years after it was last fished. Restricted spatial (▲) is the mean catch rate over only those cells that were actually fished each year. Ratio (■) is simply total catch summed over all cells divided by total effort.

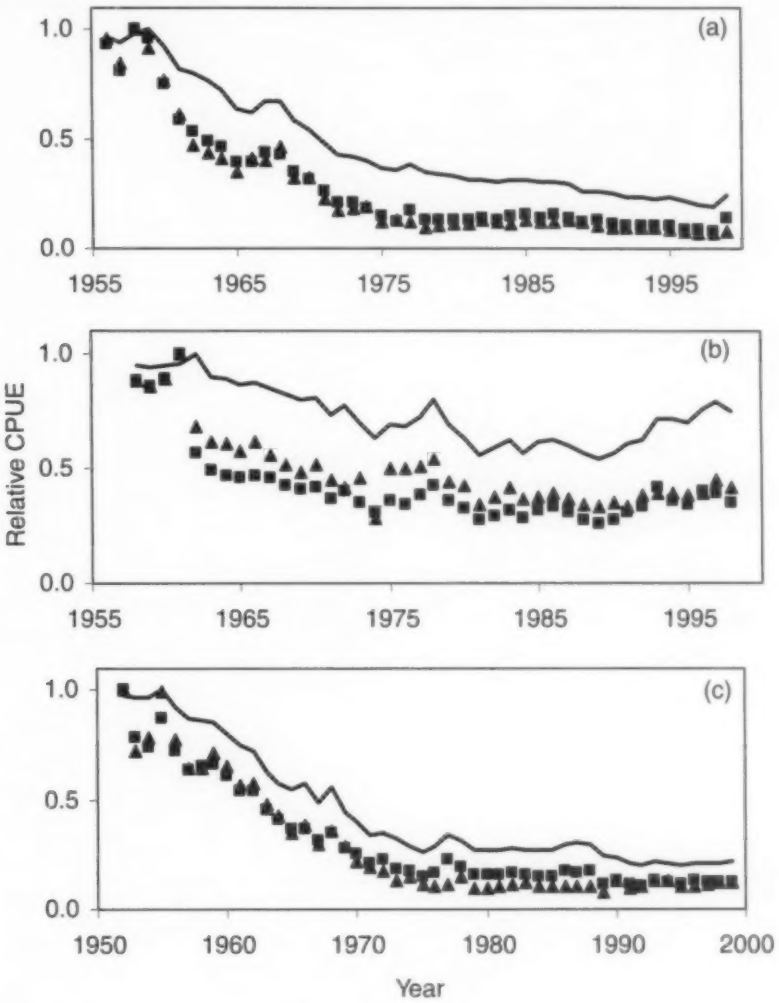

catch rate in later years was set to the rate for the last year of fishing (i.e., abundance assumed not to recover after fishing departed). The difference between these methods is very obvious; although all three indicate stock depletion, the third implies that the stocks were not as severely reduced as the fishery developed.

It has been typical in the analysis of commercial catch rate data to be very concerned about "hyperstability" (Hilborn and Walters 1992) caused by shoaling behavior and range contraction during stock declines. In terms of the table representation of trend index construction, hyperstability is represented by having a shrinking number of cells (if cells are small enough) occupied by fishers over time. In this case, to use the average catch rate in just the fished cells as an overall index (i.e., to fill the unfished cells with that average catch rate) would obviously create a hyperstable index. To avoid this hyperstability, a simple estimation tactic is to fill the unfished cells outside the fished area for each year with zeros (to represent the notion that fishers would still have been going to those cells if there had still been fish in them).

Discussion

It is apparently not often realized that constructing a long-term abundance trend index from catch-rate data is necessarily equivalent to filling in a large data table with many missing entries. And it may also be surprising to realize that using only the data at hand can be equivalent to (produces same numerical result as) filling in the table with obviously incor-

© 2003 NRC Canada

rect averages. But for far too long, we have been "putting our heads in the sand", pretending that things will average out in the end and that routine application of statistical techniques will somehow absolve us of responsibility for thinking carefully about what we are assuming in analysis. That in fact is a much more dangerous fantasy than to use various gap-filling methods, and it has to come to an end; examples like Fig. 1, where anyone who has examined overall catch trends would suspect that the stock declines could not have been as bad as indicated by ratio catch rate trends, can seriously undermine the credibility of fisheries assessment scientists. This will in turn make it harder to argue for conservation measures in cases where there really has been severe overfishing. Further, to simply ignore the long-term data entirely would, in most cases, be an invitation to the potentially even worse errors of the shifting baseline syndrome (Pauly 1995).

Once we realize the importance of gap-filling spatial catch rate tables to avoid both hyperstability and hyperdepletion in indices, we open the door to various innovative and relatively inexpensive approaches to design of field survey programs that can make the gap-filling more objective. For example, in cases in which behavior (shoaling, etc.) would lead us to suspect hyperstability, even a very simple, wide-area system for presence–absence sampling may be all that is needed to fill the spatial data gaps. Likewise, in many cases there may be simple, local information to warn us of whether back-filling of tables with prefishing catch rates for spreading fisheries would be misleading because of changes in stock distribution and (or) impacts of fishing on dispersal rates of fish to (from) areas that have not yet been heavily fished.

Even with care in the spatial data analysis, there always remains a serious risk that catch per effort is not in fact proportional to abundance, even at the scale of small spatial cells. Hyperstability at small scales can arise as the result of gear saturation and handling time effects. Hyperdepletion can arise as the result of localized depletion of fine-scale spatial aggregations within cells. Apparent hyperdepletion can be caused by interference competition (Gillis and Peterman 1998; Swain and Wade 2003), exploitation of a pool of more vulnerable fish that exchanges with a pool of less vulnerable individuals (Walters and Bonfil 1999), and perhaps other mechanisms than can cause direct decrease in catch per effort with increasing effort, even when stock size is not being depleted.

References

Cochran, W.G. 1963. Sampling techniques. John Wiley and Sons, New York.

Gillis, D.M., and Peterman, R.M. 1998. Implications of interference among fishing vessels and the ideal free distribution to the interpretation of CPUE. Can. J. Fish. Aquat. Sci. **55**: 37–46.

Hilborn, R., and Walters, C. 1992. Quantitative fisheries stock assessment: choice, dynamics, and uncertainty. Chapman and Hall Inc., New York.

Myers, R.A., and Worm, B. 2003. Rapid world-wide depletion of predatory fish communities. Nature (Lond.), **423**: 280–283.

Pauly, D. 1995. Anecdotes and the shifting baseline syndrome of fisheries. Trends Ecol. Evol. **10**: 430.

Swain, D.P., and Wade, E.J. 2003. Spatial distribution of catch and effort in a fishery for snow crab (*Chionoecetes opilio*): tests of predictions of the ideal free distribution. Can. J. Fish. Aquat. Sci. **60**: 897–909.

Walters, C., and Bonfil, R. 1999. Multispecies spatial assessment models for the British Columbia groundfish trawl fishery. Can. J. Fish. Aquat. Sci. **56**: 601–628.

© 2003 NRC Canada

RAPID COMMUNICATION / COMMUNICATION RAPIDE

Fish as potential dispersal agents for floodplain plants: first evidence in North America

John H. Chick, Robert J. Cosgriff, and Lori S. Gittinger

Abstract: In river–floodplain ecosystems with seasonal flood pulses, many species display adaptations to take advantage of resources in the aquatic–terrestrial transition zone. Frugivory and seed dispersal by fishes is a clear example of such adaptations, known primarily from South American river–floodplain systems. Here, we document consumption of red mulberry (*Morus rubra*) and swamp privet (*Forestiera acuminata*) fruit by channel catfish (*Ictalurus punctatus*) in the floodplain of the Mississippi River, U.S.A., and demonstrate that red mulberry and swamp privet seeds will germinate after being consumed by channel catfish. In a common-garden experiment, consumption of fruits and seeds by channel catfish improved germination success of these riparian plants relative to a treatment simulating fruit dropped during a flood without being consumed by fish. This is the first study to provide evidence of frugivory and viability of seeds ingested by fish in a North American river–floodplain ecosystem. Frugivory and seed dispersal by fishes may be more widespread than previously thought.

Résumé : Dans les écosystèmes des plaines d'inondation des rivières qui subissent des épisodes saisonniers de crue, plusieurs espèces possèdent des adaptations pour profiter des ressources qu'offre la zone de transition entre les milieux aquatique et terrestre. La consommation de fruits et la dispersion des graines par les poissons, observées surtout dans les systèmes des plaines d'inondation des rivières d'Amérique du Sud, sont un exemple évident de telles adaptations. Nous signalons ici la consommation de fruits du mûrier rouge (*Morus rubra*) et du troène des marécages (*Forestiera acuminata*) par la barbue de rivière (*Ictalurus punctatus*) dans la plaine d'inondation du Mississipi, États-Unis, et démontrons que les graines des deux plantes peuvent germer après avoir été consommées par la barbue. Dans une expérience de jardin commun, la consommation de fruits et de graines par la barbue améliore le succès de la germination chez ces plantes de rivage, par rapport à une expérience où l'on simule la chute des fruits durant une crue, sans qu'il y ait de consommation par les poissons. C'est la première fois que, dans un écosystème de plaine d'inondation d'une rivière d'Amérique du Nord, on prouve l'existence de la consommation de fruits par les poissons et la viabilité des graines ingérées; la consommation de fruits et la dispersion des graines par les poissons sont peut-être des phénomènes plus répandus qu'on ne le croyait jusqu'ici.

[Traduit par la Rédaction]

River–floodplain systems differ from other lotic ecosystems in that seasonal flood pulses connect rivers to floodplain resources that drive biotic production (Sparks 1995; Sparks et al. 1998). In South America, over 200 species of fish consume fruits and seeds, underscoring the importance of floodplain resources to biotic communities in large rivers (Gottsberger 1978; Araujo-Lima and Goulding 1997). Several of these fishes pass viable seeds through their digestive tract, thereby acting as potential seed-dispersal agents (Gottsberger 1978; Horn 1997; Araujo-Lima and Goulding 1997). Many riparian plants in these systems produce floating fruits and show concordance of fruiting with seasonal flood pulses, which may be adaptations to take advantage of fishes for seed dispersal (Goulding 1980; Kubitzki and Ziburski 1994). Reports of seed dispersal by fishes in South American river–floodplains, however, are usually based only on stomach content analysis, and actual experiments demonstrating viability of seeds digested by fishes are rare (Horn 1997). Frugivory by fishes also has been reported in Asia (Corlett 1998) and Africa (Welcomme 1985), but apparently no studies outside of South America have reported the viability of riparian plants seeds after ingestion by fishes. This may indicate that South American river–floodplain ecosystems differ from those in the rest of the world, or that researchers have not thoroughly investigated this topic in other regions. Gottsberger (1978) suggested that seed dispersal by fishes is more common in nutrient-poor systems, such as the Amazon, where fish depend on allochthonous food sources. Additionally, human alterations of flow regimes and riparian habitats in river–floodplain ecosystems, particularly in North

Received 26 September 2003. Accepted 28 October 2003. Published on the NRC Research Press Web site at http://cjfas.nrc.ca on 10 December 2003.
J17736

J.H. Chick,[1] R.J. Cosgriff, and L.S. Gittinger. Great Rivers Field Station, Illinois Natural History Survey, Brighton, IL 62012, U.S.A.

[1]Corresponding author (e-mail: chick@inhs.uiuc.edu).

 doi: 10.1139/F03-155 © 2003 NRC Canada

Table 1. Frequency of occurrence of prey items consumed by channel catfish collected from the Mississippi River in May 2001 (N = 23) and June 2002 (N = 26).

	Frequency of occurrence (%)	
Prey item	2001	2002
Red mulberry	69.5	53.8
Swamp privet	0.0	53.8
Unidentified seeds	21.7	0.0
All seeds	78.2	73.1
Chironomids	17.4	38.5
Other insects	52.2	42.3
Crayfish	13.0	7.7
Fish	8.7	7.7
Detritus	0.0	23.1
Vegetation	0.0	7.7

Note: Frequency of occurrence is percent of channel catfish that consumed a given prey item. Both terrestrial and aquatic species are included in the categories "other insects" and "vegetation".

America and Europe, have reduced connectivity between rivers and their floodplains (Welcomme 1985; Sparks 1995; Galat and Lipkin 2000), which may have reduced or eliminated frugivory and seed dispersal by fishes.

In late May of 2001, we initiated a study to verify reports from Illinois Department of Natural Resources biologists of channel catfish consuming mulberries and to test the viability of ingested seeds. We used boat electrofishing to collect channel catfish from flooded terrestrial habitats in a contiguous backwater lake located in the interior of an island in the Mississippi River near Alton, Illinois (U.S.A.). The riparian zone of this lake contains abundant red mulberry and swamp privet trees that are accessible to fishes during floods. We collected 23 channel catfish (28–57.5 cm total length (TL)) and checked for the presence of fruit or seeds throughout the entire digestive tract. A majority of these fish (69.5%) had consumed red mulberries (Table 1), with individuals consuming from two to over 1000 seeds. In early June of 2002, we collected 26 channel catfish (16.8–63 cm TL) from the same location and similar habitats, a majority of which (73.1%) had consumed red mulberries and (or) swamp privet fruit (Table 1). Individual channel catfish consumed from two to over 100 mulberry seeds and from two to 12 swamp privet fruits. Channel catfish in both years were not exclusively frugivorous and consumed several other prey items of aquatic and terrestrial origin (Table 1).

Seeds from the lower digestive tract (intestine) were used in experiments to assess seed viability. We conducted a pilot study in May and June 2001, planting seeds in plug trays to assess germination of seeds in five treatments: (1) seeds planted directly from channel catfish intestines; (2) seeds taken from channel catfish intestines and held in water for 14 days; (3) seeds extracted from berries picked from trees; (4) seeds extracted after allowing berries to dry and ferment for 14 days; and (5) seeds extracted from berries held in water for 14 days. We allowed 30 days for seeds to germinate for each treatment, but most seeds germinated within 10 days. On average, the floodplain of this reach of the Mississippi River is inundated for 35 days each year, with a

Fig. 1. Percent of seeds germinating (±1 standard error) from (*a*) red mulberry (*Morus rubra*) and (*b*) swamp privet (*Forestiera acuminata*) fruit from two treatments: fish — seeds removed from channel catfish (*Ictalurus punctatus*) intestines and held in river water for 7 days; no fish — seeds extracted and planted from fruit that was harvested from the Mississippi River floodplain and held in river water for 7 days.

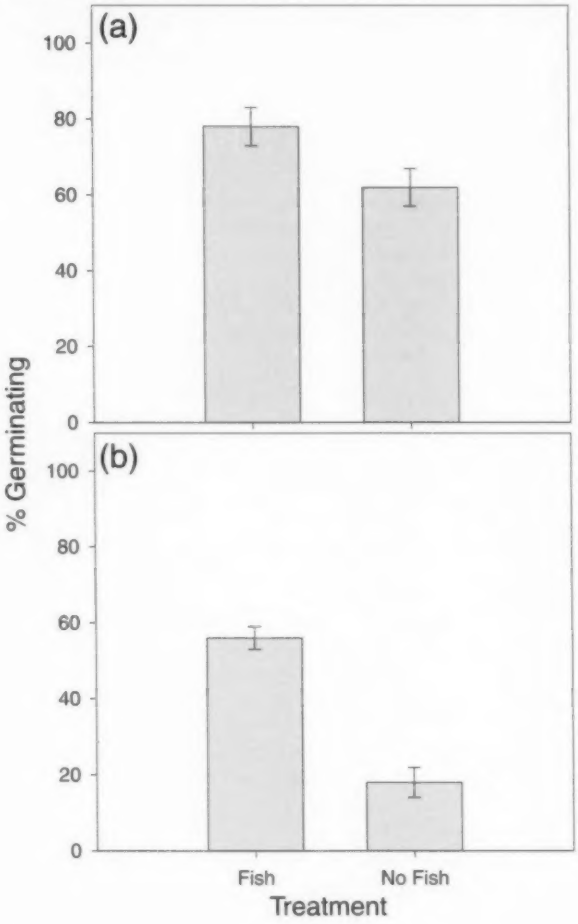

flood peak in May (U.S. Geological Survey, unpublished gauge data). Red mulberry and swamp privet fruit begin to ripen in May and June (Young and Young 1992), so we chose to hold berries and seeds in water for 14 days (i.e., about half of the duration of an average flood pulse). Plug trays were kept outside during the day and brought indoors at night and during rainstorms. Germination success for seeds consumed by channel catfish was 75.7% (N = 185) when seeds were planted directly and 70.5% (N = 173) when seeds were subsequently held in water for 14 days. Seeds extracted directly from berries had a germination success of 82.4% (N = 357), but germination success was only 30% (N = 390) when berries were fermented and only 0.3% (N = 360) when berries were held in water for 14 days.

To test whether ingestion of seeds by channel catfish improves germination success for red mulberry and swamp

© 2003 NRC Canada

privet seeds, we conducted a common-garden experiment in June 2002. We examined two treatments, one simulating the fate of seeds consumed by channel catfish, and one simulating the fate of seeds from fruit dropped during a flood without being consumed by fish. In the fish treatment, seeds were planted after being removed from channel catfish intestines and held in river water (4-L open plastic container) for 7 days (a less drastic inundation time than in our pilot study). For the no-fish treatment, seeds were extracted from fruit and planted after holding mulberry and swamp privet fruit in river water (separate 4-L open containers) for 7 days. We chose to pool all seeds ingested by catfish and all seeds extracted from berries because the relatively high and comparable germination success for seeds ingested by catfish and seeds extracted from berries suggests that variation in germination success among individual fish or berries is slight (i.e., most seeds germinated). Seeds were planted in plug trays under similar conditions (outdoors) to those in the pilot study. We considered a row of seven plugs (one seed per plug) an experimental unit and calculated the proportion of seeds germinating in each row. Six rows formed a block and each of the two treatments was randomly assigned to three rows per block. We used a total of five blocks for red mulberry seeds and four blocks for swamp privet seeds. After 10 days, a significantly greater proportion of seeds germinated in the fish treatment compared with the no-fish treatment for both red mulberry (Fig. 1*a*; $F = 7.05$, df = 1,20, $P = 0.0152$) and swamp privet (Fig. 1*b*; $F = 21.79$, df = 1,16, $P = 0.0003$). Differences among blocks and interactions between block and treatment were not significant for either red mulberry ($F_{block} = 0.04$, df = 4,20, $P = 0.9972$; $F_{block \times treatment} = 2.48$, df = 4,20, $P = 0.0772$) or swamp privet ($F_{block} = 0.09$, df = 3,16, $P = 0.9672$; $F_{block \times treatment} = 0.57$, df = 3,16, $P = 0.6444$).

To our knowledge, this is the first study to provide evidence of frugivory and viability of riparian seeds ingested by fish in a North American river–floodplain ecosystem. Channel catfish are known to undertake longitudinal and lateral migrations to gain access to floodplain habitats during seasonal floods (Flotemersch et al. 1997). This behaviour combined with their frugivory and nondestructive ingestion of seeds suggests that channel catfish could act as seed dispersers by defecating viable seeds in habitats that are suitable for germination after flooding subsides. Future research needs to expand on this work to examine catfish diet across a broader spatial area, sampling throughout the entire duration of the flood pulse, and repeating this effort across multiple years. Similarly, studies are needed to determine to what extent fruiting of riparian plants in temperate river–floodplain systems coincides with seasonal flood pulses and to examine the likelihood of plants benefiting from seed dispersal and improved germination success associated with frugivory by fishes. The variation in consumption of swamp privets between years suggests that annual variation in the timing and duration of flooding will be critical to these interactions. Finally, because access to the floodplain has been dramatically altered in most temperate river–floodplain systems, it will be vital to examine these interactions in areas with varying access to floodplain habitats to determine the extent to which anthropogenic habitat alterations may have limited frugivory and seed dispersal by fishes.

Acknowledgements

We thank the Illinois Natural History Survey for supporting this study. Patty Brown, Eric Ratcliff, Eric Gittinger, Ben Lubinski, Jim Lamer, and Schuyler Sampson assisted with field and laboratory work. We thank Rob Maher (IDNR) for alerting us to channel catfish consuming mulberries in the Mississippi River. Rip Sparks, Mathew Leibold, Amy Downing, Pamela Geddes, and two anonymous reviewers provided valuable comments on an earlier version of this manuscript. This is publication number 3 of the National Great Rivers Research and Education Center.

References

Araujo-Lima, C., and Goulding, M. 1997. So fruitful a fish: ecology, conservation, and aquaculture of the Amazon's Tambaqui. Columbia University Press, New York.

Corlett, R.T. 1998. Frugivory and seed dispersal by vertebrates in the Oriental (Indomalayan) Region. Biol. Rev. **73**: 413–448.

Flotemersch, J.E., Jackson, D.C., and Jackson, J.R. 1997. Channel catfish movements in relation to river channel–floodplain connections. Proc. Annu. Conf. Southeast. Assoc. Fish Wildl. Agencies, **51**: 106–112.

Galat, D.L., and Lipkin, R. 2000. Restoring ecological integrity of great rivers: historical hydrographs aid in defining reference conditions for the Missouri River. Hydrobiologia, **422/423**: 29–48.

Gottsberger, G. 1978. Seed dispersal by fish in the inundated regions of Humaita, Amazonia. Biotropica, **10**: 170–183.

Goulding, M. 1980. The fishes and the forest: explorations in Amazonian life history. University of California Press, Berkely, Calif.

Horn, M.H. 1997. Evidence for dispersal of fig seeds by the fruit-eating characid fish *Brycon guatemalensis* Regan in a Costa Rican tropical rain forest. Oecologia, **109**: 259–264.

Kubitzki, K., and Ziburski, A. 1994. Seed dispersal in flood plain forests of Amazonia. Biotropica, **26**: 30–43.

Sparks, R.E. 1995. Need for ecosystem management of large rivers and their floodplains. BioScience, **45**: 168–182.

Sparks, R.E., Nelson, J.C., and Yin, Y. 1998. Naturalization of the flood regime in regulated rivers. BioScience, **48**: 706–720.

Welcomme, R.L. 1985. River fisheries. FAO Fish. Tech. Pap. No. 262. United Nations, Rome.

Young, J.A., and Young, G.C. 1992. Seeds of woody plants. Dioscorides Press, Portland, Oreg.

© 2003 NRC Canada

Spread of hybridization between native westslope cutthroat trout, *Oncorhynchus clarki lewisi*, and nonnative rainbow trout, *Oncorhynchus mykiss*

Nathaniel P. Hitt, Christopher A. Frissell, Clint C. Muhlfeld, and Fred W. Allendorf

Abstract: We examined spatial and temporal patterns of hybridization between native westslope cutthroat trout, *Oncorhynchus clarki lewisi*, and nonnative rainbow trout, *O. mykiss*, in streams of the Flathead River system in Montana, U.S.A. We detected hybridization in 24 of 42 sites sampled from 1998 to 2001. We found new *Oncorhynchus mykiss* introgression in seven of 11 sample populations that were determined to be nonhybridized in 1984. Patterns of spatial autocorrelation and linkage disequilibrium indicated that hybridization is spreading among sites and is advancing primarily via post-F_1 hybrids. Although hybridized populations were distributed widely throughout the study area, the genetic contribution from *O. mykiss* decreased with increasing upstream distance from the Flathead River mainstem, suggesting that *O. mykiss* introgression is spreading in an upstream direction. The spread of hybridization may be constrained more by demographic than by environmental factors, given that (*i*) hybridized populations generally encompassed the range of environmental variability in nonhybridized populations, and (*ii*) hybridization status was more strongly associated with neighborhood statistics than measured environmental gradients.

Résumé : Nous avons examiné les patterns spatiaux et temporels de l'hybridation de la truite fardée indigène du versant occidental, *Oncorhynchus clarki lewisi*, avec la truite arc-en-ciel non indigène, *Oncorhynchus mykiss*, dans des cours d'eau du système hydrographique de la Flathead au Montana, États-Unis. Il y avait de l'hybridation dans 24 des 42 sites examinés de 1998 à 2001. De nouvelles introgressions d'*O. mykiss* ont été trouvées dans sept de 11 populations qui ne montraient aucun signe d'hybridation en 1984. Les patterns d'autocorrélation spatiale et de déséquilibre d'association indiquent que l'hybridation se répand d'un site à l'autre, surtout par l'intermédiaire des hybrides post-F_1. Bien que les populations hybrides soient largement réparties dans la zone d'étude, la contribution génétique d'*O. mykiss* décroît en fonction de la distance en amont depuis le cours principal de la Flathead, ce qui laisse croire que l'introgression d'*O. mykiss* se répand vers l'amont. La propagation de l'hybridation semble être davantage contrôlée par des facteurs démographiques qu'environnementaux, puisque (*i*) les populations hybrides subissent la même gamme de variations des conditions de l'environnement que les populations pures et (*ii*) le statut de l'hybridation est plus fortement associé aux mesures de proximité qu'aux gradients environnementaux étudiés.

[Traduit par la Rédaction]

Introduction

Introductions of nonnative fishes often result in unintended consequences for freshwater biota and ecosystems (Moyle et al. 1986). One such consequence is hybridization among native and nonnative fishes and the potential loss of locally adapted gene complexes in native populations (Allendorf et al. 2001). Conservation of native fishes will require an understanding of the genetic and ecological mechanisms that permit and constrain hybridization with nonnative taxa.

Hybridization is perhaps the primary threat facing westslope cutthroat trout, *Oncorhynchus clarki lewisi* (Allendorf and Leary 1988). Nevertheless, the distribution of hybridized populations and the limits to their expansion remain poorly understood. In this study, we examined spatial and temporal patterns of hybridization between *O. c. lewisi* and nonnative rainbow trout, *Oncorhynchus mykiss*, within a reported stronghold for the native cutthroat trout, the Flathead River system, Montana, U.S.A.

The native range of *O. c. lewisi* encompasses the headwaters of the Columbia, Missouri, Milk, Fraser, and Saskatchewan rivers in western North America (Behnke 1992). Native, disjunct populations extend from southern British Columbia to the John Day River in Oregon (Behnke 1992).

Received 23 January 2003. Accepted 31 August 2003. Published on the NRC Research Press Web site at http://cjfas.nrc.ca on 15 December 2003.
J17302

N.P. Hitt[1,2] **and F.W. Allendorf.** Division of Biological Sciences, University of Montana, Missoula, MT 59812, U.S.A.
C.A. Frissell. Pacific Rivers Council, Polson, MT 59860, U.S.A.
C.C. Muhlfeld. Montana Fish, Wildlife and Parks, Kalispell, MT 59901, U.S.A.

[1]Corresponding author (e-mail: than@vt.edu).

[2]Present address: Department of Fisheries and Wildlife Sciences, Virginia Polytechnic Institute and State University, Blacksburg, VA 24061, U.S.A.

 doi: 10.1139/F03-125 © 2003 NRC Canada

The *O. mykiss* populations of concern in this study originate from hatchery stocks containing a mixture of coastal rainbow trout (*Oncorhynchus mykiss irideus*) and inland redband rainbow trout (*Oncorhynchus mykiss gairdneri*), although the coastal subspecies is believed to have made up most of the broodstock (Needham and Behnke 1962). The native range of coastal *O. mykiss* encompasses a north–south band along the Pacific Ocean from northern Baja California to central Alaska and eastern Asia. Inland *O. mykiss* inhabit sections of the interior Columbia and Fraser River basins as their native range (Behnke 1992).

Both *O. c. lewisi* and *O. mykiss* spawn during the spring. Females excavate gravel redds and deposit eggs, and males fertilize eggs immediately after deposition (Behnke 1992). Naturally sympatric populations of *O. mykiss* and *O. c. lewisi* exhibit substantial reproductive segregation (e.g., coastal cutthroat trout, *Oncorhynchus clarki clarki*; Campton and Utter 1985). In contrast, introductions of *O. mykiss* into *O. c. lewisi* waters often result in genetically admixed populations (i.e., hybrid swarms; Allendorf et al. 2001).

Experimental *O. mykiss* × *O. c. lewisi* hybrids have shown evidence of developmental instability (i.e., increased bilateral asymmetry) and decreased growth and survival rates (Leary et al. 1985), but fitness characteristics of *O. mykiss* × *O. c. lewisi* hybrids have not been assessed within natural settings. *Oncorhynchus mykiss* introgression is expected to decrease fitness in native *O. c. lewisi* populations as the result of genetic homogenization and disruption of locally adapted gene complexes (Allendorf et al. 2001). However, these effects may only become evident after extreme environmental conditions, which do not occur every year but nevertheless pose selective pressures on local populations (e.g., 100-year floods).

The distribution and abundance of *O. c. lewisi* have declined as a result of introductions of nonnative salmonids (i.e., hybridization, competition, predation), habitat degradation and fragmentation, and angler exploitation (Liknes and Graham 1988; Behnke 1992). The Flathead River system in northwest Montana is recognized as a regional stronghold for *O. c. lewisi* throughout their historic range (Liknes and Graham 1988). Although *O. mykiss* introgression is prevalent in the Flathead River mainstem upstream of Flathead Lake (Deleray et al. 1999), the potential upstream expansion of *O. mykiss* introgression has not been previously assessed.

Our objectives were (*i*) to map the distribution of *O. mykiss* × *O. c. lewisi* hybridization in the study area, (*ii*) to assess spatial and temporal patterns of hybridization, and (*iii*) to evaluate the relative importance of environmental and spatial factors for further *O. mykiss* introgression into *O. c. lewisi* populations.

Materials and methods

Study area

The Flathead River system encompasses 7730 km^2 in northwest Montana and 1580 km^2 in southwest British Columbia. Our study area extended from the Flathead River mainstem (above Flathead Lake) approximately 100 km upstream within North Fork and Middle Fork of Flathead River (Fig. 1*a*). Within this area, we surveyed first-, second-, and third-order streams (as defined by Strahler 1957) within Glacier National Park and the Flathead National Forest (Fig. 1*b*).

Stocking records indicated that over 20 million *O. mykiss* individuals were released into the Flathead River system beginning in the late 1800s and ending in 1969 (M. Deleray, Montana Fish, Wildlife and Parks, 490 North Meridian Road, Kalispell, MT 59901, unpublished data). The vast majority of these introductions targeted the lower elevation areas within the basin (Flathead Lake and the Flathead River mainstem), whereas few headwater streams received *O. mykiss*. However, the complete stocking history is unknown because stocking records in Montana are poor before 1952 and virtually nonexistent before 1931, even though hatcheries were active at this time (J. Huston, 18 Yellowstone Street, Kalispell, MT 59901, personal communication). Stocking data from British Columbia showed no records of *O. mykiss* introductions into North Fork of Flathead River.

Anglers first suspected *O. mykiss* × *O. c. lewisi* hybridization in the Flathead River mainstem during the mid-1950s. The state of Montana discontinued stocking *O. mykiss* in 1969. However, self-sustaining *O. mykiss* and *O. mykiss* × *O. c. lewisi* populations have recently been documented in the mainstem of Flathead River (Deleray et al. 1999). The most recent genetic survey of the North Fork basin detected *O. mykiss* × *O. c. lewisi* hybridization in just two of 15 stream sites (Huston 1988). Because nonnative Yellowstone cutthroat trout, *Oncorhynchus clarki bouvieri*, have hybridized with *O. c. lewisi* in some Glacier National Park lakes (Marnell et al. 1987), we included this taxon in our genetic surveys.

Hybridization assessment

The genetic status of fish populations was assessed at 42 sites from 1998 through 2001 (Fig. 1*b*; Table 1). Sites within North Fork tributaries (n = 30) generally encompassed within- and among-stream gradients, whereas sites within Middle Fork tributaries (n = 9) encompassed only an among-stream gradient. In 41 of 42 sites, single-pass electrofishing was conducted to capture *Oncorhynchus* sp. individuals within sample reaches (>300 m). Site 42 (Whitefish River) was sampled by electrofishing from a drift boat. Captured fish were anesthetized and a small portion of the anal fin was excised and stored in 95% ethanol for laboratory analyses. We refer to the set of individuals from each site as sample "populations".

Paired interspersed nuclear element polymerase chain reaction (PINE PCR) techniques were used to assess the hybridization status of each sample population (Spruell et al. 2001; Kanda et al. 2002). We used combinations of primer pairs to evaluate specific regions ("fragments") of anonymous nuclear DNA for each taxon. We examined six nDNA fragments for *O. mykiss*, seven for *O. c. lewisi*, and nine for *O. c. bouvieri* (Table 2).

We first tested for suspected *O. c. lewisi* polymorphisms (i.e., mutations within *O. c. lewisi* producing fragments with the same electrophoretic properties as diagnostic *O. mykiss* fragments). Following Forbes and Allendorf (1991), sites with individuals showing nonnative fragments only at a single locus (i.e., one fragment size) were assumed to be *O. c. lewisi* polymorphisms. Alternatively, the presence of more

© 2003 NRC Canada

Fig. 1. (*a*) Study area location (solid circle). (*b*) Study site identification. Site codes correspond to Table 1. (*c*) Distribution of *Oncorhynchus mykiss* × *O. clarki lewisi* hybridization in the study area. Hybridized populations are indicated with solid circles; nonhybridized populations are indicated with open circles. (*d*) Relative percent genetic contributions of *O. mykiss* (pie chart, solid area) and *O. c. lewisi* (pie chart, open area) within hybridized sites. Site 38 includes *O. c. bouvieri* introgression in the solid area of the pie chart. Hatch-marked circles indicate sites with *O. mykiss* introgression but where percent calculations were inappropriate because of significant linkage disequilibrium.

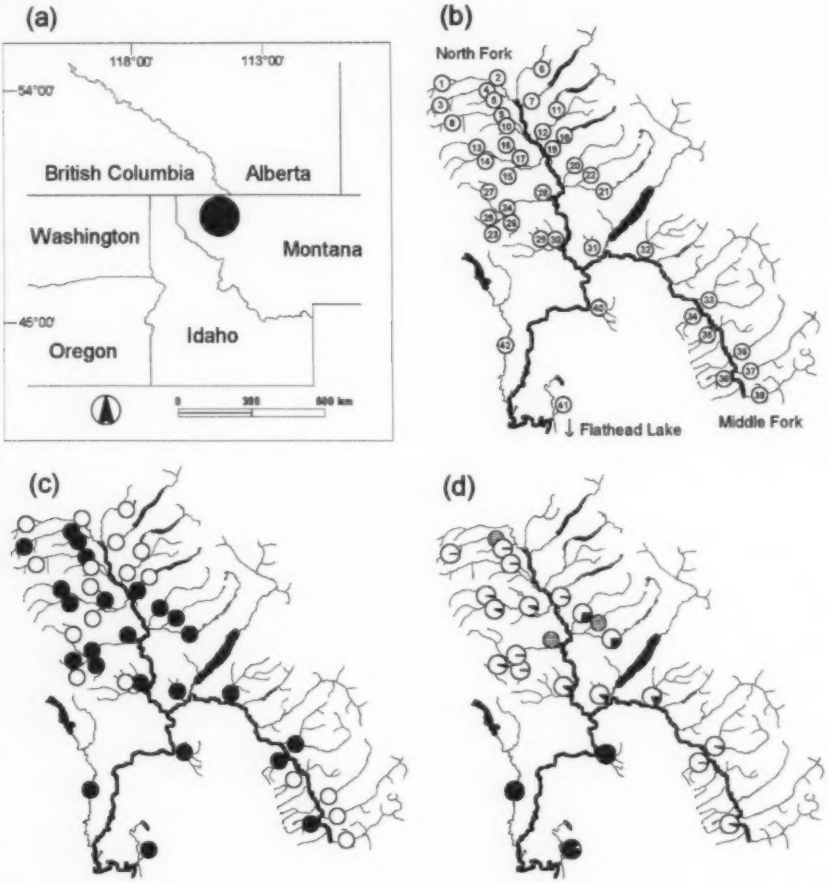

than one nonnative fragment in a sample population was assumed to indicate introgression.

Hybridized populations were evaluated for linkage disequilibrium (i.e., nonrandom association of alleles between loci) as a means to distinguish between hybrid swarms and populations with recent introgression of relatively pure *O. mykiss*. Because alleles are sorted independently during meiosis (i.e., Mendel's second law), the distribution of parental nDNA fragments will tend to equilibrate over many generations. However, recent introgression will maintain a nonrandom distribution of parental nDNA fragments. For instance, F_1 hybrids would be expected to yield strong linkage disequilibrium in a sample population.

We used Fisher's exact test (Uitenbroek 1997) to evaluate the distribution of *O. mykiss* fragments among all pairwise comparisons. Statistical significance was determined by testing against Bonferroni-corrected error rates based on the number of *O. mykiss* fragments evaluated. Sample populations showing significant linkage disequilibrium were included in binary analyses of introgression but were not used to estimate the percent genetic contribution of *O. mykiss* because of evidence against Hardy–Weinberg proportions. Although it may be possible to remove individual hybrid fish from a linkage disequilibrium population to reduce further introgression, this is not a feasible strategy for management of hybrid swarms (Allendorf et al. 2001).

For hybridized populations lacking significant linkage disequilibrium, the genetic contribution of *O. mykiss* (GC_r) was calculated as

$$(1) \qquad GC_r = \frac{\sum_{i=1}^{n}\left(1 - \sqrt{\frac{L_i}{N_i}}\right)}{n}$$

where the number of diagnostic *O. mykiss* fragments runs from 1 to n, L_i is the number of individuals lacking fragment i, and N_i is the total number of individuals genotyped for fragment i. Parallel calculations were conducted for the ge-

© 2003 NRC Canada

Table 1. Sample site information (site codes correspond to Fig. 1*b*).

Site code	Region	Site name	Sample size	Sample year(s)
1	North Fork	Moose Creek, upper	19	2000
2		Moose Creek, lower	25	2000
3		Red Meadow Creek, upper	25	2000
4		Red Meadow Creek, lower	25	1998, 2000
5		South Fork, Red Meadow Creek	20	2000
6		Akokala Creek	25	2000
7		Bowman Creek	25	2001
8		Hay Creek, upper	24	2000
9		Hay Creek, lower	24	2000
10		Moran Creek	21	2000
11		Quartz Creek, upper	24	2000
12		Quartz Creek, lower	20	2000
13		Coal Creek[a]	15	2000
14		South Fork, Coal Creek	10	2001
15		Deadhorse Creek	23	2001
16		Cyclone Creek, upper	24	2001
17		Cyclone Creek, lower	25	1998
18		Logging Creek, upper	16	2000
19		Logging Creek, lower	16	2000
20		Anaconda Creek	20	1998
21		Camas Creek	6	1998
22		Dutch Creek	23	1998
23		Big Creek, upper	25	2001
24		Big Creek, middle	12	1998, 2000
25		Nicola Creek	15	2000
26		Skookoleel Creek	20	2000, 2001
27		Kletomas Creek	25	2001
28		Langford Creek	20	1998
29		Depuy Creek	25	2001
30		McGinnis Creek	12	2000
31	Middle Fork	Rubideau Creek	12	2000
32		Lincoln Creek	22	1998
33		Coal Creek[a]	5	1998
34		Stanton Creek	15	2001
35		Tunnel Creek	25	2001
36		Park Creek	22	1998
37		Ole Creek	20	1998
38		Essex Creek	25	1998
39		Bear Creek	13	1998
40	Mainstem	Abbot Creek	18	1998
41		Mill Creek	15	1998
42		Whitefish River	15	2001

[a]North Fork Coal Creek and Middle Fork Coal Creek are different streams.

netic contribution of *O. c. bouvieri* (GC_y). The genetic contribution of *O. c. lewisi* (GC_w) was then calculated as the converse of the total nonnative fragment proportion. Percent genetic contributions were then calculated as $100(GC_x)$.

These estimations assumed that individuals at each site were sampled from the same population and that this population exhibited Hardy–Weinberg proportions. For sample populations classified as *O. c. lewisi*, we had at least a 95% chance for detecting as little as 2% nonnative trout introgression, assuming

$$(2) \qquad A^{2NX} = B$$

where A equals one minus the percent introgression to be detected, B equals one minus the percent chance to detect that level of introgression, N is the number of fish sampled, and X denotes the number of diagnostic nDNA fragments evaluated.

Spatiotemporal patterns of introgression

We assessed the spatial structure of *O. mykiss* introgression among North Fork sites (n = 30) and North Fork – Middle Fork sites (n = 39). For each region, we evaluated patterns of spatial autocorrelation in (*i*) coincident presence of introgression and (*ii*) percent introgression (for sites lacking significant linkage disequilibrium). Coincident introgression was coded in a binary site × site matrix where both sites hybridized was represented by 1 and other combinations were represented by 0. Euclidean dissimilarity matrices

© 2003 NRC Canada

Table 2. Paired interspersed nuclear element polymerase chain reaction (PINE PCR) nDNA fragments used to detect hybridization among *Oncorhynchus mykiss*, *O. clarki lewisi*, and *O. c. bouvieri* populations (Spruell et al. 2001; Kanda et al. 2002).

Taxon	PINE fragment number	No. of base pairs	Primer pair	Primer pair type
O. mykiss	1	70	HpaI 5′ / HpaI 3′	SINEs
	2	66	HpaI 5′ / HpaI 3′	SINEs
	3	369	FokI 5′ / Tc1	SINE and transposon
	4	230	FokI 5′ / Tc1	SINE and transposon
	5	395	HpaI 5′ / 33.6+2	SINE and Jeffreys' core fragment
	6	266	HpaI 5′ / 33.6+2	SINE and Jeffreys' core fragment
O. clarki lewisi	1	153	HpaI 5′ / HpaI 3′	SINEs
	2	72	HpaI 5′ / HpaI 3′	SINEs
	3	69	HpaI 5′ / HpaI 3′	SINEs
	4	366	FokI 5′ / Tc1	SINE and transposon
	5	110	FokI 5′ / Tc1	SINE and transposon
	6	388	HpaI 5′ / 33.6+2	SINE and Jeffreys' core fragment
	7	148	HpaI 5′ / 33.6+2	SINE and Jeffreys' core fragment
O. c. bouvieri	1	232	HpaI 5′ / HpaI 3′	SINEs
	2	72	HpaI 5′ / HpaI 3′	SINEs
	3	69	HpaI 5′ / HpaI 3′	SINEs
	4	366	FokI 5′ / Tc1	SINE and transposon
	5	159	FokI 5′ / Tc1	SINE and transposon
	6	138	FokI 5′ / Tc1	SINE and transposon
	7	388	HpaI 5′ / 33.6+2	SINE and Jeffreys' core fragment
	8	248	HpaI 5′ / 33.6+2	SINE and Jeffreys' core fragment
	9	148	HpaI 5′ / 33.6+2	SINE and Jeffreys' core fragment

Note: SINE, small interspersed nuclear elements.

were constructed from percent introgression data (SPSS version 10.0; SPSS Inc., Chicago, Ill.). We used Mantel tests (Mantel 1967) to assess associations between introgression and spatial location, considering both fluvial and straight-line distances between sites.

Correlograms were developed from simple Mantel test results (Legendre and Fortin 1989). The number of distance classes for correlograms was determined at each spatial scale in order to exceed 25 site × site comparisons within each distance category. Significance of correlations was assessed with a Bonferroni-corrected error rate, $\alpha' = 0.05/6$ (six distance classes) = 0.008. All simple Mantel tests were conducted with SMT version 1.2 (MS-DOS program by E. Bonnet, Department of Plant Systems Biology, Ghent University, KL Ledeganckstraat 35, B-9000 Ghent, Belgium).

Allozyme data from Huston (1988) were used to assess temporal changes in *O. mykiss* introgression for 13 sites within North Fork tributaries sampled in 1984. Although allozymes are codominant fragments and PINE PCR techniques utilize dominant nDNA fragments, these two types of analyses have shown concordance in hybrid detection at the population level (Spruell et al. 2001).

The spatial distribution of linkage disequilibrium also provided inferences on the spread of *O. mykiss* introgression. In this study, the presence of linkage disequilibrium indicated relatively recent introgression of relatively pure *O. mykiss* into *O. c. lewisi* populations. However, the absence of linkage disequilibrium in hybridized populations may be explained by either recent introgression of post-F_1 hybrid individuals or introgression of relatively pure *O. mykiss* several generations ago. In either case, hybridized sites that lack linkage disequilibrium are probably best classified as hybrid swarms (Allendorf et al. 2001).

Environmental regulation of introgression

We evaluated the hypothesis that environmental parameters restrict the spread of *O. mykiss* introgression in the study area. First, we posited that limiting factors would result in discrete environmental conditions from nonhybridized sites. Conversely, hybridized populations encompassing the range of environmental variability in nonhybridized populations would constitute evidence against environmental limiting factors. Secondly, we posited that if environmental factors restricted introgression, the association between hybridization status and environmental conditions would be stronger than for purely spatial (i.e., neighborhood) statistics.

Collection of environmental data was organized around three categories: water temperature regime, channel geomorphology, and watershed condition. These divisions represent coarse categories of environmental conditions that have been demonstrated to influence assemblage structure in stream fishes (Schlosser 1995; Poff 1997). We used principal components analysis (PCA) to reduce covariation and to permit standardized comparisons of environmental conditions relative to hybridization status. All principal components were derived from correlation matrices (SPSS version 10.0). The first two principal components explained >80% of the variance within each data category (Table 3).

Water temperature metrics included measures of magnitude and variability (Moyle and Light 1996), including max-

© 2003 NRC Canada

Table 3. Principal component analysis (PCA) loadings for environmental data.

Category	Variable	PCA I	PCA II
Thermal	Summer maximum	0.98	–0.01
	Summer range	0.83	0.51
	Average daily maximum	0.98	–0.18
	Average daily standard deviation	0.89	0.21
	Days >15 °C, %	–0.89	0.01
	Days <10 °C, %	0.84	–0.51
	Cumulative variance explained, %	81.76	91.65
Geomorphology	Stream gradient	0.68	0.73
	Upstream basin size	–0.81	0.24
	Elevation	0.79	–0.39
	Cumulative variance explained, %	58.19	82.69
Watershed condition	Upstream road density	0.92	–0.03
	Number upstream road crossings	0.73	0.65
	3 km radius road density	0.77	–0.58
	Cumulative variance explained, %	65.91	90.93

imum temperature, thermal range, mean daily maximum temperature, standard deviation of daily mean temperatures, percent mean temperature days <10 °C, and percent mean temperature days >15 °C. Thermographs were deployed at each site to record water temperatures at 2-h increments. The sampling period extended from 27 June to 20 September (85 days) between 1998 and 2001. Thermographs were calibrated to ±0.2 °C before and after use.

Channel geomorphology metrics were derived from U.S. Geological Survey 7.5 min maps and GIS (geographical information system) data. Site gradient and elevation were determined from contour intervals and stream order (Strahler 1957) was calculated from mapped perennial streams. Upstream basin size (i.e., flow volume covariate) and channel sinuosity (i.e., microhabitat availability covariate) were calculated using ArcView® Spatial Analyst (ESRI, Redlands, Calif.).

We used road density metrics as indicators of watershed condition. Forest roads affect the physical, biotic, and chemical conditions in downstream areas by altering geomorphic and hydrologic regimes (Trombulak and Frissell 2000), and road densities are strongly associated with land use pattern, in particular the spatial extent of timber harvest activity in the Flathead River system (Hauer and Blum 1991). We calculated upstream road densities, number of upstream road – stream intersections (Baxter et al. 1999), and road densities within a 3-km radius from each site. Road data were obtained from U.S. Forest Service's Flathead National Forest INFRA database and road densities were calculated with ArcView® Spatial Analyst. This database includes current and historic logging roads in the study area.

To compare sites relative to environmental factors, we conducted *t* tests on environmental PCA scores among hybridized and nonhybridized sample populations. To assess the relative importance of environmental data and neighborhood statistics, we used simple and partial Mantel tests (Mantel 1967) for North Fork sites (n = 27) and North Fork – Middle Fork sites (n = 36) that lacked significant linkage disequilibrium. Introgression was represented by the percent genetic contribution of *O. mykiss* (GC_r). Environmental data were represented by first principal component scores in each data category. To identify potential environmental correlations that are not influenced by fluvial connections, spatial position was represented by straight-line distances between sites. Additionally, the spatial structure of hybridization was represented by the percent *O. mykiss* introgression of the nearest neighboring site based on fluvial distances. Euclidean dissimilarity matrices were then derived for each data category (i.e., introgression, thermal, geomorphology, watershed condition, neighbors).

Mantel test significance was assessed at a Bonferroni-corrected error rate, $\alpha' = 0.05/25$ (25 possible comparisons) = 0.002. In the presence of significant spatial autocorrelation, partial Mantel tests were used to examine associations with the spatial component of the data set removed (sensu Wilkinson and Edds 2001). Partial Mantel tests were conducted with PMT version 1.1 (MS-DOS program by E. Bonnet, Department of Plant Systems Biology, Ghent University, KL Ledeganckstraat 35, B-9000 Ghent, Belgium).

Results

Hybridization assessment

Of the 42 sample populations, 24 (57%) showed *O. mykiss* introgression (Fig. 1*c*; Table 4). Of the 18 nonhybridized populations, six showed "diagnostic" *O. mykiss* fragments that were assumed to be natural polymorphisms within nonhybridized *O. c. lewisi*. For these populations, additional sampling of individuals or loci would be required to distinguish between introgression and true *O. c. lewisi* polymorphisms. Of the 24 hybridized populations, three showed statistically significant patterns of linkage disequilibrium. *Oncorhynchus c. bouvieri* introgression was detected only at the Essex Creek site (38), which also contained *O. mykiss* introgression (Table 4).

Within the 21 hybridized populations lacking significant linkage disequilibrium, GC_r (percent genetic contribution of *O. mykiss*) ranged from 0.9% to 98.2% (Table 4). Most hybridized populations (14/21) contained less than 10% genetic contribution from *O. mykiss*. All populations that exhibited greater than 10% *O. mykiss* introgression in the North Fork and Middle Fork tributaries were located within

© 2003 NRC Canada

Table 4. Percent genetic contributions of rainbow trout, *Oncorhynchus mykiss* (GC_r), westslope cutthroat trout, *O. clarki lewisi* (GC_w), and Yellowstone cutthroat trout, *O. c. bouvieri* (GC_y), detected in the study area.

Site code	Site name	GC_r	GC_w	GC_y
3	Red Meadow Creek, upper	1.4	98.6	0
4	Red Meadow Creek, lower	*	*	0
5	South Fork, Red Meadow Creek	0.9	99.1	0
9	Hay Creek, lower	1.1	98.9	0
13	Coal Creek (I)	3.6	96.4	0
14	South Fork, Coal Creek	6.1	93.9	0
17	Cyclone Creek, lower	7.4	92.6	0
19	Logging Creek, lower	2.1	97.9	0
20	Anaconda Creek	27.4	72.6	0
21	Camas Creek	24.5	75.5	0
22	Dutch Creek	*	*	0
24	Big Creek, middle	1.4	98.6	0
25	Nicola Creek	4.0	96.0	0
26	Skookoleel Creek	1.7	98.3	0
28	Langford Creek	*	*	0
30	McGinnis Creek	9.8	90.2	0
31	Rubideau Creek	11.1	88.9	0
32	Lincoln Creek	18.5	81.5	0
33	Coal Creek (II)	5.3	94.7	0
34	Stanton Creek	2.3	97.7	0
38	Essex Creek	1.4	95.2	3.5
40	Abbot Creek	97.5	2.5	0
41	Mill Creek	89.4	10.6	0
42	Whitefish River	98.2	1.8	0

Note: Asterisk (*) indicates hybridized site that showed statistically significant patterns of linkage disequilibrium.

25 km above the confluence of the North and Middle forks. Mainstem tributary sites (sites 40, 41, and 42) showed GC_r values in excess of 89% (Table 4).

Spatiotemporal patterns of introgression

Binary measures of *O. mykiss* introgression showed significant positive spatial autocorrelation with the closest fluvial distance category for North Fork sites (Mantel $r = 0.14$, $P < 0.005$; Fig 2*a*). Fluvial distances greater than 38 km showed negative spatial autocorrelation with introgression in the North Fork, but this trend was not statistically significant. Straight-line distances showed no patterns of spatial autocorrelation with introgression among North Fork sites (Fig. 2*b*). When North Fork and Middle Fork sites were aggregated ($n = 39$), significant spatial autocorrelation was not observed for either fluvial or straight-line distances.

Within the North Fork basin, more nonhybridized populations were sampled from tributaries entering the mainstem above 30 km upstream from the Middle Fork confluence than below (11 and three sites, respectively). In contrast, hybridized populations were equally distributed between these areas (eight sites each). All Middle Fork sample populations contained introgression within 40 km upstream from the North Fork confluence, above which four of five sites were nonhybridized *O. c. lewisi*.

The magnitude of *O. mykiss* introgression generally decreased with increasing upstream distance from Flathead Lake (Fig. 3). North Fork and Middle Fork sites showed similar distance effects with mainstem sites and excluding mainstem sites (analysis of covariance interaction terms, $P > 0.45$). Although the mainstem sites (sites 40, 41, and 42) were influential points, their absence did not change the general pattern of decreasing *O. mykiss* introgression with increasing distance from Flathead Lake in either the North Fork or Middle Fork sites (Fig. 3).

Oncorhynchus mykiss introgression has spread within the study area since the mid-1980s. We detected new *O. mykiss* introgression in seven of 11 sites determined to be nonhybridized *O. c. lewisi* in 1984 (Huston 1988) (Table 5). In contrast, we detected nonhybridized *O. c. lewisi* in upper

Fig. 2. Mantel correlograms for *Oncorhynchus mykiss* introgression in North Fork of the Flathead River system ($n = 30$). Spatial matrices were derived from (*a*) fluvial distances and (*b*) straight-line distances among sites. The star indicates a significant correlation, using a Bonferroni-corrected error rate, $\alpha' = 0.05/6$ (six distance classes) = 0.008.

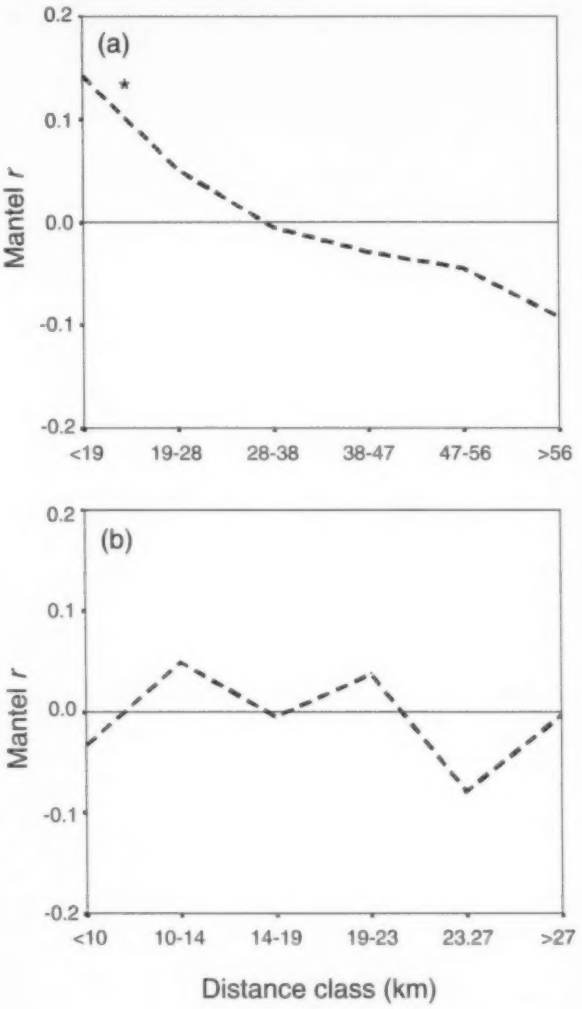

© 2003 NRC Canada

Fig. 3. Relationship between the percent genetic contribution of *Oncorhynchus mykiss* (GC_r) and upstream distance from Flathead Lake for (*a*) all hybridized populations and (*b*) hybridized populations within North Fork and Middle Fork, which lacked statistically significant linkage disequilibrium. Circles indicate North Fork sites (n = 14). Triangles indicate Middle Fork sites (n = 5); and triangles within circles indicate mainstem sites (n = 3). Upstream distance patterns within Middle Fork (solid line) and North Fork (broken line) sites were not significantly different at either spatial scale (analysis of covariance interaction terms, P > 0.45).

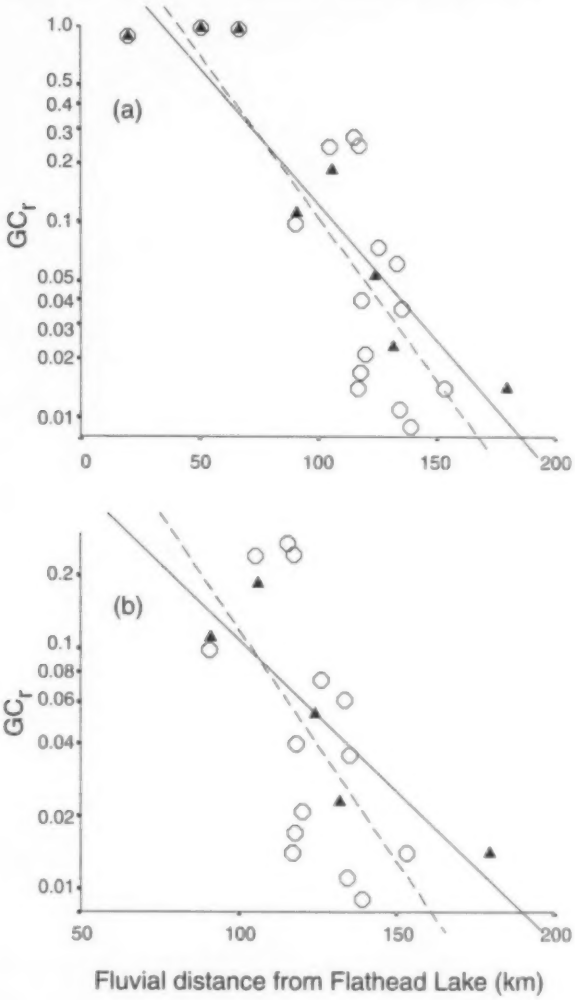

Moose Creek (site 1) where Huston (1988) reported low levels of *O. mykiss* introgression. Langford Creek (site 28) showed introgression in both surveys, but we did not calculate percent introgression for this population because of the presence of linkage disequilibrium.

Environmental regulation of introgression

Hybridized populations largely encompassed the range of environmental variability found in nonhybridized *O. c. lewisi* populations (Fig. 4). Mean thermal and geomorphological PCA scores were not statistically different among hybridized and nonhybridized sites (t test, P > 0.50 for all comparisons). However, sites with the highest elevations, steepest slopes, and smallest upstream basin sizes tended to support

Fig. 4. Environmental variability among hybridized (solid circle) and nonhybridized (open circle) populations for (*a*) thermal, (*b*) geomorphological, and (*c*) watershed condition principal component analysis (PCA) scores. PCA loadings are given in Table 3.

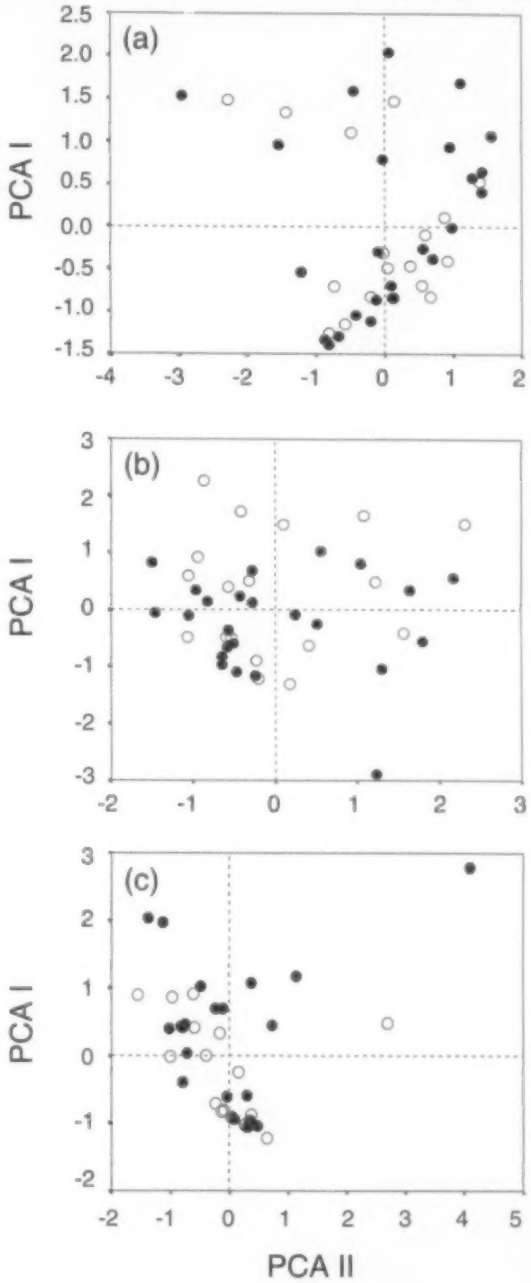

© 2003 NRC Canada

Table 5. Temporal change of *Oncorhynchus mykiss* × *O. clarki lewisi* hybridization in North Fork of the Flathead River system, Montana, U.S.A.

Site code	Site name	*N* (1988)	GC_T (1988)	GC_T (current study)
1	Moose Creek, upper	27	1.5	0
2	Moose Creek, lower	25	0	0
4	Red Meadow Creek, lower	22	0	Introgression present
5	South Fork, Red Meadow Creek	24	0	0.9
9	Hay Creek, lower	27	0	1.1
10	Moran Creek	29	0	0
13	Coal Creek	26	0	3.6
14	South Fork, Coal Creek	25	0	6.1
17	Cyclone Creek	23	0	7.4
25	Nicola Creek	25	0	4.0
27	Kletomas Creek	25	0	0
28	Langford Creek	15	2.0	Introgression present
29	Depuy Creek	27	0	0

Note: Allozyme data were reported by Huston (1988). Percent genetic contribution of *O. mykiss* (GC_T) was not calculated for sites 4 and 28 because of linkage disequilibrium in the sample population.

Table 6. Mantel correlations between percent *Oncorhynchus mykiss* introgression (1), environmental factors (2–4), the introgression status of nearest neighboring sites (5), and straight-line distances among sites.

		1	2	3	4	5
		Introgression	Thermal	Geomorphology	Watershed condition	Neighbors
North Fork (n = 27)	Distance	0.194	0.137	0.222	0.338*	0.192
	1	—	0.199	–0.040	0.107	0.860*
	2		—	0.409*	0.336*	0.151
	3			—	0.109	0.004
	4		0.308*		—	0.030
North Fork – Middle Fork (n = 36)	Distance	–0.089	–0.044	0.047	0.011	–0.101
	1	—	0.108	–0.080	0.033	0.819*
	2		—	0.118	0.155	0.064
	3			—	0.115	–0.066
	4				—	–0.040

Note: Statistical significance was assessed using a Bonferroni-corrected error rate, $\alpha' = 0.05/25$ (25 possible comparisons for each site group) = 0.002. Probability is based on 10 000 permutations; *, $P < 0.002$. Upper diagonals show simple Mantel correlations; lower diagonals show partial Mantel correlations with the distance effect removed.

nonhybridized *O. c. lewisi* populations. This potential transition corresponds to an approximate elevation of 1450 m. Watershed condition data showed a stronger separation of hybridized and nonhybridized sites ($t = 1.73$, $P < 0.10$) such that sites with the highest road densities tended to support introgression.

The presence of introgression was more strongly correlated with the introgression status of neighboring sites than with any of the environmental variables (Table 6). Within North Fork sites (n = 27) and North Fork – Middle Fork sites (n = 36), neighbors data were significantly correlated to *O. mykiss* introgression (Mantel, $r = 0.86$, $P < 0.002$; Mantel, $r = 0.82$, $P < 0.002$, respectively), whereas environmental data were not. Significant spatial autocorrelation was detected only for watershed condition data in North Fork sites (Mantel, $r = 0.34$, $P < 0.002$).

Mantel tests also revealed significant associations among environmental categories. In North Fork sites, water temperature data were significantly correlated with geomorphology (Mantel, $r = 0.41$, $P < 0.002$) and watershed condition (Mantel, $r = 0.34$, $P < 0.002$). The correlation between watershed condition and thermal data was not an artifact of spatial autocorrelation, given the persistence of significant results in partial Mantel tests, which controlled for autocorrelation in the analysis (Table 6). Specifically, increased road density was associated with increased magnitude and variability of summer water temperatures.

Discussion

Introgressive hybridization presents a special case for invasion biology. Although all invasive taxa are subject to environmental constraints during establishment and expansion, hybridization presents the additional requirement of genetic compatibility. However, if this genetic criterion is satisfied, the invasive genome may benefit by its integration into the locally adapted native species. In this study, the initial establishment of *O. mykiss* may be limited by the suitability of the hydrologic regime (Fausch et al. 2001), but *O. mykiss* introgression may not be subject to such restrictions once source populations are established.

© 2003 NRC Canada

Our findings indicate that (*i*) *O. mykiss* introgression is spreading rapidly in the study area; (*ii*) native *O. c. lewisi* populations are declining rapidly in the study area; (*iii*) hybridization is spreading among sites and in an upstream direction from the Flathead River mainstem; and (*iv*) environmental factors should not be expected to prevent the additional spread of hybridization in the study area.

In comparisons against 1984 data, we found new *O. mykiss* introgression at seven sites and the apparent disappearance of introgression in one site (Moose Creek). Huston (1988) attributed the *O. mykiss* introgression in Moose Creek to accidental introductions of hybridized broodstock in the headwater lake above this creek. The apparent disappearance of hybridization in this area may be explained by natural selection against hybrid individuals, emigration of hybridized fish from the area, or sampling error. Nonetheless, our primary finding is that hybridization has spread dramatically over approximately five cutthroat generations.

Our results suggest that that the spread of *O. mykiss* introgression will not be prevented by the observed ecological gradients. We found that hybridized populations generally encompass the range of environmental variability in nonhybridized populations and that introgression shows stronger associations with neighborhood statistics than measured environmental gradients. These findings are consistent with the hypothesis that *O. mykiss* introgression is constrained more by straying rates than by measured environmental factors.

Although we found some weak evidence for geomorphological limiting factors corresponding to an elevation of 1450 m, it is unlikely that this gradient will prevent additional introgression in the study area. Over 95% of the stream segments above this elevation are less than 8 km in length, a distance unlikely to support isolated populations of cutthroat trout (Hilderbrand and Kershner 2000). However, it remains possible that environmental factors outside of this study area might pose ecological restrictions to *O. mykiss* introgression.

Spatial patterns of linkage disequilibrium and percent *O. mykiss* introgression are consistent with a stepping-stone model of genetic invasion. Under this model, F_1 hybrids (and perhaps parental *O. mykiss*) breed into lower-elevation *O. c. lewisi* subpopulations, which subsequently produce post-F_1 hybrids that then disperse and pioneer headwater streams. This model is supported by our observations that sites closer to the Flathead River mainstem tended to support more extensive hybridization than sites further upstream. Specifically, *O. mykiss* introgression in the Camas, Anaconda, and Dutch creeks in the southwest portion of Glacier National Park may have led to the subsequent upstream expansion of hybridization. Future research should assess straying rates of hybridized populations within this area of Glacier National Park.

Theoretical models of invasive species spread have highlighted the importance of rare long-distance dispersal events (Kot et al. 1996; Neubert and Caswell 2000; Clark et al. 2001). The presence of significant linkage disequilibrium in lower Red Meadow Creek (site 4) suggests that long-distance dispersal may also advance the spread of *O. mykiss* introgression in the study area. Alternatively, our observations could also be explained by unreported *O. mykiss* stocking in Red Meadow Creek.

Our findings are concordant with a recent study of hybrid trout movements in the Flathead River system. In 2002, radiotelemetry surveys documented upstream spawning migrations by *O. mykiss* × *O. c. lewisi* hybrids from the Flathead River mainstem to Dutch Creek (near site 22), Hay Creek (near site 9), and Lincoln Creek (near site 33) (C. Muhlfeld, Montana Fish, Wildlife and Parks, 490 North Meridian Road, Kalispell, MT 59901, unpublished data). We detected hybridized populations in each of these streams.

Similar temporal and spatial patterns of *O. mykiss* × *O. c. lewisi* hybridization were reported by Rubidge et al. (2001) in tributaries of the upper Kootenay River of British Columbia. Temporal comparisons against allozyme data from 1987 showed new *O. mykiss* introgression in previously pure *O. c. lewisi* populations in four of seven sampled streams (Rubidge et al. 2001). In their analysis, upstream distance from Lake Koocanusa was negatively correlated with the proportion of hybridized individuals in each sample site, although this relationship was not statistically significant (Rubidge et al. 2001).

In contrast to our study, Weigel et al. (2003) found stronger evidence for ecological barriers to the spread of *O. mykiss* × *O. c. lewisi* hybridization in the Clearwater River system of Idaho, U.S.A. Although they detected widespread *O. mykiss* introgression in tributaries, hybridized populations were absent from some areas near known *O. mykiss* stocking locations. In addition, the degree of hybridization showed negative associations with site elevation and positive associations with stream width (Weigel et al. 2003). However, hybridized sites largely encompassed the range of environmental variability in their study, in concordance with our findings suggesting that there is no ultimate refuge from introgression unless discrete physical barriers to dispersal exist.

Spatial autocorrelation analyses in this study demonstrated the importance of fluvial measurements in assessing contagious processes in stream ecology. Although straight-line distances lacked significant Mantel correlations with hybridization status in North Fork, fluvial distances showed significant positive autocorrelation. As a result, Mantel correlations in stream ecology that rely exclusively on straight-line distances may underestimate spatial autocorrelation by overlooking processes driven by fluvial connections (e.g., cf. Magnan et al. 1994; Wilkinson and Edds 2001). This finding also suggests that straying rates can influence the spread of *O. mykiss* introgression. To the extent that homing has a genetic basis, straying to nonnatal populations could be facilitated by genomic disruption caused by hybridization, but this remains a subject for future research.

This study contributes new insight into the determination of *O. c. lewisi* status. Interpolating from our data to stream reaches delineated by Montana Fish, Wildlife and Parks, the spatial extent of *O. mykiss* × *O. c. lewisi* hybridization is more than triple that considered in the recent U.S. Fish and Wildlife Service Status Review for *O. c. lewisi* (Anonymous 1999) within the study area. Additionally, our results suggest that the Status Review's assumption that headwater streams "are relatively secure from colonization by non-native fishes..." (Anonymous 1999, p. 158) is inaccurate for ge-

© 2003 NRC Canada

netic introgression. Studies of invasion by nonnative brook trout *Salvelinus fontinalis* (Adams et al. 2000, 2002), which compete for space with native cutthroat trout, also contradict the assumption that headwater streams offer secure refuge. Although hybridized populations might ultimately play some role in restoration, nonhybridized *O. c. lewisi* populations with intact genetic heritage should be carefully distinguished when assessing the status of the native taxon.

Acknowledgements

Funding for this project was provided by the Bonneville Power Administration and Montana Fish, Wildlife, and Parks. We thank A. Sheldon, L. Broberg, M. Deleray, L. Knotek, B. Marotz, G. Michaels, J. Cavigli, T. Weaver, D. Daniels, W. Fredenberg, J. Huston, L. Marnell, S. Kem, S. Somerville, N. Kanda, and M.A. Hitt for their assistance in this project. We also thank B. Shepard, E. Taylor, and an anonymous reviewer for thorough and instructive reviews of this manuscript. Logistical support was provided by the University of Montana's Division of Biological Sciences, Flathead Lake Biological Station and Wild Trout and Salmon Genetics Laboratory.

References

Adams, S.A., Frissell, C.A., and Rieman, B.E. 2000. Movements of non-native brook trout in relation to stream channel slope. Trans. Am. Fish. Soc. **129**: 623–638.

Adams, S.B., Frissell, C.A., and Rieman, B.E. 2002. Changes in distribution of nonnative brook trout in an Idaho drainage over two decades. Trans. Am. Fish. Soc. **131**: 561–568.

Allendorf, F.W., and Leary, R.F. 1988. Conservation and distribution of genetic variation in a polytypic species, the cutthroat trout. Conserv. Biol. **2**: 170–184.

Allendorf, F.W., Leary, R.F., Spruell, P., and Wenburg, J.K. 2001. The problems with hybrids: setting conservation guidelines. Trends Ecol. Evol. **16**: 613–622.

Anonymous. 1999. Status review for westslope cutthroat trout in the United States. U.S. Fish and Wildlife Service, Regions 1 and 6, Portland, Oregon, and Denver, Colorado.

Baxter, C.V., Frissell, C.A., and Hauer, F.R. 1999. Geomorphology, logging roads, and the distribution of bull trout spawning in a forested river basin: implications for management and conservation. Trans. Am. Fish. Soc. **128**: 854–867.

Behnke, R.J. 1992. Native trout of western North America. American Fisheries Society, Bethesda, Md.

Campton, D.E., and Utter, F.M. 1985. Natural hybridization between steelhead trout (*Salmo gairdneri*) and coastal cutthroat trout (*Salmo clarki clarki*) in two Puget Sound streams. Can. J. Fish. Aquat. Sci. **42**: 110–119.

Clark, J.S., Lewis, M., and Horvath, L. 2001. Invasion by extremes: population spread with variation in dispersal and reproduction. Am. Nat. **157**: 537–554.

Deleray, M., Knotek, L., Rumsey, S., and Weaver, T. 1999. Flathead Lake and River system fisheries status report. Montana Department of Fish, Wildlife, and Parks, Kalispell, Mont.

Fausch, K.D., Taniguchi, Y., Nakano, S., Grossman, G.D., and Townsend, C.R. 2001. Flood disturbance regimes influence rainbow trout invasion success among five holarctic regions. Ecol. Appl. **11**: 1438–1455.

Forbes, S.H., and Allendorf, F.W. 1991. Associations between mitochondrial and nuclear genotypes in cutthroat trout hybrid swarms. Evolution, **45**: 1332–1349.

Hauer, F.R., and Blum, C.O. 1991. The effect of timber management on stream quality. Flathead Basin Commission, Flathead Basin Forest Practices, Water Quality and Fisheries Cooperative Program, Kalispell, Mont.

Hilderbrand, R.H., and Kershner, J.L. 2000. Conserving inland cutthroat trout in small streams: how much stream is enough? N. Am. J. Fish. Manag. **20**: 513–520.

Huston, J. 1988. Statewide Fisheries Investigations, Fisheries Division job progress report. Project F-46-R-1. Job No. I-a, II-a (partial). Montana Department of Fish, Wildlife and Parks, Kalispell, Mont.

Kanda, N., Leary, R.F., Spruell, P., and Allendorf, F.W. 2002. Molecular genetic markers identifying hybridization between the Colorado River – greenback cutthroat trout complex and Yellowstone cutthroat trout or rainbow trout. Trans. Am. Fish. Soc. **131**: 312–319.

Kot, M., Lewis, M.A., and van den Driessche, P. 1996. Dispersal data and the spread of invading organisms. Ecology, **77**: 2027–2042.

Leary, R.F., Allendorf, F.W., and Knudsen, K.L. 1985. Developmental instability and high meristic counts in interspecific hybrids of salmonid fishes. Evolution, **39**: 1318–1326.

Legendre, P., and Fortin, M.J. 1989. Spatial pattern and ecological analysis. Vegetatio, **80**: 107–138.

Liknes, G.A., and Graham, P.J. 1988. Westslope cutthroat trout in Montana: life history, status, and management. Am. Fish. Soc. Symp. **4**: 53–60.

Magnan, P., Rodriguez, M.A., Legendre, P., and Lacasse, S. 1994. Dietary variation in a freshwater fish species: relative contributions of biotic interactions, abiotic factors, and spatial structure. Can. J. Fish. Aquat. Sci. **51**: 2856–2865.

Mantel, N. 1967: The detection of disease clustering and a generalized regression approach. Cancer Res. **27**: 209–220.

Marnell, L.F., Behnke, R.J., and Allendorf, F.W. 1987. Genetic identification of cutthroat trout, *Salmo clarki*, in Glacier National Park, Montana. Can. J. Fish. Aquat. Sci. **44**: 1830–1839.

Moyle, P.B., and Light, T. 1996. Biological invasions of fresh water: empirical rules and assembly theory. Biol. Conserv. **78**: 146–161.

Moyle, P.B., Li, H.W., and Barton, B.A. 1986. The Frankenstein effect: impact of introduced fishes on native fishes in North America. *In* Fish culture in fisheries management. *Edited by* R.H. Stroud. American Fisheries Society, Bethesda, Md. pp. 415–426.

Needham, P.R., and Behnke, R.J. 1962. The origin of hatchery rainbow trout. Prog. Fish-Cult. **24**: 156–158.

Neubert, M.G., and Caswell, H. 2000. Demography and dispersal: calculation and sensitivity analysis of invasion speed for structured populations. Ecology, **81**: 1613–1628.

Poff, N.L. 1997. Landscape filters and species traits: towards mechanistic understanding and prediction in stream ecology. J. N. Am. Benthol. Soc. **16**: 391–409.

Rubidge, E., Corbett, P., and Taylor, E.B. 2001. A molecular analysis of hybridization between native westslope cutthroat trout and introduced rainbow trout in southeastern British Columbia, Canada. J. Fish Biol. **59**(Suppl. A): 42–54.

Schlosser, I.J. 1995. Critical landscape attributes that influence fish population dynamics in headwater streams. Hydrobiologia, **303**: 71–81.

Spruell, P., Bartron, M.L., Kanda, N., and Allendorf, F.W. 2001. Detection of hybrids between bull trout (*Salvelinus confluentus*) and brook trout (*S. fontinalis*) using PCR primers complementary to interspersed nuclear elements. Copeia, 2001: 1093–1099.

© 2003 NRC Canada

Strahler, A.N. 1957. Quantitative analysis of watershed geomorphology. Trans. Am. Geophys. Union, **38**: 913–920.

Trombulak, S., and Frissell, C.A. 2000. Review of the ecological effects of roads on terrestrial and aquatic communities. Conserv. Biol. **14**: 18–30.

Uitenbroek, D.G. 1997. Binomial. SISA (http://home.clara.net/sisa/binomial.htm).

Weigel, D.E., Peterson, J.T., and Spruell, P. 2003. Introgressive hybridization between native cutthroat and introduced rainbow trout. Ecol. Appl. **13**: 38–50.

Wilkinson, C.D., and Edds, D.R. 2001. Spatial pattern and environmental correlates of a midwestern stream fish community: including spatial autocorrelation as a factor in community analyses. Am. Midl. Nat. **146**: 271–289.

© 2003 NRC Canada

Determining long-term water quality change in the presence of climate variability: Lake Tahoe (U.S.A.)

Alan D. Jassby, John E. Reuter, and Charles R. Goldman

Abstract: We developed a time series model of Secchi depth for Lake Tahoe incorporating a mechanistic understanding of interannual variability with sufficient simplicity to allow data-based parameter estimation. Secchi depth is still occasionally over 40 m at Lake Tahoe, but mean annual Secchi depth has declined nearly 10 m since 1967, prompting a large-scale restoration program. Year-to-year variability is extremely high, obscuring restoration actions and compliance with water quality standards. The model focused on Secchi depth during summer, when the lake is least transparent and most heavily used. Interannual variability for the summer season is driven largely by precipitation differences. The model offers a means for determining compliance with water quality standards when precipitation anomalies may persist for years. As demonstrated by means of an ex-post forecast, increasing Secchi depths during 1999–2001 were simply climate-driven and do not represent a recovery of the lake. The long-term trend for summer is most likely due to the accumulation of allochthonous mineral suspensoids.

Résumé : Nous avons mis au point un modèle de série chronologique des profondeurs de Secchi pour le lac Tahoe, modèle basé sur une interprétation mécaniste de la variabilité inter-annuelle suffisamment simple pour permettre l'estimation de paramètres à partir des données. La profondeur mesurée au disque de Secchi au lac Tahoe dépasse encore à l'occasion 40 m, mais la profondeur de Secchi annuelle moyenne a diminué de presque 10 m depuis 1967, ce qui a mené à l'instauration d'un programme de récupération à grande échelle. La variabilité d'une année à l'autre est extrêmement élevée, ce qui masque les effets des actions de récupération et les conséquences du respect des normes de qualité de l'eau. Le modèle prend en considération surtout les profondeurs de Secchi durant l'été quand la transparence est minimale et l'utilisation du lac maximale. La variabilité d'une année à l'autre durant l'été s'explique en grande partie par des différences dans les précipitations. Le modèle fournit un moyen de vérifier le respect des normes de qualité de l'eau lorsque des anomalies dans les précipitations persistent pendant plusieurs années. Ainsi, une prédiction ex post facto démontre que l'accroissement des profondeurs de Secchi de 1999 à 2001 s'explique simplement par des facteurs climatiques et ne représente pas une récupération de la condition du lac. La tendance à long terme en été est sans doute explicable par une accumulation de matière minérale allochtone en suspension.

[Traduit par la Rédaction]

Introduction

Lake Tahoe is renowned for its water clarity, but the transparency decline over the past four decades has been a source of concern to residents of the Tahoe basin and millions of recreational visitors (Goldman 1988). In a visit to the lake during the nineteenth century, the author Mark Twain described it as "the fairest sight the whole earth affords". More recently, these waters have been losing their famed transparency, at least since systematic observation of Secchi depth began in 1967. Although occasional Secchi depths of over 40 m can still be observed during winter upwelling events, mean annual Secchi depth has declined at a rate of 0.27 m·year^{-1} for the past 34 years, a total loss of nearly 10 m.

Received 10 December 2002. Accepted 15 October 2003. Published on the NRC Research Press Web site at http://cjfas.nrc.ca on 15 December 2003.
J17232

A.D. Jassby,[1] J.E. Reuter, and C.R. Goldman. Department of Environmental Science and Policy, University of California, Davis, CA 95616, U.S.A.

[1]Corresponding author (e-mail: adjassby@ucdavis.edu).

A watershed approach to management has been taken at Lake Tahoe since the late 1970s based on the belief that successful implementation of land and air restoration projects is the only likely avenue to arrest further decline in lake clarity. In 1997, the Environmental Improvement Program (EIP) was formulated by the Tahoe Regional Planning Agency, a bistate (California and Nevada) regulatory and planning agency created by the U.S. Congress. The EIP is a regional document that presents restoration projects considered necessary to achieve environmental restoration in the Tahoe basin.

The success of this restoration program will ultimately be measured by changes in the long-term decline of water transparency. Although the effectiveness of individual mitigation projects may be high, ecosystem restoration depends on their cumulative ability to address the underlying imbalance between lake inputs and outputs, ultimately reflected in lake response. The ability to perceive a response to rehabilitation measures is therefore of fundamental importance. Given the potentially long time scales associated with ecosystem restoration and the large demand that these types of projects can have on financial and personnel resources, it is not surprising that trend detection has received much attention among ecologists and in related disciplines (Esterby 1996).

 doi: 10.1139/F03-127 © 2003 NRC Canada

A major obstacle to assessing long-term systemic change on the scale of years or decades in Lake Tahoe and many other systems is the presence of interannual variability, often due, at least in part, to climate but also including other processes such as intrinsic population dynamics. Resource scientists must have a reliable methodology for separating long-term change due to environmental management from interannual variability driven by other factors, such as natural wet–dry climate cycles. This is especially true for Lake Tahoe, where apparent recovery periods lasting several years occur despite the overall declining trend in clarity.

The background variability can often be reduced by incorporating one or more explanatory variables into a statistical model to account for this shorter-term variability. Flow rate, for example, is often used to account for short-term variability of stream water quality (Helsel and Hirsch 1992). The simplest method is to describe the contemporaneous relation between the response variable and some function of the explanatory variable(s) through a regression model. This method, however, makes implicit assumptions about the dynamics of the relation, e.g., no lagged effects of predictors, and violation of these assumptions can lead to false conclusions about anthropogenic trends. The analysis model must therefore respect the underlying mechanisms.

In this paper, our goal is to describe a procedure for extracting trends in systems with strong interannual variability, using Lake Tahoe water transparency as a specific example, as well as to test our understanding of year-to-year change in the lake's transparency. The method rests on prior identification of factors underlying year-to-year change and incorporation of their effects into a model that, while simple, addresses the essential mechanism. We use the model to examine whether observed Secchi depth increases in 1999–2001 reflected a fundamental change in lake transparency or only a response to short-term climate variability. We also examine the implications of the model for water clarity dynamics.

Materials and methods

Site description

Lake Tahoe lies in a subalpine graben, with its surface at an altitude of 1898 m when full. The lake surface area is approximately 501 m^2, and its watershed area is 812 m^2. Mean depth is 333 m and maximum depth is 499 m (Gardner et al. 2000). The low ratio of watershed to lake area and the great depth lead to a long hydraulic residence time of approximately 650 years. This warm monomictic lake is free of ice the entire year. Thermal stratification intensifies during February–April, achieves a maximum in August when the thermocline is located approximately 20 m below the surface, and then begins to weaken slowly again through midwinter. Conditions of near-isothermy occur for a few weeks during late winter or early spring, but complete mixing does not necessarily take place unless meteorological conditions are appropriate during that window of time (Goldman et al. 1989).

Monitoring data

Monitoring data used in this study include Secchi depth, precipitation, and chlorophyll *a*. Secchi depth measurements at the index station (Fig. 1) began in July 1967 and have been repeated every 12 days on average since that time. Measurements at the midlake station began in December 1969 and have been repeated every 30 days on average since that time. The two time series are similar at monthly and longer scales, and so the index time series is used because of its higher resolution and greater length. Secchi depth measurements were averaged by trapezoidal integration (i.e., by assuming that the Secchi depth time series is piecewise linear between sample times) for the period June–September. Precipitation data were obtained from the Tahoe City station (near the Truckee River outlet) of the National Weather Service. Data were summed for the water year (WY), which extends from the previous October through September. Almost all of this precipitation falls before June as rain and snow. Stream flow usually reaches a maximum during May–June in response to melting snow. Measurements of chlorophyll *a* corrected for phaeophytin began in November 1987. Sampling and methods are described by Jassby et al. (1999).

Modeling interannual variability

A preliminary consideration is the nature of the response variable. Secchi depth, S, can be described by

$$(1) \qquad S = \Gamma/(c + K)$$

where c is the beam attenuation coefficient for luminance, K is the attenuation coefficient for illuminance, and Γ is approximately constant (Preisendorfer 1986). Because K covaries with c, Secchi depth is highly correlated inversely with c, which in turn is dominated by total scattering of dissolved and suspended materials (Davies-Colley et al. 1993; Larson et al. 1996). The Secchi depth slope will therefore become less steep over time, even if dissolved and suspended materials are increasing at a constant rate. Inverse Secchi depth, on the other hand, is directly proportional to total scattering and concentration to the extent that the relative composition of scattering materials is unchanged. It is therefore most direct to use inverse Secchi depth as our response variable.

In particular, we use the inverse of average Secchi depth during the period June–September, denoted by $1/S_t$ for year t. This period is important because June is the month of lowest Secchi depth and the summer months are when the open waters of the lake are most heavily used and observed. Also, since about 1990, the trend in annual mean Secchi depth is due mostly to the decrease during June–September. A previous study demonstrated two independent modes of interannual variability for Secchi depth, a summer mode and a winter one (Jassby et al. 1999). The summer mode, which encompasses the June–September period of interest here, is driven by watershed inputs of mineral suspensoids and, to a minor extent, nutrients.

We specify the model by treating inverse Secchi depth as a surrogate for the total concentration of scattering materials and constructing a simple mass balance that incorporates our current understanding of interannual variability for the summer months. We also assume implicitly that phytoplankton and limiting nutrient concentration are interchangeable on an annual scale in this ultra-oligotrophic lake. Watershed inputs of mineral particles and nutrients are largely dependent on stream flow during the spring, which in turn reflects cumulative winter and spring precipitation. Atmospheric deposition — both wet

© 2003 NRC Canada

Fig. 1. Map of Tahoe basin on the border of California and Nevada, U.S.A., showing location of the two long-term sampling stations on the lake.

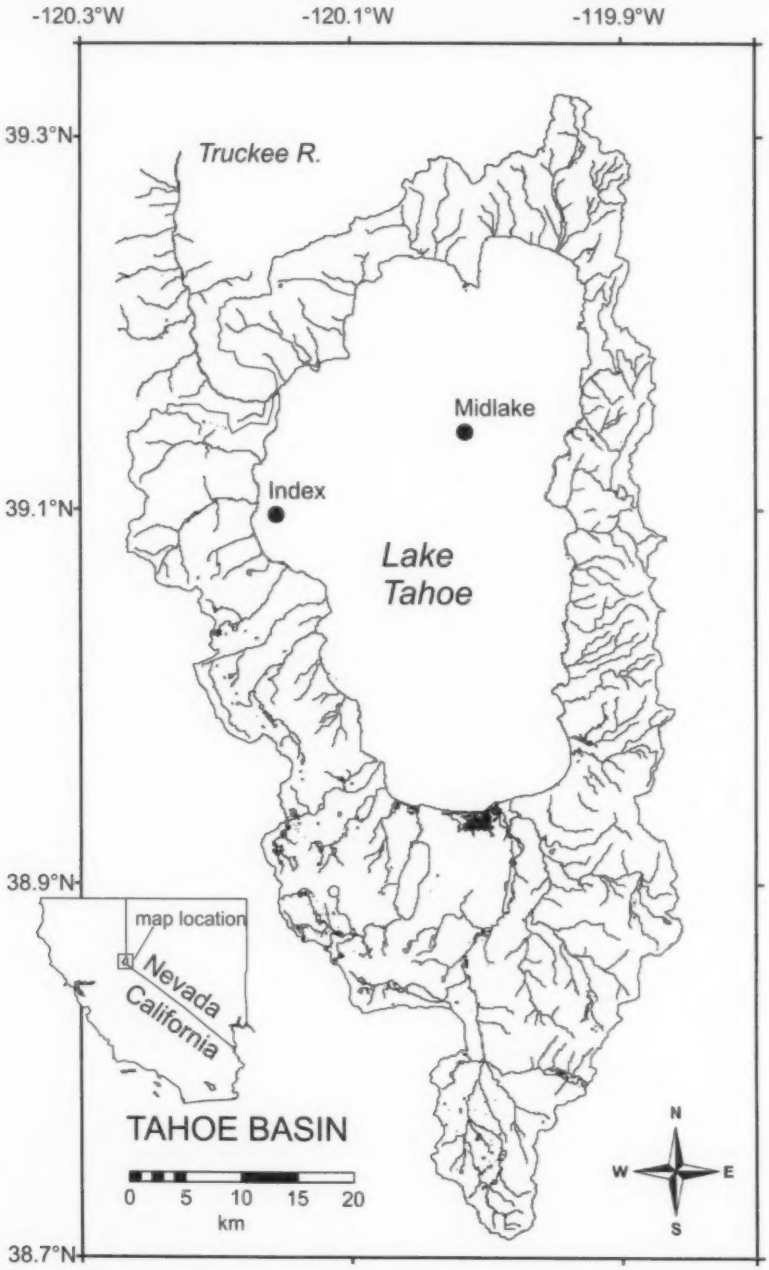

and dry — is also a major source of nutrients and, to a lesser extent, of mineral particles such as dust from vehicle traffic (Jassby et al. 1994). The simplest way to describe loading is by a constant to represent precipitation-independent sources (dry deposition) plus a term directly proportional to precipitation (wet deposition and runoff).

Because the lake has such a long hydraulic residence time (650 years), outflow is negligible and sedimentation represents the major known output for particles and nutrients (Jassby et al. 1995; Heyvaert 1998). Also, neither nitrogen fixation nor denitrification is thought to play a significant role in the nutrient balance of Tahoe's pelagic zone (Reuter et al. 1986), and bottom waters remain near oxygen saturation with consequent suppression of internal loading. The simplest way to formulate output under these circumstances is as a first-order loss process.

© 2003 NRC Canada

The annualized mass balance can therefore be expressed in difference-equation form (cf. Chapra 1997) as

$$(2) \qquad \nabla \frac{1}{S_t} = (c_1 + c_2 P_t) - c_3 \frac{1}{S_{t-1}}$$

where $\nabla x_t = x_t - x_{t-1}$ is the notation for the difference operator, P_t is water-year (October–September) precipitation, c_1 represents precipitation-independent sources, c_2 the proportionality constant for precipitation-dependent sources, and c_3 the fraction lost annually.

Modeling long-term change

Equation 2 quantifies the main mechanism underlying interannual variability for June–September, but it contains no information regarding a longer-term trend that is not simply a trend in precipitation. Loftis et al. (2001) describe how dummy or indicator variables can be used to determine a treatment effect using a covariance model to account for natural variability arising from precipitation or similar processes. Applying such a test to eq. 2 amounts to replacing each parameter c_i with $c_{i1} + c_{i2}I$, where I is an indicator variable set to 0 for the pretreatment period and 1 for the treatment period. One can conclude that a treatment effect is statistically significant if the confidence interval involving any subset of the c_{i2} parameters excludes 0.

For Lake Tahoe, the data are relatively extensive for an instrumental time series but still too short to support the estimate of three additional parameters. Instead, we test only for an overall additive change. Furthermore, we cannot assume a priori that the change is a step or, for that matter, a linear trend or any other particular form. If the specification for a predictor is incorrect, then the test of its significance will have diminished power. So, for example, testing for a step trend in long-term data may be misleading if the trend is some other shape. Instead, we first use a restricted cubic spline to model the trend (Gu 2002). A cubic spline is a piecewise polynomial of order three that is smooth (specifically, it has continuous first and second derivatives) at the knots (i.e., points joining the different polynomial pieces). A restricted cubic spline is further constrained by being linear beyond the outer knots. The use of splines in general and restricted cubic splines in particular has many advantages over other methods in representing nonlinear functions in a regression model when the exact form of the nonlinearity is unknown (Harrell 2001, p. 26). To minimize the number of parameter estimates, we use a restricted cubic spline with only three knots, requiring only two parameters. The knot positions — fifth earliest, median, and fifth latest year — were chosen based on the numbers of knots and observations, using general recommendations from simulation studies (Harrell 2001), and were not tailored in any way for the current data set. Designating this spline-estimated transformation of t as f_t and adding a term η_t to designate the residual, unexplained variability for year t yields

$$(3) \qquad \nabla \frac{1}{S_t} = (c_1 + c_2 P_t) - c_3 \frac{1}{S_{t-1}} + f_t + \eta_t$$

f_t is thus the trend in $1/S_t$ that cannot be attributed to precipitation variability or expected losses from the lake. Expressed in terms of the so-called "truncated power" basis,

$$(4) \qquad f_t = c_4 t + c_5 [(t - k_1)_+^3 - 2(t - k_2)_+^3 + (t - k_3)_+^3]$$

where

$$x_+ = \begin{cases} 0 & x \le 0 \\ x & x > 0 \end{cases}$$

k_i is the ith knot, and c_4 and c_5 are additional constants to be estimated. Note that long-term change implied by f_t cannot be interpreted simply as evidence that c_1 has changed; changes in other parameters could be responsible (see Discussion).

Model estimation and validation

Parameters were estimated by ordinary least squares (OLS) using data from 1968–2001. The most serious potential problem in using OLS for time series regression is autocorrelation of the residuals (Ostrom 1990). Normality of the residuals is also necessary for certain significance tests such as t tests. Residuals and their variance should also have no systematic trend with the fitted response variable or any predictor variable. The residuals were examined accordingly.

Equation 3 requires the estimation of four parameters, apart from the intercept. Given that data are complete for only 34 years (1968–2001), overfitting is a danger. Overfitting refers to distorted parameter estimates (and predictions) that can result from a small ratio of observations to predictors. Overfitting was estimated by using the 0.632 bootstrap estimator of prediction error (Efron 1983; Jassby 1999) to produce corrected values of R^2 and MSE (mean square error). In this method, the model is refitted many times using bootstrap samples of the original observations. For each bootstrap sample, observations not included in the sample are compared with model predictions. The average error rate is then calculated for each observation over all bootstrap samples, and an overall error rate is determined by averaging over all observations. Based on theoretical considerations, the prediction error can then be estimated from the original R^2 and the overall average error rate. The corrected slope and intercept of the calibration plot, i.e., the plot of observed versus predicted values, were also estimated. When the same data set is used for estimation and prediction, these values are 1 and 0, respectively. When an estimated model is applied to a new data set, however, overfitting causes the slope to be less than 1. This "shrinkage" of the slope means that extreme response values are estimated less accurately than intermediate values. Ordinary bootstrap estimation was used to plot a bias-corrected calibration plot. Bootstrap samples of 2000 were used in all calculations, sufficient for at least two significant digits. Harrell (2001) describes all bootstrapping techniques used here.

Results

Monitoring data

The time series used in this analysis include summer mean Secchi depth (S_t), WY precipitation (P_t), and summer mean chlorophyll a in the 0- to 20-m layer (Fig. 2). The long-term decline in Secchi depth is obvious, although much of the decline occurred in the last half of the record. The overall linear trend is –0.21 m·year^{-1} ± 0.05 standard error (SE). Strong year-to-year variability can exceed the long-term trend. Secchi depth ranged from 17.4 m to 29.8 m, with a

© 2003 NRC Canada

Fig. 2. Observed time series of (*a*) mean Secchi depth (m) for June–September, (*b*) water year precipitation (WY precip., cm) at Tahoe City, and (*c*) mean chlorophyll a (Chl *a*) for June–September, 0–20 m.

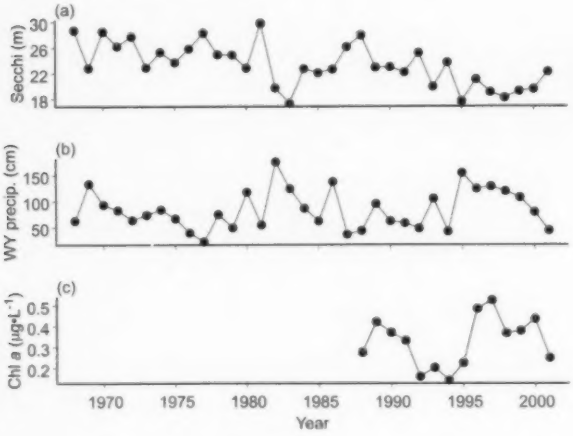

median of 22.9 m, and individual measurements, as opposed to these 4-month averages, can be much higher or lower (Jassby et al. 1999). Note that transparency has increased consistently during the last three years (1999–2001) for a total gain of 4 m.

Model diagnosis

As pointed out above, parametric inferences regarding the model presuppose certain properties for the residuals. In fact, there are no problems with autocorrelation, lack of normality, or systematic trend in residual mean with the fitted response (Fig. 3). The Breusch–Godfrey test for serial correlation, which is the appropriate test when lagged response variables are included as predictors (Ostrom 1990), confirms the absence of serial correlation ($F = 0.251$, $P = 0.780$). Although the residual variance appears to decrease with the fitted response (Fig. 3*c*), the data are actually too sparse at these higher values to make any definitive conclusions in this regard. There are also no systematic trends in residual mean with predictors (not shown).

Because the residuals satisfy the assumptions of OLS, we can conduct various partial F tests of hypotheses regarding the model, the most important of which concerns the existence of a trend apart from interannual variability (Table 1). All predictors are significant, including — as indicated by the results for f_t — the trend. Note, however, that the nonlinearity in the trend is not significant.

The partial residual for each predictor here refers to the response minus the sum of all other predictor terms. The partial residual plot is simply the partial residual for a predictor plotted against the predictor itself. It is a visual guide to the effects — both magnitude and shape — of individual predictors in a model (Cook and Croosdabrera 1998). The three predictors have effects of similar magnitude, as evidenced by the sizes of their y-axis ranges (Fig. 4). In accordance with model assumptions, the partial residual plots for P_t and $1/S_{t-1}$ are approximately linear. The trend term is not

Fig. 3. Residual diagnostic plots for the model of eq. 3 with the trend f_t represented as a restricted cubic spline: (*a*) autocorrelation function with 95% confidence limits (broken lines); (*b*) normality plot; and (*c*) residuals versus fitted response.

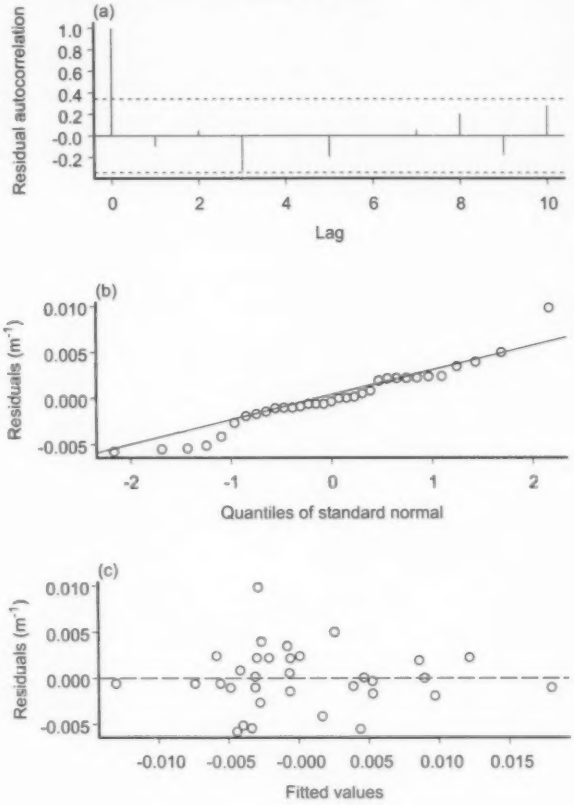

constrained to linearity but shows almost no curvature and is essentially linear, consistent with the partial F test.

The statistical (Table 1) and visual (Fig. 4) evidence therefore do not support nonlinearity in the trend term. To minimize overfitting, we eliminate the nonlinearity (i.e., set $c_5 = 0$) and treat f_t in what follows as being linear in t.

The fitted response demonstrates that the model with linear trend describes inverse Secchi depth well, and the residuals are not obviously correlated or otherwise nonrandom (Fig. 5). In fact, the residual diagnostic plots resemble those of the model with spline trend very closely (Fig. 3). All parameter estimates for the model with linear trend are significantly nonzero (Table 2). Note that the rate constant for settling of 0.92 year^{-1}, combined with the mean lake depth of 333 m, implies a settling velocity of 0.84 m·day^{-1}, which is characteristic of clay and many algal cells (Wetzel 2001).

The R^2 value (Table 3) confirms the visual evidence (Fig. 5) that the model closely fits the data used to estimate it. As indicated above, however, the usual method of calculation can be optimistic if overfitting is a problem. Using the 0.632 bootstrap method, which provides estimates of R^2 and MSE that are more realistic when the model is used to predict new observations, R^2 falls to 0.69, whereas MSE in-

© 2003 NRC Canada

Table 1. Partial F tests for the model of eq. 3.

Factor	df	Partial SS	F	P
P_t	1	5.00×10^{-4}	40.90	<0.0001
$1/S_{t-1}$	1	6.93×10^{-4}	56.70	<0.0001
f_t	2	1.70×10^{-4}	6.96	0.0035
Nonlinearity of f_t	1	1.50×10^{-6}	0.12	0.7290
Regression	4	1.27×10^{-3}	26.10	<0.0001
Error	28	3.42×10^{-4}		

Fig. 4. Partial residual plots for (*a*) water-year (WY) precipitation, (*b*) lagged inverse Secchi depth, and (*c*) trend. Each line is the respective fitted term from the model.

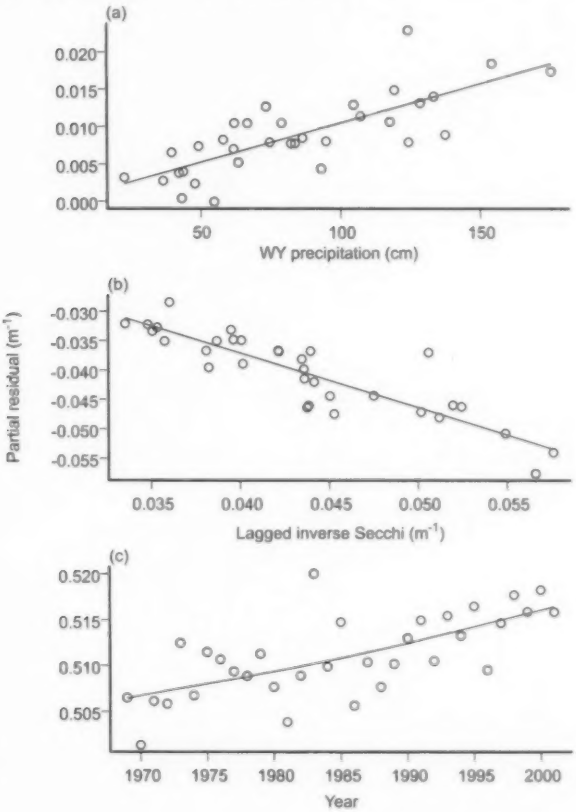

creases by 31%. The bias-corrected calibration statistics, namely, the intercept and slope of observed versus predicted values, are very close to the ideal, i.e., shrinkage is small (Table 3). The actual bias-corrected calibration plot for predicting new observations is close to the ideal (Fig. 6).

Change detection

The underlying long-term trend in Secchi depth can be described by simulating the data with precipitation held constant and equal to its long-term (1968–2001) median of 76.8 cm. The simulation is a "dynamic" one in the sense that each year's value is based on the simulated value — not the observed value — for the previous year. Uncertainty in the true coefficient values was incorporated by repeating the simulation, varying coefficients randomly, consistent with their mean and standard error, at the beginning of each simulation. Each individual simulated time series evolves according to eq. 3, with $\eta_t = 0$ and with precipitation constant. The mean and 95% confidence limits were calculated from 10 000 simulations (Fig. 7). The underlying trend in the observed time series is disguised especially by heavy precipitation during the 1982–1983 El Niño Southern Oscillation (ENSO) and then a prolonged drought during 1987–1992. As a result, the raw data obscure the long-term summer decline through 1992.

We also asked if the consistent increase in Secchi depth during the last three years (1999–2001) represents an underlying change in the lake's transparency trend or simply reflects climate variability. The development and validation of eq. 3 provide a quantitative context for addressing this issue. Specifically, we asked what Secchi depth values would be expected had the trend in inverse Secchi (declining clarity)

Fig. 5. (*a*) Observed (thin solid line) and fitted (thick shaded line) response for the model of eq. 3 and (*b*) corresponding residuals.

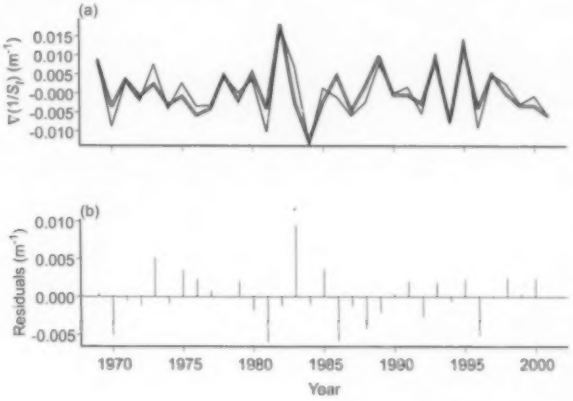

Table 2. Coefficient estimates for the model of eq. 3 with linear trend.

	Value	Standard error	t	P
Intercept	–0.583	0.159	–3.66	0.0003
P_t	1.05×10^{-4}	1.61×10^{-5}	6.56	<0.0001
$1/S_{t-1}$	0.920	0.120	7.69	<0.0001
t	3.09×10^{-4}	8.20×10^{-5}	3.77	0.0002

Table 3. Corrected measures of predictive accuracy for the model of eq. 3.

	R^2	MSE	Intercept	Slope
Original value	0.787	1.04×10^{-5}	0.000	1.000
Corrected value	0.688	1.36×10^{-5}	0.000	0.976

Note: MSE, mean square error; intercept, intercept of calibration curve (observed vs. predicted values); slope, slope of calibration curve. Corrected values are based on Efron's 0.632 bootstrap method using 2000 samples.

© 2003 NRC Canada

Fig. 6. Ideal (broken line) and bias-corrected (solid line) calibration plots for the model of eq. 3.

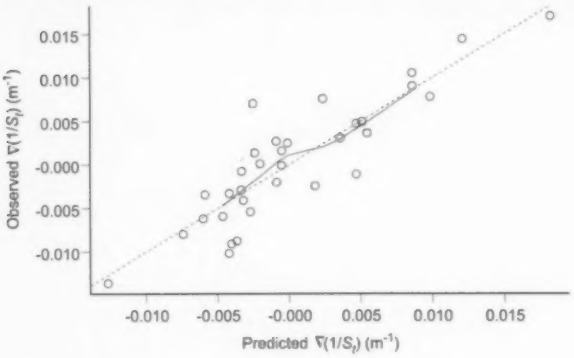

ceased in 1998, i.e., if $f_t = f_{1998}$, $t > 1998$. The model was re-estimated using only data collected before 1999 and an ex-post forecast was made for the subsequent three years. The forecast was a "dynamic" one in the sense described above. Forecast values were similar to observed values (Fig. 8), suggesting that the observations of 1999–2001 do not represent a fundamental recovery of the lake's transparency.

Discussion

Model specification and diagnosis

This simple time series model has several important and desirable qualities. The variable chosen — winter–spring precipitation — reflects the main cause of interannual variability as revealed through prior analysis of historical data and was not selected during the model-building process to produce the best fit. Similarly, the model was prespecified to reflect mass balance constraints, not formulated simply to provide a best fit. In addition, the initial use of a restricted cubic spline for the trend enables departures from linearity without searching for the best shape. The model therefore largely avoids problems that result from treating an empirically derived model as if it were the correct prespecified model, such as distorted standard errors (Faraway 1992; Chatfield 1995).

The restricted cubic spline allows us to prespecify complexity in the trend by choosing the number of knots while still allowing for a wide range of shapes. This trend term normally should not be simplified simply because the nonlinear component may lack statistical significance. The important criterion for retaining the spline-transformed trend term is the joint test of all of its components, and temptations to simplify the term should be avoided (Grambsch and O'Brien 1991). Future evolution of f_t may very well be nonlinear, especially if restoration efforts are successful.

A separate problem that may warrant simplification of the model, however, is overfitting, i.e., an overly optimistic R^2 and MSE that are not borne out when it comes to predicting future data. Overfitting results from a relatively small number of observations compared to predictors. Studies show that a regression model is likely to avoid overfitting when there are at least 10–20 observations per predictor (Harrell et al. 1996). In contrast, the original model of eq. 3 with a spline trend used four predictors (including two associated with the trend) or only about eight observations per predictor. We found that the extra predictor led to excessive overfitting (not shown) that could seriously increase parameter and forecast uncertainty, which prompted us to simplify the trend term to a linear one. The simpler model still exhibits moderate overfitting, as evidenced by the difference ("optimism") between R^2 values calculated in the normal way and with the bootstrap method. Nonetheless, the corrected R^2 remains high, shrinkage is small, and the bias-corrected calibration curve is close to the ideal. Given the performance of the model and behavior of the residuals, the model can therefore be used with relative confidence.

Fig. 7. Dynamic simulation of Secchi depth assuming precipitation is constant and equal to the 1968–2001 median. Solid line, observed June–September mean Secchi depth; long-dashed line, mean of constant-precipitation scenarios; short-dashed lines, 95% confidence interval of constant-precipitation scenarios.

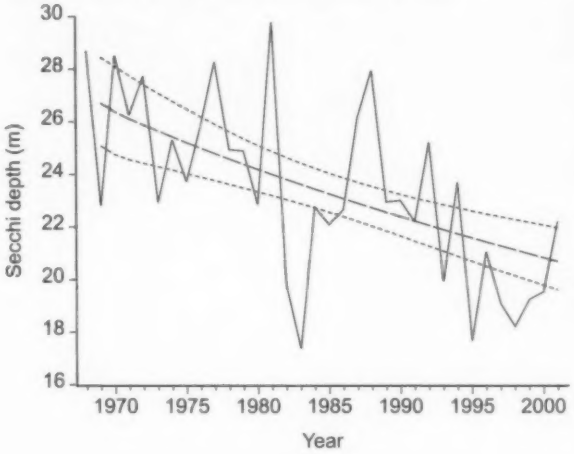

Fig. 8. Dynamic forecast of 1999–2001 under the hypothesis that $f_t = f_{1998}$. Solid line, observed June–September mean Secchi depth; long-dashed line with solid circles, forecast; short-dashed lines, approximate 95% forecast interval.

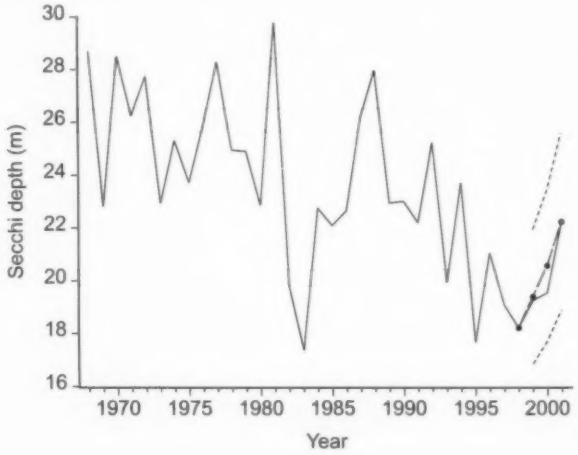

© 2003 NRC Canada

Assessing long-term change

One of the motivations for this model was speculation that watershed management may have been responsible for the improvement in water transparency seen in recent years (1999–2001). Only one other example of at least three years of improvement can be seen in the record, namely 1986–1988. The deterioration in Secchi depth after 1988 illustrates how a three-year improvement can easily be transient. Indeed, the 1999–2001 forecasts are similar to or slightly higher than observed values. Thus, the Secchi depth increases during 1999–2001 provide no evidence that the underlying ecosystem response has changed markedly since 1998 and that transparency is improving in the longer term.

The forecast for 1999–2001 has 95% confidence limits of at least 2 m above and below, implying that large changes would be required before we could conclude either that the trend continued or reversed for 1999–2001 based on a null hypothesis significance test. Recall that the long-term linear trend for summer is only –0.21 m·year^{-1}, whereas the absolute year-to-year difference averages 3.0 m and can be over 10 m (1981–1982). Although the model of interannual variability presented here performs quite well, the variability is so high that much uncertainty remains relative to the trend. It is therefore difficult to make judgments about underlying change for short time intervals. We may have to wait many years for highly significant evidence that the underlying trend has reversed, depending on the speed of recovery, as well as the uncertainty surrounding the long-term trend.

The model may have additional uses in determining compliance with transparency standards for the lake. As shown here, the interannual variability is enormous and driven almost entirely by precipitation differences. Multiyear periods of drought (and high rainfall) are common in the coastal U.S., the last major one extending from 1987 through 1992. A simple, percentile-based approach — such as requiring that at most 10% of samples or even annual means not violate water quality standards — is not appropriate when perceived violations are actually due to climate anomalies that may persist for years. With the model developed here, the extracted long-term trend determined as in our study can be used as a basis for assessing compliance and determining effectiveness of restoration. Alternately, an "equilibrium value" of Secchi depth (see below) determined by setting f_t equal to its current value can be used as the basis for assessment. Our goal here is not to address this issue in detail, but rather to show the need for explicit consideration of climate variability and offer a tool for possible incorporation into the regulatory process.

Can we make long-term forecasts of Secchi depth, given future scenarios of climate and other relevant variables? The trend term (f_t) is, in essence, structure that we have extracted from the residuals after accounting for our knowledge of interannual variability. It is simply a device for describing and testing hypotheses about the long-term change that has taken place and cannot be extrapolated safely into the future. An out-of-sample (or ex-ante) forecast requires that we incorporate the processes underlying the trend explicitly into the model. At the same time, however, the relatively small number of years precludes estimating additional parameters solely from the data set. This implies the need for a model incorporating the controlling mechanisms in more detail and in a fashion that allows parameters to be based on fundamental scientific knowledge or experience from a wide range of lakes. Such a model is well under way for Lake Tahoe (Perez-Losada 2001).

Water transparency dynamics

What is responsible for the overall and probably ongoing trend in transparency? Although we cannot answer this question based on the data and analysis presented here, eqs. 2 and 3 provide a useful framework for understanding the question more deeply. As emphasized by Carpenter and Turner (2001): "...the essential dynamics of a given ecosystem phenomenon can be captured by including the key processes with longer and shorter turnover times (slower or faster turnover rates). Slow processes are treated as parameters, whereas fast processes may be solved at equilibrium". Here, we make such a distinction between the "fast" process of interannual variability in Secchi depth and the "slow" process of long-term transparency decline. Equation 2 is a linear difference equation in $1/S_t$. Over a period of less than one decade, long-term trend is small, and eq. 2 describes transparency dynamics well. It has a stable equilibrium value of

$$\frac{1}{S_e} = \frac{c_1 + c_2\overline{P}}{c_3} \quad (5)$$

where $\overline{P}$ represents the long-term precipitation average. Because the system has a response time of $1/c_3$ or approximately 1 year, Secchi depth can approach its equilibrium value within a few years (although in practice it will fluctuate around it because of variable P_t). The fast response time is demonstrated most dramatically by the reaction to and recovery from record precipitation in 1982–1983. A likely reason for this fast response is the loading of larger mineral particles during high flows; the particles then sink out relatively rapidly (Jassby et al. 1999).

The trend term can be seen as slowly shifting this equilibrium value from decade to decade through changes in any of the c_i. The simplest mechanism would be an increase in precipitation-independent loading (c_1) or in the yield (c_2) of precipitation-dependent loading. These could arise from, for example, increases in dry deposition of dust originating from road surfaces or higher erosion yield of the watershed, respectively. A trend could also be generated through c_3 by changes in biological pumping, i.e., altered sedimentation rate of suspensoids arising from food web changes, especially involving macrozooplankton (Turner 2002) such as the *Mysis relicta* population in Tahoe. A difficulty with these explanations is that changes would have to be ongoing to maintain the observed trend. In other words, despite the many rehabilitation activities and restrictive land-use policies enacted in the Tahoe basin, loading of materials would have to be increasing year by year or, at least, decade by decade. Similarly, food web changes would have to be ongoing to sustain the trend.

A more likely possibility presents itself by relaxing the implicit assumption that the particle composition of material remaining in the lake is not changing. We hypothesize that settling processes in the lake act to sort particles based on size. The relative contributions of small size classes — known

© 2003 NRC Canada

to have a large effect on lake optical properties — build up over time because inputs and outputs are not in equilibrium. To simplify understanding of this issue, suppose that particles entering the lake could be divided into two groups: (*a*) "big" ones that settle out relatively quickly (approximately 1 year) and (*b*) "small" ones that settle out more slowly (approximately 10 years). The equilibrium value would then be given by a sum of two terms similar to the right-hand side of eq. 5, one for big and one for small particles. The big particles, with a response time of a year, generate the interannual variability, and the small particles, with a response time of a decade, generate the decadal variability or trend. In response to a step change in loading rate, the big particles would achieve equilibrium on the scale of years, whereas the small ones would take decades. Transparency, therefore, would continue to decline years after the loading increase, even though the (elevated) loading remained the same. In the context of eq. 2, it can easily be shown that $c_3 = c_b h_b + c_s h_s$, where c_b and c_s are the loss rates of big and small particles, respectively, and h_b and h_s are the proportions of big and small particles in the lake relative to the total. A step increase in loading rate would then result in a decadal-scale decline in c_3, because $c_s < c_b$ and h_s would continue to increase relative to h_b. Although we cannot say what the equilibrium Secchi depth corresponding to existing loading might be, we can say that it is smaller than the present trend value of 20 m and that loading must therefore be decreased at least until the trend reverses.

If c_3 is in fact the source of the trend, then a slightly different model specification is implied. In particular, the specific loss rate becomes $(c_3 + f_t)$. Although the model respecified in this manner may be truer to the underlying processes, the behavior of the model and forecasts change very little (not shown).

The particle composition in loading and in the lake itself is a key to distinguishing among the possible explanations. Unfortunately, the long-term instrumental record does not include particle size and composition data, and retrospective analysis therefore cannot provide an easy answer. We can infer that living phytoplankton probably do not contribute to the long-term change in summer: chlorophyll *a* in the upper layer (available only since 1988) bears no relationship to the summer trend (although it is a factor in the long-term winter decline; Jassby 1999). Accumulating diatom debris could, in principle, contribute to the long-term trend, a possibility currently under investigation by combining scanning electron microscopy – x-ray fluorescence identification of particles with an optical model. Results so far, however, support at most a secondary role for biogenic silica contributions to transparency losses (T. Swift, Department of Environmental Science and Policy, University of California, Davis, CA 95616, personal communication).

In conclusion, we presented a model of interannual variability using mass balance concepts to guide the exact formulation. Models that incorporate a mechanistic understanding of ecological dynamics with sufficient simplicity to allow data-based parameter estimation are becoming increasingly important for environmental management. Such models are characterized by better predictions, more appropriate parameter values, and explicit incorporation of parameter and residual uncertainty (Borsuk et al. 2001). The model for interannual variability was then "hybridized" with an empirical model for the long-term trend because the existing time series, while extensive, are not sufficient to support the estimate of many more parameters. A restricted cubic spline was used initially for the empirical portion because of its flexibility in shape and other desirable properties, but a linear term was needed ultimately to avoid overfitting. The model described the data well and satisfied traditional diagnostic tests, as well as bootstrap validation and calibration tests.

In application to Lake Tahoe, the model showed via an ex-post forecast that recent clarity improvements are caused by climate variability and are not indicative of a change in the lake's behavior. However, because of the low signal-to-noise ratio — and the resulting uncertainty in model parameters — it is possible to overlook real change taking place over just a few years. A probable explanation for the long-term trend is that the lake is not in equilibrium with respect to the particle size spectrum. The particles in question appear to be mainly inorganic mineral suspensoids rather than living phytoplankton and mainly allochthonous rather than biogenic. Elevated loading of mineral suspensoids is therefore the most likely primary cause of the long-term summer trend, and limiting the atmospheric and watershed inputs of mineral particles is the most likely solution. Still, the actual spectrum of mineral particle sizes responsible for the trend has important bearing on mitigation measures and expected response times and should be resolved as soon as possible.

Acknowledgements

We thank Bob Richards and Scott Hackley for their essential roles in the field and laboratory measurements; Patty Arneson for data management; and Ted Swift, Geoff Schladow, Joaquim Losada, and Alan Heyvaert for helpful discussions on limnological processes at Lake Tahoe. Robert Shumway provided invaluable guidance on statistical issues, and two anonymous reviewers helped to improve the presentation. Data collection was supported by contracts from the Tahoe Regional Planning Agency, the U.S. Geological Survey, and the State of California Water Resources Control Board through the Lake Tahoe Interagency Monitoring Program. Data analysis and the preparation of this article were supported by the U.S. Environmental Protection Agency (U.S. EPA; R819658) through the Center for Ecological Health Research at the University of California, Davis. Although preparation of this document was partially funded by the U.S. EPA, it does not necessarily reflect the views of the agency, and no official endorsement should be inferred.

References

Borsuk, M.E., Higdon, D., Stow, C.A., and Reckhow, K.H. 2001. A Bayesian hierarchical model to predict benthic oxygen demand from organic matter loading in estuaries and coastal zones. Ecol. Model. **143**: 165–181.

Carpenter, S.R., and Turner, M.G. 2001. Hares and tortoises: interactions of fast and slow variables in ecosystems. Ecosystems, **3**: 495–497.

Chapra, S.C. 1997. Surface water-quality modeling. McGraw-Hill, New York.

© 2003 NRC Canada

Chatfield, C. 1995. Model uncertainty, data mining and statistical inference (with discussion). J. R. Stat. Soc. A, **158**: 419–466.

Cook, R.D., and Croosdabrera, R. 1998. Partial residual plots in generalized linear models. J. Am. Stat. Assoc. **93**: 730–739.

Davies-Colley, R.J., Vant, W.N., and Smith, D.G. 1993. Colour and clarity of natural waters: science and management of optical water quality. Ellis Horwood, New York.

Efron, B. 1983. Estimating the error rate of a prediction rule: improvements on cross-validation. J. Am. Stat. Assoc. **78**: 316–331.

Esterby, S.R. 1996. Review of methods for the detection and estimation of trends with emphasis on water quality applications. Hydrol. Process. **10**: 127–149.

Faraway, J.J. 1992. The cost of data analysis. J. Comput. Graph. Stat. **1**: 213–229.

Gardner, J.V., Mayer, L.A., and Clarke, J.E.H. 2000. Morphology and processes in Lake Tahoe (California–Nevada). Geol. Soc. Am. Bull. **112**: 736–746

Goldman, C.R. 1988. Primary productivity, nutrients, and transparency during the early onset of eutrophication in ultra-oligotrophic Lake Tahoe, California–Nevada. Limnol. Oceanogr. **33**: 1321–1333.

Goldman, C.R., Jassby, A.D., and Powell, T. 1989. Interannual fluctuations in primary production: meteorological forcing at two subalpine lakes. Limnol. Oceanogr. **34**: 310–323.

Grambsch, P.M., and O'Brien, P.C. 1991. The effects of transformations and preliminary tests for non-linearity in regression. Stat. Med. **10**: 697–709.

Gu, C. 2002. Smoothing spline ANOVA models. Springer-Verlag, New York.

Harrell, F.E., Jr. 2001. Regression modeling strategies: with applications to linear models, logistic regression, and survival analysis. Springer-Verlag, New York.

Harrell, F.E., Jr., Lee, K.L., and Mark, D.B. 1996. Multivariable prognostic models: issues in developing models, evaluating assumptions and adequacy, and measuring and reducing errors. Stat. Med. **15**: 361–387.

Helsel, D.R., and Hirsch, R.M. 1992. Statistical methods in water resources. Elsevier, Amsterdam.

Heyvaert, A. 1998. The biogeochemistry and paleolimnology of sediments from Lake Tahoe, California–Nevada. Ph.D. dissertation, University of California, Davis, Calif.

Jassby, A.D. 1999. Uncovering mechanisms of variability from short ecological time series. *In* Integrated assessment of ecosystem health. *Edited by* K.M. Scow, G.E. Fogg, D.E. Hinton, and M.L. Johnson. Lewis Publishers, Boca Raton, Fla. pp. 285–306.

Jassby, A.D., Reuter, J.E., Axler, R.P., Goldman, C.R., and Hackley, S.H. 1994. Atmospheric deposition of nitrogen and phosphorus in the annual nutrient load of Lake Tahoe (California–Nevada). Water Resour. Res. **30**: 2207–2216.

Jassby, A.D., Goldman, C.R., and Reuter, J.E. 1995. Long-term change in Lake Tahoe (California–Nevada, U.S.A.) and its relation to atmospheric deposition of algal nutrients. Arch. Hydrobiol. **135**: 1–21.

Jassby, A.D., Goldman, C.R., Reuter, J.E., and Richards, R.C. 1999. Origins and scale dependence of temporal variability in the transparency of Lake Tahoe, California–Nevada. Limnol. Oceanogr. **44**: 282–294.

Larson, G.L., McIntire, C.D., Hurley, M., and Buktenica, M.W. 1996. Temperature, water chemistry, and optical properties of Crater Lake. Lake Reserv. Manag. **12**: 230–247.

Loftis, J.C., MacDonald, L.H., Streett, S., Iyer, H.K., and Bunte, K. 2001. Detecting cumulative watershed effects: the statistical power of pairing. J. Hydrol. **251**: 49–64.

Ostrom, C.W. 1990. Time series analysis. 2nd ed. Sage University Paper series on Quantitative Applications in the Social Sciences No. 07-009, Sage, Newbury Park, Calif.

Perez-Losada, J. 2001. A deterministic model for lake clarity: application to Lake Tahoe (California, Nevada), U.S.A. Ph.D. dissertation, University of Girona, Spain.

Preisendorfer, R.W. 1986. Secchi disk science: visual optics of natural waters. Limnol. Oceanogr. **31**: 909–926.

Reuter, J.E., Loeb, S.L., and Goldman, C.R. 1986. Inorganic nitrogen uptake by epilithic periphyton in a nitrogen deficient lake. Limnol. Oceanogr. **31**: 149–160.

Turner, J.T. 2002. Zooplankton fecal pellets, marine snow and sinking phytoplankton blooms. Aquat. Microb. Ecol. **27**: 57–102.

Wetzel, R.G. 2001. Limnology. 3rd ed. Academic Press, New York.

© 2003 NRC Canada

Testing a model of drift-feeding using three-dimensional videography of wild brown trout, *Salmo trutta*, in a New Zealand river

Nicholas F. Hughes, John W. Hayes, Karen A. Shearer, and Roger G. Young

Abstract: We tested the assumptions and predictions of a foraging model for drift-feeding fish. We used three-dimensional videography to describe the foraging behavior of brown trout, *Salmo trutta*, mapped water depth and velocity in their foraging area, sampled invertebrate drift to determine length class specific drift densities, and captured trout to determine the size composition of their diet. The model overestimated the fish's prey capture rate and gross energy intake rate by a factor of two. Most of this error resulted from the fact that prey detection probabilities within the fish's foraging area averaged only half the expected value. This was the result of a rapid decrease in capture probability with increasing lateral distance from the fish's focal point. Some of the model's assumptions were accurate: equations for predicting reaction distance and minimum prey size supported reliable predictions of the shape and size of the fish's foraging area and the size composition of the diet. Other assumptions were incorrect: fish detected prey within the predicted reaction volume, not on its upstream surface as expected, fish intercepted prey more slowly than the expected maximum sustainable swimming speed, and fish captured about two-thirds of their prey downstream of their focal point, rather than upstream.

Résumé : Nous avons évalué les présuppositions et les prédictions d'un modèle de quête de nourriture mis au point pour les poissons qui se nourrissent de la dérive. La vidéographie à trois dimensions nous a permis de décrire le comportement de quête de nourriture chez des truites brunes, *Salmo trutta*. Nous avons établi la répartition de la profondeur de l'eau et de la vitesse du courant dans l'aire d'alimentation des truites et échantillonné la dérive des invertébrés pour en déterminer la densité par classes de longueur. Nous avons enfin capturé des truites pour connaître la composition en taille de leur régime alimentaire. Le modèle surestime le taux de capture des proies par les poissons et leur ingestion brute d'énergie par un facteur de 2. La cause principale de cette erreur est que les probabilités de détection des proies dans l'aire d'alimentation sont en moyenne seulement la moitié des valeurs attendues. C'est là le résultat d'une diminution importante de la probabilité de capture en fonction de la distance latérale de la proie du point focal du poisson. Quelques-unes des présuppositions du modèle s'avèrent justes : les équations qui servent à prédire la distance de réaction et la taille minimale des proies produisent des prédictions fiables de la forme et de la taille de l'aire de quête de nourriture du poisson et de la structure en taille du régime alimentaire. D'autres présuppositions sont fausses : les poissons détectent leurs proies au sein du volume de réaction prédit et non sur sa surface d'amont, comme on s'y attendait; les poissons interceptent leurs proies plus lentement qu'à la vitesse de nage maximale soutenue; enfin, les poissons capturent environ les deux tiers de leurs proies en aval, plutôt qu'en amont, de leur point focal.

[Traduit par la Rédaction]

Introduction

During the last few years, biologists interested in the ecology of stream salmonids have begun to develop mechanistic models of the way in which habitat characteristics influence the net energy intake rates of drift-feeding fish. The main impetus for the development of these models has been to predict habitat selection (Fausch 1984; Hughes and Dill 1990; Hill and Grossman 1993), habitat quality (Baker and Coon 1997; Braaten et al. 1997; Guensch et al. 2001), and growth rates (Hughes 1998; Hayes et al. 2000). Similar models have been developed for drift-feeding reef fish (Kiflawi and Genin 1997). The current research trend is to adapt these foraging models to predict how stream morphology, and seasonal changes in stream discharge, invertebrate drift abundance, and water temperature combine to shape the population dynamics of stream salmonids (see Armstrong 1997; Nislow et al. 2000).

This research activity shows that mechanistic foraging models already play a significant role in stream fish ecology. This makes it surprising to discover that the ability of these models to actually predict a fish's energy intake rate has

Received 14 May 2003. Accepted 13 August 2003. Published on the NRC Research Press Web site at http://cjfas.nrc.ca on 17 December 2003.
J17529

N.F. Hughes.[1] School of Fisheries and Ocean Sciences, University of Alaska Fairbanks, Fairbanks, AK 99775-7220, U.S.A.
J.W. Hayes, K.A. Shearer, and R.G. Young. Cawthron Institute, Private Bag 2, Nelson, New Zealand.

[1]Corresponding author (e-mail: ffnfh@uaf.edu).

 doi: 10.1139/F03-126 © 2003 NRC Canada

never been tested. In this paper, we address this situation by using three-dimensional videography of wild brown trout (*Salmo trutta*) to test the assumptions and predictive power of an updated version of the model that Hughes and Dill (1990) developed to predict the energy intake rate and habitat selection behavior of Arctic grayling (*Thymallus arcticus*). We update the original model to incorporate several recent advances, particularly from Guensch et al. (2001) and Hayes et al. (2000), and also add some improvements of our own. The results of this test should be directly relevant to researchers developing or using mechanistic models of drift-feeding and also to the assessment and development of more empirically based models of drift-feeding such as those described by Hill and Grossman (1993) and Nislow et al. (2000).

The model

The original formulation

Hughes and Dill's (1990) original model is essentially a geometrical description of the way that the foraging capabilities of a drift-feeding fish interact with the stream habitat to determine the fish's net rate of energy intake (Fig. 1). Intriguingly, Kiflawi and Genin (1997) developed a model of drift-feeding for zooplanktivorous damselfish that incorporates many of the same assumptions and constraints as Hughes and Dill's (1990) model. Together these two models provide arguably the most comprehensively mechanistic models of drift-feeding, and the test that we describe here is applicable to both.

Incorporating recent advances

In this section, we describe how we incorporate recent advances and some improvements of our own to update Hughes and Dill's (1990) model. Equations describing the updated model are listed in Table 1.

Size-selective predation

Hughes and Dill (1990) assume that fish can eat all sizes of prey, but this is not true. Both morphology and behavior can restrict the range of prey sizes that a fish consumes. We rectify this situation by incorporating morphological constraints following Wankowski (1979) and Hayes et al. (2000). We set minimum prey length to 1.15% of fish length to reflect constraints due to gill raker spacing and maximum prey length to 45.2% of fish length to reflect the constraint of mouth gape. We also incorporate the logic of Charnov's (1976) diet model to account for the fact that rate-maximizing fish should drop less profitable prey from their diet when the time spent handling them could be better used to search for and handle more profitable prey, where we equate interception time with handling time (Table 1).

Velocity shear and capture area

Hughes and Dill's (1990) model only represents lateral water velocity shear, neglecting vertical velocity shear. Guensch et al.'s (2001) model rectifies this, recreating vertical velocity shear from average velocity by assuming a logarithmic vertical velocity profile. In this paper, we adopt a more general approach by simply dividing a cross section into rectangular cells and assigning a velocity to each cell based on field measurements. If the cells are small enough, this procedure can provide a computationally versatile means of describing water velocity in the vertical and lateral dimensions. We divide the cross section into 0.1 m × 0.1 m cells (Fig. 2*a*). We also incorporate Guensch et al.'s (2001) technique of accounting for the ways in which vertical and horizontal velocity shear influence the size and shape of the fish's capture area (Fig. 2*b*).

Holling's (1959) disk equation

Hughes and Dill's (1990) original formulation does not incorporate the logic of Holling's (1959) disk equation. As a result, it predicts a linear increase in prey capture rate with increasing prey density, rather than the type II (decelerating) functional response expected (e.g., Ringler and Brodowski 1983). Several researchers have tried to rectify this problem by incorporating the logic of the disk equation and a way to estimate handling time. Hughes (1998) equates handling time to the time taken to intercept prey ($h_i = RD_i/VMAX$), Hayes et al. (2000) use a similar approach but assume that the mean prey detection distance is $0.5RD_i$ so that $h_i = 0.5RD_i/VMAX$, and Guensch et al. (2001) equate handling time to the total time taken to recognize, intercept, and swallow the prey and return to the focal point, using a value of 5 s, based on Bachman's (1984) observations of brown trout. In this paper, we use Hughes' (1998) method to estimate handling time.

Energetics

Hughes and Dill (1990) used the total energy content of the prey to calculate the fish's energy intake. Here we use assimilable energy content, which should improve the model's accuracy because fish assimilate significantly less than 100% of their prey's total energy content (Table 1). We do not update Hughes and Dill's rather simplistic approach to predicting swimming costs to include the cost of prey interception maneuvers (e.g., Hughes and Kelly 1996*b*) because we can not directly test predictions of swimming costs with the work described here. For this reason, we confine our attention to testing the model's predictions of gross energy intake. More sophisticated approaches to predicting swimming costs are certainly justified (see later).

Testing the model

To evaluate the model just described, we test the following assumptions and predictions. (1) When fish are searching from their focal points, they detect all prey on the upstream surface of the reaction volume (Fig. 3). (2) Fish intercept prey at their maximum sustainable swimming speed. (3) Fish capture all prey upstream of their focal point. (4) Prey capture probability is uniform across each capture area. (5) The model makes accurate predictions of the length–frequency distribution of prey in the diet. (6) The model makes accurate predictions of the prey capture rate (number·s^{-1} or number·h^{-1}) and gross energy intake rate (J·s^{-1} or J·h^{-1}). Note that our incorporation of Holling's disk equation means that the model will no longer predict that the fish should capture 100% of potential prey passing through a capture area, as assumed by Hughes and Dill (1990), because the fish will miss some prey while it is handling others.

© 2003 NRC Canada

Fig. 1. A summary of the foraging model described by Hughes and Dill (1990). (*a*) The geometry of prey interception. The fish is assumed to detect prey as they hit the surface of a hemispherical reaction volume with a radius equal to its reaction distance (RD) for prey length in question. The half circle in the figure describes the upstream surface of this volume in cross section. The fish intercepts prey at its maximum sustainable swimming speed (VMAX) and may only capture those prey that it is able to intercept before they cross the line *D–E*. Under these conditions, when water velocity is V, the maximum lateral capture distance (MCD) is $[RD^2 - (V \cdot RD/VMAX)^2]^{1/2}$. (*b*) Description of the influence of water velocity on MCD. (*c*) Part of a cross section occupied by a fish. The cross section is divided into vertical strips j, each characterised by a width, depth, and mean water velocity V_j. The fish's focal point is equidistant from the sides of its chosen strip and 25% of the depth from the stream bed. (*d*) Illustration of the way that MCD is used to calculate the area within strip j where the fish captures prey in length class i, $CA_{i,j}$. This is the overlap between a circle with a radius equal to the $MCD_{i,j}$ calculated with the distance-weighted water velocity, $AVEL_j$, traversed to forage in strip j, and the reaction distance RD_i appropriate to prey in length class i. The model assumes that the fish will capture 100% of the prey passing through this capture area. To estimate the fish's net rate of energy intake (NREI), prey availability is described by categorizing prey into i length classes, each with a density, PC_i (number·m^{-3}), and mean energy content, PE_i (J). The fish is assumed to pay swimming costs (SC) appropriate to swimming at the mean water velocity in its chosen strip, neglecting interception costs. Then, if i = 1, ..., 3 and j = –3, ..., +3, then the fish's net rate of energy intake (NREI) can be calculated as $NREI = -SC + \sum_{i=1}^{3} \sum_{j=-3}^{+3} CA_{i,j} V_j PC_i PE_i$. (Reproduced from Hughes and Dill (1990).)

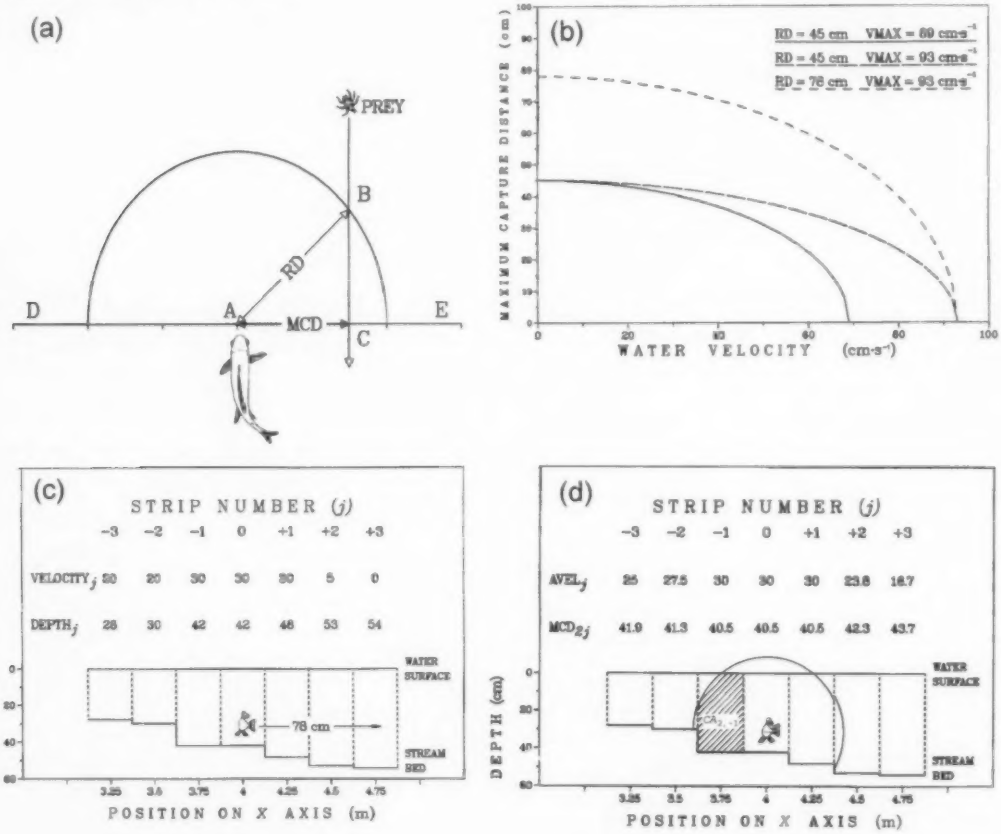

Fieldwork

Study site

The fieldwork was carried out on the Travers River (41°57′S, 172°48′E) in the northern region of South Island, New Zealand, the main tributary of Lake Rotoiti in Nelson Lakes National Park. The Traver's catchment is predominately beech forest (*Nothofagus* spp.) with open grassland and shrubby river terraces on the valley floor. In the study reach, the river has a predominantly cobble and gravel bed, a well-developed pool–riffle sequence, a mean width of 15 m, a gradient of 0.01%, a discharge of 1–3 m^3·s^{-1} at base to low flow, and very clear water (10- to 20-m underwater visibility). Brown trout are the only salmonid present in the river. They occur at relatively low densities (~13 fish·km^{-1} or 40 fish·ha^{-1}) but are generally large (0.40–0.65 m).

Trout video

To obtain the data needed to test the model, we videotaped trout in one run and three pools. Progressing from upstream to downstream through the study reach, we named these Cicada Run, Plunge Pool, Rockslide Pool, and Dead-

© 2003 NRC Canada

tree Pool. At each of these locations, we videotaped the fish occupying the most upstream position in the pool or run, and in Plunge Pool, we also videotaped the second-largest drift-feeding fish, for a total of five fish. We videotaped over a period of 2 weeks in midsummer, between 18 February and 4 March 1999. We located feeding fish from the bank, set up our video equipment in the evening, training our cameras on the fish's feeding position, and returned to tape the fish the following day. The timing of our observations were somewhat contingent on fish behavior, and the length of time taping varied from 23 min for the fish in Cicada Run to 139 min for the fish in Rockslide Pool.

We used three-dimensional (3-D) videography techniques (Hughes and Kelly 1996*a*) to describe foraging behavior. We videotaped each fish with two underwater video cameras, positioned close to the stream bank and spaced some distance apart. One of these cameras provided a view of the fish from the side, or upstream, so we could discern prey captures, and custom made pan-tilt devices allowed us to point the cameras using push–pull throttle cables.

3-D quadrat and habitat mapping

To provide 3-D calibration, we placed a 3-D quadrat in the fish's foraging area after videotaping, recording its image on both video tapes. The quadrat was a 1 m × 1 m × 0.6 m cuboid cage made of welded 8-mm-diameter aluminum tubing. Each of its six faces comprised a grid of 0.2 m × 0.2 m squares. We aligned the quadrat so that one face was perpendicular to the current, one face was parallel to the current, and one face was parallel to the stream surface. We registered the location of the quadrat on a tape measure stretched across the river at the fish's focal point.

We mapped the habitat on this cross section by measuring water depth and velocity at 0.5-m intervals. We measured velocity with a Marsh-McBirney current meter (model 2000; Marsh-McBirney Inc., Frederick, Md.). Outside the fish's foraging area, we measured velocity at 0.4 × depth from the stream bed. Inside the fish's foraging area, we measured velocity at 0.2 and 0.8 × depth in Plunge Pool, 0.2, 0.4, and 0.8 × depth in Cicada Run, and 0.2, 0.4, 0.6, and 0.8 × depth in Rockslide Pool and Deadtree Pool.

Invertebrate drift sampling

To estimate the density and size composition of drifting prey in the study area, we sampled drift in two runs 350- to 700-m downstream of the four observation pools. We chose sampling locations with depth and mean column velocities similar to those of trout feeding locations observed in the Travers River by Hayes and Jowett (1994). We scheduled our drift sampling to overlap the time that we videotaped trout, for a total of five sample periods, one for each fish.

At each of our two drift sampling sites, we sampled drift at two locations, about 0.25 m apart on the same cross section. At each location, we stacked three drift nets vertically to sample water just below the surface, at midcolumn depth, and just above the stream bed. Each net had a mouth area of 0.0052 m^2 and mesh size of 0.5 mm. We measured water velocity at the mouth of each net with a Gurley pigmy meter (Gurley Precision Instruments, Troy, N.Y.) to estimate the volume of water filtered during the sample period. We preserved the samples in 4% formaldehyde and later counted invertebrates in each sample and measured each individual to the nearest millimetre.

We estimated mean drift density of each length class at each location by summing samples from the three vertically stacked nets and dividing by the total water volume sampled. We then averaged over the four locations and the five observation periods to obtain a single estimate of length class specific daytime drift density for the 2-week study period.

Trout diet sampling

We estimated the size composition of the prey captured by trout using stomach samples from eight trout caught in a handheld net by a snorkel diver on 4 March. We anesthetised these fish with 2-phenoxyethanol and collected a sample of their prey with a stomach pump (Giles 1980). We preserved and processed these stomach contents in the same manner as the drift samples.

3-D videography and data analysis

Spatiotemporal description of foraging maneuvers

We used the 3-D videography techniques developed by Hughes and Kelly (1996*a*) to describe prey interception maneuvers in the coordinate system defined by our calibration quadrat. The x axis of this system points downstream, the y axis points towards the true left bank, and the z axis points downwards from the surface. For each fish, we determined the 3-D coordinates of its nose and tail at the start of each maneuver, at the moment of prey capture, and at the moment that it settled back to the stream bed. If the fish intercepted more than one prey item during the course of a maneuver, we determined the fish's nose and tail coordinates for each capture. We took considerable care to determine whether the fish actually captured a prey item during the course of a maneuver by watching for the telltale flash that occurs when a fish opens its mouth and exposes the white skin on the side of its lower jaw. We attached the appropriate video time code to each pair of nose and tail coordinates to provide a description of the fish's position in both time and space during the course of each maneuver.

Hydraulic conditions in the foraging area

We used the depth and velocity information collected on the cross section through the fish's focal point to describe the habitat in the fish's foraging area (Fig. 2). We assumed that the depth and velocity conditions at this cross section continued upstream and downstream far enough to encompass the fish's foraging area.

Prey detection locations

To estimate the 3-D coordinates of prey detection, we took the y and z coordinates of prey capture and looked up the corresponding water velocity on our habitat map (Fig. 2*a*). We assumed that the prey traveled downstream at this velocity before being eaten by the fish, moving parallel to the x axis but maintaining its position on the y and z axes. Next we looked up the time that the fish took to intercept the prey and back-calculated the 3-D coordinates of prey detection. Note that this analysis assumes that fish initiate interception at the moment that they detect prey.

To simplify our analysis of prey detection locations, we normalized the 3-D coordinates of each detection location

© 2003 NRC Canada

Table 1. Parameters and equations defining the model of drift-feeding tested in this paper.

Parameter	Definition	Equation or method of computation	Source
NP	Number of prey length classes	NP = 8	This paper
i	Subscript designating prey length class	i = 1, ..., NP	This paper
PLW	Width of prey length class (m)	PLW = 1×10^{-3}	This paper
PL_i	Prey length for length class i (m)	$Pl_i = i + 1.5 \times 10^{-3}$	This paper
PC_i	Density of prey in length class i (number·m^{-3})	Determined by drift sampling	This paper
PM_i	Dry mass (mg) of prey in length class i	$PM = e^{(-5.021 + 2.88 \ln(1000PL_i))}$	Smock (1980)
PE_i	Energy content (J) of prey in length class i	$PE_i = 28.3PM_i$	Cummins and Wuycheck (1971)
PEA_i	Assimilable energy content (J) of prey in length class i	$PEA_i = 0.7PE_i$	Based on Elliott (1982)
FL	Fish length (m)	Determined by 3-D videography	This paper
PLMIN	Minimum length of prey included in the fish's diet (m)	PLMIN = 0.0115FL	Wankowski (1979)
PLMAX	Maximum length of invertebrate prey included in the fish's diet (m)	PLMAX = 0.452FL	Modified from Hayes et al. (2000)
RD_i	Reaction distance of fish to prey in length class i (m)	$RD_i = 0.12PL_i(1 - e^{(-20FL)})$	Modified from Hughes and Dill (1990)
NC	Number of 0.1 × 0.1 m cells used to make the cross section discrete	Sufficient to blanket cross section	This paper
k	Subscript designating a particular cell	k = 1, ..., NC	This paper
AC	Area of a cell (m^2)	AC = 0.1 × 0.1 = 0.01	This paper
V_k	Water velocity in cell k (m·s^{-1})	Estimated from field measurements	This paper
NR	Number of radials originating from focal point and used to describe capture area	NR = 35	Following Guensch et al. (2001)
j	Subscript designating a particular radial	j = 1, ..., NR	This paper
$AVEL_j$	Mean water velocity along radial j from focal point to point of interest (m·s^{-1})	Estimated from V_k during calculation of $MCD_{i,j}$, as described in text	This paper
VMAX	Maximum sustainable swimming speed (m·s^{-1})	$VMAX = 0.87FL^{0.19}$	Modified from Hughes and Dill (1990)
$MCD_{i,j}$	Maximum lateral capture distance for prey in length class i along radial j (m)	Calculated using iteration as described in text	This paper
CA_i	Polygon formed by projecting the fish's capture area for prey in length class i onto cross section	Polygon intersects each radial $MCD_{i,j}$ metres from fish's focal point, j = 1, ..., NR	Guensch et al. (2001)
$PD_{i,k}$	Probability that searching fish will detect a prey in length class i approaching cell k	$PD_{i,k}$ = 1 if center of cell k lies inside CA_i; $PD_{i,k}$ = 0 otherwise	This paper
PAM_i	Proportion of prey in length class i that fish's morphology will allow it to eat	PAM_i = Proportion of length class falling between PLMIN and PLMAX	Following Wankowski (1979) and Hayes et al. (2000)
λ_i	Encounter rate for prey in length class i (number·s^{-1})	$\lambda_i = \sum_{k=1}^{NC} PD_{i,k} PC_i V_k AC$	This paper
h_i	Interception (handling) time of fish for prey in length class i (s)	$h_i = RD_i/VMAX$	Hughes (1998)

© 2003 NRC Canada

Table 1 (*concluded*).

Parameter	Definition	Equation or method of computation	Source
PAC_i	Probability fish will attack prey in length class i, given detection	$PAC_i = 1$ if $\frac{PEA_i}{h_i} \geq \frac{\sum_{j=i+1}^{NP} PAM_j \lambda_j PEA_j}{1 + \sum_{j=i+1}^{NP} PAM_j \lambda_j h_j}$; $PAC_i = 0$ otherwise	Charnov (1976)
CR_i	Capture rate for prey in length class i (numbers·s^{-1})	$CR_i = \frac{PAM_i PAC_i \lambda_i}{1 + \sum_{j=1}^{NP} PAM_j PAC_j \lambda_j h_j}$	Based on Holling (1959)
TCR	Total capture rate for prey in all length classes (numbers·s^{-1})	$TCR = \sum_{i=1}^{NP} CR_i$	This paper
GEI	Gross energy intake (J·s^{-1})	$GEI = \sum_{i=1}^{NP} CR_i PEA_i$	This paper

by subtracting the fish's starting coordinates and adding the result to the fish's median focal point coordinates. We then rotated these normalized detection coordinates into the same horizontal plane as the focal point, preserving the horizontal bearing and the distance between the fish's starting point and the prey detection location. We then projected that part of each prey size specific predicted reaction volume lying above this plane (see Fig. 3) onto the plane. This presentation allows a visual assessment of the model's assumption that prey will be detected on the surface of the reaction volume. For this analysis, we selected only prey detected while the fish was searching from its focal point, excluding prey captures that occurred when the fish was still off the bottom after a prior prey capture.

To supplement our analysis of the model's ability to predict the size and shape of the fish's reaction volume, we fitted a two-dimensional (2-D) reaction field to the observed prey detection locations and compared this to the size and shape of a 2-D projection of the 3-D reaction volume (Fig. 3) predicted by the model. The fitted reaction field has a shape like a pie slice and points downstream, so that its point rests on the fish's focal point. We specify the size and shape of the fitted reaction field using the two angles between its left and right edges and the upstream–downstream axis, which sum to give its apical angle, and the radius of the resulting arc.

To fit the reaction field to a set of prey detection locations, we selected an angle for the left side just large enough to include 95% of the total number of prey detected on that side and an angle for the right side just large enough to include 95% of the total number of prey detected on that side. We then chose a radius that was just large enough to include 90% of the distances between prey detection locations and the fish's focal point. This technique provided an empirically fitted reaction field that included 80–90% of prey detection locations and gave a fairly satisfying fit to the observed data. Next we used randomization techniques (Manly 1991) to calculate the probability that the observed differences between the shape and size of the predicted and fitted reaction fields could be produced by chance. We constructed a conservative test by allowing modest ranges for radius (0.5–1.5 m) and apical angle (30–180 degrees) in our null model.

Interception speed

To test the assumption that fish will intercept prey at their maximum sustainable swimming speed, we calculated each fish's actual interception speeds, dividing the distance traveled during prey interception by the time taken to intercept the prey. Following Hughes and Dill (1990), we equated the distance traveled to the distance between the fish's nose and the prey at the moment of prey detection. This calculation estimates speed relative to the water surrounding the fish.

Prey capture locations

To test the model's assumption that all prey are captured upstream of the focal point, we projected prey capture locations directly downward onto the horizontal plane and analysed the resulting 2-D distribution.

Prey capture probability

To test the model's assumption that prey capture probability is uniform across the capture area, we mapped the spatial

© 2003 NRC Canada

Fig. 2. Methods used to describe habitat in the fish's foraging area and the shape of the fish's capture area. (*a*) Depth and velocity in the foraging area are described by dividing that part of the cross section occupied by the fish into 0.1 m × 0.1 m cells, mapping field measurements of water velocity into the appropriate cells and populating empty cells by interpolating horizontally and vertically, assuming zero water velocity in the cells nearest the stream bed. (*b*) The shape of the fish's capture area is determined by plotting the observed fish position onto the cross section and drawing 35 radials from its focal point. The boundary of the capture area for prey in length class i, CA_i, is then described by clipping each radial, j, at $MCD_{i,j}$ and joining the tips of the trunkated radials. $MCD_{i,j} = [RD_i^2 - (AVEL_j RD_i/VMAX)^2]^{1/2}$, where RD_i is the fish's reaction distance to prey in length class i, $AVEL_j$ is the distance-weighted water velocity that the fish must traverse to travel $MCD_{i,j}$ along radial j, and VMAX is the fish's maximum sustainable swimming speed. This equation must be solved numerically.

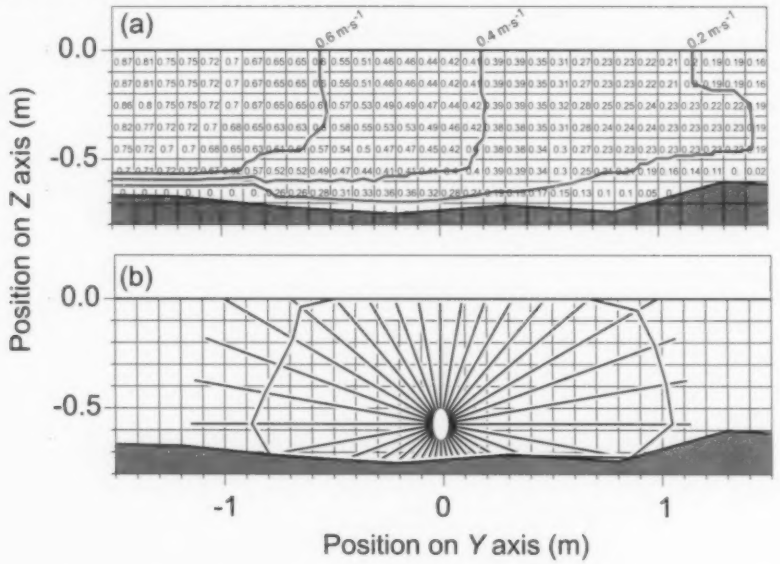

Fig. 3. A three-dimensional representation of the fish's reaction volume. The model predicts that when the fish is searching at its focal point, it will detect all prey as soon as they encounter the partial hemisphere (shaded) that forms the upstream surface of this volume.

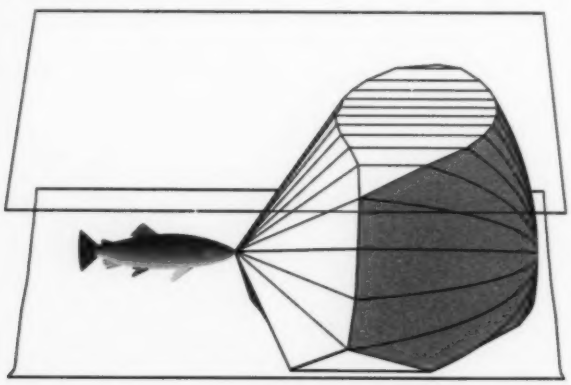

pattern of prey capture probability onto the cross section perpendicular to the flow and examined the prey capture probability contours. We estimated a capture probability for each hydraulic cell, k, by counting up all of the prey captures within that cell and dividing that sum by an estimate of the total number of potential prey passing through that cell during the time that we observed the fish. Counting the number of prey captures in each cell was simply a matter of mapping prey captures into the appropriate cell and tallying them up. Using the relevant variables (Table 1), we then estimated the number of potential prey (NPP) passing through a cell k as

$$(1) \qquad NPP = \sum_{i=1}^{NP} AC V_k PC_i PAM_i PAC_i$$

Size composition of the drift and trout diets

To test the model's ability to predict the length frequency of prey captured by trout, we compared its predictions of mean and minimum prey size with values for the diver-captured trout. We also determined how well the model could explain the difference between the size composition of the drift and the diet of the diver-captured trout. To do this we followed the work of Dunbrack and Dill (1983) and compared our model's predictions with those of a simpler model in which the trout are assumed to feed unselectively on the different size classes of drifting invertebrates, consuming each length class in the same proportion as it occurred in the drift.

Prey capture rates and gross energy intake rate

To test the model's ability to predict the fish's prey capture rate, we compared its predictions of total capture rate (TCR, number·h^{-1}; Table 1) with observed prey capture rates for each of the five trout observed. To test the model's prediction of the fish's gross energy intake rate, we estimated

© 2003 NRC Canada

Fig. 4. Comparison of (*a–e*) predicted and (*f–j*) fitted reaction volumes superimposed on observed prey detection locations. Predicted volumes for the three largest prey length classes for each of the five trout (*Salmo trutta*) are shown, and fitted reactions fields encompass 80–90% of detection locations, as described in the text. Prey detection locations have been rotated into the two-dimensional plane so as to preserve distance and horizontal bearing from the fish's focal point. Only prey detected while the fish was searching at its focal point are included, and all prey detection locations have been normalized to the fish's median focal point location. Grid spacing is 0.2 m.

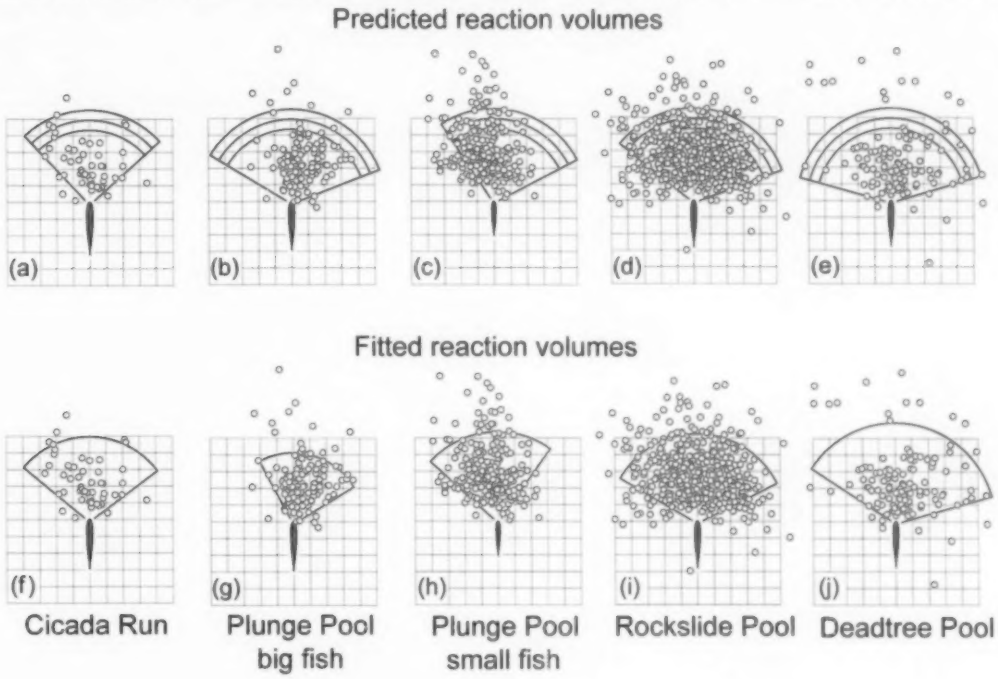

the actual gross energy intake for the fish that we observed using the size composition of the diet for the diver-captured trout, observed capture rates, and equations relating prey size to assimilable energy content (Table 1). We then compared these estimates with the model's predictions of gross energy intake rate for the four largest trout that we videotaped, which closely resembled the diver-captured trout in size.

Results

Prey detection locations

Our results do not support the model's assumption that a brown trout searching from its focal point will initiate interception as prey hit the upstream surface of its reaction volume. In fact, in most cases, fish initiated interception when prey were well within the predicted reaction volume, (Fig. 4), and mean reaction distances for the five fish averaged only 66% (range 57–73%) of the model's predictions. However, the reaction volume predicted by the model does provide a fairly reasonable outer boundary for the observed prey detection locations, as can be seen by comparing predicted and fitted reaction volumes (Fig. 4). The predicted reaction volumes had a mean apical angle of 117 degees vs. an observed mean of 105 degrees, a predicted mean radius of 1.14 m vs. an observed mean of 1.05 m, and a mean area of 1.32 m^2 vs. an observed mean of 1.06 m^2. Our randomization test showed that the probability of fits this good being obtained by chance was 0.01 for apical angle, 0.02 for radius, and 0.03 for projected area. Because our test is conservative, we can conclude that the model's predictions of the shape and size of the fish's reaction volume is much better than we could expect from chance alone.

Interception speed

Our results do not support the assumption that brown trout intercept prey at VMAX, our estimate of their maximum sustainable swimming speed. In fact, fish used a fairly wide range of interception speeds distributed well below VMAX (Fig. 5). Values for VMAX ranged between 0.74 and 0.79 $m \cdot s^{-1}$, depending on fish size, whereas observed mean interception speeds averaged only 0.47 $m \cdot s^{-1}$, ranging from 0.33 to 0.59 $m \cdot s^{-1}$. The only fish observed to intercept prey at speeds greater than VMAX was the small fish in Plunge Pool.

One interesting and unanticipated finding was that the trout's mean interception speed was very similar to mean prey speed (Fig. 5). In fact, regression analysis showed that mean prey speed "explained" 97% of the variation in mean interception speed ($p < 0.002$). The slope of this regression was 0.82, showing that mean interception speed increased less quickly than mean prey velocity. At low water velocities, fish tend to move a little faster than their prey, and in faster water, they tend to move more slowly.

Interception speed also increased with the distance upstream to the prey, p values for linear regressions were be-

© 2003 NRC Canada

Fig. 5. Frequency distributions of prey interception speeds in relation to maximum sustainable swimming speed, VMAX, for each of the five trout (*Salmo trutta*): (*a*) Cicada Run; (*b*) Plunge Pool big fish; (*c*) Plunge Pool small fish; (*d*) Rockslide Pool; and (*e*) Deadtree Pool. Vertical lines denote VMAX, mean interception speed, and the mean downstream speed of the prey.

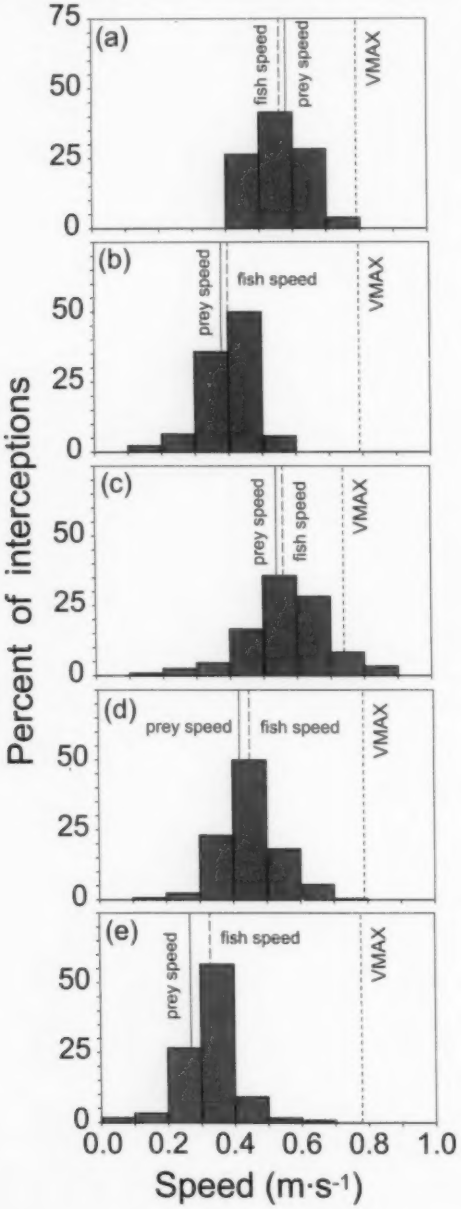

low 0.005 for four fish and nonsignificant for the fish in Deadtree Pool; R^2 values ranged from 0.01 to 0.17.

Trout did not make any extra effort to speed up interception of prey detected at large angles to the upstream–downstream axis. This finding is important in relation to the model's assumption that fish must capture prey upstream of their focal point, because these prey are particularly likely to be swept downstream of the focal point before capture. Regression analysis showed that prey detection angle was not significantly correlated with interception speed for three fish and was actually negatively correlated with interception speed for fish of the Cicada Run ($p < 0.001$, $R^2 = 0.21$) and Rockslide Pool ($p < 0.001$, $R^2 = 0.05$).

Prey capture locations

Trout did not capture all prey upstream of their focal point, as assumed by the foraging model (Fig. 6). In fact, of the 1326 prey captured by the five fish, only 31% were captured upstream of the fish's focal point (range 25–51%), whereas 69% were captured downstream. There was no relationship between mean prey speed and the proportion of prey that each fish captured downstream of its focal point.

Prey capture locations tended to fall within a crescent shape balanced on the fish's focal point, and the tips of this crescent are swept downstream as water velocity increases (Fig. 6). Several processes combine to produce this pattern. First, the fish's mean interception speed closely matches the mean prey speed, and it does not swim faster to catch prey detected at particularly large angles to the upstream–downstream axis. Simple geometric analysis shows that this will result in the fish being swept further downstream as it intercepts prey detected at increasingly large angles. Because prey detected at greater lateral distance tend to be detected at wider angles (linear regression, $p < 0.001$, $R^2 = 0.42$) and take longer to intercept, they tended to be captured further downstream than prey passing closer to the fish's focal point. In faster water, this effect is magnified by the fact that the fish's interception speed does not increase as rapidly as prey speed (Fig. 5). This effect was particularly evident in Rockslide Pool, where water velocity was 0.6 $m \cdot s^{-1}$ at the left tip of the prey capture crescent but only 0.2 $m \cdot s^{-1}$ at the right tip. As a result, the crescent is asymmetrical, the left arm being swept further downstream than the right.

Another interesting feature of the prey capture field is that it is more compressed in the upstream–downstream direction than the prey detection field (Fig. 6). This is not surprising because prey detected at greater distances take longer to intercept, and as a result, they travel further between detection and capture. This telescopes the prey capture field despite the fact that fish intercept prey detected at greater upstream distances more rapidly, the extra speed does not offset the added distance.

Prey capture probability

Our results do not support the model's assumption that capture probability will be uniform across the fish's capture area. Maximal prey capture probabilities close to the fish's focal point were in excess of 100% but dropped rapidly to less than about 20% at the boundary of the capture area for the smallest prey expected to be in the diet (Fig. 7). The shape of the prey capture probability contours varied from being quite circular for the fish in Deadtree Pool and the big fish in Plunge Pool to an increasingly flattened ellipse for the fish in Rockslide Pool, the small fish in Plunge Pool, and the fish in Cicada Run (Fig. 7). The prey capture probability contours for the fish in Cicada Run were quite symmetrical around the fish's focal point, both laterally and vertically,

© 2003 NRC Canada

Fig. 6. Prey (*a–e*) detection and (*f–j*) capture locations projected directly downwards onto the horizontal plane. Note that this projection of prey detection locations is not equivalent to the projection in Fig. 4. Only prey detected while the fish was searching at its focal point have been included, and all prey detection locations have been normalized to the fish's median focal point location. Grid spacing is 0.2 m.

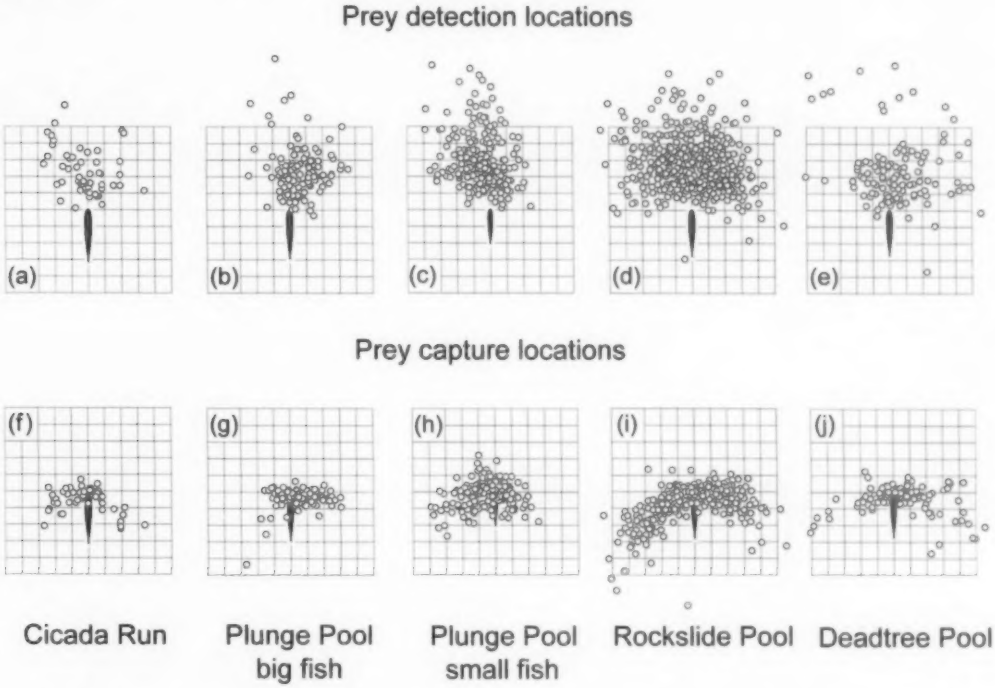

much less so for fish in the other locations. The prey capture probability contours for the small fish in Plunge Pool have a plume-like extension at the water's surface. This is probably an artifact because this fish was capturing some surface prey but our model assumes that all prey are subsurface. Linear regression showed that there was no change in the mean lateral distance traveled to capture prey over the 139 min that we observed the fish in Rockslide Pool. This suggests that the relationship between lateral distance and prey capture probability is rather stable over time.

Size composition of the diet

The model converted our estimate of the size composition of the drift (Table 2) into rather accurate predictions of the size composition of the diet for the eight diver-captured trout (Fig. 8). We restricted our test of the model's predictions to the four largest fish (mean length 0.57 m, range 0.55–0.63 m) because these were of similar size to the diver-caught trout (mean length 0.6 m, range 0.54–0.65 m). The model's prediction of the minimum prey size was accurate at 6 mm; only 3% of the 482 prey eaten by the diver-captured trout were smaller than this. The model's prediction of mean prey size was 8.0 mm, close to the observed 7.6 mm (95% confidence interval, 7.53–7.68 mm). The mean length of invertebrates in the drift was only 3.9 mm. The model explained 96% of the variance left unexplained by a null model in which the fish ate prey in direct proportion to their abundance in the drift.

Prey capture and energy intake rates

Observed prey capture rates (number·h^{-1}) averaged only 55% (range 36–67%) of the rates predicted by the model (Table 3). Instead of capturing an average of 87% (range 83–92%) of prey passing through their capture areas, as predicted by Holling's disk equation, the fish caught only 48% (range 39–59%). (Note: 0.48/0.87 = 0.55.) Charnov's (1976) prey choice model predicted that fish should not drop small prey from their diet. Predicted foraging rates were positively correlated with observed foraging rates, but linear regression showed that the relationship was nonsignificant (p = 0.3, R^2 = 0.35). Our estimate of observed gross energy intake rate (J·h^{-1}) for the four largest fish was only 45% as large as predicted by the model (range 31–57%). This is lower than the 55% value for capture rate because the model predicted a slightly larger mean prey size than we observed for the diver-captured trout.

Discussion

The foraging model tested in this paper overestimated the foraging rate and gross energy intake rate of large brown trout feeding in a New Zealand river by a factor of two. Observed prey capture rates (number·h^{-1}) averaged only 55% of the model's predictions, whereas our best estimates of the gross energy intake (J·h^{-1}) for the four largest fish averaged only 45% of the model's predictions.

A consideration of the possible errors and biases in our work suggests that the discrepancy between the observed

© 2003 NRC Canada

Fig. 7. Distribution of prey capture locations in relation to depth, velocity, and predicted capture areas for prey large enough to be included in each fish's diet (*a–e*) and prey capture probability contours (*f–j*). All prey capture locations are included and have been normalized to the fish's median focal point location. (*a* and *f*) Cicada Run; (*b* and *g*) Plunge Pool big fish; (*c* and *h*) Plunge Pool small fish; (*d* and *i*) Rockslide Pool; (*e* and *j*) Deadtree Pool.

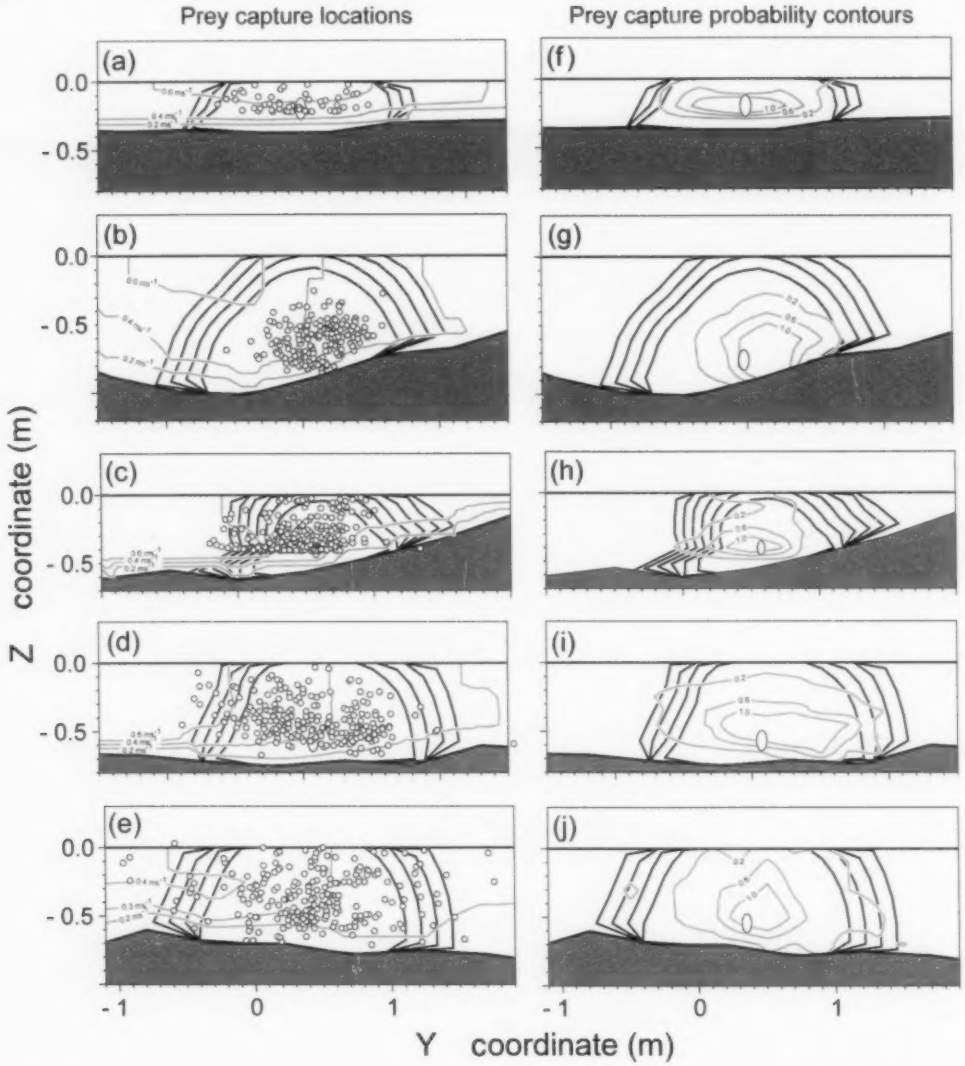

and predicted foraging rates may be even greater than suggested by our analyses. One particular cause for concern in this regard is the fact that fish captured about twice as many prey from the area around their focal point as we predicted from our estimates of drift density. This might be explained by the fact the fish ate some prey smaller than the minimum size predicted by the model. If these were captured from the area close to the fish's focal point, they might account for the unexpectedly high number of prey captures there. Calculations suggest that the percentage of smaller than predicted prey would have to be in the 6–10% range to account for the observed pattern, whereas our diet analysis of the diver-caught trout showed that about 3% of their prey were smaller than predicted. Another possible explanation for the higher than expected prey capture probabilites close to the focal point is that we underestimated drift density or overestimated prey capture rates. Either bias is plausable, and if corrected, both would increase the degree to which the model overestimates the fish's foraging rate.

The model's error in predicting gross energy intake has serious implications for researchers interested in predicting fish growth rates (e.g., Hughes 1998; Hayes et al. 2000) because a twofold error in estimating feeding rates will dramatically affect predictions of growth when fish are food-limited (e.g., Elliott and Hurley 1999). The model's error may be less worrying for researchers interested in predicting habitat selection (e.g., Hughes 1992; Guensch et al. 2001; Rosenfeld and Boss 2001), provided that the model accu-

© 2003 NRC Canada

Table 2. Mean length class specific drift density during the five trout observation periods.

Length class (mm)	Drift density (number·m^{-3})
2.5	1.456
3.5	1.036
4.5	0.315
5.5	0.165
6.5	0.178
7.5	0.179
8.5	0.119
9.5	0.039
>6.0	0.679

rately maps the relative potential for net energy intake onto the habitat.

The inaccuracy of the existing model is unsatisfactory. In the following discussion we critically assess its components, develop suggestions on how to use it as the framework for a more accurate model of drift-feeding, and suggest how to compensate for its deficiencies in the interim.

Our results show that most of the model's inaccuracy results from its incorrect assumption that prey detection probabilities will be uniform and high across each capture area. In fact, we have shown that prey capture probability declines rapidly with increasing distance from the fish's focal point. This decline is probably a reliable reflection of prey detection probability because Charnov's (1976) model showed that fish should always attack prey large enough to be retained by the gill rakers. A similar decline in prey detection probability with increasing distance from the focal point has been demonstrated experimentally by Hill and Grossman (1993). Their work suggested mean prey capture probabilities in the 80–90% range and a knife-edged decline in capture probability at the edge of the fish's reaction volume. This knife-edged decline is also consistent with Dunbrack and Dill's (1984) work on the reaction volume of juvenile coho salmon (*Oncorhynchus kisutch*) and Wankowski's (1981) work on prey detection by juvenile Atlantic salmon (*Salmo salar*). The knife-edged decline observed in these studies may be a consequence of high contrast between the prey and the background in the tank environment. Our work in the natural environment shows that mean prey capture probabilities can be much lower than suggested by Hill and Grossman and also that capture probability can decline steeply well within the fish's foraging area, a result that is more consistent with the results of Luecke and O'Brien's (1981) work on the reaction volume of bluegill sunfish (*Lepomis macrochirus*).

Our analyses also show that the way in which prey detection probability declines with distance can depend on direction (lateral or vertical) and on the physical characteristics in the fish's foraging area. Prey capture probability contours can be fairly circular (Deadtree Pool), laterally elongated (Cicada Run), or lopsided (the big fish in Plunge Pool). Some of this variation is undoubtedly in response to water depth, velocity, and the presence of bubble plumes near the fish's foraging area. The shape of these contours may also be, to some extent, an artifact of vertical or lateral gradients in drift density. These would distort the contours because the model assumes uniform drift density. No existing model of prey detection is capable of predicting or explaining these observations on the spatial variability of prey detection probability.

Fig. 8. Comparison of (*a*) length–frequency distribution of invertebrates in the drift, (*b*) predicted length–frequency distribution of the diet for the four largest trout (*Salmo trutta*), and (*c*) observed length–frequency distribution of the diet for the eight diver-captured trout.

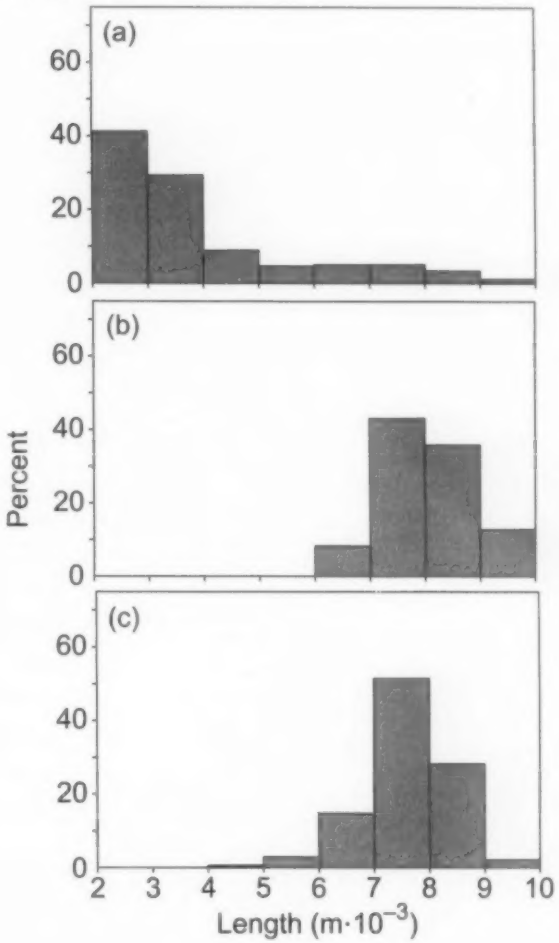

The model made impressively accurate predictions of prey size for the diver-caught trout. Nevertheless, the apparently small difference between predicted and observed prey size is magnified into a significant error when converting prey capture rate to energy intake rate. The model predicted a slightly larger mean prey size (8.0 mm) than the mean prey size actually consumed by the diver-caught trout (7.6 mm). As a result, it overestimates the energy content of each prey by about 22%. This result shows that although we, and other researchers (e.g., Dunbrack and Dill 1983; Grant and Noakes 1986), have had considerable success in predicting the length frequency of the diet for drift-feeders, these predictions need to be very accurate to support reliable predictions of gross energy intake rate.

© 2003 NRC Canada

Table 3. Observed vs. predicted foraging rates and estimated vs. predicted gross energy intake rates for the five trout.

Location of fish being videotaped	No. of prey·h^{-1} observed	No. of prey·h^{-1} predicted	No. of prey·h^{-1} observed/predicted	Gross energy intake (J·h^{-1}) estimated	Gross energy intake (J·h^{-1}) predicted	Gross energy intake (J·h^{-1}) estimated/predicted
Cicada Run	140	220	0.64	6492	11 929	0.54
Plunge Pool Big	180	500	0.36	8347	27 111	0.31
Plunge Pool Small	255	546	0.47	NA	NA	NA
Rockslide Pool	249	374	0.67	11 825	29 605	0.40
Deadtree Pool	263	432	0.61	11 547	20 279	0.57

Note: NA, not available.

To balance these rather stringent criticisms of the model, we should acknowledge that it performed some tasks rather well. It made reasonably accurate predictions of the minimum prey size, showing that Wankowski's (1979) gill raker spacing constraint for small Atlantic salmon can be extrapolated to predict minimum prey size for much larger brown trout. It also made very reasonable predictions of the length–frequency composition of the diet. This shows that the reaction distance equations Hughes and Dill (1990) developed from Schmidt and O'Brien's (1982) data on small Arctic grayling make reasonable predictions of the way in which the brown trout's reaction distance scales with prey size. These reaction distance equations also combine with the model's assumptions about the factors influencing the apical angle of the fish's reaction volume, and the width of the foraging area, to give very reasonable predictions of the outer boundary of the reaction volume.

On the other hand, despite these successes in predicting the radius and apical angle of the reaction volume, our results show that all of the assumptions that the model uses to make these predictions are incorrect. Prey detection locations are distributed throughout the reaction volume, not concentrated on its surface, and fish intercept prey at speeds much lower than their maximum sustainable swimming speed and capture most of their prey downstream of their focal point. Furthermore, fish do not seem to make any special effort to avoid capturing prey downstream of their focal point, as prey detected at large bearings are not intercepted especially quickly. Other studies have also shown that drift-feeders often intercept prey downstream of their focal points (Stradmeyer and Thorpe 1987; Keeley and Grant 1995). These assumptions were included in the original models (Hughes and Dill 1990; Kiflawi and Genin 1997) to allow them to predict a narrowing of the fish's foraging area with increasing water velocity, an important relationship observed experimentally (Hill and Grossman 1993; O'Brien and Showalter 1993) and essential in any model of drift-feeding. Without such a relationship, these models would not be able to predict how water velocity will influence energy intake rate or explain the existence of an optimum velocity for drift-feeding.

Taken together, these criticisms show that the model that we tested has some realistic elements but fails to capture the essential mechanisms determining the energy intake rate of drift-feeding fish. We need to use the lessons learned from this critique to build better models.

Perhaps the most important lesson from our work is that we need to develop better models of prey detection by drift-feeding fish. Ideally such models will predict the shape of the reaction volume and the 3-D pattern of prey detection locations within this volume. It is very possible that the effect of water velocity on the apical angle and width of the fish's reaction volume (e.g., O'Brien and Showalter 1993) is actually determined during the prey detection process and is not the consequence of constraints on the geometry of prey interception maneuvers, as suggested by Hughes and Dill (1990) and Kiflawi and Genin (1997). O'Brien and Showalter's (1993) observations that small amounts of detritus added to the water can cause the fish to narrow the apical angle of its reaction volume are particularly interesting in this regard. They suggest that constraints on the fish's information-processing capacity may cause it to narrow its reaction volume as the task of prey detection becomes more demanding. The behavior of the large fish in Plunge Pool is consistent with this observation; this fish had a much smaller reaction volume than we predicted and was the only fish to be foraging in close proximity to a plume of entrained air bubbles. These bubbles almost certainly would have made prey detection more difficult, and because they passed to the fish's left, they may also account for its asymmetrical reaction volume. It is also important to remember that fish can reduce their reaction distance and energy intake below the maximum set by visual and information-processing constraints. Fish may reduce their reaction distance when following a lower than maximal growth trajectory (Huntingford et al. 1988) or in response to heightened predation risk (Dill and Fraser 1984). At the moment, there are no mechanistic or statistical models capable of predicting how fish size, prey size, water velocity, and direction from the focal point will influence prey detection probability, but there is great scope for both theoretical and experimental work on this problem. Integrating the effects of life history and predation risk into these models will also be a challenge.

Another lesson is that we need better mechanistic models of prey interception. Ideally such models might predict how prey detection location and water velocity will influence the handling time (interception time) and the energetic costs of prey capture. Such models would improve our ability to predict net energy intake rate in several ways. First, they would allow us to make better predictions of the fish's energy expenditure. Second, they would allow us to apply Charnov's (1976) prey model to determine whether rate-maximizing fish should drop laterally distant prey from their diets as water velocity increases. If so, this might explain why fish narrow their foraging as water velocity increases. Finally, the predictive power of a maneuver model might prove essential to a realistic prey detection model. This is because when information processing capacity limits a fish's prey detection

© 2003 NRC Canada

ability, it should focus its attention on areas where it will be most profitable to detect prey. A maneuver model could be used to predict where this will be. Currently there are no models of the way fish should intercept prey and there is plenty of opportunity for interesting work in this area. Our observation that interception speed closely matches prey speed might provide a clue as to how such models should be designed for large fish, suggesting that the fish may be using inertial effects to their advantage when maneuvering to capture prey in vertical and lateral velocity shears.

It may be some time before researchers successfully address the problems identified here with existing models. In the interim, it would be useful for biologists using the models to have a simple technique to improve their predictions. For large brown trout, we suggest applying empirical correction factors: multiplying the predictions of the model by 0.55 for prey capture rate and 0.45 for gross energy intake rate; using mean prey speed (i.e., mean water velocity) rather than maximum sustainable swimming speed to estimate the cost of prey interception; and assuming that prey interception distance is only 63% of the value predicted by the model.

In summary, our test of an updated version of Hughes and Dill's (1990) model shows that it overestimates the fish's gross energy intake by a factor of two. We also found that the conceptual basis of existing mechanistic models of drift-feeding is flawed and needs revision. We particularly need to develop integrated models of prey detection and prey interception. Despite these problems, our test showed that some components of the model worked well: it made accurate predictions of the size of the prey detection field and size composition of the diet. These results suggest that if we can build more realistic models of prey detection and prey capture, it should be possible to develop models that make accurate predictions of the behavior and net energy intake rates of drift-feeding fish.

Acknowledgements

We thank Rowan Strickland for capturing trout, Aaron Quarterman for his assistance with the organization of equipment and fieldwork, and the Department of Conservation for providing research permits to work in Nelson Lakes National Park. We also thank Lon Kelly, Senior Technical Specialist, and the U.S. Department of the Interior, Bureau of Land Management, for developing the software tools used for 3-D videographic analysis of fish–habitat interactions. The study was funded by the Foundation for Research, Science and Technology (contract No. CAW802), and Fish and Game New Zealand.

References

Armstrong, J.D. 1997. Self-thinning in juvenile sea trout and other salmonid fishes revisited. J. Anim. Ecol. **66**: 519–526.

Bachman, R.A. 1984. Foraging behavior of free-ranging wild and hatchery brown trout in a stream. Trans. Am. Fish. Soc. **113**: 1–32.

Baker, E.A., and Coon, T.G. 1997. Development and evaluation of alternative habitat suitability criteria for brook trout. Trans. Am. Fish. Soc. **126**: 65–76.

Braaten, P.J., Dey, P.D., and Annear, T.C. 1997. Development and evaluation of a bioenergetic-based habitat suitability criteria for trout. Regul. Rivers Res. Manag. **13**: 345–356.

Charnov, E.L. 1976. Optimal foraging: attack strategy of a mantid. Am. Nat. **110**: 141–151.

Cummins, K.W., and Wuycheck, J.C. 1971. Caloric equivalents for investigations in ecological energetics. Mitt. Int. Ver. Theor. Angew. Limnol. **18**: 1–158.

Dill, L.M., and Fraser, A.H.G. 1984. Risk of predation and the feeding behavior of juvenile coho salmon (*Oncorhynchus kisutch*). Behav. Ecol. Sociobiol. **16**: 65–71.

Dunbrack, R.L., and Dill, L.M. 1983. A model of size dependent surface feeding in a stream dwelling salmonid. Environ. Biol. Fishes, **8**: 203–216.

Dunbrack, R.L., and Dill, L.M. 1984. Three-dimensional prey reaction field of the juvenile coho salmon (*Oncorhynchus kisutch*). Can. J. Fish. Aquat. Sci. **41**: 1176–1182.

Elliott, J.M. 1982. The effects of temperature and ration size on the growth and energetics of salmonids in captivity. Comp. Biochem. Physiol. **73**: 81–91.

Elliott, J.M., and Hurley, M.A. 1999. A new energetics model for brown trout, *Salmo trutta*. Freshwater Biol. **42**: 235–246.

Fausch, K.D. 1984. Profitable stream positions for salmonids: relating specific growth rate to net energy gain. Can. J. Zool. **62**: 441–451.

Giles, N. 1980. A stomach sampler for use on live fish. J. Fish Biol. **16**: 441–444.

Grant, J.W.A., and Noakes, D.L.G. 1986. A test of a size-selective predation model with juvenile brook charr, *Salvelinus fontinalis*. J. Fish Biol. **29**(Suppl. A): 15–23.

Guensch, G.R., Hardy, T.B., and Addley, R.C. 2001. Examining feeding strategies and position choice of drift-feeding salmonids using an individual-based, mechanistic foraging model. Can. J. Fish. Aquat. Sci. **58**: 446–457.

Hayes, J.W., and Jowett, I.G. 1994. Microhabitat models of large drift-feeding brown trout in three New Zealand rivers. Trans. Am. Fish. Soc. **14**: 710–725.

Hayes, J.W., Stark, J.D., and Shearer, K.A. 2000. Development and test of a whole-lifetime foraging and bioenergetics growth model for drift-feeding brown trout. Trans. Am. Fish. Soc. **129**: 315–332.

Hill, J., and Grossman, G.H. 1993. An energetic model of microhabitat use for rainbow trout and rosyside dace. Ecology, **74**: 685–698.

Holling, C.S. 1959. Some characteristics of simple types of predation and parasitism. Can. Entomol. **91**: 385–398.

Hughes, N.F. 1992. Selection of positions by drift-feeding salmonids in dominance hierarchies: model and test for Arctic grayling, *Thymallus arcticus*, in subarctic mountain streams, interior Alaska. Can. J. Fish. Aquat. Sci. **49**: 1999–2008.

Hughes, N.F. 1998. A model of habitat selection by drift-feeding stream salmonids at different scales. Ecology, **79**: 281–294.

Hughes, N.F., and Dill, L.M. 1990. Position choice by drift-feeding salmonids: model and test for Arctic grayling (*Thymallus arcticus*) in subarctic mountain streams, interior Alaska. Can. J. Fish. Aquat. Sci. **47**: 2039–2048.

Hughes, N.F., and Kelly, L.H. 1996*a*. New techniques for 3-D video tracking of fish swimming movements in still or flowing water. Can. J. Fish. Aquat. Sci. **53**: 2473–2483.

Hughes, N.F., and Kelly, L.H. 1996*b*. A hydrodynamic model for estimating the energetic cost of swimming maneuvers from a description of their geometry and dynamics. Can. J. Fish. Aquat. Sci. **53**: 2484–2493.

Huntingford, F.A., Metcalfe, N.B., and Thorpe, J.E. 1988. Choice of feeding station in Atlantic salmon, *Salmo salar*, parr: effects

© 2003 NRC Canada

of predation risk, season and life history strategy. J. Fish Biol. **33**: 917–924.

Keeley, E.R., and Grant, J.W.A. 1995. Allometric and environmental correlates of territory size in juvenile Atlantic salmon (*Salmo salar*). Can. J. Fish. Aquat. Sci. **52**: 186–196.

Kiflawi, M., and Genin, A. 1997. Prey flux manipulation and the feeding rates of reef-dwelling planktivorous fish. Ecology, **78**: 1062–1077.

Luecke, C., and O'Brien, W.J. 1981. Prey location volume of a planktivorous fish: a new measure of prey vulnerability. Can. J. Fish. Aquat. Sci. **38**: 1264–1270.

Manly, B.F.J. 1991. Randomization and Monte Carlo methods in biology. Chapman and Hall, New York.

Nislow, K.H., Folt, C.L., and Parrish, D.L. 2000. Spatially explicit bioenergetic analysis of habitat quality for age-0 Atlantic salmon. Trans. Am. Fish. Soc. **129**: 1067–1081.

O'Brien, W.J., and Showalter, J.J. 1993. Effects of current velocity and suspended debris on the drift feeding of Arctic grayling. Trans. Am. Fish. Soc. **122**: 609–615.

Ringler, N.H., and Brodowski, D.F. 1983. Functional response of brown trout *(Salmo trutta* L.) to invertebrate drift. J. Freshw. Ecol. **2**: 45–57.

Rosenfeld, J.R., and Boss, S. 2001. Fitness consequences of habitat use for juvenile cutthroat trout: energetic costs and benefits in pools and riffles. Can. J. Fish. Aquat. Sci. **58**: 585–593.

Schmidt, D., and O'Brien, W.J. 1982. Planktivourous feeding ecology of Arctic grayling (*Thymallus arcticus*). Can. J. Fish. Aquat. Sci. **39**: 475–482.

Smock, L.A. 1980. Relationships between body size and biomass of aquatic insects. Freshwater Biol. **10**: 375–383.

Stradmeyer, L., and Thorpe, J.E. 1987. Feeding behaviour of wild Atlantic salmon, *Salmo salar* L., parr in mid- to late summer in a Scottish river. Aquacult. Fish. Manag. **18**: 33–49.

Wankowski, J.W. 1979. Morphological limitations, prey size selectivity, and growth response of juvenile Atlantic salmon (*Salmo salar* L.). J. Fish Biol. **14**: 89–100.

Wankowski, J.W. 1981. Behavioural aspects of predation by juvenile Atlantic salmon (*Salmo salar* L.) on particulate, drifting prey. Anim. Behav. **29**: 557–571.

© 2003 NRC Canada

Cladoceran body length and Secchi disk transparency in northeastern U.S. lakes

Richard S. Stemberger and Eric K. Miller

Abstract: Mean cladoceran body length of 59 northeastern U.S. lakes was estimated from functional groups that broadly define taxonomic, body size, and grazing potential. Multiple regression of body length, color, and chlorophyll *a* or total phosphorus against Secchi disk transparency explained 72% and 83% of the variation across lakes, respectively. Analysis that included body length, color, and particulate carbon, a proxy for light backscattering and absorption by suspended organic particles, explained 85% of the variance in transparency. Body length was as important a predictor of water clarity as chemical factors. Furthermore, body length was significantly correlated to temporal variation in transparency within lakes. Because cladocerans primarily filter organic particles in size ranges having high light attenuation efficiencies, body length was consistently more strongly correlated to transparency than to chlorophyll *a*. Monitoring cladoceran body length should help to distinguish changes in lake transparency due to nutrient loading from changes that reflect fish population size structure and predation intensity on zooplankton. This simple size index can greatly increase the interpretative value of Secchi transparency observations to lake managers.

Résumé : Nous avons estimé la longueur corporelle moyenne des cladocères de 59 lacs du nord-est des États-Unis à partir des groupes fonctionnels qui définissent de façon générale l'identité taxonomique, la taille du corps et le potentiel de broutage. Des régressions multiples de la longueur du corps, de la couleur, de la chlorophylle *a* ou alors du phosphore total sur la transparence mesurée au disque de Secchi expliquent respectivement 72 et 83 % de la variation entre les lacs. Une analyse qui inclut la longueur du corps, la couleur et le carbone particulaire (une variable qui remplace la rétrodispersion de la lumière et l'absorption par les particules organiques en suspension) explique 85 % des la variance de la transparence. La longueur du corps est une variable prédictive de la clarté de l'eau aussi importante que le sont les facteurs chimiques. De plus, la longueur du corps est en corrélation significative avec la variation temporelle de la transparence de l'eau dans les lacs. Parce que les cladocères récoltent par filtration surtout une gamme de tailles de particules organiques qui atténuent fortement la lumière, les longueurs du corps sont toujours plus fortement corrélées à la transparence qu'à la chlorophylle *a*. La surveillance des longueurs des cladocères devrait permettre de distinguer les changements dans la transparence des lacs reliés aux charges de nutriments de ceux qui sont dus à la structure en taille des populations de poissons et à l'intensité de la prédation sur le zooplancton. Ce simple indice de taille peut augmenter considérablement la valeur interprétative des mesures de transparence au disque de Secchi pour les gestionnaires des lacs.

[Traduit par la Rédaction]

Introduction

Secchi disk transparency is perhaps the most widely measured optical property of lakes. It is commonly used as an indicator of lake trophic condition because it is easily measured and has clear intuitive meaning regarding water quality as a function of phytoplankton production (Edmondson 1980; Preisendorfer 1986). Factors that control transparency also affect thermal inputs and the depth of the mixing layer (Mazumder et al. 1990; Fee et al. 1996).

The primary factors that affect transparency include (1) absorption and scattering of light by water molecules, (2) absorption of incident light by colored dissolved organic and particulate matter, and (3) and backscattering of incident light by suspended organic particles such as bacteria, phytoplankton, and detritus and suspended minerals such as clay and calcite. Upward irradiance from backscattering reduces the visual contrast between the Secchi disk and the viewer at the surface. The Secchi disk vanishes at the depth at which contrast from background luminance and light intensity falls below a threshold of human vision (Davies-Colley et al. 1993).

Factors that affect particle concentrations in the near-surface waters or alter particle sizes and shapes have the potential to affect water clarity. Zooplankton filter particles continuously from the water column as a positive exponential function of body size (Burns 1969; Peters and Downing 1984; Knoechel and Holtby 1986). Therefore, transparency should vary with community clearance rate and grazer popu-

Received 16 October 2002. Accepted 31 August 2003. Published on the NRC Research Press Web site at http://cjfas.nrc.ca on 19 December 2003.
J17147

R.S. Stemberger.[1] Department of Biological Sciences, Dartmouth College, Hanover, NH 03755, U.S.A.
E. K. Miller. Environmental Studies Program, Dartmouth College, Hanover, NH 03755, U.S.A.

[1]Corresponding author (e-mail: Richard.S.Stemberger@dartmouth.edu).

 doi: 10.1139/F03-124 © 2003 NRC Canada

lation biomass. The attenuation of contrast in water is approximately exponential with depth (Tyler 1968), so that the relationship between clearance rate and Secchi transparency should be approximately linear. By extension, the relationship between grazer body length and Secchi transparency should be exponential but only under conditions in which light absorption by particulates and colored DOC are relatively constant.

Organic particles in the range of 1–10 μm have high light-attenuation cross sections (i.e., capacity to scatter and absorb light based on particle surface area per unit mass; see Davies-Colley et al. 1993). Zooplankton strongly select particles within and around this range of optimal attenuation effect (cf., McCauley and Downing 1985). Hence, the preference and removal of small particles by grazers should significantly affect water transparency. This relationship with the zooplankton has not been previously exploited for assessment of Secchi disk transparency across a spatially diverse set of lakes that range widely in trophic condition and zooplankton assemblage structure.

Secchi transparency is strongly correlated to average and seasonal total phosphorus concentrations and to phytoplankton populations measured as chlorophyll *a*, but often with substantial residual variance (Mazumder and Havens 1998). Populations of large-bodied grazers such as *Daphnia* are positively and significantly related to Secchi disk transparency within individual lakes in which they contribute a significant proportion of the total zooplankton biomass (Lampert et al. 1986; Kasprzak et al. 1999; Lathrop et al. 1999). However, relationships between zooplankton community biomass with chlorophyll *a* are often weak or not significant across populations of lakes (Currie et al. 1999). This is partly explained by the covariance between zooplankton biomass and lake productivity and the confounding effects of fish predation on assemblage biomass and body size of key grazers.

Increasing predation by forage fish drives the size structure of zooplankton assemblages from large- to small-bodied species with system-wide consequences on nutrient concentrations, phytoplankton abundance, and trophic condition (Carpenter and Kitchell 1993; Christoffersen et al. 1993; Carpenter et al. 1998). Several studies support body size as a more consistent measure of factors that define lake trophic condition rather than metrics of population biomass. Mean individual body size is significantly correlated to chlorophyll *a* and total phosphorus concentrations, whereas biomass of all zooplankton or of the cladoceran assemblage is uncorrelated to these factors (Currie et al. 1999). Furthermore, body size is negatively related to planktivore abundance and planktivore growth rates and positively correlated to the abundance of piscivores, whereas assemblage biomass is not significantly related to fish trophic structure (Mills and Shiavone 1982; Currie et al. 1999). Hence, body size is also a metric that most effectively indicates the impact of fish predation on variables used to define lake trophic condition. Therefore, body size also provides indirect evidence for the trophic structure of fish populations.

In this study, we evaluate Secchi disk transparency measurements from 59 northeastern U.S. lakes as a function of mean cladoceran body length, a proxy for potential grazing efficiency, in analysis with colored dissolved organic carbon and total phosphorus, chlorophyll *a*, or particulate carbon. Total phosphorus, chlorophyll *a*, and Secchi disk transparency are widely measured variables used to assess lake trophic status. Water transparency may be modulated directly by changes in phytoplankton concentrations and indirectly by the size structure of forage and piscivorous fish populations. The signature response of zooplankton body size to fish predation has been largely overlooked as a tool in lake management for the assessment of lake trophic condition based on Secchi transparency records. We attempt to simplify the process of acquiring body size data to produce a cost-effective metric that can be easily applied to routine monitoring of lake trophic status.

Methods

Zooplankton and water chemistry samples were collected from 59 lakes in New York, Vermont, and New Hampshire, U.S.A., over a 24-week sampling period (June through November) from 1999 though 2001. Lakes were selected along a gradient of water column concentrations of total nitrogen and total phosphorus and N–P ratios (N:P) using data available from the United States Environmental Protection Agency, Environmental Monitoring and Assessment Program (EMAP) pilot survey 1991–1994, the Vermont Department for Environmental Conservation, and the New Hampshire Department of Environmental Services (Table 1).

Of the 59 lakes surveyed for zooplankton, 18 lakes were visited just once in the 3-year period, 31 lakes were visited at least twice, and five lakes in the 2001 survey were sampled 3–7 times for a total of 123 lake visits. Three lakes included in the present study also were previously sampled during the 1991–1996 EMAP survey (Stemberger et al. 2001). The EMAP data set provided 11 additional visits for a total of 5–7 revisits in the time-series lakes. Zooplankton length and biomass estimates were done on these archived samples in conjunction with the current study. The mean values of repeated visits across and within years were calculated for both zooplankton and chemistry variables to avoid inflation of the degrees of freedom for the error terms in multiple regression and correlation analyses.

Water samples for chemistry were collected at the 1.5-m depth for a total of 142 lake visits for the 3-year survey. In the zooplankton data set, eight samples had missing chlorophyll *a* measurements and two samples had missing data for total phosphorus. Zooplankton length, dissolved organic carbon (DOC), and morphometric variables were complete for all samples. Data for particulate carbon ($n = 78$) were available only for the 1999 and 2000 surveys, of which 61 samples were collected concurrently with zooplankton.

Zooplankton

Zooplankton were collected with a single vertical net tow taken in the deepest location from 0.5 m off the bottom to the surface. A cone net (30-cm diameter, 202-μm mesh) was used for macrozooplankton (4:1 net length-to-diameter ratio) and a Wisconsin net (48-μm mesh) with a 15-cm-diameter reducing collar was used for the microzooplankton (7:1 net length-to-diameter ratio). Both nets were hung on a bongo

© 2003 NRC Canada

Table 1. Mean, range, and standard deviation (SD) of selected variables in the study lakes for all visits.

Variable	Minimum	Maximum	Mean	SD
Secchi depth (m)	0.45	9.55	4.21	1.97
TP (μmol)	0.023	5.737	0.321	0.577
TN (μmol)	0	149.9	23.41	17.47
TN/TP	0	1494.7	143.9	178.5
DOC ($mg \cdot L^{-1}$)	0.83	23.40	4.99	2.78
Color (absorbance DOC at 320 nm)	0	0.195	0.039	0.036
Chlorophyll *a* ($\mu g \cdot L^{-1}$)	0.1	47.8	3.7	7.3
Site depth (m)	0.45	46.8	10.2	9.6
Lake area (ha)	0.2	803.6	98.0	141.5
pH	5.1	8.6	6.8	0.8
Cladoceran biomass ($\mu g \cdot L^{-1}$)	0.17	233.5	13.5	25.1
Total zooplankton biomass ($\mu g \cdot L^{-1}$)	1.5	641.1	88.0	97.8

Note: TP, total phosphorus; TN, total nitrogen; DOC, dissolved organic carbon.

frame. These nets have large surface to volume ratios providing high filtration efficiencies over typical net designs. Zooplankton were anesthetized for 1–3 min in CO_2-charged water and preserved in buffered formalin and sucrose. Standardized abundances ($individuals \cdot L^{-1}$) of species were estimated using 2-, 5-, or 10-mL counting chambers with either a stereomicroscope or inverted microscope at 40× to 100×. Abundances of species were aggregated into functional groups sharing similar taxonomic, body size, and trophic features (Stemberger and Lazorchak 1994) (Fig. 1). The biomass of individual cladocerans was estimated from body length measurements using length-to-mass regression equations (Dumont et al. 1975; Culver et al. 1985). The biomass of each functional group is the product of the average body mass of individuals in the group and their abundance. The assemblage biomass is the sum of the biomass contributions of the individual functional groups.

Body size measurements were done on a Macintosh computer (Apple Computer, Inc., Cupertino, Calif.) using the public-domain NIH Image program (developed at the U.S. National Institutes of Health and available on the Internet at http://rsb.info.nih.gov/nih-image/). Images of individual zooplankton from each sample were digitized with a video camera mounted on an inverted microscope and stored on a hard drive or CD-ROM. A macro program was used to gather the image data and to process body length measurements for conversion to individual biomass using length-to-mass regression equations (Dumont et al. 1975; Culver et al. 1985; Stemberger and Gilbert 1985). The length and biomass data were recorded to a spreadsheet for later processing.

Gently mixed concentrated subsample (4–5 mL) was withdrawn using a large bore pipette and placed into a 5-mL glass-bottomed counting cell. Ninety to 125 images were taken from each sample based on one to several subsamples. Images of the coarse net samples were taken at 65 or 100 magnifications and those of the fine mesh net were taken at either 100 or 200 magnifications. Typically, 1–5 individuals were present on each image, but only individuals that were laying along the long axis of the body and that could be positively identified were measured. Generally, 30–75 measurements were taken for each taxon. If a particular group was rare, we took additional subsamples to get a minimum of 10 measurements. However, in some instances, this minimum number could not be achieved even after searching the entire sample.

Body length of cladocerans was measured from the top of the head to the base of the shell spine, regardless of age. Copepods were measured from the tip of head to the end of the caudal rami, and rotifers were measured from the anterior margin of the body to the posterior end, excluding anterior and posterior spines. The precision determined from calibrated digital micrographs was ±10, 7.1, and 4.4 μm for 63, 100, and 200 magnifications, respectively. A trained technician easily made 200–250 measurement per hour.

Rationale for mean body size and functional groups

Our analysis is limited to cladocerans collected from the coarse mesh net because these grazers have the greatest potential to affect commonly measured trophic indicators such as chlorophyll *a* and, consequently, have the greatest potential to influence lake transparency. For routine monitoring purposes, this emphasis on cladocerans also has significant benefits in processing effort and costs.

Cladoceran species were arranged in four groups based on size and taxonomic affiliation: *Daphnia*; large Cladocera excluding *Daphnia* (*Diaphanosoma*, *Sida*, *Latona*, *Simocephalus*, and *Scaphrolebris*); small cladocerans (bosminids, chydorids, ceriodaphnids, and macrothricids); and *Holopedium gibberum* — the latter species has a unique gelatinous sheath. *Daphnia* and *Holopedium* were often major contributors to the zooplankton assemblage, comprising up to 70 and 36%, respectively, of the total biomass of samples in our survey. Ninety-five percent of the lakes having *Holopedium* also had *Daphnia*. However, 35% of the lakes with *Daphnia* did not have *Holopedium*. Furthermore, *Holopedium* may spend part or most of the daylight hours near or at the bottom in some lakes (R. Stemberger, personal observation). Hence, their occurrence in lakes may reflect different environmental conditions and behavioral interactions with fish predators.

Miscellaneous large cladocerans did not contribute significantly to total biomass (maximum 9% of the total assemblage) but they often occurred in shallow lakes having abundant macrophytes that may provide cover from fish predators. They also occurred at mid-water stations in deep lakes where the epilimnion may provide a thermal refuge

© 2003 NRC Canada

Fig. 1. Box-and-whiskers diagram of zooplankton mean body length functional groups: ■, median; open outside box, 25–75 percentiles; whiskers, minimum and maximum values.

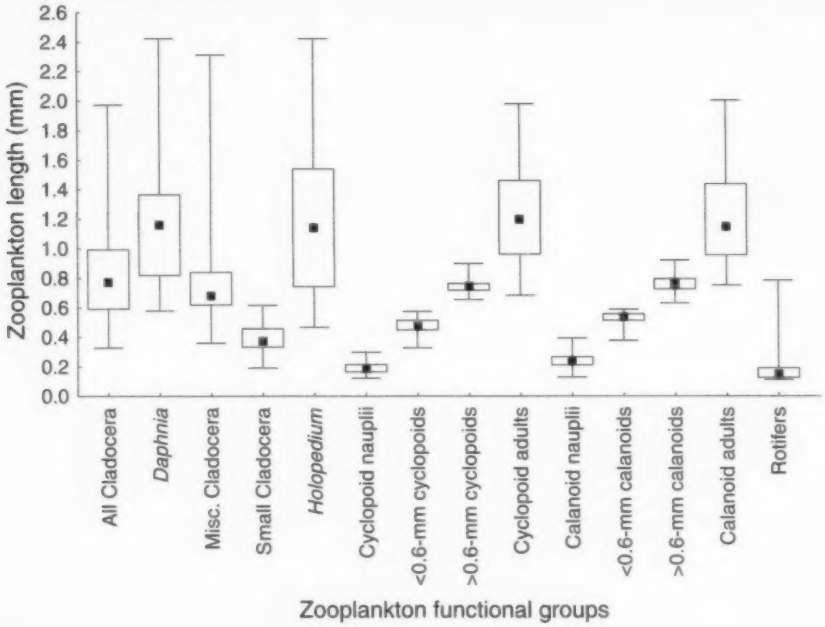

against cool-water predators. Morphometric and physical factors that potentially reduce predation on large grazers should also indirectly affect lake transparency. Hence, we distinguished these species from other large cladocerans. These functional groups are easily identified from digital micrographs from which length measurements were taken. The cladocerans (*Leptodora kindtii* and *Polyphemus pediculus*) were excluded from the analysis because they are primarily omnivorous and were not efficiently sampled.

Our index of mean cladoceran body length is simply the unweighted grand mean of the average length of individuals in each of the four cladoceran categories. We also evaluated other statistics of central tendency, including the median and geometric mean of body length for individuals within functional groups and for all cladoceran individuals irrespective of functional group. We tested these statistics and their log transformations in correlation analyses with Secchi disk depth and chlorophyll *a* and in multiple regression with chemical variables.

Chemistry

Total phosphorus, DOC, and chlorophyll *a* samples were collected in conjunction with zooplankton at a depth of 1.5 m or 0.5 m off the bottom in shallow lakes. Samples were collected with a 1.5-L polyvinyl chloride (PVC) plastic water sampler and filtered through precombusted Whatman GF/F glass-fiber filters (Whatman Inc., Clifton, N.J.) using 60-mL syringes fitted with Nuclepore™ 47-mm filter holders (Whatman Inc., Nuclepore Process Business, Newton, Mass.). Syringes were repeatedly filled from a port on the water sampler and filtered until the filter was fully loaded. The total filtered volume was recorded and the filters were removed with tweezers, wrapped in aluminum foil, and stored on ice until they could be frozen, usually within 6–8 h after collection. Three sets of filters were collected in this manner. One set of filters was later sent to the University of Maine for chlorophyll *a* analysis using in vitro acetone extraction. One set of filters was analyzed for total particulate N and P by persulfate oxidation (Grasshoff et al. 1983), followed by colorimetric assay (Lachat Instruments 1993; American Public Health Association (APHA) 1998). The third set of filters (collected on 25-mm supports) was analyzed for total particulate C by combustion – gas chromatography on a Carlo Erba NA 1500 (Carlo Erba Instruments, Milano, Italy). A 250-mL aliquot of the filtrate was collected, kept on ice during transport, and stored at 4 °C until analysis for dissolved chemical constituents. Total dissolved N and P were determined by persulfate oxidation (Grasshoff et al. 1983), followed by colorimetric assay (Lachat Instruments 1993; APHA 1998). Total water column N and P were computed from the sum of measured particulate and dissolved fractions.

DOC was determined as the difference between total carbon and inorganic carbon measured on a Shimadzu TOC-5000 (Shimadzu Scientific Instruments, Inc., Columbia, Md.). Ultraviolet light absorbance at 285 nm was measured and the ratio of absorbance at 285 nm to DOC was used as an indicator of the carboxylic and phenolic group content of the DOC (Buffle 1988).

In the time-series lakes that were sampled in 2001, we also measured light absorbance at 320 nm, a proxy for the color and light attenuation properties of DOC (Williamson et al. 1999). We developed a regression model using DOC, the ratio of absorbance at 285 nm to DOC, and pH that ex-

© 2003 NRC Canada

plained 94% of the variance in absorbance at 320 nm. We used the regression model to estimate the 320-nm color index in samples collected in 1999 and 2000.

Lake characteristics

A suite of variables useful for describing and partitioning populations of lakes were measured for each lake. However, only the variables used in the current analysis are presented here (Table 1). The zooplankton and chemistry sampling station was located in the deepest portion of the lake using acoustic or manual sounding. Secchi transparency depth was based on a 20-cm-diameter disk. We estimated transparency to the nearest centimetre as the mean of the depth of disappearance and reappearance of the disk when viewed from the shaded side of the boat. We also deployed an Endeco/YSI sonde (model UPG 6600; Endeco/YSI Inc., Yellow Springs, Ohio) fitted with chlorophyll and turbidity sensors, pH, dissolved oxygen, and temperature and pressure sensors for vertical profiling of these attributes.

Data analysis

Total phosphorus, chlorophyll *a*, color, and length metrics were $\log_e$-transformed. Secchi depth was not transformed because transformation did not improve on a normal distribution. Furthermore, light attenuation or water transparency represented by the depth at which the Secchi disk disappears is approximately an exponential decay function with surface irradiance (Davies-Colley et al. 1993). Hence, a logarithmic transformation is unnecessary. Although significantly different from a normal distribution (Shapiro–Wilk's test, $p = 0.01$), normal quantile plots qualitatively showed that the untransformed Secchi depth data yielded the best linear fit.

Secchi disk transparency was treated as the dependent variable in multiple stepwise regression with total phosphorus or chlorophyll *a*, colored DOC (absorbance at 320 nm), and mean cladoceran body length in among-lake analysis. We evaluated residuals in these models with site depth. Finally, we evaluated the time-series lakes using simple correlation analysis of body length, color, chlorophyll *a*, and total phosphorous to Secchi disk transparency.

Standardized regression coefficients (Beta coefficients), partial coefficients of determination, and the part correlation squared were calculated for the independent variables in the multiple regression models. Beta coefficients permit the comparison and assessment of the relative importance of each independent variable to predict the dependent variable (Neter and Wasserman 1974). For example, a Beta coefficient of 0.50 means that a half standard deviation change in the independent variable causes a half standard deviation response in transparency. The part correlation squared gives the unique variance that an independent variable contributes to the model when other independent variables are held constant. All analyses were done using STATISTICA version 6 (StatSoft Inc. 2001).

Results

The log of mean cladoceran body length estimated from functional groups gave the highest correlation to Secchi disk transparency relative to other statistics of central tendency such as the median and geometric mean or their logarithmic transformations. We report only results for the mean of the functional groups (Table 2). Secchi transparency was a linear function of the log of mean body length. The Secchi transparency depth depends not only on light backscattering, but also on light absorption by particulates and colored DOC; thus, lakes having large-bodied grazers may have lower than expected Secchi transparencies if light absorption efficiencies by particulates and colored DOC are high (and visa versa). Hence, light extinction may dampen the expected exponential response between lake transparency and cladoceran body length, making the relationship approximately linear.

Cladoceran body length ranged from 0.23 to 1.97 mm, with mean length of 0.81 mm and upper (75 percentile) and lower quartile (25 percentile) values of 1.02 mm and 0.59 mm, respectively. The range of variation in body length across zooplankton groups was greatest among cladocerans with the exception of small cladocerans (Fig. 1). Mean body length of adults of calanoid and cyclopoid copepods were similar to large cladocerans but with considerably smaller ranges (Fig. 1). Individuals in the upper size ranges of species are generally the most vulnerable to fish predators. We assume that the lower quartile of mean cladoceran body length (0.6 mm) reasonably reflects conditions in which fish predation on zooplankton is likely to be high. This length also corresponds to the diameter (0.2 mm) of copepods with lengths (<0.6 mm) that will pass through the coarse 202-μm mesh net (Stemberger and Lazorchak 1994).

Secchi disk transparency was significantly and negatively related to total phosphorus, chlorophyll *a*, DOC, color, and particulate carbon and positively correlated to the log of mean cladoceran length (Table 2). Secchi transparency depth was positively correlated to site depth, consistent with observations reported elsewhere (Davies-Colley et al. 1993). Cladoceran mean body length was positively related to Secchi disk transparency and site depth. It was also significantly and negatively correlated to chlorophyll *a* but was not significantly correlated to total phosphorus or color. Body length of *Daphnia* and small Cladocera was not significantly related to total phosphorus or chlorophyll *a* ($p \geq 0.05/21$; Table 2). With the exception of cyclopoid nauplii, body length of noncladocerans was either not correlated or weakly correlated to Secchi depth and chlorophyll *a*, which is consistent with expectation of their weaker grazing impact. Assemblage biomass of cladocerans was not significantly correlated to any of the trophic variables of interest. Particulate carbon had the highest correlation coefficients to trophic variables.

Variation across lakes

Multiple regression models that included zooplankton body length, color, and chlorophyll *a* or total phosphorus accounted for 72% and 83%, respectively, of the variation in Secchi disk transparency across lakes (Table 3). Cladoceran body length was as important in predicting transparency as total phosphorus, chlorophyll *a*, or colored DOC. Each variable contributed significant amounts of variance to the models, and all factors were highly significant ($p < 0.0001$). Standardized Beta coefficients for cladoceran body length were about equal in size, as were chemical variables. The Beta coefficients varied from 0.30 to 0.34 for cladoceran

© 2003 NRC Canada

Table 2. Pairwise correlation coefficients of the log of body length to selected variables.

Variable	Secchi depth	Total phosphorus	Chl *a*	Color	Site depth
Secchi depth (n = 55)	1				
Total phosphorus (n = 55)	**–0.75**	1			
Chl *a* (n = 55)	**–0.70**	**0.54**	1		
Color (n = 54)	**–0.71**	**0.47**	**0.55**	1	**–0.51**
Site depth (n = 55)	**0.83**	**–0.57**	**–0.48**	**–0.51**	1
Particulate carbon (n = 53)	**–0.82**	**0.82**	**0.73**	**0.60**	**–0.66**
Cladoceran assemblage biomass (n = 53)	–0.12	0.19	0.05	0.01	0.12
Cladoceran length (n = 54)	**0.58**	–0.37	**–0.40**	–0.29	**0.63**
Daphnia (n = 48)	0.36	–0.31	–0.38	–0.13	**0.47**
Misc. large Cladocera (n = 44)	**0.51**	**–0.44**	–0.32	–0.33	0.40
Small Cladocera (n = 52)	**0.43**	–0.22	–0.20	–0.31	0.38
Holopedium (n = 37)	**0.61**	**–0.49**	**–0.50**	–0.18	**0.65**
Cyclopoid nauplii (n = 53)	**0.64**	**–0.55**	–0.31	**–0.45**	**0.60**
Cyclopoids <0.6 mm (n = 52)	0.32	–0.15	–0.14	–0.25	0.31
Cyclopoids >0.6 mm (n = 51)	0.22	–0.09	–0.14	–0.31	0.26
Cyclopoid adults (n = 49)	0.35	–0.28	–0.21	–0.14	**0.48**
Calanoid nauplii (n = 35)	–0.31	0.13	0.33	0.29	–0.04
Calanoids <0.6 mm (n = 39)	–0.03	–0.04	0.04	0.22	0.05
Calanoids >0.6 mm (n = 47)	–0.02	0.09	–0.09	–0.03	–0.10
Calanoid adults (n = 47)	0.27	–0.24	–0.11	–0.07	0.34
Rotifers (n = 54)	–0.34	0.32	0.36	0.12	–0.08

Note: Significance values are Bonferroni corrected for multiple comparisons. Bold type indicates $p < 0.05/21 = 0.0023$. Color is the absorbance by dissolved organic carbon (DOC) at 320 nm; Chl *a*, chlorophyll *a*; sample size (n) is indicated in parentheses; misc., miscellaneous.

Table 3. Multiple regression of Secchi disk transparency vs. log cladoceran mean length and log color in analysis with (*a*) log total phosphorus, (*b*) log chlorophyll *a*, and (*c*) log particulate carbon.

Source	df	Beta coefficient	Partial R^2	Part correlation squared	R^2 change	F	Full model R^2
(*a*) Full model	3,50					81.17	0.83
Total phosphorus	1	–0.48	0.57	0.18	0.57		
Color	1	–0.42	0.48	0.14	0.18		
Cladoceran length	1	0.30	0.35	0.07	0.07		
(*b*) Full model	3,50					45.65	0.72
Chlorophyll *a*	1	–0.36	0.50	0.08	0.50		
Color	1	–0.40	0.48	0.11	0.13		
Cladoceran length	1	0.34	0.35	0.10	0.10		
(*c*) Full model	3,47					88.66	0.85
Particulate carbon	1	–0.53	0.66	0.19	0.65		
Cladoceran length	1	0.32	0.36	0.09	0.12		
Color	1	–0.32	0.51	0.07	0.04		

Note: The magnitude and sign of the Beta coefficient represents the relative contribution of the independent variable in the prediction of Secchi disk transparency. The partial coefficient of determination (partial R^2) is the bivariate regression of the independent variable against Secchi disk transparency, and the part correlation squared is the proportion of variance in Secchi transparency that is not explained by the other independent variables but which is unique to the given independent variable. Independent variables are listed in their order of entry into the model; $p < 0.0001$ for all factors and overall model results; df, degrees of freedom.

mean body length compared with from –0.36 to –0.53 for chemical variables (Table 3). The unique variance contributed by cladoceran body length (part correlation squared) ranged from 0.07 to 0.10 and was also similar in size to the contribution by chemical variables (0.07–0.18) in the various models (Table 3). These results further support the importance of cladoceran body size as an indirect factor driving variation in lake transparency. When particulate carbon is included in place of chlorophyll *a* or total phosphorus, the model gives the best overall fit ($R^2 = 0.85$, $F = 88.66$, $p < 0.0001$) (Table 3; Fig. 2). The Beta coefficients and part correlation squared are –0.53 and 0.19 (particulate carbon), 0.32 and 0.09 (cladoceran length), and –0.32 and 0.07 (color), respectively.

© 2003 NRC Canada

Fig. 2. Predicted vs. observed Secchi disk transparency values in multiple regression with particulate carbon, color, and cladoceran mean length as independent variables. $R^2 = 0.85$, $F = 88.66$. Solid lines denote 0.95 prediction bands; broken lines denote 0.95 confidence intervals; $N = 51$; ●, mean cladoceran length <0.6 mm; ○, mean cladoceran length >0.6 mm. Note that large-bodied cladocerans may be associated with low Secchi transparency values when color or concentrations of organic particulates are high.

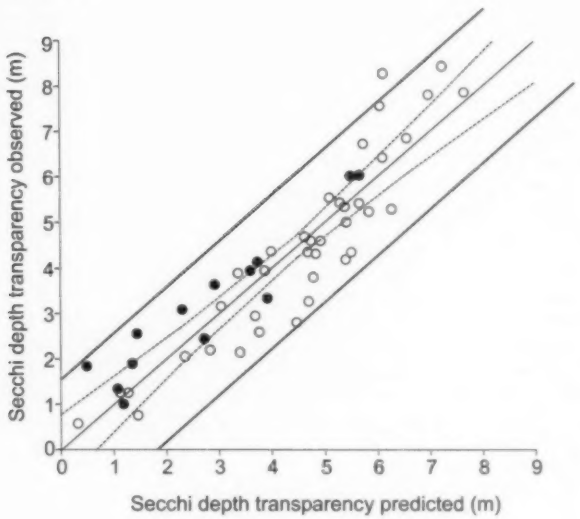

Temporal variation

Secchi disk transparency was significantly and positively related to zooplankton body length and (or) negatively related to chlorophyll *a* in seven of the nine time-series lakes (Table 4). Autocorrelation coefficients between Secchi depth transparency and body length were not significant except for the trivial case of time lag zero. Cladocerans were significantly correlated to transparency or chlorophyll *a* in five of nine lakes, and late stage copepods were significantly correlated to these variables in two lakes (Table 4). In contrast to the between-lake comparisons, color and total phosphorus were not significant factors in time-series lakes. This is likely explained because within-lake variation was small relative to the variation of these factors in lakes across the region (Table 4).

Discussion

This analysis provides a simple framework for interpreting spatial and temporal variation in water clarity using data that are routinely collected in volunteer lake-monitoring programs, with the exception of zooplankton body size. Body length is an effective indicator of the grazing capacity of the cladoceran assemblage to remove organic particles in size ranges having high light backscattering and absorption properties. These particles potentially include bacteria, protists, phytoplankton, and detritus. The relative predictive importance of body length and the part correlation squared in multiple regression analysis were consistently similar in size to the contributions of chemical variables in the models. These results support the importance of zooplankton size as an indirect driver of lake transparency. The inclusion of zooplankton body size measurements to routine lake-monitoring programs would permit more conclusive interpretations of the causes for observed changes in water clarity.

The log of the arithmetic mean of body length of cladoceran functional groups appears to capture the grazing signature between clearance rate potential and lake transparency that would be expected from community clearance rates estimated from population size–frequency distributions. In analysis with chemical variables, the index predicts Secchi transparency over a wide range of trophic conditions in a spatially extensive set of lakes. The metric is also well correlated to Secchi disk transparency in most lakes having time-series data. Functional groups partition the population size–frequency distribution that is typically lognormal into size–frequency distributions that are approximately normal (Shapiro–Wilk's test, $p > 0.05$). Because the mean is independent of the size–frequency distribution of the sample, it should be relatively insensitive to sampling error from net filtration efficiency factors and to spatial variance associated with horizontal patchiness or collection effort. Estimating the mean of cladoceran body length from functional groups also has significant time and costs savings that would be advantageous in routine lake monitoring.

Particulate carbon was the most important variable explaining transparency in this analysis because it incorporates a wide range of organisms and detritus that are potentially consumed by zooplankton and affect the optical scattering and light absorption components of Secchi transparency. Consequently, it explains more of the variance than chlorophyll *a*. For similar reasons, total phosphorus explains more of the variance in Secchi disk transparency than chlorophyll *a* because it is principally a proxy for bound phosphorus associated with organic particles like bacteria, phytoplankton, zooplankton, and detritus. Soluble forms of phosphorus contribute to unexplained variance if they do not represent colored dissolved organic compounds. However, except in highly eutrophic lakes, soluble forms of phosphorus are dominantly associated with colored organic compounds.

In time-series lakes, Secchi disk transparency was consistently correlated to zooplankton body length and to chlorophyll *a* with the expected direction (±) of effects. Secchi disk transparency was not significantly correlated to color and total phosphorus within lakes, probably because the within-lake variation of these factors was small relative to their variation across lakes. An analysis of the components of variance (between-lakes vs. within-lakes) using all visits showed that color and total phosphorus had relative within-lake variances of 11 and 20%, respectively. This compares with 43 and 53% for relative within-lake variance for chlorophyll *a* and cladoceran mean body length, respectively. In two lakes, late-stage copepods were more strongly correlated to transparency than cladocerans. High densities of cyclopoid copepods have been reported to mediate lower transparencies through predation on microzooplankton grazers (Elser et al. 1995), but in this study, cyclopoids were positively correlated to transparency. In the majority of the time-series

© 2003 NRC Canada

Table 4. Pairwise correlations of zooplankton taxonomic groups with Secchi disk transparency and chlorophyll *a* in time series lakes.

Lake	Taxon	Secchi depth	Chl *a*	Total visits
Crystal Lake, NY	Cladocerans	× (+)	× (–)	6
Grafton Pond, NH	Cladocerans	NS	NS	8
Harvey Lake, VT	*Daphnia*	NS	× (–)	6
Messer Pond, NH	Calanoids >0.6 mm	NS	× (–)	5
Moose Lake, NY	*Daphnia*	× (+)	NS	7
Spectacle Pond, NY	Cladocerans	× (+)	NS	5
Trout Lake, NY	Cladocerans	NS	NS	6
Willis Pond, NY	Cyclopoids >0.6 mm	× (+)	NS	6

Note: Color and total phosphorus were not significantly correlated to Secchi disk transparency in the time series. Chl *a*, chlorophyll *a*; ×, $p < 0.05$; sign of correlation is indicated in parentheses; NS, $p > 0.05$; NY, New York; NH, New Hampshire; VT, Vermont.

lakes, mean body length of cladocerans was negatively correlated to chlorophyll *a* and positively correlated to lake transparency. These observations are consistent with the well-established relationship of body size and grazing potential in cladocerans (Bogdan and McNaught 1975; Knoechel and Holtby 1986).

Other sources of variance

The precision in Secchi depth measurements at a single sampling location can vary up to 10% for multiple observers (Davies-Colley et al. 1993). In addition to observer error, we consider other factors that may account for residual variance in multiple regression models.

The models that included chlorophyll *a* had residuals that were significantly and positively correlated to site depth (the maximum depth of the lake). Site depth accounted for nearly 12% of residual variance in the model with chlorophyll *a* and about 5.4% and 2.6% of residual variance in models with total phosphorus and particulate carbon, respectively. This suggests that the implied effect of site depth might be spurious or that site depth might be related to particle sinking rates. Net loss of particles from the mixing layer is more likely to occur in stratified lakes with steep density gradients that are resistant to wind mixing. A negative relationship between Secchi transparency and particulate carbon (partial $R^2 = 0.66$) is consistent with a mechanism that involves sinking and net loss of particles with increasing lake depth.

Lower than predicted transparency values in the models suggest several possible causative mechanisms. Particulates may be resuspended during windy sampling conditions, especially in shallow lakes, thus reducing transparency. Lower than predicted Secchi disk transparencies may also occur when phytoplankton growth rates exceed grazing rates by low population densities of large grazers.

Suspended mineral particles may be predominately in clays that have high light backscattering and absorption properties. However, suspended clay was not evident in the majority of lakes, at least not in concentrations that were noticeable to the human eye. Nearly all of the lakes that we sampled had relatively low pH, so calcite precipitation is unlikely to be significant. Hence, lakes with large negative residuals were more likely to be shallow and eutrophic, having high phytoplankton densities and low grazing potential as indicated by small-bodied grazers.

Theoretical and experimental studies suggest both positive and negative effects of zooplankton grazing on phytoplankton sedimentation rates. Particle flux in the mixing layer involves the balance between productivity, nutrient recycling, grazing, fecal particle production, sinking rates, microbial degradation, and the effects of wind mixing. In low productivity systems, like many of the deeper lakes in our study, zooplankton are more likely to have a positive effect on sedimentation rate (Sarnelle 1999). This is also consistent with the positive relationship between site depth and water clarity observed in our study and reported elsewhere (Davies-Colley et al. 1993).

Large zooplankton grazers can reduce mortality of size-selective fish predation by undergoing diurnal vertical migrations to deeper waters where low light provides a visual refuge. Grazers also could spend a significant amount of time in the upper water column and undergo limited vertical migrations in stratified lakes that support salmonid fisheries. In these systems, the warmer epilimnion may provide a temporary summertime thermal refuge from temperature-sensitive planktivores. The clearest and deepest lakes in our survey support cold-water fisheries. Harvey Lake, Vermont, had the largest positive residual, greatest site depth (47 m), and an assemblage characterized by large copepods and cladocerans with red body pigments. Presumably these pigments support photoprotection against harmful exposure to solar ultraviolet radiation (Williamson et al. 2001). The presence of pigments is consistent with increased residence time in near-surface waters.

Quality of DOC

The quality, color, and light-attenuating properties of DOC are another influence on water transparency that may differ between lakes. Different-sized lakes tend to receive different relative contributions of DOC from terrestrial and pelagic sources. Allochthonous DOC is more strongly colored than that formed from autochthonous sources (Buffle 1988). This is in contrast to DOC generated from bottom sediments, which can be more similar to refractory terrestrial DOC (E.K. Miller and R.S. Stemberger, unpublished data).

Autochthonous DOC may be both less colored and more labile and susceptible to photobleaching by solar ultraviolet radiation than allochthonous DOC (Reche et al. 2000). The largest and deepest lakes that we sampled had the lowest DOC color indices. Hence, DOC in larger and deeper sys-

© 2003 NRC Canada

tems may be less colored and have less capacity to absorb and filter sunlight, resulting in greater Secchi transparencies for a given nutrient loading and grazing pressure. Thus, differences in the quality of DOC related to lake size may also explain the positive relationship in our data between site depth and water transparency.

The highest observed transparencies occurred in 1999, a drought year in the northeastern region. Tributary streams with substantial flow observed in later years were found to be dry, or nearly so, in many of the lakes visited in 1999. This suggests that climate-driven variation in terrestrial inputs of DOC may also have been a significant factor in explaining some of the high transparency values observed in 1999 (cf., Schindler et al. 1997).

Relevance to lake monitoring and trophic state assessment

Crustacean body size estimated from length–frequency distributions is significantly correlated to growth and size structure of fish populations (Mills and Schiavone 1982). Clearance rates are a power function of cladoceran body length (Knoechel and Holtby 1986), and Secchi transparency is a linear function of potential clearance rate in cladoceran assemblages when weighted for the size–frequency distribution (Kasprzak et al. 1999). Our analysis further suggests that mean cladoceran body size estimated from size-based taxonomic functional groups that do not depend on abundance weightings from the sample size–frequency distribution is also an effective index that is highly correlated to spatial and temporal variation in lake transparency. The index represents a significant simplification in sample processing for the acquisition of body size data while still retaining the fundamental relationship between grazing potential, fish population structure, and water clarity.

A decrease in water transparency may occur from a shift in fish population size structure, but without information on zooplankton body size, it might appear to be a response to changes in nutrient loading. Few lake-monitoring programs can make such distinctions. If water clarity and mean cladoceran body size decrease over time, then one can evaluate the likelihood of potential causes such as excessive harvesting of game fishes, introductions of nonnative zooplanktivores such as alewife (*Alosa pseudoharengus*) and gizzard shad (*Dorosoma cepedianum*), high stocking rates of juvenile game fish, winter kill, or decline of cool-water habitat capable of supporting salmonid fisheries. Monitoring that relies predominantly on water transparency to identify changes in water quality may misinterpret the underlying causes of transparency changes. Without information on zooplankton size structure, an evaluation of the proximate causes of change in lake transparency or trophic condition is far more speculative.

In conclusion, estimates of mean zooplankton body size from randomly chosen individuals sampled over the entire water column in a deep location are easily acquired using computer-based imaging technology. The integration of commonly measured trophic and chemical variables with a key indicator of middle food web structure provides a relatively simple interpretative tool for assessing variation and trends in lake transparency. However, in lakes and reservoirs with large amounts of suspended solids, the body length relationship with transparency is likely to be weak or absent.

Observations of zooplankton body size provide additional insight into spatial and temporal variability in lake transparency that has not been widely available in lake-monitoring programs. Body size is pertinent to understanding variation and trends in trophic condition. First, it indicates grazing potential on small phytoplankton and other organic particulates with light attenuation effect on Secchi transparency greater than that of larger particles. Second, zooplankton body size reflects the intensity of predation by fish and gives insight into the trophic structure of fish populations. This simple index of middle food web structure can therefore contribute to understanding the sources of variation and long-term trends in lake transparency and lake trophic condition of major interest in lake-monitoring efforts.

Acknowledgements

This research was supported by The National Center for Environmental Research (NCER) STAR Program, Environmental Protection Agency (grant No. R826591), awarded to R.S.S. and E.K.M. Charles P. Daghlian wrote the NIH IMAGE macro. The comments of Phil Larsen, Alan Herlihy, Kenneth Sedmak, and two anonymous reviewers improved the manuscript. Jess Fortin, Anne Fleck, Tii McLane, Carrie Bassage, Daisy Hebb, Lauren Hierl, Dick Ziegler, Gail Steinhart, Paul Zietz, Allison Warner, and Marinn Mansell assisted us in the field and lab. A.T. Packard and B. Mayes did the species counts, and A. Fleck and S. Heath did the image processing. We thank the private and public landowners and managers who gave us access to many of the water bodies in the study. The research described in this article does not necessarily reflect the views of the EPA, and no official endorsement should be inferred.

References

American Public Health Association. 1998. Standard methods for the examination of water and wastewater. American Public Health Association, American Water Works Association and Water Pollution Control Federation. Washington, D.C.

Bogdan, K., and McNaught, D.C. 1975. Selective feeding by *Diaptomus* and *Daphnia*. Int. Ver. Theor. Angew. Limnol. Verh. **19**: 2935–2942.

Buffle J. 1988. Complexation reactions in aquatic systems: an analytical approach. Ellis Horwood Ltd., Chichester, U.K.

Burns, C.W. 1969. Relation between filtering rate, temperature, and body size in four species of *Daphnia*. Limnol. Oceanogr. **14**: 693–700.

Carpenter, S.R., and Kitchell, J.F. (*Editors*). 1993. The trophic cascade in lakes. Cambridge University Press, Cambridge.

Carpenter, S.R., Cole, J.J., Kitchell, J.F., and Pace, M.L. 1998. Impact of dissolved organic carbon, phosphorus, and grazing on phytoplankton biomass and production in experimental lakes. Limnol. Oceanogr. **43**: 73–80.

Christoffersen, K., Rieman, B., Klysner, A., and Sondergaard, M. 1993. Potential role of fish predation and natural populations of zooplankton in structuring a plankton community in eutrophic lake water. Limnol. Oceanogr. **38**: 561–573.

Culver, D.A., Boucherle, M.M., Bean, D.J., and Fletcher, J.W. 1985. Biomass of freshwater crustacean zooplankton from length–weight regressions. Can. J. Fish. Aquat. Sci. **42**: 1380–1390.

© 2003 NRC Canada

Currie, D.J., Dilworth-Christie, P., and Chapleau, F. 1999. Assessing the strength of top-down influences on plankton abundance in unmanipulated lakes. Can. J. Fish. Aquat. Sci. **56**: 427–436.

Davies-Colley, R.J., Vant, W.N., and Smith, D.G. 1993. Colour and clarity of natural waters: science and management of optical water quality. Ellis Horwood Ltd., Chichester, U.K.

Dumont, H.J., Van de Velde, I., and Dumont, S. 1975. The dry weight estimate of biomass in a selection of Cladocera, Copepoda, and Rotifera from the plankton, periphyton, and benthos of continental waters. Oecologia, **19**: 75–97.

Edmondson, W.T. 1980. Secchi disk and chlorophyll. Limnol. Oceanogr. **25**: 378–379.

Elser, J.J., Luecke, C., Brett, M.T., and Goldman, C.R. 1995. Effects of food web compensation after manipulation of rainbow trout in an oligotrophic lake. Ecology, **76**: 52–69.

Fee, E.J., Hecky, R.E., Kasian, S.E.M., and Cruikshank, D.R. 1996. Effects of lake size, water clarity, and climatic variability on mixing depths in Canadian Shield lakes. Limnol. Oceanogr. **41**: 912–920.

Grasshoff, K., Ehrhardt, M., Kremling, K., and Almgren, T. 1983. Methods of seawater analysis. Verlag Chemie, Weinheim, Germany.

Kasprzak, P., Lathrop, R.C., and Carpenter, S.R. 1999. Influence of different sized *Daphnia* species on chlorophyll concentration and summer phytoplankton community structure in eutrophic Wisconsin lakes. J. Plankon Res. **21**: 2161–2174.

Knoechel, R., and Holtby, L.B. 1986. Construction and validation of a body-length-based model for the prediction of cladoceran community filtering rates. Limnol. Oceanogr. **31**: 1–16.

Lachat Instruments. 1993. Quick-chem automated ion analyzer methods manual. Lachat Instruments, Milwaukee, Wis.

Lampert, W., Fleckner, W., Rai, H., and Taylor, B.E. 1986. Phytoplankton control by grazing zooplankton: a case study on the spring clear-water phase. Limnol. Oceanogr. **31**: 478–490.

Lathrop, R.C., Carpenter, S.R., and Robertson, D.M. 1999. Summer water clarity responses to phosphorus, *Daphnia* grazing, and internal mixing in Lake Mendota. Limnol. Oceanogr. **44**: 137–146.

Mazumder, A., and Havens, K.E. 1998. Nutrient–chlorophyll–Secchi relationships under contrasting grazer communities of temperate versus subtropical lakes. Can. J. Fish. Aquat. Sci. **55**: 1653–1662.

Mazumder, A., Taylor, W.D., McQueen, D.J., and Lean, D.R.S. 1990. Effects of fish and plankton on lake temperature and mixing depth. Science (Wash., D.C.), **247**: 312–315.

McCauley, E., and Downing, J.A. 1985. The prediction of cladoceran grazing rate spectra. Limnol. Oceanogr. **30**: 202–212.

Mills, E.L., and Schiavone, A., Jr. 1982. Evaluation of fish communities through assessment of zooplankton populations and measures of lake productivity. N. Am. J. Fish. Manag. **2**: 14–27.

Neter, J., and Wasserman, W. 1974. Applied linear statistical models. Richard D. Irwin, Inc., Homewood, Ill.

Peters, R.H., and Downing, J.A. 1984. Empirical analysis of zooplankton filtering and feeding rates. Limnol. Oceanogr. **29**: 763–784.

Preisendorfer, R.W. 1986. Secchi disk science: visual optics of natural waters. Limnol. Oceanogr. **31**: 909–926.

Reche, I., Pace, M.L., and Cole, J.J. 2000. Modeled effects of dissolved organic carbon and solar spectra on photobleaching in Lake Ecosystems. Ecosystems, **3**: 419–432.

Sarnelle, O. 1999. Zooplankton effects on vertical particulate flux: testable models and experimental results. Limnol. Oceanogr. **44**: 357–370.

Schindler, D.W., Curtis, P.J., Bayley, S.E., Parker, B.R., Beaty, K.G., and Stainton, M.P. 1997. Climate-induced changes in the dissolved organic carbon budgets of boreal lakes. Biogeochemistry, **36**: 9–28.

StatSoft Inc. 2001. STATISTICA (data analysis software system), version 6. StatSoft Inc., Tulsa, OK 74104.

Stemberger, R.S., and Gilbert, J.J. 1985. Body size, food concentration, and population growth in plankton rotifers. Ecology, **66**: 1151–1159.

Stemberger, R.S., and Lazorchak, J.M. 1994. Zooplankton assemblage responses to disturbance gradients. Can. J. Fish. Aquat. Sci. **51**: 2435–2447.

Stemberger, R.S., Larsen, D.P., and Kincaid, T.M. 2001. Sensitivity of zooplankton for regional lake monitoring. Can. J. Fish. Aquat. Sci. **58**: 2222–2232.

Tyler, J.E. 1968. The Secchi disk. Limnol. Oceanogr. **13**: 1–6.

Williamson, C.E., Morris, D.P., Pace, M.L., and Olson, O.G. 1999. Dissolved organic carbon and nutrients as regulators of lake ecosystems: resurrection of a more integrated paradigm. Limnol. Oceanogr. **44**: 795–803.

Williamson, C.E., Neale, P.J., Gabriella, G., De Lange, H.J., and Hargreaves, B.R. 2001. Beneficial and detrimental effects of UV on aquatic organisms: implications of spectral variation. Ecol. Appl. **11**: 1843–1857.

© 2003 NRC Canada

Demographic attributes of yellow-phase American eels (*Anguilla rostrata*) in the Hudson River estuary

Wendy E. Morrison and David H. Secor

Abstract: Management of American eels (*Anguilla rostrata*) requires an understanding of how demographic attributes vary within large estuaries. Yellow-phase American eel length and age structure, growth, dispersal, nematode infestation rates, loss rate (natural mortality and emigration), and production were measured at six sites throughout the tidal portion of the Hudson River. Short-term dispersal was low, with >70% of eels at all sites captured <1 km from their original tagging area. Length was similar among sites (total length = 45.7 ± 0.3 cm), whereas age was substantially lower for brackish-water sites (8 ± 4 years) than for freshwater sites (17 ± 4 years). Growth was higher for brackish-water sites than for freshwater sites (8.0 cm·year^{-1} and 3.4 cm·year^{-1}, respectively). From 1997 to 2000, infestation by the exotic nematode *Anguillicola crassus* increased dramatically in mean intensity as well as prevalence. Annual loss rates measured for the six sites varied between 9% and 24%, with no statistical difference between freshwater and brackish-water sites. Estimated eel production was higher in a brackish-water habitat (1.10–1.77 kg·ha^{-1}·year^{-1}) than in a freshwater location (0.21–0.58 kg·ha^{-1}·year^{-1}). The results of this study support a recent proposal to establish freshwater areas as exploitation reserves.

Résumé : La gestion des anguilles d'Amérique (*Anguilla rostrata*) exige une compréhension de la variation des caractéristiques démographiques à l'intérieur des grands estuaires. Nous avons mesuré la structure en longueur et en âge, la croissance, la dispersion, le taux d'infection par les nématodes, les taux de perte par mortalité naturelle et par émigration, ainsi que la production chez des anguilles jaunes à six sites situés dans la section du fleuve Hudson affectée par les marées. La dispersion à court terme est réduite et >70 % des anguilles à tous les sites sont recapturées à <1 km de leur point original de marquage. La longueur est la même à tous les sites (longueur totale = 45,7 ± 0,3 cm), alors que l'âge est considérablement plus bas aux sites d'eau saumâtre (8 ± 4 ans) qu'aux sites d'eau douce (17 ± 4 ans). La croissance est plus forte en eau saumâtre qu'en eau douce, respectivement de 8,0 cm/an et de 3,4 cm/an. De 1997 à 2000, l'infection par le nématode exotique *Anguillicola crassus* a augmenté de façon spectaculaire, tant en intensité qu'en prévalence. Les taux de pertes annuelles aux six sites varient de 9 à 24 %, sans qu'il n'y ait de différence statistique entre les sites d'eau douce et d'eau saumâtre. La production estimée des anguilles est plus forte dans l'habitat d'eau saumâtre (1,10–1,77 kg·ha^{-1}·an^{-1}) qu'en eau douce (0,21–0,58 kg·ha^{-1}·an^{-1}). Les résultats de notre étude appuient la suggestion récente de l'établissement des zones d'eau douce comme réserves d'exploitation.

[Traduit par la Rédaction]

Introduction

Estuaries are very productive habitats for yellow-phase American eels (*Anguilla rostrata*) (Helfman et al. 1987), but the ecology and stock dynamics of American eels in estuarine waters is not well understood. During the past 20 years, U.S. landings of American eels, which mostly occur from estuarine waters, have declined from 1500 to 400 tons during the period 1980 to 2001 (NMFS 2002). To evaluate regional and species-wide sustainability, managers and scientists have placed priority on conducting stock assessments for American eels, focusing particularly on the estuarine yellow-phase eel (Anonymous 2001).

In estuarine habitats, a principal hypothesis is that growth, abundance, and productivity of yellow-phase eels is higher in downstream brackish-water habitats than in upstream freshwater locations (Helfman et al. 1987). This hypothesis was drawn from diverse monitoring and research projects but is also a corollary to the general observation that large coastal estuaries support higher fishery yields (Houde and Rutherford 1993). Despite the recognized importance of estuaries as productive habitats, few studies have investigated eel production in estuaries (Helfman and Bozeman 1984; Bozeman et al. 1985) or compared differences in age, length, and growth between eels in freshwater and brackish-water habitats in the same estuary (Helfman and Bozeman

Received 12 September 2002. Accepted 25 September 2003. Published on the NRC Research Press Web site at http://cjfas.nrc.ca on 19 December 2003.
J17092

W.E. Morrison and D.H. Secor.[1] University of Maryland Center for Environmental Science, Chesapeake Biological Laboratory, P.O. Box 38, Solomons, MD 20688-0038 U.S.A.

[1]Corresponding author (e-mail: secor@cbl.umces.edu).

 doi: 10.1139/F03-129 © 2003 NRC Canada

1984). No single study has investigated demographic trends throughout an entire large estuary.

To compare demographic attributes between different regions within the Hudson River, it was necessary to determine the degree of dispersal of eels. A recent otolith microchemistry investigation in the Hudson River suggested that yellow-phase (~5–25 years old) eels showed three migration behaviors: freshwater residency, brackish-water residency, and a single habitat shift during the yellow-phase from fresh water to brackish water (Morrison et al. 2003). At seasonal and annual time scales, past tagging studies indicate that eels occupy a limited home range and suggest that home ranges are larger in freshwater than in brackish-water areas (Helfman et al. 1987; Table 1). Here, we evaluated home range at six sites within the Hudson River estuary to support demographic comparisons among regions represented by these sites.

Because of PCB (polychlorinated biphenyl) contamination, the Hudson River eel fishery has been closed (except for a small bait fishery) since 1976. This long-term closure provided an opportunity to study eels in an unexploited state, allowing for isolation of growth and losses without the effects of fishing. Losses of yellow-phase eels in the Hudson River include both natural mortality and silver eel emigration, when eels return to the Sargasso Sea to spawn. In *Anguilla* species, researchers have found that maturity and the resultant emigration as silver eels was dependent more on length and fat content than age (Helfman et al. 1987; De Leo and Gatto 1996; Oliveira 1999).

This investigation measured dispersal, age and length structure, growth, mortality, and other demographic attributes of yellow-phase eels across freshwater and brackish-water regions of the Hudson River estuary during the period 1997–1999. The presence of the introduced parasitic nematode *Anguillicola crassus* (Barse and Secor 1999) was monitored to evaluate the rate at which infection is spreading. Finally, total production was estimated for 1998 and 1999, at one upriver and one downriver site, to evaluate possible productivity differences between freshwater and brackish-water zones within the Hudson River estuary.

Methods

The Hudson River estuary (Fig. 1) occupies a long, straight, and relatively deep basin formed by glaciers during the Pleistocene. The estuary is well mixed, with tidal influence from New York City Harbor to Troy Dam, 255 km upriver. The salt wedge is usually found near Yonkers (river kilometre (river km) 25) in high-flow months (late winter to early spring) and moves upriver to Newburgh (river km 100) when water flow decreases during summer (Dovel et al. 1992). For this study, sites below Newburgh (George Washington Bridge (GWB) and Haverstraw (HAV)) were designated brackish-water sites and Newburgh and the sites north (Newburgh (NEW), Kingston (KIN), Athens (ATH), and Albany (ALB)) were considered freshwater sites. These designations were based on past longitudinal studies (e.g., Dovel et al. 1992) and were corroborated by salinity measurements collected during this study.

Mark–recapture experiments were conducted at the six sites during summers 1997–1999. Sites were distributed through the entire length of the estuary but also were chosen to represent similar depths and bottom characteristics. All sites were located in shoal habitats 2–10 m deep. Bottom sediments were fine-grained clay and silt at all sites. Yellow-phase eels were captured in standard 100 cm long × 25 cm diameter double funnel eel pots (1.3 cm × 1.3 cm mesh), which were baited with a single large (>25 cm total length) menhaden *Brevoortia tyrannus* and soaked overnight. The use of bait to attract eels removes the possibility of collecting silver eels, which do not feed (Tesch 1977). A grid of 36 pots was deployed in either a 12 × 3 (HAV, NEW, and KIN sites), 18 × 2 (ATH and ALB sites), or 36 × 1 (GWB site) configuration, depending on the dimensions of the river at each site. Pots were deployed approximately 200 m apart at all sites. The pots efficiently captured eels between 30 and 75 cm long. In earthen ponds, Hornberger (1977) found that 1.3 cm × 1.3 cm mesh pots captured eels of a similar length distribution (total length range = 30–70 cm) as that of eels released into the ponds. Helfman and Bozeman (1984) poisoned a section of the stream after potting and found that 1.3 cm × 1.3 cm mesh pots effectively captured eels between 20 cm and 80 cm. Based on these studies and size distributions of eels captured during this study, we have assumed unbiased sampling of eels ≥30 cm.

Eels were tagged using liquid nitrogen brands (Sorenson et al. 1983) and insertion of PIT (passive integrated transponder) tags. Branding was used to identify batches of eels according to site and day of capture, whereas PIT tags identified individual eels for growth measurements. Eels were sedated using MS-222 or clove oil, tagged, and then placed temporarily (approximately 15 min) into a recovery tank before being returned to the water near their location of capture. To brand the eels, a copper letter 0.75 cm high was attached to a copper nut (the nut allowed letter brands to be easily changed). This copper nut was attached to a long copper rod inserted into a 4-L thermos containing liquid nitrogen. Sedated eels were placed against the cold copper brand for 3–8 s, depending on humidity (branding took longer on humid days). Laboratory holding trials showed that brands were visible for at least 30 days after they were applied; eels showed no adverse responses as a result of the branding procedure. PIT tags were injected using a hypodermic needle into the dorsal musculature (1998) or visceral cavity (1999) of a subsample of eels. Eels (n = 12) held in pots for 6 days showed no adverse effects or loss of PIT tags over the 6-day period. In the field, retention of PIT tags was measured through identification of a scar at the place of insertion. In 1998, 250 eels at two sites, Athens (river km 190) and Haverstraw (river km 60), were tagged with PIT tags. In 1999, 75–150 PIT tags were utilized at all six sites (total = 600 tags). PIT tag recaptures were attempted twice, at both 2 months and 1 year after tagging, to record growth and dispersal. Brands (>18 000 eels branded) were recorded for all eels at all times to document movement between sites.

To measure home range at different temporal scales, we returned to the same site twice, 2 months and 1 year after the original tagging. A single line of pots was placed inside the original potting grid and extended 7–11 km above (north)

© 2003 NRC Canada

Table 1. North American yellow-phase eel home range estimates from the literature, noting collection and tagging methods.

Location	Home range estimate	Methods	Source
Louisiana	Moved <400 ft (121.92 m)	Electrofishing; fin clip and wire tag	Gunning and Shoop 1962
Georgia tidal creek	1 ha	Potting; anchor tags	Bozeman et al. 1985
Rhode Island river	Maximum movement 4.7 km; 87% recaptured where tagged	Electrofishing; branding	Oliveira 1997
Hudson River, N.Y.	Maximum movement 4.2 km; >80% recaptured where tagged	Potting; brands	This study
Massachusetts tidal stream	2 ha	Potting; fin clip	Ford and Mercer 1986
Penobscot Estuary, Maine	6.7±1.6 km or 325±64 ha	Potting; transmitters	Parker 1995
Vermont lake	0.6±4.9 km or 2.4±65 ha	Electrofishing; transmitters	LaBar and Facey 1983

Fig. 1. Map of the Hudson River, New York, U.S.A. Study sites are depicted by stars, the distance upriver is presented on the right, and salinity is presented on the left. Oligohaline, 0.1–5‰; mesohaline, 6–18‰.

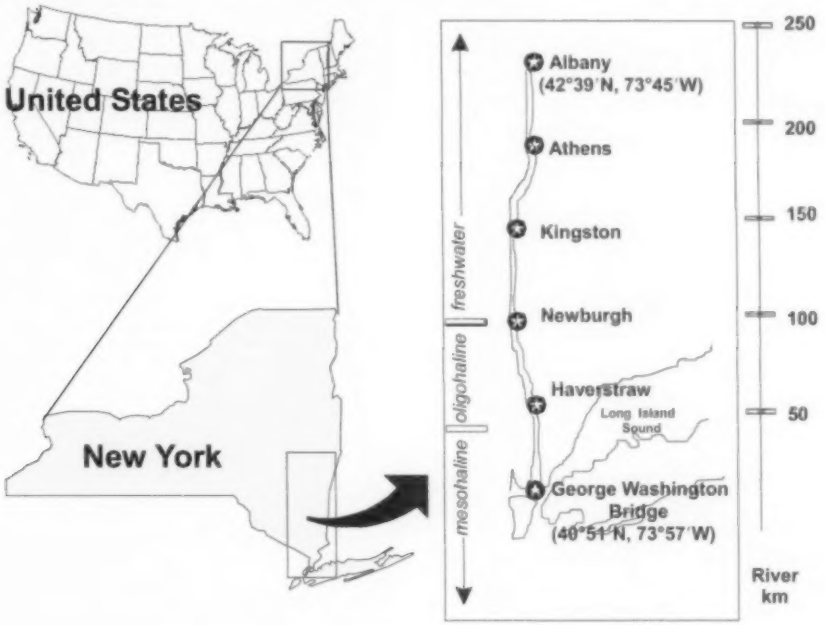

and below (south) the tagging area. In 1998, local dispersal was measured for two sites (ATH and HAV). For this year, there was no documentation of tagging location within the grid, and therefore dispersal was estimated as the distance that eels had moved away from the center of the original tagging grid. In 1999, local dispersal was measured at all sites except HAV (because of equipment failure). At this time, location of the eels within the grid during tagging was recorded, permitting more precise estimates of dispersal.

For laboratory analysis, 100 eels were collected during June or July from three sites (HAV, NEW, and ATH) in 1997 and from all six sites in 1998 and 1999. In 2000, only eels with PIT tags were collected for laboratory analysis. Eels were euthanized with MS-222 (1997 and 1998) or clove oil (1999, 2000) and frozen for later analysis. Length was measured on a subset of eels before and after being frozen, and it was determined that freezing caused approximately 3% decrease in total length (n = 30). All lengths reported here are based on uncorrected preserved length measurements. Morphological measurements recorded on each eel varied between years, with weight and head width recorded for 1999 and 2000 only. Gender was identified through gross visual inspection. Histological subsamples (46 females and 8 males) were prepared according to methods described in Dolan and Power (1977). All specimens showed histological characteristics that confirmed gross visual identification. An index of condition was calculated as Fulton's condition factor K (in $g \cdot mm^{-3} \cdot 10^5$; Ricker 1975) for eels collected in 1999. Differences between male and female condition were not testable because of the small sample of males collected. For this study, gut fullness was not recorded, which may have introduced small (2–6%) error (based on adjustment from Helfman and Bozeman 1984) to weight measurements. Head width (HW) was measured using calipers to the nearest millimetre at the widest section of the head. Head width to total length ratio (HW:TL) was calculated to determine if different ecotypes of eels are present in the Hudson River as has been reported in European yellow-phase eels (*Anguilla*

© 2003 NRC Canada

anguilla). Eels with HW:TL greater than 0.033 have been designated as "fat-headed" eels and have shown differences in relative weight, growth, and diet (Tesch 1977; Proman and Reynolds 2000). No study has reported head width in American eels. The presence and number of *Anguillicola crassus* nematodes found inside the swim bladder were recorded. Prevalence (number of infected eels divided by total number of eels examined) and mean intensity (average number of nematodes found among the infected eels) are defined as in Bush et al. (1997) and were calculated for each site.

To evaluate age structure, growth rate, and loss rate of estuarine yellow-phase eels, we required a valid ageing method. Annual periodicity of annuli within sagittal otoliths has been verified for American and European eels (Berg 1985; Oliveira 1996). Supernumerary rings or "false annuli" are common in eel otoliths and can introduce substantial bias if not correctly distinguished from true annuli. New techniques and criteria that minimize impacts from false annuli were recently introduced. We utilized a slight modification of Oliveira's (1996) and Graynoth's (1999) sectioning and dying techniques combined with Graynoth's (1999) criteria for identifying real annuli. Sagittal otoliths were extracted, soaked briefly (3 min) in 10% hypochlorite solution, rinsed in deionized water, and stored until dry. Right and left otoliths were randomly selected and embedded in epoxy resin. Transverse sections were cut using a wafering saw and then polished using wetted carborundum paper and alumina powder until the primordium was exposed (Secor et al. 1991). Otoliths were cleaned and etched with a solution of 5% toluidine blue and 2% EDTA (ethylenediaminetetraacetic acid). Under this treatment, transmitted light exposed blue opaque zones that correspond to annuli.

Ages represent the entire life span, including the marine leptocephalus stage, rather than the duration of the estuarine phase of life. There are two distinct checks on the otolith during the early life of an eel. The first check represents metamorphosis from the leptocephalus to the glass eel stage (Otake et al. 1997). The second check is described as the "transition" check (Michaud et al. 1988; Cieri and McCleave 2000), but its origin is uncertain. It may be associated with first feeding during the glass eel stage, entrance into fresh water, the end of metamorphosis, or settlement to demersal habitats. Because spawning occurs in March–April and eels enter the estuary (coincident to the deposition of this check) during March and April in the Hudson River (Mattes 1989), we assigned the transition check as age = 1 year.

Annular rings were counted at least four times for each section, with estimated age calculated as the mean of the counts. Two counts were made each along dorsal and ventral regions immediately adjacent to the sulcal groove (Fig. 2). The same counts were repeated at least 2 weeks later, and those with discrepancies >1 year were recounted a fifth time. Error in counts was estimated as the difference between the minimum and maximum counts for each otolith. The effect of site and number of annuli on ageing error was tested.

Seasonal and annual growth measured in the field through mark–recapture experiments and lifetime growth (size-at-age relationships) were measured and analyzed for differences due to capture location and time. For each eel aged, average lifetime growth was calculated by dividing total length by age. To account for growth before entering the Hudson River, the first year of life was discounted by subtracting 7.66 cm (Mattes 1989) and 1 year from the length and age, respectively. Results from field mark–recapture experiments suggested that female eels >30 cm exhibited linear growth across age classes. Therefore, we assumed that linear growth was a reasonable approximation. Estimates of seasonal and annual growth from recaptured eels were adjusted to reflect growth over 1-year or 2-month periods by dividing actual growth by the number of days at large (334–403 and 41–68 days for 1-year or 2-month growth periods, respectively) and then multiplying by either 365 or 61.

Loss rate was analyzed through catch-curve analysis. Because of the fishing ban, fishing mortality can be assumed to be negligible. For this analysis, all years were combined; age counts from 1997 and 1999 were increased and decreased by 1 year, respectively, to allow pooling by year class. In addition, individual eels were assigned to 3-year age-class bins based on mean measured error for all aged eels. For example, all eels aged 10, 11, or 12 years were combined into one group. We assumed that eels were fully recruited to the gear at and above the age at which the highest frequency occurred. Other important assumptions include constant rates of recruitment, natural mortality, and catchability across sites (Hilborn and Walters 1991).

Ricker (1975) defines total production as "the total growth in weight of fish during the year, including growth in the part of the population that dies before the year is finished". Because only length measurements were taken in the field, length measurements were converted to weight (W) estimates based on the following relationship $W = 0.001\mathrm{TL}^{3.2}$ (1999; $N = 543$, $r^2 = 0.92$).

Average biomass throughout the year was estimated as

$$\overline{B} = B_0(e^{G-Z} - 1)/(G - Z)$$

where B_0 is initial biomass (calculated by measuring average biomass of eels at a site and multiplying it by the abundance of eels at that site), G is an average yearly instantaneous growth for each site calculated from mark–recapture growth estimates, and Z is the instantaneous yearly loss rate calculated from the catch curve. Abundance was estimated using a modified Peterson mark–recapture estimate that minimized effects due to trap-shy behavior and immigration from outside areas adjacent to grid sample sites (mean recapture rate model; Morrison and Secor 2004). Production was estimated by multiplying the average biomass ($\overline{B}$) throughout the year by instantaneous growth (G) (Ricker 1975). This equation does not explicitly account for new recruitment of small eels to the pots during the period of production estimates. Still, because abundance is estimated during week-long trials, the assumption of negligible effects of new recruits may be valid. Sufficient data existed to compare production rates between HAV (brackish-water site) and ATH (freshwater site) in 1998 and 1999.

All site comparisons were made with standard one-way and two-way analyses of variance and covariance. For many analyses, assumptions of normality and homogeneous variances of the residuals were not met. Transformations (natural log and square root) were attempted, and if successful, the results were analyzed and the use of a transformation

© 2003 NRC Canada

Fig. 2. Micrograph of an otolith from a yellow-phase eel (*Anguilla rostrata*) collected in the Hudson River. Transects where annuli were identified are shown. Stars designate annuli.

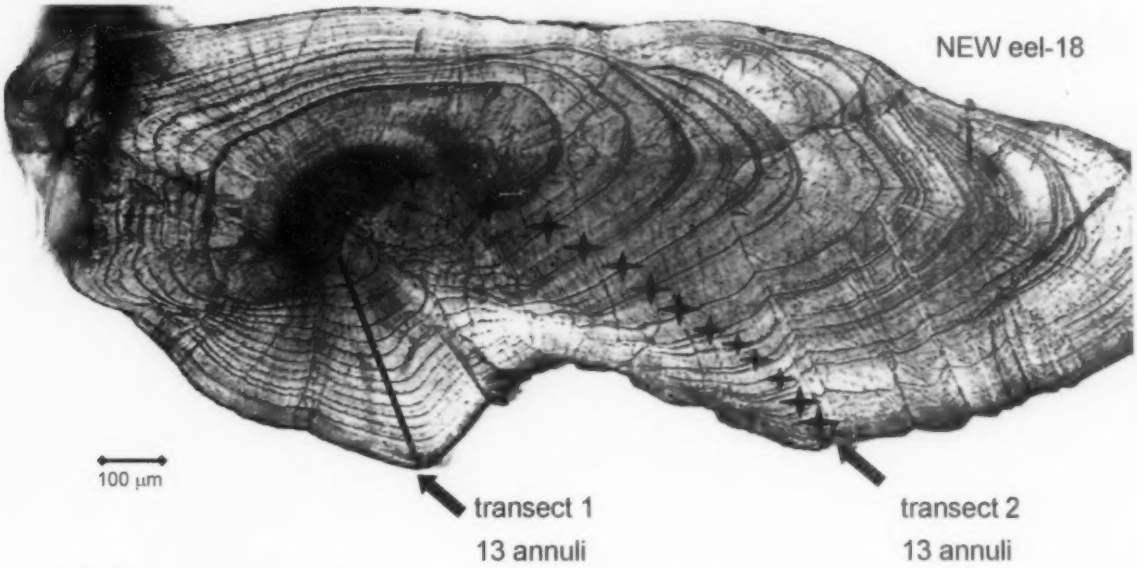

was noted. Where transformations did not remedy the violations, nonparametric Kruskal–Wallis rank tests were used and noted. All pairwise comparisons were made with Tukey's multiple comparisons.

Results

Dispersal

Retention of PIT tags was 89%; at two sites in 1999, 72 out of 81 eels retained PIT tags 2 months after tagging. PIT-tagged eels showed expected home range behaviors. For eels tagged in 1998 at ATH, 80% (54/67) and 88% (51/58) of recaptured eels were within the original tagging grid 2 months and 12 months after they were originally tagged, respectively. Ninety percent (n = 9/10) of recaptured eels at HAV in 1998 were sampled within the original tagging grid 1 year later. For eels tagged in 1999, dispersal was evaluated at all sites and results were similar across sites, with >70% (mean = 88%) of eels recaptured within 1 km of their original tagging location 2 months and 12 months later (Table 2). Recapture rate within 1 km of release site was variable among sites, with highest recapture rates at upriver locations. The longest individual dispersal was measured at NEW, where one eel moved 4.2 km from its tagging location. For the 2-month interval, the dispersal at GWB was significantly less than at all other sites except ALB.

Only four recaptured branded eels showed evidence of long distance dispersal. In 1998, four eels branded at ATH during June were recaptured 1 month later at KIN, 55 river km downstream. Estimated mean dispersal rate for those four eels was approximately 3.5 km·day^{-1}. During 1998–2000 field seasons, no other branded eels were recaptured (N > 18 000 branded eels) at sites other than where they were originally branded.

Gender, condition, and head morphometry

Nearly all (97%) examined eels (1999 samples; n = 543) were female. Of the 14 male eels identified, 11 were from GWB, two were from HAV, and one was from NEW. The mean length of males was 33.3 ± 2.2 cm; all were less than 37 cm TL. Because of insufficient sample size, gender differences in condition, growth, dispersal, or nematode mean intensity were not tested.

Condition factor K varied significantly between sites (1999, N = 542, df = 5, P < 0.0001). The condition factor at NEW was significantly higher than at the other five sites, and the condition factor at ATH was significantly lower than that at GWB and NEW (Table 3). According to criteria established for European eels, 98% of eels collected in the Hudson River in 1999 were "wide-headed" (HW:TL > 0.033; Proman and Reynolds 2000). Although no modalities in HW:TL occurred, the metric varied significantly between sites (N = 530, df = 5, P < 0.0001), with significantly greater head widths at NEW, KIN, and ATH than at ALB, GWB, and HAV (Table 3).

Nematode infection

The percent of infected eels increased during the 1997–2000 study (Fig. 3). In 1997, only four sites were analyzed (HAV, NEW, KIN, and ATH) and all sites had prevalences less than 20%. At HAV in 1997, no parasites were noted. By 2000, >60% of eels were infected by *A. crassus* at all freshwater sites. Prevalence of the parasite tended to be less at the two most saline, down-estuary sites in 1999–2000. The number of nematodes per infected eel (mean intensity) also increased with time (Fig. 3). The mean number of nematodes found in infected eels was low in 1997 and 1998, with all sites except ATH showing average mean intensities <4. By 1999, mean intensities were between 3.2 and 23.7 among sites. The maximum number of adult nematodes recorded

© 2003 NRC Canada

Table 2. Short-term dispersal of yellow-phase American eels tagged in the Hudson River, 1999.

Site	Duration	*N*	Recapture (%)	Maximum distance (m)	Mean distance (m)	Recaptured <1 km from release site (%)
GWB	2 month	8	11	200	138	100
	1 year	7	10	600	243	100
HAV	2 month	7	5	1400	843	71
	1 year					
NEW	2 month	13	12	4200	1008	85
	1 year	14	14	1400	714	93
KIN	2 month	22	20	3600	655	91
	1 year	4	5	1600	750	75
ATH	2 month	18	24	1900	544	89
	1 year	4	7	1800	575	75
ALB	2 month	24	32	1000	383	100
	1 year	17	33	1600	618	88

Note: GWB, George Washington Bridge; HAV, Haverstraw; NEW, Newburgh; KIN, Kingston; ATH, Athens; ALB, Albany. No data were collected in Haverstraw after 1 year because of technical difficulties with the PIT (passive integrated transponder) tag reader.

for an individual eel increased from 17 during 1997–1998 to 82 during 1999–2000. Mean intensities were not influenced by total length but were significantly different among sites (analysis of variance (ANOVA) on 1999 TL data, $N = 542$, df = 1, $P = 0.62$; Kruskal–Wallis test on 1999 site data, df = 5, $P < 0.0001$). Mean intensities were significantly lower at the brackish-water sites and NEW than at the three most upriver sites ($P < 0.05$). Data at KIN, ATH, and ALB indicate that between 1998 and 1999, there was at least a five-fold increase in mean intensity.

Age and length structure

Mean precision in age estimates was 1.4 ± 0.95 years. Sixty-four percent of the estimates had an error less than 1.5 years, and 95% of age differences were less than 3.5 years. There was a significant relationship between the number of annuli and error ($r^2 = 0.045$, $P < 0.0001$), but the difference was slight: mean error was 1.1, 1.5, 1.6, and 1.6 for ages 3–10, 10–15, 15–20, and 20–39, respectively. Using a two-way ANOVA, there was no significant effect on error due to capture locations after accounting for effects on error due to age (df = 5, $P = 0.26$).

Estimated ages differed significantly among sites but not among years ($n = 543$; Kruskal–Wallace rank test on year effect, df = 2, $P = 0.25$; site effect, df = 5, $P < 0.001$). Overall, ages were much lower for the two brackish-water sites than for the freshwater sites (Fig. 4). For pooled years (1997–1999), mean ages at GWB, HAV, NEW, KIN, ATH, and ALB were 8.2, 8.7, 17.1, 19.5, 16.4, and 16.9 years, respectively. The oldest eels tended to occur at KIN, with mean ages at that site of 19.1 and 19.8 years for 1998 and 1999, respectively. The oldest individual eel aged during the entire study was from GWB and was estimated to be 38 years old with a total length of 39.5 cm. The youngest eel, from HAV, was estimated to be 3 years old at 29 cm TL. Age structure was skewed towards older ages at one freshwater site (ALB) and skewed towards younger ages at both lower river sites (HAV and GWB).

Length frequencies were similar among sites (Fig. 5; Table 3) and were skewed towards smaller sizes at four of the six sites (GWB, NEW, ATH, ALB). When comparing mean total lengths with ANOVA, both site and year were significant ($n = 649$; year, df = 3, $P = 0.03$; site, df = 3, $P = 0.001$), but differences in mean lengths between sites and years were small; mean lengths varied <4 cm among sites and years. Only four site combinations out of 15 were significantly different using Tukey's pairwise comparison: HAV and GWB were significantly different from NEW and ATH. For pooled years (1997–1999), mean lengths at GWB, HAV, NEW, KIN, ATH, and ALB were 44.2, 44.1, 47.3, 46.0, 47.4, and 45.4 cm, respectively.

Growth

Length-at-age plots indicated high individual growth rate variation within sites (Fig. 6). Based on estimated ages, a 50-cm eel could range from 5 to 29 years old. Within sites and years, correlations (r) between age and length were low, ranging from 0.09 to 0.79. Only eight of 15 possible regressions were significant ($P < 0.05$). The highest correlation was for HAV in 1999 ($r = 0.79$). Overall, there was a significant relationship between age and length ($n = 649$, $r = 0.30$, $P < 0.0001$), but the relationship was weak. Annual growth calculated for individual eels based on length-at-age was higher in brackish-water sites (5.48 ± 1.80 cm) than in freshwater sites (2.48 ± 0.64 cm) for all years (Kruskal–Wallis rank test, $n = 649$; site, df = 5, $P < 0.0001$; year, df = 2, $P = 0.19$; Table 3).

Summer growth (June to August), estimated from mark–recapture, were higher for eels caught at brackish-water locations (2.5–2.8 cm·(2 months)$^{-1}$; Table 3) than those from freshwater sites (0.2–2.1 cm·(2 months)$^{-1}$). Two-way analysis of variance for 2-month growth increments showed that differences in growth among sites were significant, but interannual differences in growth between 1998 and 1999 were not detected ($n = 94$; site, df = 5, $P < 0.0001$; year, df = 1, $P = 0.12$). Similar results were found for annual growth increments ($n = 135$; site, df = 5, $P < 0.0001$; year, df = 1, $P = 0.10$). Two-month growth increments were not significantly related to length or age ($n = 94$; Kruskal–Wallis test on length, df = 1, $P = 0.30$; age, df = 1, $P = 0.33$). Annual growth rates estimated from mark–recapture ranged from 2.4 to 10.4 cm·year^{-1} and were in general similar in range to growth estimated through size at age (Table 3). Growth rates were significantly higher at brackish-water sites (8.0 cm·year^{-1}) than at fresh-

© 2003 NRC Canada

Table 3. Demographic characteristics of yellow-phase American eels for the Hudson River.

Site	Total length (cm)	Estimated age (years)	Condition index ($g \cdot mm^{-3} \cdot 10^5$)	HW:TL	Mark–recapture 2-month growth (cm)	Mark–recapture 12-month growth (cm)	Growth based on age-at-length (cm)
GWB	44±9 (118)	8±5 (118)	0.191±0.002b (86)	0.04±0.05a (97)	2.8±0.5a (7)	8±3a (7)	6.5±1.7 (54)
HAV	44±8 (117)	9±2 (117)	0.192±0.003ab (70)	0.04±0.04b (99)	2.5±1.6a (7)	10±3a (12)	5.2±1.1 (30)
NEW	47±8 (123)	17±4 (123)	0.205±0.003c (76)	0.05±0.07cd (76)	0.5±0.7b (13)	3±2b (37)	2.8±0.5 (31)
KIN	46±6 (89)	19±3 (89)	0.186±0.003ab (99)	0.05±0.06d (71)	2.1±1.1a (21)	4±2b (17)	2.6±0.5 (50)
ATH	47±6 (117)	16±3 (117)	0.181±0.003a (99)	0.05±0.05c (97)	0.7±0.7b (24)	3±2b (42)	3.1±0.9 (30)
ALB	45±6 (85)	17±2 (85)	0.187±0.003ab (96)	0.04±0.06b (96)	0.1±0.7c (22)	2±3b (20)	2.7±0.4 (33)

Note: Total length and age are means for 1997–1999; condition index, age-at-length growth, and the head width to tail length ratio (HW:TL) are for 1999; and mark–recapture growth is for 1999–2000. Values reported are mean ± standard deviation and sample size (*N*). Different letters represent significant differences using Tukey's multiple comparisons at $\alpha = 0.05$. GWB, George Washington Bridge; HAV, Haverstraw; NEW, Newburgh; KIN, Kingston; ATH, Athens; ALB, Albany.

water sites (3.4 cm·year^{-1}). Year did not influence annual growth increments ($n = 135$; site, df = 5, $P < 0.0001$; year, df = 1, $P = 0.10$). The annual growth increments, although not related to length, were significantly related to estimated age ($n = 135$; $\log_{10}$(age), df = 1, $P = 0.03$; length, df = 1, $P = 0.44$).

At ATH, 53 eels were captured both 2 months and 1 year after tagging, allowing for a comparison between summer and annual growth for individual eels. On average, 40% of their annual growth occurred during the 60-day summer interval (June to August; $n = 53$). Thirty-one eels tagged at ATH in 1998 were recaptured in 1999 and 2000. Analysis of these data indicated no significant difference in mean annual growth increments between 1998–1999 and 1999–2000, using a paired t test ($n = 31$, $t = 1.54$, $P = 0.13$). Individual growth was variable between years, with some eels exhibiting up to three times higher growth in one year versus the other. Despite this variability, there was a positive correlation between individual growth rates between the two years ($n = 31$, $r = 0.55$).

Loss rate and production

Loss rates estimated from age-class frequencies were similar across sites (Fig. 7). The overall mean loss rate was 0.16 ± 0.06 (15%·year^{-1}), with maximum and minimum rates of 0.27 (24%·year^{-1}) and 0.09 (9%·year^{-1}), estimated at ALB and NEW, respectively. Loss rates were similar between the two brackish-water sites (GWB = 12%·year^{-1}; HAV = 15%·year^{-1}) but were more variable among freshwater locations (Fig. 7). Estimated loss rates were not significantly different between freshwater and brackish-water sites (analysis of covariance, df = 1, $P = 0.13$). There was, however, a difference in the most frequent age (age at which the catch curve began). The descending portion of the age–frequency distributions began at age classes 5 and 8 for the two most down-estuary sites and between ages 17 and 20 for the other four up-estuary sites.

Total production of yellow-phase eels was higher at the brackish-water site (HAV) than at the freshwater site (ATH) in both 1998 and 1999, but the magnitude of the difference was variable. Across years, estimated production at HAV was approximately 2–3 times higher than estimated at ATH. HAV showed slightly higher production in 1998 (1.77 kg·ha^{-1}·year^{-1}) compared with 1999 (1.10 kg·ha^{-1}·year^{-1}), but ATH showed higher production in 1999 (0.58 kg·ha^{-1}·year^{-1}) compared with 1998 (0.21 kg·ha^{-1}·year^{-1}).

Discussion

Large differences in growth between brackish-water and freshwater sites affected the age structure and productivity of the eels in the Hudson River. These differences in growth, production, and age structure were supported by mark–recapture experiments that documented very limited exchange of yellow-phase eels among sites during summer. Other attributes that varied among freshwater and brackish-water habitats included condition, head morphometry, and prevalence of infection by the parasitic nematode *A. crassus*. Loss rates did not differ between estuarine regions.

© 2003 NRC Canada

Fig. 3. (*a*) Percentage of Hudson River yellow-phase eels (*Anguilla rostrata*) infected (prevalence rate) with *Anguillicola crassus*, 1997–2000. (*b*) Mean intensity (number of nematodes per eel) of yellow-phase American eels in the Hudson River, 1997–2000. Error bars represent standard deviations in mean intensity. GWB, George Washington Bridge; HAV, Haverstraw; NEW, Newburgh; KIN, Kingston; ATH, Athens; ALB, Albany. Solid bars, 1997; open bars, 1998; hatched bars, 1999; shaded bars, 2000.

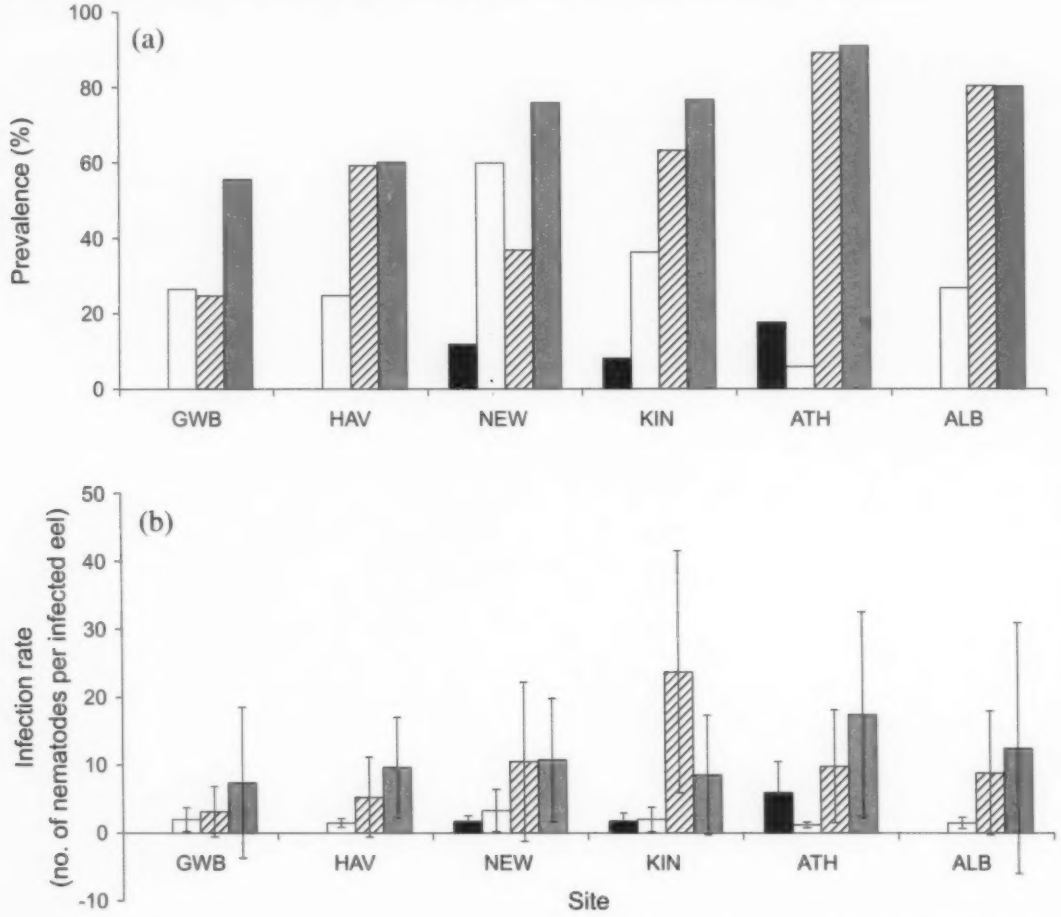

Dispersal

The limited home range and seasonal attachment to a location measured in this study were similar to results found by other researchers in various habitat types. Despite strong evidence for limited dispersal within a 1-year period, other evidence indicated that some yellow-phase eels did disperse among estuarine regions over longer periods of time. Otolith Sr-to-Ca ratios showed that some eels will spend the first 2–19 years of their life in fresh water before moving to, and residing in, brackish-water habitats (Morrison et al. 2003). The four branded eels observed to have migrated 55 km downriver could have been initiating such a migration. Otolith microchemistry showed no evidence of regular seasonal movements into and out of water of different salinity (Morrison et al. 2003), but the method cannot distinguish movements within freshwater areas, so it is possible that eels have undetected seasonal migrations within freshwater portions of the river. The long-distance migration that we documented for four eels occurred during the first weeks of the 1998 field season, suggesting that it might have been a seasonal migration. Still, because only four recaptures between sites were recorded among >18 000 marked eels during the 4-year study, interannual long-distance migration (>10 km) appears to be rare.

Helfman et al. (1987) hypothesized that eel home ranges are smaller in brackish water compared with fresh water. Dispersal was quite different at the two brackish-water sites in this study, with limited dispersal at GWB and comparatively high dispersal at HAV. The habitat characteristics of these sites may have influenced dispersal. GWB contained only a thin band of shallow habitat next to a deep channel, whereas HAV was located in an extensive shallow-water bay. Both sites had lower recapture rates (5–11% recaptured) compared with freshwater habitats (12–33% recaptured). Low recapture rates in brackish water could suggest a difference in home range and feeding behavior between the freshwater and brackish-water areas but could also be the result of higher growth and higher loss rates for brackish-water

© 2003 NRC Canada

Fig. 4. Age–frequency distributions for Hudson River yellow-phase eels (*Anguilla rostrata*), 1997–1999 combined: (*a–d*) freshwater locations; (*e* and *f*) brackish-water locations. (*a*) Albany; (*b*) Athens; (*c*) Kingston; (*d*) Newburgh; (*e*) Haverstraw; (*f*) George Washington Bridge.

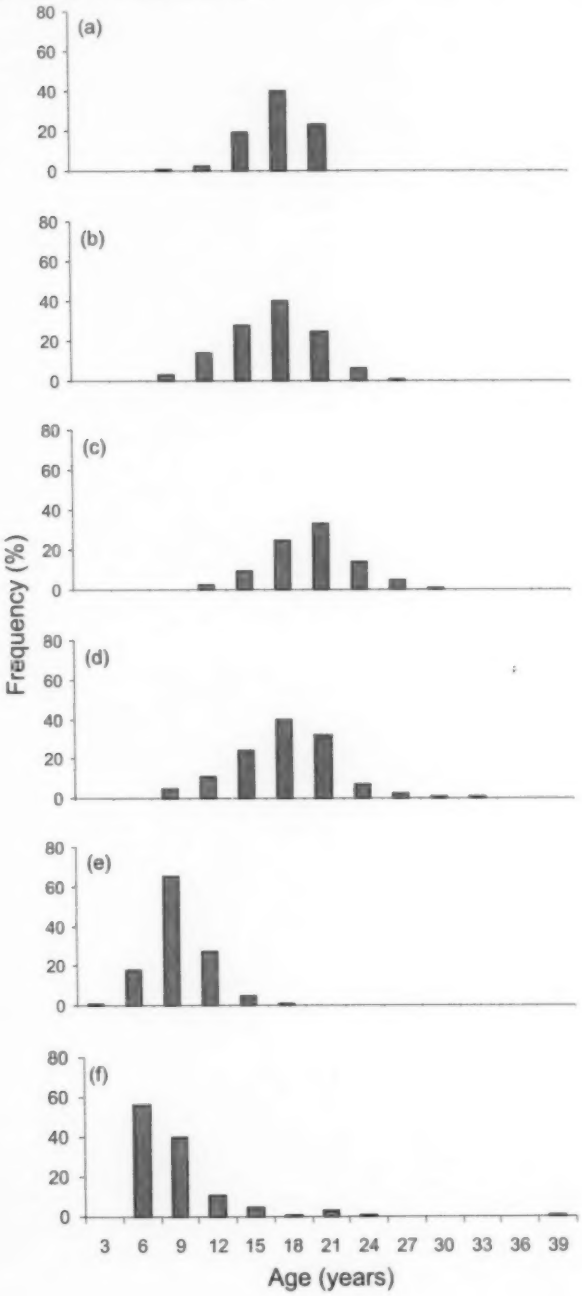

Fig. 5. Length–frequency distributions for Hudson River yellow-phase eels (*Anguilla rostrata*), 1997–1999 combined: (*a–d*) freshwater locations; (*e* and *f*) brackish-water locations. (*a*) Albany; (*b*) Athens; (*c*) Kingston; (*d*) Newburgh; (*e*) Haverstraw; (*f*) George Washington Bridge.

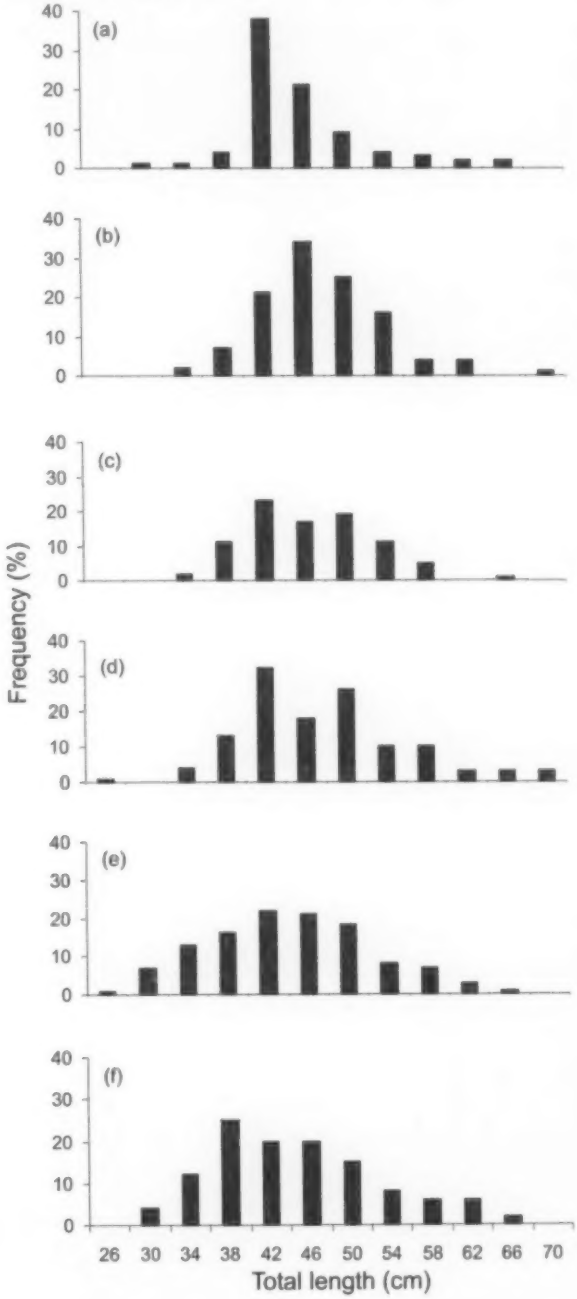

© 2003 NRC Canada

Fig. 6. Length versus age for yellow-phase American eels (*Anguilla rostrata*) collected from the Hudson River, 1997–1999: (*a*) Albany; (*b*) Athens; (*c*) Kingston; (*d*) Newburgh; (*e*) Haverstraw; (*f*) George Washington Bridge. Solid triangles, 1997; solid diamonds, 1998; open squares, 1999.

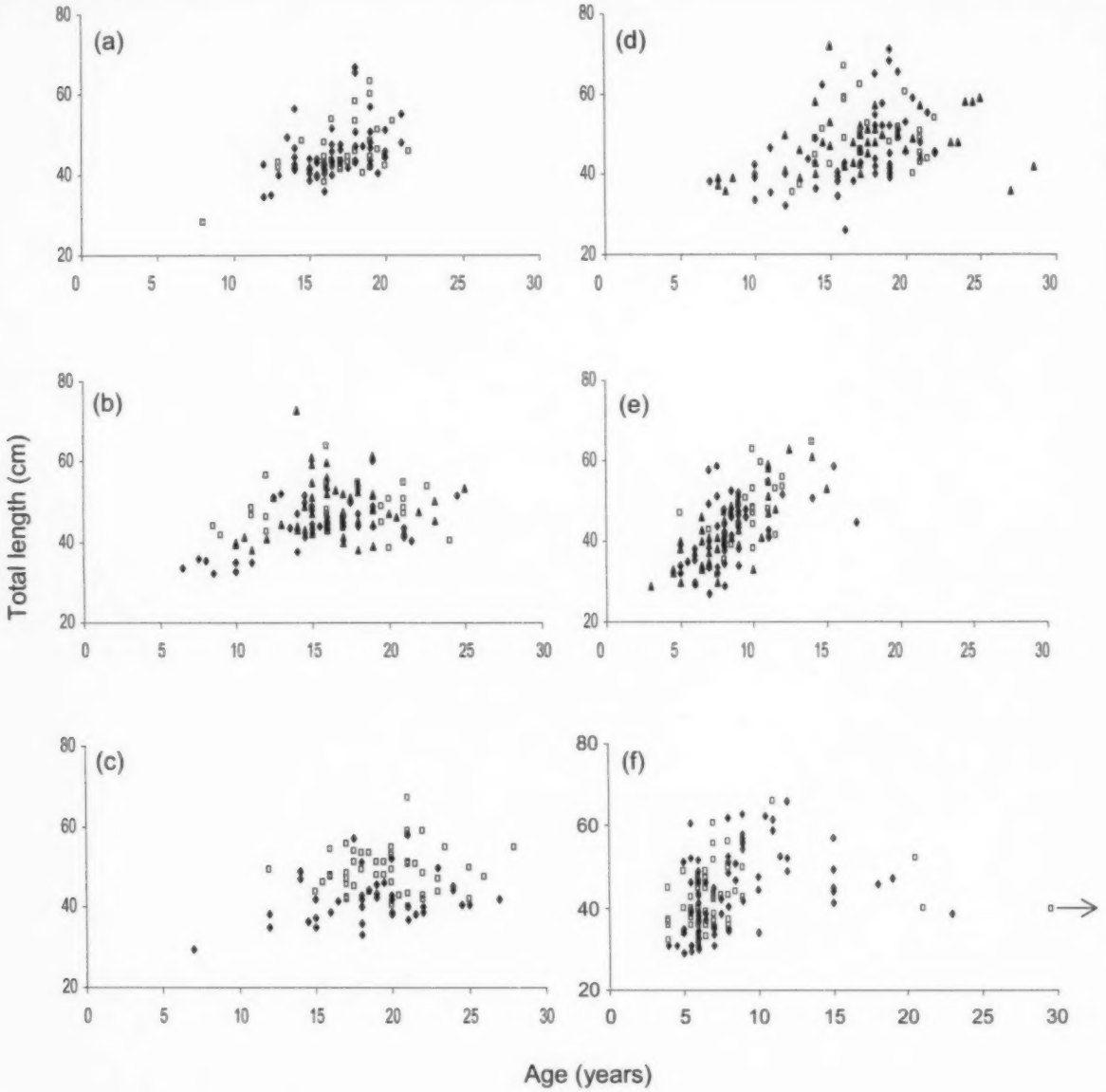

eels. Mean dispersal distance showed no obvious trend between brackish-water and freshwater sites.

Sex, condition, and head morphometry

Captured Hudson River American eels mainly consisted of female "wide headed" eels with mean condition indexes that varied little among sites. Males are smaller than females and rarely exceed 40 cm TL (Oliveira 1999); however, it is unlikely that males would emigrate before being vulnerable to pots, and the low abundance of males is probably an accurate reflection of their relative abundance ≥30 cm TL.

Differences in condition index, albeit small (<15%), coincided with growth differences between sites. The three most upriver sites (ALB, ATH, and KIN) had the lowest condition index, whereas the two brackish-water sites showed relatively high condition indexes. The NEW site was an exception to this trend: the highest condition index was observed, despite growth rates that were low relative to other sites. Yellow-phase eels from this site also had the widest heads, suggesting that for whatever reason, the morphometry of eels was different at NEW than at other sites. Interestingly, eels at NEW were significantly more contaminated by

© 2003 NRC Canada

Fig. 7. Catch curves among sites for yellow-phase American eels (*Anguilla rostrata*) from the Hudson River, 1997–1999. Frequencies were binned into 3-year age classes. GWB, George Washington Bridge; HAV, Haverstraw; NEW, Newburgh; KIN, Kingston; ATH, Athens; ALB, Albany.

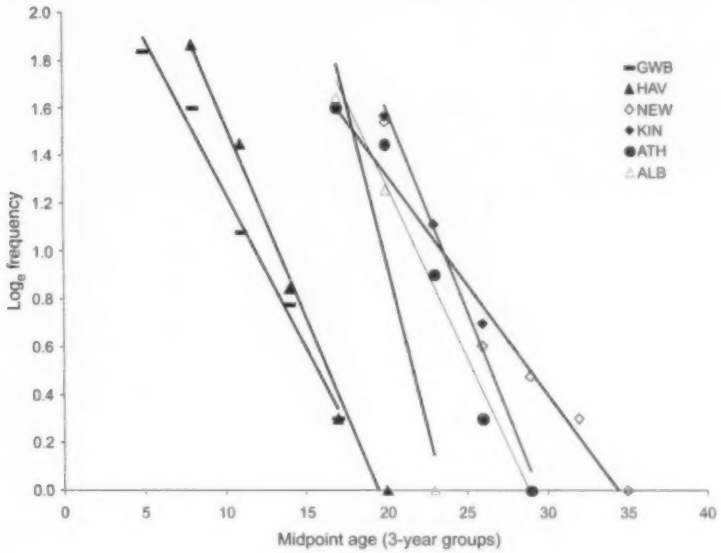

PCBs than eels at other sites, except ALB (Steinbacher 2001).

Nematode parasitism

Anguillicola crassus, native to Japanese eels (*A. japonicus*), infects the swimbladder of *Anguilla* spp. and has spread across most of Europe and recently into several areas in North America (Barse and Secor 1999; Barse et al. 2001; Moser et al. 2001). The large increase in prevalence and mean infection documented here demonstrated the capacity of the nonindigenous *A. crassus* to quickly invade an entire estuary. Overall, both prevalence and mean intensity were higher in freshwater than brackish-water areas. Results were comparable with those of Moser et al. (2001), who found mean prevalence in North Carolina rivers in 1998 and 1999 to be 52% (range 26–100%), with a mean intensity of 3.9 (range 1–12). Research has shown that the nematode prefers fresh water but that a smaller percentage can survive in brackish water, and even full salt water (Kirk et al. 2000). The ecological consequences of the parasite have been studied for European eel (*A. anguilla*), and studies have documented changes in growth (Thomas and Ollevier 1992), swimming speed (Sprengel and Lüchtenberg 1991), and serum cortisol levels (Sures et al. 2001), as well as changes to the morphology of the swimbladder (Nimeth et al. 2000; Lefebvre et al. 2002). We were unable to analyze the effect of parasite intensity on growth because nematode infection rates were confounded by underlying differences in growth between freshwater and brackish-water regions.

Age and length structure

American eel lengths were relatively similar across sites, whereas eel ages were substantially and significantly younger in brackish-water sites vs. freshwater sites. This difference in age based on salinity is similar to results of Helfman and Bozeman (1984) in Georgia, where average age was younger in brackish water (4.6 years) than in fresh water (6.2 years). The age composition of freshwater eels measured in this study was similar to that found in Maine rivers (Oliveira and McCleave 2000) but older than most other studies on eels from freshwater habitats (Table 4). Annuli in otolith sections have been validated for *A. rostrata* in other systems (Oliveira 1996), and the similarity between growth rates determined from mark–recapture and those determined by estimated age at capture provides some evidence that our age interpretations were accurate.

The results of this study support the hypothesis that silver eel metamorphosis and emigration are more dependent on length than on age (Helfman et al. 1987; De Leo and Gatto 1996). This conclusion is based on the observed sharp reduction in the number of eels >55 cm across sites and the concurrent lack of a sharp decline at a given age across the same sites. In addition, the decrease in abundance of eels between 50 and 55 cm is similar to sizes of emigrating female silver eels in Rhode Island and Maine (Oliveira 1999; Oliveira and McCleave 2000).

Growth

Growth calculated from mark–recapture was substantially higher (twofold) in brackish-water eels than in freshwater eels, corresponding to the age differences recorded in these areas. Faster growth by eels in brackish water has been documented (Helfman et al. 1987), but Gray and Andrews (1971) found the opposite trend. Average growth was much higher at both ATH and HAV in 1998 than in 1999, suggesting that conditions that affect growth act on an estuary-wide scale.

Growth rates measured in the Hudson River were similar to those estimated for other systems (Table 5). The highest estimate of mean brackish-water growth in our study

© 2003 NRC Canada

Table 4. North American eel age estimates from the literature, noting stage of eels.

Location	Salinity	Phase	Age (years)	Source
Georgia tidal creek	Brackish	Yellow	2–7	Helfman et al. 1984
	Fresh	Yellow	3–13	Helfman and Bozeman 1984
	Brackish	Yellow	3–7	
South Carolina river	Both	Yellow	2–11	Hansen 1978
New Jersey streams	Fresh	Yellow	3–19	Ogden 1970
Rhode Island river	Fresh	Silver	4–20	Oliveira 1999
Hudson River, New York	Both	Yellow	1–12	Mattes 1989
	Brackish	Yellow	3–39	This study
	Fresh	Yellow	7–30	This study
Maine rivers	Fresh	Elver and Yellow	1–33	Oliveira and McCleave 2000
Newfoundland	Both	Silver	12–13	Gray and Andrews 1971

Table 5. North American yellow-phase eel growth estimates from the literature, noting estimation method.

Location	Salinity	Growth rate ($cm \cdot year^{-1}$)	Method	Source
Louisiana creek	Fresh	up to 32.5	Based on one fin clipped eel	Gunning and Shoop 1962
Georgia creek and marsh	Brackish	5	Age–length regression	Helfman and Bozeman 1984
	Fresh	5.3		
Georgia creek	Brackish	5.5–6.2	Mark–recapture study	Helfman et al. 1984
		4.4	Age–length regression	
Rhode Island river	Fresh	4.0 (F), 3.1 (M)	Age–length regression	Oliveira 1999
Rhode Island river	Fresh	3	Mark–recapture study	Oliveira 1997
Hudson River	Both	3.9	Age–length regression	Mattes 1989
Hudson River	Brackish	8	Mark–recapture study	This study
Hudson River	Fresh	3.4	Mark–recapture study	This study
Hudson River	Brackish	5.5	Age and length at capture	This study
Hudson River	Fresh	2.8	Age and length at capture	This study

Note: Where known, gender is specified: F, female; M, male.

($10.4\ cm \cdot year^{-1}$) was based on a small sample size (12 eels; mean TL = 41 cm) captured in HAV during the 1999–2000 season. Because of the random order of sampling sites, these 12 eels were at large for 400 days, approximately 1 month longer than most other recapture eels. Although growth was adjusted for time at large (measured growth/400 × 365), the extra month during the high growth season (see below) could explain the high growth measured that year. Growth rates at GWB in 1999–2000 and HAV in 1998–1999 ($7.5\ cm \cdot year^{-1}$ and $6.1\ cm \cdot year^{-1}$, respectively) were similar to those estimated in Georgia (Helfman and Bozeman 1984).

Our estimation that summer growth comprises 40% of the annual growth is supported by Helfman et al. (1984), who found the highest growth in summer, with lower growth in spring and fall, and no growth in winter. The correlation between growth in 1999 and 2000 was noteworthy and suggests that either some eels have a genetic predisposition for faster growth and (or) some eels consistently choose or outcompete other eels for better food or habitat resources. Feeding hierarchies have been observed in eels in captivity, which lends credence to the latter explanation (Tesch 1977).

Estimates of growth from size at age of capture were slightly lower than mark–recapture growth rates. Mark–recapture estimates of growth could have been negatively affected by the tagging procedure or positively affected by supplementing diets with bait. However, highly variable growth rates and the presence of both high (5.5 cm) and no (0 cm) growth documented 2 months after tagging suggest that these influences may be minimal. Length was a poor predictor of age in this study. Despite poor fits of size at age regressions, estimated lifetime growth rates were similar in amplitude to those estimated through mark–recapture. Still, we advise that given the large variance in size at age and errors associated with ageing eels, tagging studies are a much more rigorous method for estimating growth rate assuming minimal effects from capturing and tagging.

Loss rate and production

Loss rate estimates (natural mortality and emigration) for eels >30 cm were similar between brackish-water and freshwater locations but showed differing age-specific patterns. Few young eels were captured at freshwater sites, and we believe that this was due to slow growth, with the younger, smaller eels escaping from the pots. Loss rates included both emigration plus natural mortality. There are only two estimates of natural mortality in American eels: (*i*) $0.25\ year^{-1}$ ($22\% \cdot year^{-1}$) for natural mortality and emigration on Prince Edward Island, and (*ii*) $0.13–0.79\ year^{-1}$ ($12–55\% \cdot year^{-1}$) for 10-year-old eels in the northwestern Gulf of St. Lawrence (Anonymous 2001). Compared with these estimates, the rates of loss measured in this study ($15\% \cdot year^{-1}$) were low. However, eels less than 30 cm, with potentially much higher predation, were not included in these estimates.

One of the assumptions for using the catch equation is that recruitment is stable through time. By binning eels into 3-year age classes, the effect of interannual recruitment vari-

© 2003 NRC Canada

ability will be reduced. Evidence suggests that eel recruitment varies from year to year but also follows longer-term decadal shifts associated with oceanographic conditions (Castonguay et al. 1994). If recruitment has been declining throughout the American eel's range (including the Hudson River; Anonymous 2001), then our loss rates may be underestimated (less than expected representation of younger age classes).

Production for 1998 and 1999 were both substantially higher for the brackish-water location (HAV) than for the freshwater location (ATH). The high production calculated for HAV in 1998 was influenced by the high eel abundance measured for that year (18 and 8 eels·ha^{-1} in 1998 and 1999, respectively; Morrison and Secor 2004), whereas the high production in 1999 was influenced by the high growth rate for that year. Even though ATH experienced a slightly higher growth in 1998 than in 1999, the abundance was lower (5 eels·ha^{-1} and 9 eels·ha^{-1} in 1998 and 1999, respectively), leading to an overall reduction in production. A simple sensitivity analysis found that the abundance parameter affects production estimates the most and that implementing a length–weight equation or adjusting weights for food in the stomach (according to correction factor from Helfman and Bozeman 1984) reduced the production estimate by only 1%.

Vøllestad and Jonsson (1988) estimated European eel production at 3.51 kg·ha^{-1}·year^{-1} in the Imsa River, Norway, which is much higher than the estimates for this study (0.43–1.44 kg·ha^{-1}·year^{-1}). The difference could be due to the low mortality rates and abundance estimates measured here compared with those of other systems. The low production in the Hudson River might also be related to the lack of commercial harvests. Fishing may increase the productivity of an area by keeping the population below carrying capacity, decreasing competition between conspecifics and perhaps allowing for increased regional recruitment by elvers (Tyler and Gallucci 1980).

Management implications

The results from this study suggest that brackish-water areas could support a higher fishing mortality level than freshwater areas. The mechanism for higher growth and production in brackish water is not yet understood. Possible causes include an increase in quality or quantity of food, increase in habitat quality (Barker and Cone 2000), lower resting metabolism resulting from living in near-isoosmotic conditions, increased water temperature, which reduces the amount of time that eels are dormant during winter (Walsh et al. 1983), reduced effects from parasites, decreased predation, or decreased intra- or inter-specific competition.

We hypothesize that the higher brackish-water eel production measured here is general to most large North American estuaries. Therefore, allowing harvest in brackish-water areas only, as recently proposed by an international team of scientists (Anonymous 2001), may be a defensible management policy. The lower productivity and the late age of maturity of eels in freshwater habitats suggests that fisheries would have a much larger impact in these areas. Keeping freshwater areas as a "reserve" or protected area would allow a certain percent of the population to mature, emigrate (escape), and reproduce. Freshwater areas in the Hudson River supported only female eels, and it is the female eels that are most impacted by fishing (because of their large size and older ages) and most in the need of protection. Such a strategy of escapement would depend on the assumption that freshwater eels effectively contribute to the spawning stock, evidence for which exists for congeneric species (Tsukamoto and Arai 2001; Limburg et al. 2003).

Acknowledgements

This research is dedicated to Mr. Ron Ingold, a fisherman in Valley Lee, N.J., who provided assistance in fieldwork and perspective related to this project and the heritage of the lower Hudson River. Mr. Ingold passed away in April 2002, a loss for the Hudson River fishing community, which is endangered as a result of persistent ecosystem pollution. We thank Mr. Steve Nack, who assisted with most of the fieldwork. Troy Gunderson and Steve Larsen assisted in the field and laboratory. We appreciate assistance from the Riverkeeper in providing accommodations and laboratory space during field seasons. Drs. Ed Houde and Chris Rowe provided comments on an earlier version of this manuscript. The Hudson River Foundation supported this research. This is Contribution No. 3678 of the University of Maryland Center for Environmental Science, Chesapeake Biological Laboratory.

References

Anonymous. 2001. Report of the EIFAC/ICES working group on eels. Advisory Committee on Fisheries Management, International Council for the Exploration of the Sea, CM 2001/ASFM:03.

Barker, D.E., and Cone, D.K. 2000. Occurrence of *Ergasilus celestis* (Copepoda) and *Pseudodactylogryrus anguillae* (Monogenea) among wild eels (*Anguilla rostrata*) in relation to stream flow, pH, and temperature and recommendations for controlling their transmission among captive eels. Aquaculture, **187**: 261–274.

Berg, R. 1985. Age determination of eels, *Anguilla anguilla*: comparison of field data with otolith ring patterns. J. Fish Biol. **26**: 537–544.

Barse, A.M., and Secor, D.H. 1999. An exotic nematode parasite of the American eel. Fisheries, **24**: 6–10.

Barse, A.M., McGuire, S.A., Vinores, M.A., Eierman, L.E., and Weeder, J.A. 2001. The swimbladder nematode *Anguillicola crassus* in American eels (*Anguilla rostrata*) from middle and upper regions of Chesapeake Bay. J. Parasitol. **87**: 1366–1370.

Bozeman, E.L., Helfman, G.S., and Richardson, T. 1985. Population size and home range of American eels in a Georgia tidal creek. Trans. Am. Fish. Soc. **114**: 821–825.

Bush, A.O., Lafferty, K.D., Lotz, J.M., and Shostak, A.W. 1997. Parasitology meets ecology in its own terms: Margolis et al. revisited. J. Parasitol. **83**: 575–583.

Castonguay, M., Hodson, P.V., Couilard, C.M., Eckersley, M.J., Dutil, J.D., and Verreault, G. 1994. Why is recruitment of the American eel, *Anguilla rostrata*, declining in the St. Lawrence River and Gulf? Can. J. Fish. Aquat. Sci. **51**: 479–488.

Cieri, M.D., and McCleave, J.D. 2000. Discrepancies between otoliths of larvae and juveniles of the American eel: is something fishy happening at metamorphosis? J. Fish Biol. **57**: 1189–1198.

De Leo, G.A., and Gatto, M. 1996. Trends in vital rates of the European eel: evidence for density dependence? Ecol. Appl. **6**: 1281–1294.

© 2003 NRC Canada

Dolan, J.A., and Power, G. 1977. Sex ratio of American eels, *Anguilla rostrata*, from the Matamek River System, Quebec, with remarks on problems in sexual identification. J. Fish. Res. Board Can. **34**: 294–299.

Dovel, W.L., Pekovitch, A.W., and Berggren, T.J. 1992. Biology of shortnose sturgeon (*Acipenser brevirostrum*) in the Hudson River Estuary, New York. *In* Estuarine Research in the 1980's. The Hudson River Environmental Society Seventh Symposium on Hudson River Ecology. *Edited by* Lavett C. Smith. State University of New York Press, Albany, N.Y. pp. 187–216.

Ford, T.E., and Mercer, E. 1986. Density, size distribution and home range of American eels, *Anguilla rostrata*, in a Massachusetts salt marsh. Environ. Biol. Fishes, **17**: 309–314.

Gray, R.W., and Andrews, C.W. 1971. Age and growth of the American eel (*Anguilla rostrata* (LeSueur)) in Newfoundland waters. Can. J. Zool. **49**: 121–128.

Graynoth, E. 1999. Improved otolith preparation, ageing and back-calculation techniques for New Zealand fresh water eels. Fish. Res. **42**: 137–146.

Gunning, G.E., and Shoop, C.R. 1962. Restricted movements of the American eel, *Anguilla rostrata*, in fresh water streams, with comments on growth rate. Tulane Stud. Zool. **9**: 265–272.

Hansen, R.A. 1978. Age, growth, and sex ratio study. M.Sc. thesis, Clemson University, Clemson, S.C.

Helfman, G.S., and Bozeman, E.L. 1984. Size, age, and sex of American eels in a Georgia River. Trans. Am. Fish. Soc. **113**: 132–141.

Helfman, G.S., Bozeman, E.L., and Brothers, E.B. 1984. Comparison of American eel growth rates from tag returns and length–age analyses. Fish. Bull. **82**: 519–522.

Helfman, G.S., Facey, D.E., Hales, L.S., and Bozeman, E.L. 1987. Reproductive ecology of the American eel. *In* Common strategies of anadromous and catadromous fishes. Proceedings of an international symposium, 9–13 March 1996, Boston, Mass. Am. Fish. Soc. Symp. Ser. 1. pp. 42–56.

Hilborn, R., and Walters, C.J. 1991. Quantitative fisheries stock assessment — choice, dynamics and uncertainty. Chapman and Hall, New York.

Hornberger, M.L. 1977. Gear selectivity study. *In* Progress Report. S.C. Department of Natural Resources, Bonneau, S.C. pp. 30–59.

Houde, E.D., and Rutherford, E.S. 1993. Recent trends in estuarine fisheries: predictions of fish production and yield. Estuaries, **16**: 161–176.

Kirk, R.S., Kennedy, C.R., and Lewis, J.W. 2000. Effect of salinity on hatching, survival, and infectivity of *Anguillicola crassus* (Nematoda: Dranculoidea) larvae. Dis. Aquat. Org. **40**: 211–218.

LaBar, G.W., and Facey, D.E. 1983. Local movements and inshore population sizes of American eels in Lake Champlain, Vermont. Trans. Am. Fish. Soc. **112**: 111–116.

Lefebvre, F., Contournet, P., and Crivelli, A.J. 2002. The health state of the eel swimbladder as a measure of parasite pressure by *Anguillicola crassus*. Parasitology, **124**: 457–463.

Limburg, K.E., Wickstrom, H., Svedang, H., Elfman, M., and Kristiansson, P. 2003. Do stocked fresh water eels migrate? Evidence from the Baltic suggests "yes". *In* Biology, management, and protection of catadromous eels. *Edited by* D.A. Dixon. American Fisheries Society, Symposium 33, Bethesda, Md. pp. 275–284.

Mattes, K.C. 1989. The ecology of the American eel, *Anguilla rostrata* (LeSueur), in the Hudson River. Dissertation, Fordham University, New York.

Michaud, M., Dutil, J.D., and Dodson J.J. 1988. Determination of the age of young American eels, *Anguilla rostrata*, in fresh water, based on otolith surface area and microstructure. J. Fish Biol. **32**: 179–189.

Morrison, W.E., and Secor, D.H. 2004. Local abundance of yellow-phase American eels in the Hudson River estuary. Trans. Am. Fish. Soc. In press.

Morrison, W.E., Secor, D.H., and Piccoli, P.M. 2003. Estuarine habitat use by Hudson River American eels as determined by otolith strontium:calcium ratios. *In* Biology, management, and protection of catadromous eels. *Edited by* D.A. Dixon. American Fisheries Society, Symposium 33, Bethesda, Md. pp. 87–100.

Moser, M.L., Patrick, W.S., and Crutchfield, J.U. 2001. Infection of American eels, *Anguilla rostrata*, by an introduced nematode parasite, *Anguillicola crassus*, in North Carolina. Copeia, 2001(3): 848–853.

National Marine Fisheries Service. 2002. Statistics and Economics Division. Available at http://www.st.nmfs.gov/st1/commercial/landings/annual_landings.htm/.

Nimeth, K., Zwerger, P., Wurtz, J., Salvenmoser, W., and Pelster, B. 2000. Infection of the glass-eel swimbladder with the nematode *Anguillicola crassus*. Parasitology, **121**: 75–83.

Ogden, J.C. 1970. Relative abundance, food habits, and age of the American eel, *Anguilla rostrata*, in certain New Jersey streams. Trans. Am. Fish. Soc. **99**: 54–59.

Oliveira, K. 1996. Field validation of annular growth rings in the American eel, *Anguilla rostrata*, using tetracycline-marked otoliths. Fish. Bull. **94**: 186–189.

Oliveira, K. 1997. Movements and growth rates of yellow-phase American eels in the Annaquatucket River, Rhode Island. Trans. Am. Fish. Soc. **126**: 638–646.

Oliveira, K. 1999. Life history characteristics and strategies of the American eel, *Anguilla rostrata*. Can. J. Fish. Aquat. Sci. **56**: 795–802.

Oliveira, K., and McCleave, J.D. 2000. Variation in population and life history traits of the American eel, *Anguilla rostrata*, in four rivers in Maine. Environ. Biol. Fishes, **59**: 141–151.

Otake, T., Ishii, T., Nakahara, M., and Nakamura, R. 1997. Changes in otolith strontium:calcium ratios in metamorphosing *Conger myriaster* leptocephali. Mar. Biol. **128**: 586–572.

Parker, S.J. 1995. Homing ability and home range of yellow-phase American eels in a tidally dominated estuary. J. Mar. Biol. **75**: 127–140.

Proman, J.M., and Reynolds, J.D. 2000. Differences in head shape of the European eel, *Anguilla anguilla*. Fish. Manag. Ecol. **7**: 349–354.

Ricker, W.E. 1975. Computation and interpretation of biological statistics of fish populations. Bull. Fish. Res. Board Can., Ottawa.

Secor, D.H., Dean, J.M., and Laban, E.H. 1991. Manual for otolith removal and preparation for microstructural examination. University of South Carolina Press, Columbia, S.C.

Sorensen, P.W., Bianchini, M., and Winn, H.E. 1983. Individually marking American eels by freeze branding. Prog. Fish Cult. **45**: 62–63.

Sprengel, G., and Lüchtenberg, H. 1991. Infection by endoparasites reduces maximum swimming speed of European smelt, *Osmerus eperlanus*, and European eel, *Anguilla anguilla*. Dis. Aquat. Org. **11**: 31–35.

Steinbacher, J. 2001. The American eel, *Anguilla rostrata*, as a sentinel species of polychlorinated biphenyl contamination in the Hudson River. M.Sc. thesis, University of Maryland, College Park, Md.

Sures, B., Knopf, K., and Kloas, W. 2001. Induction of stress by the swimbladder nematode *Anguilicola crassus* in European eels, *Anguilla anguilla*, after repeated experimental infection. Parasitology, **123**: 179–184.

Tesch, E.W. 1977. The eel: biology and management of anguillid eels. Chapman and Hall Ltd., Halsted Press, New York.

© 2003 NRC Canada

Thomas, K., and Ollevier, F. 1992. Paratenic hosts of the swimbladder nematode *Anguillicola crassus*. Dis. Aquat. Org. **13**: 165–174.

Tsukamoto, K, and Arai, T. 2001. Facultative catadromy of the eel *Anguilla japonica* between fresh water and seawater habitats. Mar. Ecol. Prog. Ser. **220**: 265–276.

Tyler, A.V., and Gallucci, V.F. 1980. Dynamics of fished stocks. *In* Fisheries management. *Edited by* R.T. Lackey and L.A. Nielson. John Wiley and Sons, New York. pp. 111–132.

Vøllestad, L.A. 1985. Age determination and growth of yellow eels, *Anguilla anguilla* (L.), from a brackish water, Norway. J. Fish Biol. **26**: 521–525.

Vøllestad, L.A., and Jonsson, B. 1988. A 13-year study of the population dynamics and growth of the European eel *Anguilla anguilla* in a Norwegian river: evidence for density-dependent mortality, and development of a model for predicting yield. J. Anim. Ecol. **57**: 983–997.

Walsh, P.J., Foster, G.D., and Moon, T.W. 1983. The effects of temperature on metabolism of the American eel: compensation in the summer and torpor in the winter. Physiol. Zool. **56**: 532–540.

© 2003 NRC Canada

Upstream movement by nonnative brook trout (*Salvelinus fontinalis*) promotes invasion of native cutthroat trout (*Oncorhynchus clarki*) habitat

Douglas P. Peterson and Kurt D. Fausch

Abstract: To understand how immigration and emigration influence the processes by which invading nonnative brook trout (*Salvelinus fontinalis*) displace native cutthroat trout (*Oncorhynchus clarki*), we studied trout movement in long segments of three mountain streams in Colorado during 1999–2001. Over 3500 trout were captured and marked at weirs and during electrofishing, both within and downstream of stream segments. Nearly 80% of brook trout captured at weirs were moving upstream, whereas almost 65% of cutthroat trout were moving downstream. Brook trout movements peaked in early summer and again in fall. Brook trout immigration rates from downstream source populations were high, and in one stream, invaders repopulated a segment where they were removed within 8 months. Immigrant brook trout were typically mature adults in similar body condition to the general population. Brook trout immigrated from a range of distances, with local movement within 250 m more frequently detected, but fish also moved from many distances up to 2 km away within a summer. Brook trout encroachment and invasion was characterized by a wave of local movement exerting biotic pressure on the downstream limit of the cutthroat trout population and jump dispersers moving upstream beyond the invasion front promoting rapid population spread.

Résumé : Nous avons suivi en 1999–2001 les déplacements des salmonidés sur de longs segments de trois cours d'eau de montagne au Colorado pour comprendre comment l'immigration et l'émigration influence les processus par lesquels l'omble de fontaine (*Salvelinus fontinalis*), une espèce envahissante non indigène, déplace la truite fardée indigène (*Oncorhynchus clarki*). Nous avons capturé et marqué plus de 3500 poissons près de barrages et lors de pêches électriques dans les segments étudiés ou en aval de ceux-ci. Près de 80 % des ombles de fontaine capturés aux barrages se déplaçaient vers l'amont, alors que presque 65 % des truites fardées se dirigeaient vers l'aval. Le déplacement des ombles de fontaine était maximal au début de l'été et à l'automne. Les taux d'immigration des ombles de fontaine à partir des populations de l'aval sont élevés et, dans un cours d'eau, les ombles ont recolonisé en moins de 8 mois un segment d'où ils avaient été éliminés. Les ombles immigrants étaient généralement des adultes matures dont la condition physique correspondait à celle de la population en général. Les ombles provenaient de points de distances variables; des déplacements locaux de moins de 250 m étaient fréquents, mais certains poissons s'étaient déplacés de points éloignés jusqu'à 2 km au cours d'un été. L'empiètement et l'invasion de l'omble de fontaine se caractérisent par une série de déplacements locaux qui exercent une pression biotique sur la limite aval de la répartition de la population de truites fardées; de plus, certains ombles se dispersent par bonds, se déplaçant loin vers l'amont au-delà du front d'invasion, provoquant ainsi une expansion rapide de la population.

[Traduit par la Rédaction]

Introduction

Invasions are a major factor in the imperilment, extinction, and homogenization of aquatic fauna (Rahel 2002). Salmonid fishes have been widely introduced, and those that successfully invade are known to produce large ecological effects from the genetic to ecosystem levels (Krueger and May 1991). For example, invasion by brook trout (*Salvelinus fontinalis*) in the western U.S. has been implicated in population declines of native subspecies of inland cutthroat trout (*Oncorhynchus clarki*), and brook trout tend to displace cutthroat trout where they co-occur (Griffith 1988; Fausch 1989; Young 1995).

Movements of invading salmonids have not been well studied in comparison to other aspects of their invasion, such as impacts (Dunham et al. 2003; but see Adams et al. 2000, 2001). However, ranging behavior (sensu Dingle 1996) to seek suitable habitat or feeding conditions outside the home

Received 20 December 2002. Accepted 7 September 2003. Published on the NRC Research Press Web site at http://cjfas.nrc.ca on 19 December 2003.
J17252

D.P. Peterson[1,2] **and K.D. Fausch.** Department of Fishery and Wildlife Biology, Colorado State University, Fort Collins, CO 80523-1474, U.S.A.

[1]Corresponding author (e-mail: peterson@unb.ca).

[2]Present address: Canadian Rivers Institute, Department of Biology, University of New Brunswick, Bag Service 45111, Fredericton, NB E3B 6E1, Canada.

 doi: 10.1139/F03-128 © 2003 NRC Canada

Table 1. Location and habitat characteristics of three study streams in northern Colorado during 1999–2001.

Stream	Location (latitude, longitude)	Length of study segment (m)[a]	Elevation range (m)	Mean July water temperature (°C)	Mean bankfull width range (m)[b]
Little Muddy Creek	39°56′59″N, 106°02′46″W	877	2658–2694	12.7	2.5–3.8
Indiana Creek	39°25′38″N, 106°59′44″W	950–1090	3194–3246	6.6	2.9–3.8
Willow Creek	40°28′12″N, 105°46′48″W	1002–1200	3188–3219	6.9	2.1–2.6

[a]Length of study segment varied among years in two streams because of habitat changes caused by beaver (Indiana Creek) and logistical constraints (Willow Creek).
[b]Range of mean bankfull width among years as measured in the study segments.

range is common for many species of stream salmonids (Gowan et al. 1994; Gowan and Fausch 1996) and may often drive invasion success and rate of spread. Description of the pattern of displacement observed in natural populations typically has been followed by small-scale studies of competition between native and nonnative species at the individual level (Peterson and Fausch 2003). Nevetheless, movement is a critical component of the life history and ecology of salmonids (Northcote 1997) and so is likely to influence invasion dynamics at the population level and over larger spatial scales (Fausch et al. 2002).

Detailed studies of movement by invading salmonids are warranted because invasion dynamics are sensitive to age-, size-, or stage-structured differences in dispersal (Neubert and Caswell 2000; Fagan et al. 2002). Therefore, an accurate assessment of the demography of a salmonid invasion must account for age- or size-specific differences in movement and their relative contributions to the rate of population spread. Particular components of stream salmonid populations are thought to exhibit more frequent ranging behavior than others (Gowan et al. 1994; Fausch and Young 1995; Gowan and Fausch 1996) and may promote rapid, far-ranging colonization of new habitats.

Movement in isolated populations of native salmonids facing nonnative fish invasions has also rarely been considered but may be important if it contributes to their displacement. Many populations of native cutthroat trout are restricted to headwater stream reaches because of fragmentation and loss of downstream habitat, impassible barriers, or nonnative species (Behnke 1992; Harig et al. 2000). Inland salmonid species historically included migratory (e.g., fluvial or adfluvial) life history types (Northcote 1997), but these components are thought to have been lost from, or may now be maladaptive for, isolated populations (e.g., Young 1996). However, even resident populations can exhibit ranging behavior to meet life history requirements (Fausch and Young 1995), and an influx of nonnative salmonids might increase emigration rates of native species.

In this study, we measured characteristics of movement by nonnative brook trout invading mid- and high-elevation headwater streams inhabited by native Colorado River cutthroat trout (*Oncorhynchus clarki pleuriticus*). To understand how movement influences invasion dynamics, we measured the timing, direction, distance, and rate of movement by brook trout in an ongoing upstream-directed invasion. We characterize the demographic components of brook trout populations that contribute to the success of such invasions and also describe how movement of cutthroat trout may contribute to the observed pattern of displacement.

Materials and methods

Study sites

Trout movement was measured in Little Muddy, Indiana, and Willow creeks in northern Colorado during 1999 to 2001 (Table 1; Fig. 1). Sites were small, first- or second-order montane streams with baseflow $<0.05 m^3 \cdot s^{-1}$ that we classified as mid-elevation (Little Muddy Creek, ~2650 m) or high-elevation (Indiana and Willow creeks, >3175 m) sites. Habitat alternated between 1–2% gradient meadow reaches with willow (*Salix* sp.) and 2–5% gradient forested reaches with mixed stands of lodgepole pine (*Pinus contorta*), subalpine fir (*Abies lasioicarpa*), Engelmann spruce (*Picea engelmannii*), and aspen (*Populus tremuloides*). Streams contained populations of Colorado River cutthroat trout subject to ongoing brook trout invasion. Published literature (Fausch 1989) and unpublished data from the Colorado Division of Wildlife and the U.S. Forest Service indicated that the invasions progressed substantially in the previous 1–3 decades. Study areas encompassed either the leading edge of the invasion (Indiana Creek) or the most recently invaded habitat (Little Muddy and Willow creeks). However, brook trout abundances were reduced in 877- to 1200-m-long segments (hereafter, study segments) of Little Muddy and Willow creeks during 1998 to 2001 as part of a removal experiment to test mechanisms by which brook trout displace cutthroat trout (Peterson 2002).

Predictions

Based on previous studies demonstrating widespread trout movement and ranging behavior in streams (e.g., Gowan et al. 1994; Rodríguez 2002), we made a series of predictions about movements by trout in study streams. These predictions generated subsequent expectations as to how such movement would influence the processes by which brook trout invade small, headwater streams inhabited by cutthroat trout. First, we predicted that brook trout would exhibit seasonal variation in movement, with peaks in early summer during elevated stream discharge (i.e., snowmelt runoff) and in fall during spawning (Flick and Webster 1975; Gowan and Fausch 1996). Second, we predicted that brook trout would tend to move upstream in summer (Flick and Webster 1975; Gowan and Fausch 1996), whereas cutthroat trout would either emigrate (Peterson and Fausch 2003) or show no tendency to move in either direction (Young 1996). Third, we predicted that adult brook trout would move more frequently than juveniles (Gowan and Fausch 1996). If so, these adults would likely be sexually mature and capable of reproducing and establishing populations. Fourth, we predicted that brook trout moving during summer would be longer but in poorer condition than individuals in the general popula-

© 2003 NRC Canada

Fig. 1. Study segments, weirs, and downstream marking sampling locations for Little Muddy, Indiana, and Willow creeks from 1999–2001. The two-way weirs were operated during summer to early fall. The study segment was the location of an intensive mark–recapture study to estimate trout survival (see Peterson 2002), and downstream marking locations were sites where brook trout (*Salvelinus fontinalis*) were marked and released to estimate distance and rate of movement.

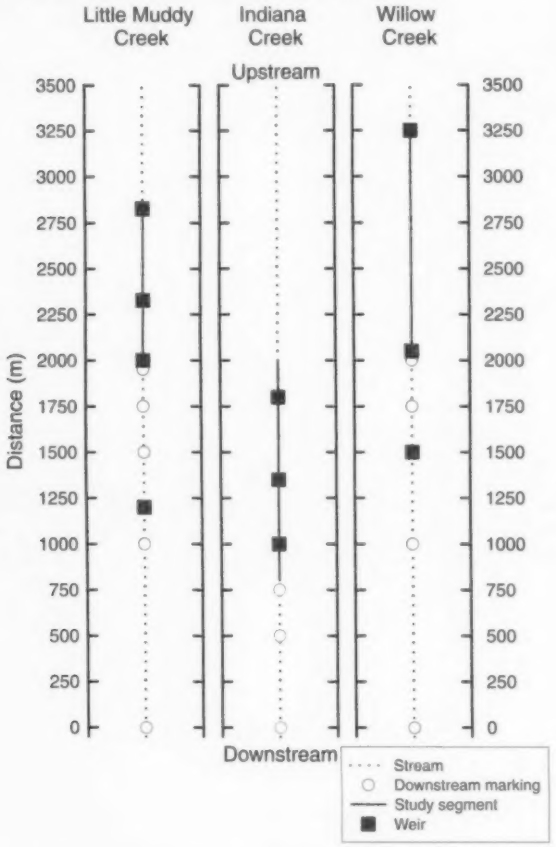

tion (Gowan and Fausch 1996). Fifth, we predicted that brook trout would move rapidly upstream from a variety of distances downstream (Gowan and Fausch 1996). Consequently, if these predictions held, we expected that invading brook trout would be primarily upstream-moving adults arriving from a variety of distances, and within-season movement rates would be high enough to promote rapid colonization.

Weirs

To measure timing and direction of trout movement and to characterize the age and size composition and body condition of moving trout, we operated two-way fish weirs in the three streams during summer to late fall from 1999 to 2001 (Table 2). Each stream had three or four weirs, one each at the upstream and downstream margins of the study segment and additional weirs either within this segment or downstream. Weirs consisted of a two-way trap box with side panels (wings hereafter) covered with 6-mm black plastic mesh that funneled trout into the traps (see Gowan and Fausch (1996) for similar design). Trap boxes consisted of a 0.9 m long × 0.8 m wide × 0.6 m tall frame of polyvinyl chloride (PVC) pipe covered with the same plastic mesh and were divided longitudinally to separate fish moving upstream from those moving down. Large cobble and plywood wedges provided velocity refuges for trout in each side. Trap openings were 6 cm wide, and a 20-cm-wide board was placed inside the trap box 10 cm from the entrance and perpendicular to flow to obscure the opening from trout already inside the trap. Beginning in 2000, entrances were constricted into a 5 cm × 8 cm opening through an angled section of plastic rain gutter fitted with a 10-cm length of flexible nylon stocking, which collapsed after trout passed through it and obscured the exit. Weirs were secured using steel posts, and a 25-cm mesh skirt extending from the bottom of the apparatus was buried in stream gravels to prevent trout from passing beneath the weir. Snorkeling was used to confirm that the weir was closed to all trout >75 mm fork length (FL). Weirs were installed during mid-June to late July, depending on when high flow from melting snow receded, and were removed in early October (see Table 2). Weirs could be monitored only during summer to fall because sites could not be reached during winter.

Weirs were visited every second day, and captured trout were anesthetized (MS-222), measured (FL, nearest mm), and weighed (nearest 0.1 g). Trout were assigned to one of three age classes (i.e., ages 0, 1, and 2 and older (= age 2+ hereafter)) based on length, using a combination of length–frequency histograms and ages determined from otoliths (Kennedy et al. 2003). Brook trout entering the study segments in Little Muddy and Willow creeks were euthanized with an overdose of anesthetic as part of the removal experiment. In all other cases, trout of both species received batch marks to indicate weir location and direction of travel, including brook trout leaving study segments of Little Muddy and Willow creeks. Fish of all sizes were marked using various colors of nontoxic Liquitex© acrylic paint (Binney and Smith, Inc., Easton, Pa.) injected into postorbital adipose tissue using an insulin syringe. In addition, brook trout ≥110 mm FL received numbered, dark-green Floy Fine Fabric Anchor tags (Floy Tag, Inc., Seattle, Wash.), and cutthroat trout ≥85 mm FL were tagged using two fluorescent visual implant (VI) tags (Northwest Marine Technology, Inc., Shaw Island, Wash.). The adipose fin was excised from all trout given individually numbered tags to identify subsequent tag loss. After recovery from anesthesia, trout were released at least 10 m away from the weir in the direction in which they were traveling. Stream stage was recorded from a staff gauge on each day that weirs were checked, and discharge was estimated using a rating curve calibrated for each stream in each year.

Downstream marking of brook trout

To characterize the origin of invading brook trout and to detect long-distance movements, we marked brook trout downstream and outside of the study segments (hereafter downstream marking; Fig. 1). Brook trout invasions were directed upstream in all streams, and source populations only existed downstream of the study segments. Batches of approximately 40–120 brook trout of all age classes and sizes were captured at minimum starting distances of 0, 250, 500,

© 2003 NRC Canada

Table 2. Dates of weir operation, downstream marking, and annual electrofishing surveys in study streams during 1999–2001.

Stream	Year	Number of weirs (unconfounded)[a]	Period of weir operation (days)[b]	Downstream marking	Electrofishing survey
Little Muddy	1999	3 (0)	24 June – 1 Oct. (100)	5–6 Aug.	10–13 Sept.
	2000	4 (1)	16 June – 16 Oct. (123)	8–9 June, 12–13 July	21–24 Sept.
	2001	4 (1)	10 June – 4 Oct. (117)	10, 16, 26 June	18–21 Sept.
Indiana	1999	3 (3)	21 July – 27 Sept. (69)	3–4 Aug.	17–19 Aug.
	2000	3 (3)	29 June – 4 Oct. (98)	14–15 July	14–18 Aug.
	2001	3 (3)	29 June – 3 Oct. (97)	3, 5 July	13–15 Aug.
Willow	1999	3 (1)	30 July – 29 Sept. (62)	[c]	17–20 Sept.
	2000	3 (1)	23 July – 3 Oct. (73)	1–3 Aug.	17–20 Sept.
	2001	3 (1)	20 July – 1 Oct. (74)	17–18 Aug.	17–20 Sept.

[a]Unconfounded weirs are those in which movement direction of brook trout was not biased by removing them from the study segments, whereas no cutthroat trout were removed so data from all weirs were used.

[b]Weirs could not be operated during winter or early spring because sites were inaccessible or discharge was too high.

[c]Downstream marking was not conducted in Willow Creek in 1999.

1000, and 2000 m downstream from the study segment during 1999 to 2001 and then marked and released (Table 2). Downstream marking was conducted in each stream in each year (except Willow Creek in 1999), but not all locations at 0 and 500 m were sampled each year, and the site 2000 m downstream in Indiana Creek could not be sampled because the stream was bordered by private property. Brook trout were captured by one-pass backpack electrofishing (Mark 10, Coffelt Manufacturing, Inc., formerly of Flagstaff, Arizona; settings, 30 Hz, 150–450 V pulsed DC) that proceeded upstream in reaches at least 100 m in length. A block net (5-mm mesh) was placed at the top of the reach. Brook trout captured were measured and tagged as above, and all fish received florescent elastomer (Northwest Marine Technology, Inc.) injected into rays of the dorsal or caudal fins to indicate year and location of capture. Trout were held overnight in live baskets placed in deep pools and then released at the capture location.

Annual electrofishing surveys

As part of the brook trout removal experiment, annual two-pass depletion electrofishing was conducted in the study segments of all streams during baseflow (Fig. 1; Table 2). The electrofishing technique was similar to that used for downstream marking, except that trout populations were enclosed by block nets at upstream and downstream margins of 150- to 300-m reaches where sampling was completed in 1 day (see Peterson 2002). Cutthroat trout in all streams and brook trout in Indiana Creek were counted, marked as above, and released into their 50-m section of capture, whereas brook trout captured in the study segments of Little Muddy and Willow creeks were euthanized. Weirs inside and at the margins of the study segments were closed during electrofishing.

Analysis

Marked trout were recaptured at weirs, during annual electrofishing surveys of the study segments, or during downstream marking. These sampling methods encompassed a total distance of 2000–3325 m per stream. We analyzed the timing of movement both graphically, in relation to date, and analytically, in relation to discharge. The relationship between the number of trout captured at weirs and stream discharge was explored using Pearson correlation on log-transformed data, by stream and year (n = 9 analyses for each species). Statistically significant correlations had 95% confidence intervals (CI) that did not overlap zero.

Direction of trout movement through weirs was estimated by logistic regression. Stream and year were primary factors, and log-transformed fork length was used as a covariate. In addition, treatment group (e.g., brook trout removal stream or not) was used as a class variable for cutthroat trout. Weir type (confounded or unconfounded) was used as an additional class variable for brook trout. Confounded weirs were those located adjacent to stream reaches where brook trout were being removed in Little Muddy and Willow creeks, so that movement direction of brook trout was potentially biased, whereas unconfounded weirs were those downstream from removal reaches (Little Muddy and Willow creeks) or in a stream where brook trout were not removed (Indiana Creek). An information-theoretic (IT) approach to model selection was used whereby Akaike's information criterion weights corrected for small sample sizes (AIC_c) were used to assess the relative likelihood of competing models (Burnham and Anderson 2002). Importance of individual factors was determined by cumulative AIC_c weights, defined as the sum of the AIC_c weights of all models containing that factor. The proportions of trout moving in a given direction were estimated using model averaging.

Lengths of marked trout in the general population that subsequently moved through weirs were compared with those that did not, using analysis of variance (ANOVA) or covariance (ANCOVA) and IT model selection. Lengths were log-transformed, and stream, year, and treatment group (cutthroat trout only) were factors. For brook trout, the general populations were defined as trout caught and individually tagged during downstream marking in Little Muddy and Willow creeks because brook trout were repeatedly removed from study segments, whereas in Indiana Creek, trout marked during annual electrofishing and downstream marking were pooled. For cutthroat trout, the general populations were also defined as all fish individually tagged inside the study segments and during downstream marking. Only individually tagged trout, generally age-1 and older, were used for these analyses so that trout recaptured at weirs could be separated from those that were not.

Fish condition of trout recaptured moving through weirs was also compared with those that did not (i.e., the general

© 2003 NRC Canada

population), using ANCOVA of the same marked trout as for length comparisons. In a typical ANCOVA, length–mass regression lines for each group are fit to the data to first test for differences in slopes (i.e., growth rates) among groups. If slopes are similar (i.e., group–length interaction not significant), one can estimate differences in body condition among treatment groups by comparing intercepts (cf. Riley and Fausch 1995; Gowan and Fausch 1996). In contrast, we used an information-theoretic approach for this analysis. Preliminary model selection for both species indicated that the relationship between length and mass (both log-transformed) depended on stream (or treatment group) and year and their interactions, so data were analyzed separately for each stream in each year ($n = 7$ analyses for brook trout because there were no brook trout recaptures in Little Muddy and Willow creeks during 1999, and $n = 9$ analyses for cutthroat trout). Three models were fit in each analysis, whereby mass was a function of (*i*) group, length, and their interaction (interaction model), (*ii*) group and length (group model), and (*iii*) length only (length-only model). Model averaging across these three models was used to estimate the mass of trout that moved through weirs versus those that did not (i.e., general population), and simple differences were calculated to determine if trout in one group were in better condition than those in the other.

Immigration into study segments by brook trout marked downstream was used to detect long-distance movements. Data from all weirs, annual electrofishing, and downstream marking were combined to estimate total and net movement of brook trout. Movement distances were estimated to within 25 m, because annual electrofishing was conducted in 50-m reaches and trout were returned to the middle of these reaches after marking. To measure the potential for brook trout to quickly colonize new habitats, we estimated within-season movement rates of brook trout during 2000–2001 using combined data from downstream marking and weirs. Data from 1999 were not analyzed because downstream marking was done relatively late in the summer (Table 2), and none of these fish, or fish initially marked at weirs, was recaptured at another location within the 1999 recapture season. Total and net movement frequencies were described, but not statistically analyzed because of potential bias. Some locations were not sampled every year, and recaptures would be expected to increase through time because more marked fish were available for recapture. In contrast, upstream movement rates were modeled as a function of stream, year, and size of brook trout using general linear models (ANOVA) and IT model selection using cumulative AIC_c weights, because these data were less subject to the biases affecting total and net movement frequencies. All statistical analyses were performed with SAS (PROC GENMOD, PROC MIXED, and PROC LOGISTIC; Version 8.2, SAS Institute Inc., Cary, N.C.).

Results

Numbers, timing, and direction of trout moving through weirs

We captured 1726 trout at weirs in the three streams during 1999–2001, but numbers captured varied by species, year, and stream (Figs. 2–4). Over twice as many brook trout ($n = 1220$) were captured than cutthroat trout ($n = 506$), and more trout of both species were captured in 2000 than in other years. Summer immigration by brook trout was substantial from 1999 to 2001, particularly in Little Muddy Creek. Between 1999 and 2001, the number of brook trout captured and removed by summer trapping at weirs on the margins of the study segment in Little Muddy Creek constituted 44–70% of the estimated 1998 (pretreatment) abundance of age-1 and older brook trout within the segment (Peterson 2002). In other streams, age-2+ brook trout immigration averaged 11% of the estimated 1998 abundance in the study segment.

Movement was more frequent in early summer and late fall, associated with higher discharge, particularly in Little Muddy and Indiana creeks (Figs. 2–4). Movement of brook trout was positively correlated with discharge in Little Muddy Creek during 2000 and 2001 ($r_{2000} = 0.65$, 95% CI 0.48–0.78; $r_{2001} = 0.60$, 0.41–0.74) but negatively correlated in Indiana Creek in 2001 ($r_{2001} = -0.30$, 95% CI –0.53 to –0.04). Cutthroat trout movement was also positively correlated with discharge every year in Little Muddy Creek ($r_{1999} = 0.33$, 95% CI 0.04–0.56; $r_{2000} = 0.73$, 95% CI 0.58–0.83; $r_{2001} = 0.50$, 95% CI 0.28–0.67) and in two of three years in Indiana Creek ($r_{1999} = 0.40$, 95% CI 0.09–0.64; $r_{2000} = 0.37$, 95% CI 0.09–0.59) but, like brook trout, was negatively correlated with discharge in Indiana Creek during 2001 ($r_{2001} = -0.33$, 95% CI –0.55 to –0.08). No correlations were significant for Willow Creek.

Brook trout tended to move upstream during summers in all streams and in most years, regardless of whether or not weirs were adjacent to brook trout removal reaches (Fig. 5*a*). Logistic regression using 24 a priori models indicated that stream, year, fish length, weir type, stream–year interaction, and year–length interaction were important factors (cumulative AIC_c weights all > 0.99). The proportion of brook trout moving in a given direction for each stream–year–weir type combination (at the mean fork length for each year) was estimated by model averaging over the top two models, which contributed 99% of the total AIC_c weight. Brook trout moved upstream through all weirs more often than downstream every year in Little Muddy Creek (84% estimated moving upstream, averaged over confounded and unconfounded weirs), two of three years in Willow Creek (73%), and one year in Indiana Creek (91%). These values estimate the proportion of brook trout captured at weirs that were moving upstream and do not make inference as to what proportion of the entire brook trout populations in these streams moved in a given direction.

In contrast, cutthroat trout moved downstream more often than upstream in two of three summers (Fig. 5*b*). Results from 23 a priori models indicated that year (cumulative AIC_c weight >0.99) and length (0.52) were important factors. The proportion of cutthroat trout moving in a given direction each year was estimated by averaging over the top 11 models (total AIC_c weight >0.99). Based on these models, an estimated 61% and 77% of cutthroat trout captured at weirs were moving downstream during 2000 and 2001, respectively.

Characteristics of trout moving through weirs

Trout of both species captured at weirs during summer ranged from 26 to 310 mm FL but were predominantly age 1 or age 2+ (Peterson 2002). Lengths of brook trout recaptured moving through weirs tended to be larger than those in the

© 2003 NRC Canada

Fig. 2. Number of brook trout (*Salvelinus fontinalis*, Bkt; ○) and Colorado River cutthroat trout (*Oncorhynchus clarki pleuriticus*, Ct; ▲) captured at all weirs, and stream discharge (—) in Little Muddy Creek during summer to late fall in (*a*) 1999, (*b*) 2000, and (*c*) 2001. Numbers of trout captured moving upstream ( ) or downstream ( ) are given for each species in each year.

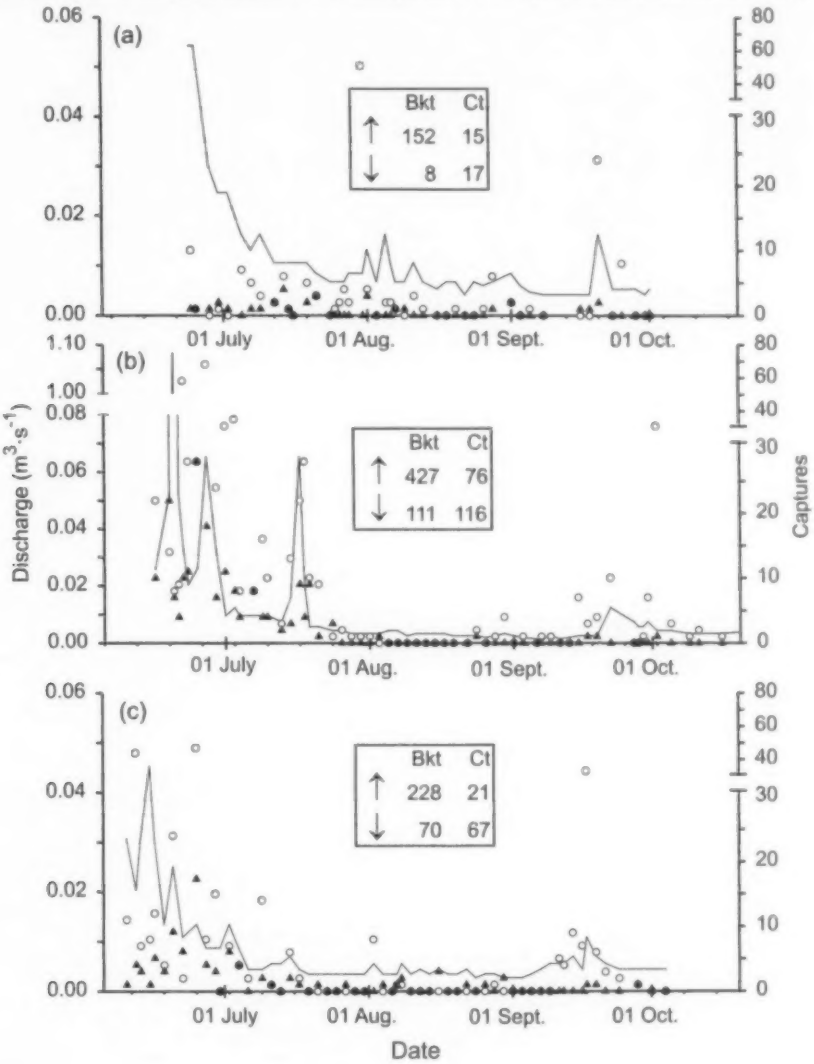

general population in Indiana and Willow creeks but smaller than those in Little Muddy Creek (Fig. 6*a*). However, the 95% confidence intervals for the two groups overlapped in every case, so there was insufficient statistical evidence to claim differences. Cumulative AIC_c weights for all single and two-way factors from 19 ANOVA models were all at least 0.99, indicating that the group effect for brook trout varied by stream and year. These effects are evident in the difference between Little Muddy Creek compared with Willow and Indiana creeks and the downward trend in length across years for all streams. In comparison, cutthroat trout moving through weirs tended to be larger than those in the general population in Little Muddy and Indiana creeks, but there was sufficient statistical evidence to show this only for Little Muddy Creek in 2001 (Fig. 6*b*). Cumulative AIC_c weights from 19 ANOVA models showed that cutthroat trout length depended on stream (weight = 1.0), group (0.99), and year (0.52) but not on the two-way (0.17 to 0.41) and three-way (<0.01) interactions, indicating that group and stream effects were consistent across years.

Fish condition

There was no evidence to suggest any biologically meaningful differences in body condition between brook trout recaptured at weirs versus the general population (Table 3). On average, brook trout in the general population were heavier in Little Muddy Creek (cumulative AIC_c weight for group 0.59–0.69), but the absolute and relative effect sizes were

© 2003 NRC Canada

Fig. 3. Number of brook trout (*Salvelinus fontinalis*, Bkt; ○) and Colorado River cutthroat trout (*Oncorhynchus clarki pleuriticus*, Ct; ▲) captured at all weirs, and stream discharge (—) in Indiana Creek during summer to late fall in 1999–2001. Numbers of trout captured moving upstream ( ) or downstream ( ) are given for each species in each year.

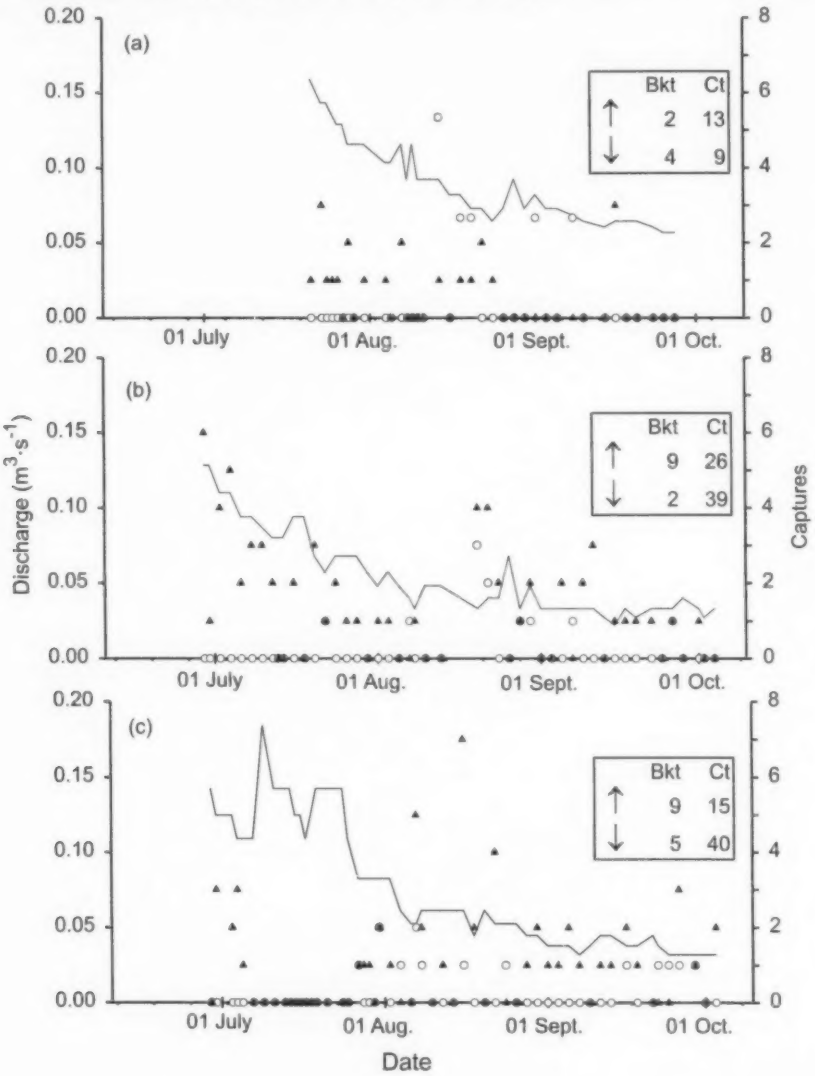

small. Similarly, condition of cutthroat trout captured at weirs and in the general population was similar except in two cases. In one of these, the absolute difference was <1 g (Little Muddy Creek in 2000), but in the other, cutthroat trout in the general population averaged 28 g heavier than those captured at weirs (Willow Creek in 2001).

Movement distances and rates

Recaptures of brook trout marked downstream of the study segments showed that brook trout immigrated from up to at least 2 km away, but local immigration from within 250 m was most frequently detected (Figs. 7–9). A total of 1872 brook trout were marked and released during downstream marking in the three streams, which resulted in 405 recaptures of 368 individual fish encountered at weirs, during downstream marking, or inside the study area during annual electrofishing surveys. Recapture rates were 19–28% among streams. The proportion of marked brook trout recaptured inside the study area could not be compared among streams because sampling effort and locations varied, but movement was detected more frequently in Little Muddy Creek than in Indiana or Willow creeks. There were sufficient recapture data for downstream marking in Little Muddy Creek to fit a logistic regression model that predicted the proportion of brook trout invading the study segment from different distances (intercept and distance, $P < 0.0001$). Batch marks of brook trout captured at 500 m downstream in 1999 quickly faded, so these data were excluded. The

© 2003 NRC Canada

Fig. 4. Number of brook trout (*Salvelinus fontinalis*, Bkt; ○) and Colorado River cutthroat trout (*Oncorhynchus clarki pleuriticus*, Ct; ▲) captured at all weirs, and stream discharge (—) in Willow Creek during summer to late fall in 1999–2001. Numbers of trout captured moving upstream ( ) or downstream ( ) are given for each species in each year.

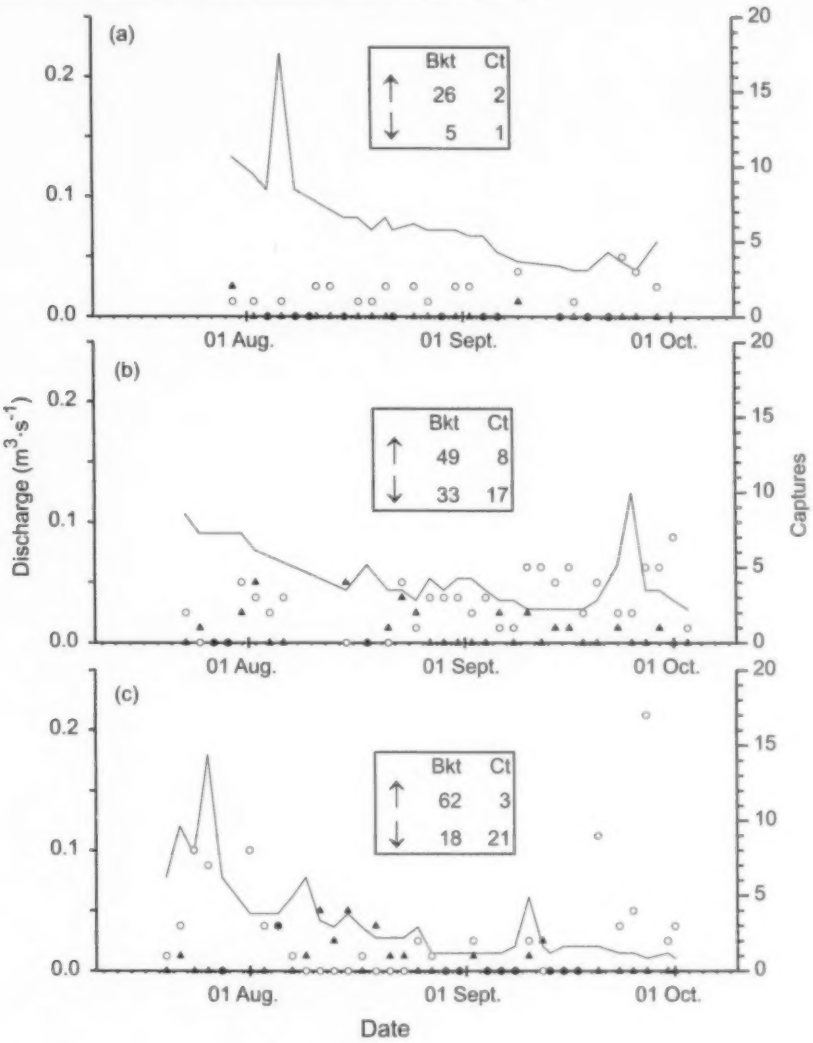

model predicts that 15% of brook trout at 250 m, 6% at 1000 m, and 2% at 2000 m would move upstream and enter the study segment.

Recaptures throughout the stream of these marked brook trout showed that the modal frequencies of total and net distances moved was ≤50 m, but substantial numbers of fish moved hundreds to thousands of metres (maximum value ≥2500 m; Figs. 8–9). For example, 54% of recaptured brook trout in Little Muddy Creek, 38% in Willow Creek, and 9% in Indiana Creek were estimated to have moved more than 50 m. Movement beyond 50 m was more commonly detected for brook trout in Little Muddy Creek than in other streams, and most individuals that did move were ultimately recaptured upstream from their original capture location (Fig. 9).

Median rates of upstream movement by brook trout captured within a summer were higher in Little Muddy Creek (33.3 m·day^{-1} in 2000, 16.7 m·day^{-1} in 2001) than in Indiana Creek (9.0 m·day^{-1} in 2001) or Willow Creek (11.5 m·day^{-1} in 2000, 12.5 m·day^{-1} in 2001; see Peterson (2002) for details). Cumulative AIC_c weights from 18 models indicated that movement rates depended on body length (weight = 0.99), year (0.91), and stream (0.61), but the length effect did not depend on stream or year (weights for all two-way interactions <0.4). The top-ranked model, in which movement rate was a function of year and length, indicated that there was a negative relationship between movement rate and size (i.e., negative regression coefficient for length with 95% CI that did not include 0). However, there was considerable uncertainty about this relationship because this model

© 2003 NRC Canada

Fig. 5. Proportion of (*a*) brook trout (*Salvelinus fontinalis*) and (*b*) Colorado River cutthroat trout (*Oncorhynchus clarki pleuriticus*) moving upstream through weirs in Little Muddy, Willow, and Indiana creeks during summer to late fall in 1999–2001 as estimated by logistic regression. Confounded estimates (□) are based on brook trout captured at weirs adjacent to study segments in Little Muddy and Willow creeks where brook trout were being removed by electrofishing, and brook trout attempting to enter the study segment were euthanized as part of a concurrent removal experiment. Thus, tests of movement direction by brook trout through these weirs were potentially confounded by the population manipulation. In contrast, unconfounded estimates (●) are based on brook trout captured at weirs downstream from the study segments in Little Muddy and Willow creeks and at all locations in Indiana Creek. Cutthroat trout abundances were not directly manipulated, so their data were unconfounded. Confidence intervals (CI) that do not intersect the horizontal broken line (proportion = 0.5) provide evidence that trout moved either upstream or downstream. The 1999 estimate for brook trout in Indiana Creek has wide confidence intervals because of small sample size (n = 6).

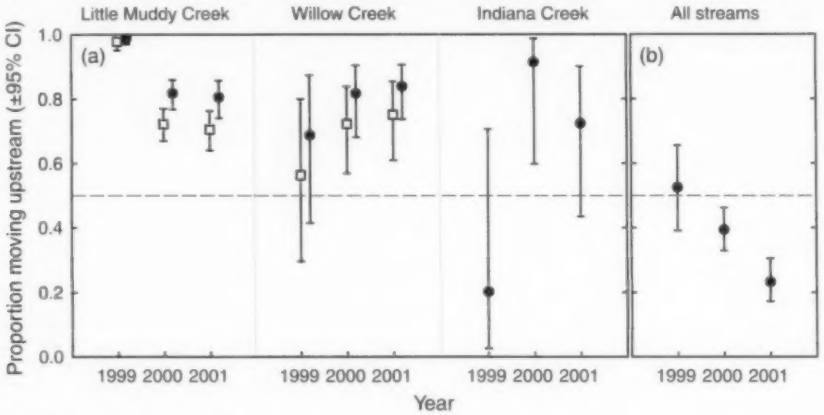

Fig. 6. Predicted sizes of (*a*) brook trout (*Salvelinus fontinalis*) and (*b*) Colorado River cutthroat trout (*Oncorhynchus clarki pleuriticus*) captured at weirs (□) and in the general population (●) in Little Muddy, Willow, and Indiana creeks from 1999–2001. Data are for individually tagged brook trout (generally ≥110 mm fork length) or cutthroat trout (generally ≥85 mm fork length) originally marked inside the study area or during downstream marking and subsequently either recaptured at a weir or not.

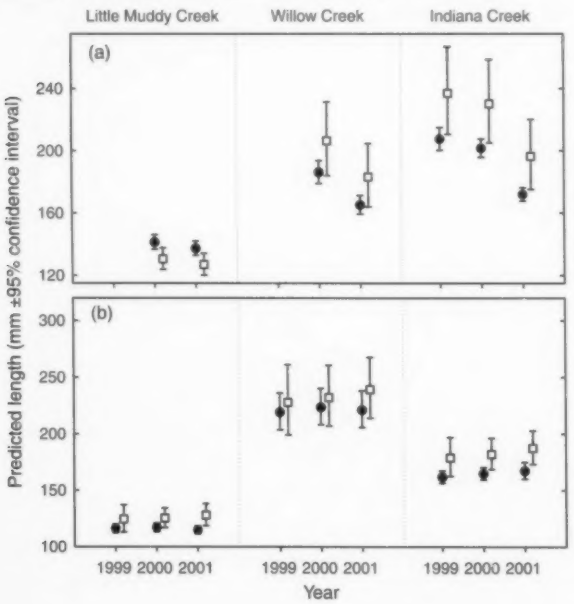

accounted for only 22% of the total AIC_c weight. For all streams in all years, only seven brook trout were recaptured moving downstream within a season (range 4–150 m·day^{-1}), so these data were not analyzed.

Tag loss and potential bias

Tag loss did occur for both trout species, but the overall effect was probably small. For example, most analyses were unbiased with respect to tag loss, including timing, direction, maturity, condition, and distance of moving trout, because they were either based on both marked and unmarked trout (e.g., timing, direction, maturity) or the trout captured were an unbiased sample for the characteristic measured (e.g., condition, distance moved). However, tag loss could affect inferences about length of moving trout. Tag loss was similar to that reported elsewhere (Mourning et al. 1994; Shepard et al. 1996) but increased with length in brook trout and decreased with length in cutthroat trout and varied by year for brook trout (logistic regression models selected using AIC_c, PROC LOGISTIC). At median length of trout captured at weirs, tag loss was ≤16% for brook trout and 35% for cutthroat trout. However, the 95% confidence intervals overlapped for tag loss by cutthroat trout at the extremes of the length range that contained 75% of trout tagged at weirs and during downstream marking (i.e., 115–223 mm, including both species). Thus, little bias would result from variation in tag loss with length for cutthroat trout. In contrast, the comparable 95% confidence intervals for tag loss by brook trout did not overlap in two of three years, so some minor bias with respect to length might be present. If larger brook trout lost tags more frequently than smaller brook trout, then the lengths estimated from those captured in weirs would be smaller than the true value (e.g., Fig. 6*a*). Thus, the statisti-

© 2003 NRC Canada

Table 3. Results of analysis of covariance (ANCOVA) comparing body condition of trout caught at weirs with those in the general population.

Stream	Year	Sample size (n)[a]		Size range (mm)	Model weights[b]			Difference in body mass (general – weir)[c]	
		General population	Weir captures		Interaction	Group	Intercept	Absolute (g, SE)	Relative (%)
Brook trout									
Little Muddy	2000	155	42	103–200	0.31	0.59	0.10	0.8 (0.37)	3.0
	2001	147	32	86–210	0.31	0.69	0.00	2.3 (0.45)	8.9
Willow	2000	113	5	78–244	0.42	0.42	0.16	11.1 (5.9)	17.4
	2001	137	10	108–243	0.13	0.38	0.49	–3.5 (4.3)	–6.9
Indiana	1999	142	2	115–330	[d]	[d]	[d]	[d]	[d]
	2000	205	5	105–300	0.11	0.25	0.64	2.9 (16.0)	2.8
	2001	300	7	110–351	0.28	0.29	0.43	–1.6 (2.3)	–2.6
Cutthroat trout									
Little Muddy	1999	145	6	81–220	0.09	0.25	0.66	0.2 (0.66)	0.9
	2000	134	30	82–211	0.42	0.57	0.01	0.9 (0.30)	5.2
	2001	182	16	82–200	0.99	0.00	0.01	[d]	[d]
Willow	1999	22	1	95–286	[d]	[d]	[d]	[d]	[d]
	2000	24	5	119–308	0.41	0.17	0.42	3.7 (7.3)	2.4
	2001	19	10	125–301	0.27	0.73	0.00	28.0 (6.5)	20.6
Indiana	1999	120	9	78–273	0.08	0.24	0.68	0.1 (1.2)	0.11
	2000	133	18	87–280	0.18	0.42	0.42	1.1 (1.1)	1.9
	2001	212	14	89–289	0.40	0.25	0.35	2.7 (1.9)	5.0

[a]The general population was defined as trout captured during electrofishing in the study segment or at downstream marking sites that received individual tags, which were generally age-1 and older. Weir recaptures were trout from the general population that were subsequently recaptured at weirs. No marked brook trout were recaptured in Little Muddy and Willow creeks during 1999.

[b]Model weights were the AIC weights of the three models under analysis of covariance. The interaction model [body weight = $\beta_0 + \beta_1$(group) + β_2(length) + β_3(group × length) + ε] tests whether the two groups are growing at similar rates. The group model [body weight = $\beta_0 + \beta_1$(group) + β_2(length) + β] tests whether the intercepts (or heights of the lines) are similar, that is, whether there is a difference in condition between groups that are growing at the same rate. The intercept only model [body weight = $\beta_0 + \beta_1$(length) + β] tests whether length is related to weight (i.e., no group effect).

[c]Differences were calculated as the difference in the model-averaged estimates of weight at the mean fork length for a given stream and year, averaging over group (SE = standard error).

[d]No estimates were calculated because of small sample size.

cal comparisons for lengths of brook trout in Willow and Indiana creeks would be conservative and the true differences might be greater, but this would likely only affect the inference in Indiana Creek. Brook trout were smaller in Little Muddy Creek, so fewer trout lost tags and results for length should be relatively unbiased. Finally, tag loss would have reduced the number of brook trout captured in weirs that were marked downstream and thus render the estimated proportion of fish moving long distances conservative (Fig. 7). However, some fish that lost tags nevertheless retained elastomer or acrylic paint marks, which permitted assigning them to a cohort released at a particular location and date and thus detecting their long distance movements.

Discussion

Movement of brook trout and cutthroat trout in headwater streams

The results demonstrated that nonnative brook trout were capable of rapid upstream invasion into habitats occupied by native cutthroat trout in small headwater streams in Colorado and that the demography of these far-ranging immigrants makes them potent colonizers. Here we address which predictions made at the outset about trout movement and brook trout invasion were supported by the data. First, our data confirmed the prediction that brook trout movement would show seasonal peaks during early summer and early fall. Although brook trout were captured at weirs throughout the summer, more were caught during mid-June to mid-July or in late September than during other periods. Movement peaks were related to hydrologic conditions because many brook trout moved through weirs during high discharge, though the relationship was most consistent in the mid-elevation stream that had the highest brook trout density (Little Muddy Creek; Peterson 2002). Similar to brook trout, cutthroat trout movement also tended to coincide with increased discharge. We assumed that increased movement by brook trout during fall was associated with spawning (e.g., Flick and Webster 1975; Gowan and Fausch 1996; Bélanager and Rodríguez 2001), because most brook trout captured at weirs during this time were extruding milt or eggs.

Second, we confirmed the prediction that brook trout move upstream during summer but found that cutthroat trout moved downstream more often than upstream. Even after accounting for potential bias caused by the removal experiment, we still found that a majority of brook trout were moving upstream when captured at weirs (73–84% on average, across years for each stream, excluding Indiana Creek in 1999 because of small sample size). Similar tendencies for upstream movement were found for brook trout in other

© 2003 NRC Canada

Fig. 7. Proportion of brook trout (*Salvelinus fontinalis*) recaptured inside or entering the study segments of (*a*) Little Muddy, (*b*) Indiana, and (*c*) Willow creeks that were originally marked downstream. Trout were marked and released during summer 1999 (solid bars), 2000 (open bars), and 2001 (hatched bars) and recaptured during any year at weirs, during downstream marking, or during annual electrofishing surveys of the study segments. Numbers of live releases for each year and location are given above each bar. No downstream marking was done in Willow Creek during 1999. The curve in (*a*) (Little Muddy Creek) shows predicted values of the proportion recaptured as a function of distance (m) downstream, estimated from a logistic regression averaged over year of release: $p(\text{recapture}) = \exp(-1.3476 - 0.00143 \cdot \text{Distance})/[1 + \exp(-1.3476 - 0.00143 \cdot \text{Distance})]$. The 500-m location in 1999 was excluded from the logistic regression analysis because of batch mark failure.

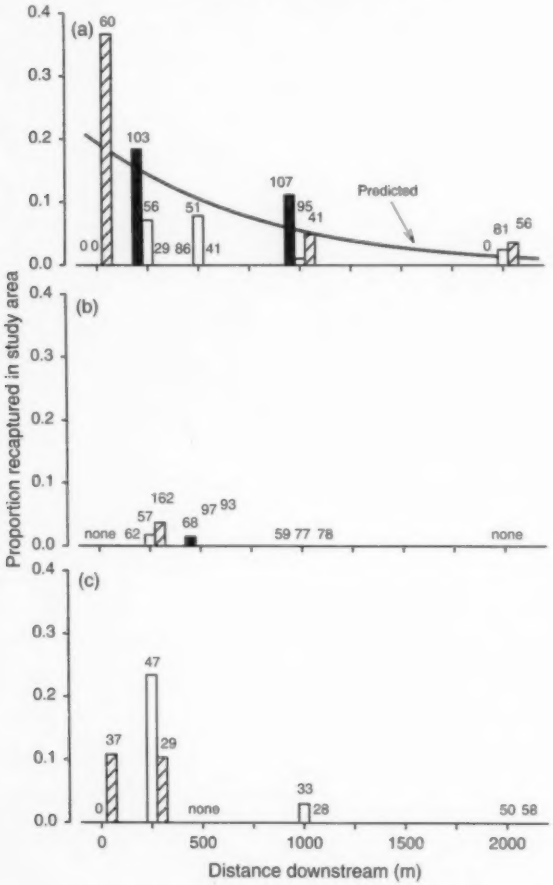

Fig. 8. Frequency of total distances moved by brook trout (*Salvelinus fontinalis*) marked downstream in (*a*) Little Muddy, (*b*) Indiana, and (*c*) Willow creeks during 1999–2001. Total distance was the sum of absolute distances between all pairs of capture locations, which included recaptures at weirs, during downstream marking, or during annual electrofishing surveys in study segments. The first (leftmost) bar contains fish that were recaptured within the section or at the same location where they were previously marked (i.e., detected movement = 0 m). The second bar contains fish estimated to have moved up to 50 m, and subsequent distance bins are in 50-m increments.

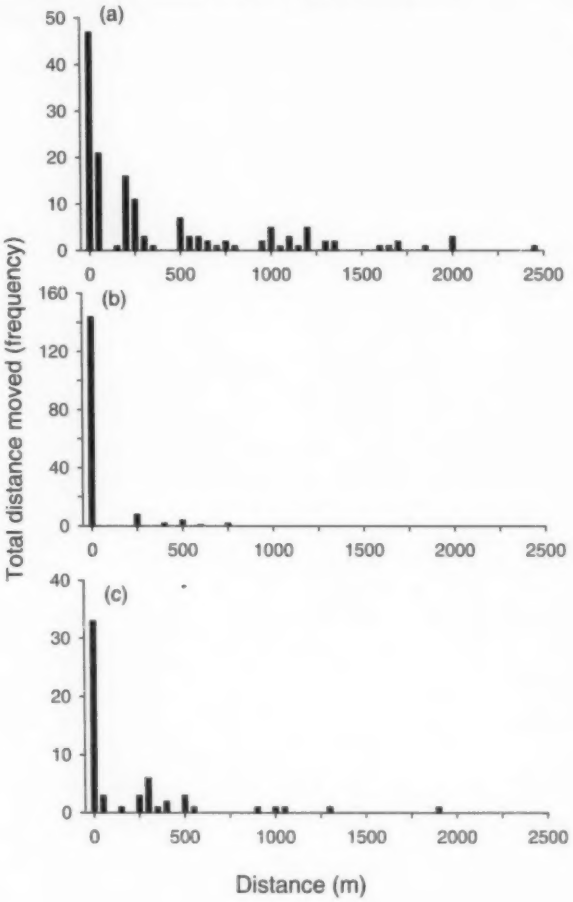

streams in Idaho (Adams et al. 2000), Colorado (Riley et al. 1992; Gowan and Fausch 1996), and New York (Flick and Webster 1975), so this pattern may be fairly general (but see Adams et al. 2001). Net movement by brook trout was also upstream, although brook trout captured within, or attempting to enter, the study segments of Little Muddy and Willow creeks were removed and never had the opportunity to move downstream. Nonetheless, upstream-moving brook trout would be expected to settle if they encountered suitable habitat (Gowan and Fausch 1996, 2002) and thus interact with cutthroat trout. Although this upstream-directed movement pattern appears to be common among salmonids (Hughes 1998), the mechanisms responsible for it are not clear and remain to be tested. Possible hypotheses include homing of fish displaced earlier in their life cycles (Hunt 1965), recruitment of certain ages or life stages to upstream reaches (Hughes 1999), olfactory cues from conspecifics or natal habitat (Bélanager and Rodríguez 2001), ranging behavior to seek suitable habitat (Gowan and Fausch 2002), or dispersal from source habitats (Adams 1999).

In contrast to brook trout, we found that at least 60% of cutthroat trout captured at weirs were moving downstream in

© 2003 NRC Canada

Fig. 9. Frequency of net distances moved by brook trout (*Salvelinus fontinalis*) marked downstream in (*a*) Little Muddy, (*b*) Indiana, and (*c*) Willow creeks during 1999–2001. Net distance was between initial and final recapture locations, which included recaptures at weirs, during downstream marking, or during annual electrofishing surveys in study segments. Negative values indicate trout that moved downstream. The bar at 0 m contains fish that were recaptured within the section or at the same location where they were previously marked (i.e., detected movement = 0 m), whereas other bars are based on 50-m distance increments.

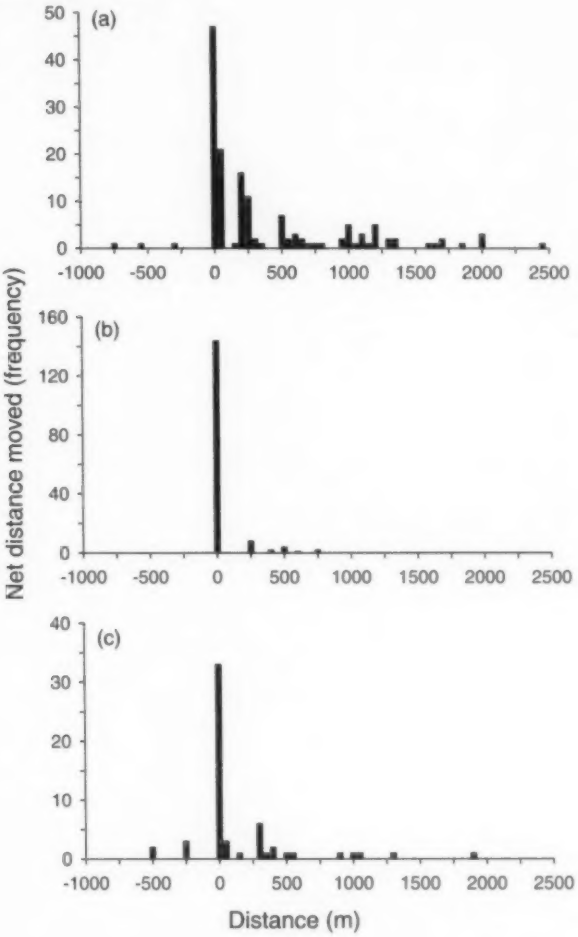

two of three summers. However, about 20% of the individually tagged cutthroat trout that left the study areas during one summer had returned by the following summer (Peterson 2002), suggesting that some may undergo seasonal reciprocal movements. Other investigators reported that fluvial cutthroat trout moved dozens of kilometres while descending from headwater or tributary streams following spawning, whether brook trout were present in the system (Schmetterling 2001) or not (Schrank 2002). In contrast, Hilderbrand and Kershner (2000) found that four times as many cutthroat trout sympatric with brook trout moved upstream than downstream during summer through weirs in Utah and Idaho, and Young (1996) found no directional bias in summer movement by radio-tagged cutthroat trout in a Wyoming stream with no brook trout. These different results may be caused by the timing of sampling, as well its spatial and temporal extent, or variation in measurement techniques (e.g., weirs, telemetry, or electrofishing), or habitat size and connectivity.

Third, our data are consistent with the prediction that adult brook trout move more often than juveniles and constitute the majority of immigrants and invaders. Brook trout captured at weirs in Indiana and Willow creeks were mostly age-2+ adults larger than 160 mm, and brook trout moving in Little Muddy Creek were primarily age-1 and age-2+ individuals larger than 100 mm. Brook trout of all age classes were present in moderate to high abundance in downstream source populations (Peterson 2002), but weirs were likely more effective at retaining larger trout. Nonetheless, juvenile trout as small as 26 mm were captured in weirs, and trout <75 mm constituted over 4% of the total weir captures. In addition, electrofishing data from these streams indicated that population turnover of brook trout was mainly attributed to age-1 and older trout (Peterson 2002). Thus, we concluded that weir captures were representative of the sizes of trout moving during summer in these streams. Most of the brook trout moving through weirs were mature adults, but even a proportion of age-1 individuals were reproductively mature in Little Muddy Creek. Using median sizes of invading brook trout in Little Muddy Creek (111–125 mm, among years), a logistic regression model predicts that 15–70% of males and up to 20% of females at these lengths would be mature (Kennedy et al. 2003). Fourth, differences between moving trout and the general population did not support the prediction that moving trout would be larger and in poorer condition than the general population. However, in the high-elevation streams, the tendency (i.e., a trend was apparent, but there was insufficient statistical evidence to claim a difference) for trout captured at weirs to be larger than the general population was consistent with the hypothesis that larger, dominant trout often search for suitable habitat and better foraging locations during summer as stream flow, habitat area, and invertebrate drift decline (Gowan and Fausch 2002). However, these fish were not necessarily in poorer condition than the general population and so were not expected to be competitively inferior. For example, Kahler et al. (2001) found that juvenile anadromous salmonids that moved grew more quickly that those that did not. In contrast, immigrant brook trout in Little Muddy Creek, which was warmer than the other streams, tended to be smaller that the general population and may represent surplus production from a source population (e.g., Adams 1999) or subdominant individuals searching for open habitat.

Fifth, the data show that brook trout moved rapidly upstream from a variety of distances downstream. Summer immigration alone supplied up to two-thirds of the existing population in Little Muddy Creek, and between-summer immigration could completely repopulate depleted stream segments where brook trout were removed (Peterson 2002). Population turnover by brook trout had both local (Rodríguez 2002) and far-ranging components (Gowan and Fausch 1996). Based on recaptures of marked individuals, local (≤250 m) movements by brook trout were most fre-

© 2003 NRC Canada

quently detected, but long-distance movements up to 2 km were detected within a summer and our sampling methods were biased against detecting long-distance movements. Moreover, between 70 and 80% of brook trout tagged at weirs and during downstream marking were never recaptured, so movement was likely more common than we measured and probably occurred outside the detection limits of this study (e.g., Gowan and Fausch 1996).

Trout movement: implications for invasion

The combination of rapid upstream movement, the inclination to move during elevated discharge, and the biological characteristics of the immigrants make brook trout potentially effective invaders of headwater streams inhabited by native cutthroat trout. In streams like the ones that we studied in Colorado, brook trout often have a source population downstream that can provide a supply of potential immigrants, whereas cutthroat trout populations are generally isolated (Fausch 1989; Behnke 1992). Upstream movement by brook trout promotes the invasion of upstream reaches that are typically the last stronghold for native cutthroat trout (Fausch and Young 1995; Young 1995), though downstream-directed invasions from headwater lakes where brook trout were stocked also occur (Adams et al. 2001). Pulses of brook trout movement were observed during elevated discharge caused by snowmelt runoff and localized summer thunderstorms, so brook trout dispersing at these times may be able to pass barriers that would normally block their movements under baseflow conditions (Thompson and Rahel 1998; Adams et al. 2000). Stream reaches in Little Muddy Creek where brook trout were removed over four consecutive years were completely repopulated between late fall and the following summer every year (Peterson 2002), so we suspect that the majority of this movement occurred during snowmelt runoff. Although the upstream movement and ranging behavior that we measured for brook trout does not necessarily constitute permanent colonization in every case, the extent of brook trout invasions in the western U.S. (e.g., Dunham et al. 2003; Peterson and Fausch 2003) suggests that it often does.

In comparison, if cutthroat trout consistently exhibit downstream-directed movement, as measured in this study, then such behavior may have negative consequences for their populations. For example, downstream emigration would increase the probability that cutthroat trout would encounter high-density brook trout reaches. If these cutthroat trout subsequently spawned in downstream reaches, their offspring would be particularly vulnerable to biotic interactions with brook trout that would reduce their survival (Peterson et al. 2004). The effect on these cutthroat trout offspring would be the same, whether or not their parents were among those 20% of downstream emigrants that later returned upstream through seasonal reciprocal movements. Brook trout removal did not appear to affect the tendency for cutthroat trout to emigrate from study reaches during summer (Peterson et al. 2004), but further investigation into how the presence and encroachment of nonnative brook trout influences cutthroat trout movement is warranted given the implications to the population ecology and management of native cutthroat trout.

Dispersal ability is typically influenced by size or age, so demography of dispersing brook trout is likely to have profound effects on the invasion (Fagan et al. 2002). Immigrant brook trout tended to be adults (Gowan and Fausch 1996; Adams et al. 2000) in similar condition to the general population. Swimming ability, position in dominance hierarchies, and fecundity are positively correlated with size in stream-dwelling trout (Fausch 1984; Nakano 1995; Moyle and Cech 2000). Thus, larger trout may be able to ascend higher, steeper barriers (Thompson and Rahel 1998; Adams et al. 2000) or move longer distances than smaller trout (Young 1994; Schrank 2002). Large immigrant brook trout could competitively displace smaller cutthroat trout and affect their growth and survival (Novinger 2000), and large adults would have the greatest reproductive potential. If these brook trout reproduced, their progeny would have a competitive advantage over young cutthroat trout (Griffith 1972; De Staso and Rahel 1994; Novinger 2000), which can cause lower survival rates and population declines (Peterson 2002).

Overall, our results indicate that in the two high-elevation streams studied, invading brook trout were mostly large adults with the potential to range into new habitats, defend profitable feeding positions, and reproduce, whereas in the mid-elevation stream, invaders were often juveniles representing surplus production from downstream habitats that could numerically swamp cutthroat trout populations. Differences in growth, longevity, and age at maturity in these streams also indicate that brook trout have flexible life histories, which may in part explain their success at establishing populations in mountain streams of the western U.S. (Kennedy et al. 2003).

Far-ranging elements of the brook trout dispersal continuum (i.e., the range of distances from and to which trout move; sensu Schrank 2002) may contribute disproportionately to invasion spread. Local movement at the invasion front was frequently detected and exerted considerable biotic pressure on cutthroat trout, facilitating rapid recolonization in streams where brook trout were removed. However, brook trout can also move upstream at least several kilometres within a summer (Riley et al. 1992; Gowan and Fausch 1996). The frequency distribution of recaptures from brook trout marked at various distances outside the study segments appears to be leptokurtic (cf. Skalski and Gilliam 2000), especially in the mid-elevation stream, indicating that many brook trout may immigrate to the study segment from long distances. Both theoretical (Kot et al. 1996; Lewis 1997) and empirical (e.g., Suarez et al. 2001) evidence indicates that such long-distance movements facilitate rapid invasion via jump dispersal. It has been suggested that brook trout may be exceptionally mobile compared with other stream-dwelling salmonids (Rodríguez 2002), and it may be just this property that makes them potent invaders of headwater streams in the western U.S. inhabited by threatened or endangered cutthroat trout.

Acknowledgements

Helpful comments from Kevin Bestgen, Jason Dunham, LeRoy Poff, Gary White, Mike Young, and an anonymous reviewer improved the manuscript. Financial support was provided by the Colorado Division of Wildlife (CDOW),

© 2003 NRC Canada

U.S. Department of Interior Central Utah Project Completion Act (CUPCA), U.S. Department of Agriculture Forest Service Fish Habitat Relationships Program (FHR), and Trout Unlimited (TU). We thank Tom Nesler (CDOW), Ralph Swanson (CUPCA), Nick Schmal (FHR), Dave Winters (FHR), Mike Young (FHR), and Whit Fosburgh (TU) for administering these funds. D. Peterson was also supported by scholarships from the West Denver Chapter of Trout Unlimited, Cook Memorial Scholarship fund, Peters Scholarship fund, and the Western Division of the American Fisheries Society. We thank the dozens of technicians and volunteers who helped collect field data.

References

Adams, S.B. 1999. Mechanisms limiting a vertebrate invasion: brook trout in mountain streams of the northwestern USA. Ph.D. thesis, University of Montana, Missoula, Mont.

Adams, S.B., Frissell, C.A., and Rieman, B.E. 2000. Movements by nonnative brook trout in relation to stream channel slope. Trans. Am. Fish. Soc. **129**: 623–638.

Adams, S.B., Frissell, C.A., and Rieman, B.E. 2001. Geography of invasion in mountain streams: consequences of headwater lake fish introductions. Ecosystems, **4**: 296–307.

Behnke, R.J. 1992. Native trout of western North American. Am. Fish. Soc. Monogr. No. 6, Bethesda, Md.

Bélanager, G., and Rodríguez, M.A. 2001. Homing behaviour of stream-dwelling brook charr following experimental displacement. J. Fish Biol. **59**: 987–1001.

Burnham, K.P., and Anderson, D.R. 2002. Model selection and multimodel inference — a practical information-theoretic approach. 2nd ed. Springer-Verlag Inc., New York.

De Staso, J., III, and Rahel, F.J. 1994. Influence of water temperature on interactions between juvenile Colorado River cutthroat trout and brook trout in a laboratory stream. Trans. Am. Fish. Soc. **123**: 289–297.

Dingle, H. 1996. Migration: the biology of life on the move. Oxford University Press, New York.

Dunham, J.B., Adams, S.B., Schroeter, R.E., and Novinger, D.C. 2003. Alien invasions in aquatic ecosystems: toward and understanding of brook trout invasions and their potential impact on inland cutthroat trout. Rev. Fish Biol. Fish. **12**: 373–391.

Fagan, W.F., Lewis, M.A., Neubert, M.G., and van den Driessche, P. 2002. Invasion theory and biological control. Ecol. Lett. **5**: 148–157.

Fausch, K.D. 1984. Profitable stream positions for salmonids: relating specific growth rate to net energy gain. Can. J. Zool. **62**: 441–451.

Fausch, K.D. 1989. Do gradient and temperature affect distribution of, and interactions between, brook char and other salmonids in streams? Phys. Ecol. Jpn. Spec. **1**: 303–322.

Fausch, K.D., and Young, M.K. 1995. Evolutionary significant units and movement of resident stream fishes: a cautionary tale. Am. Fish. Soc. Symp. **17**: 360–370.

Fausch, K.D., Torgersen, C.E., Baxter, C.V., and Li, H.W. 2002. Landscapes to riverscapes: bridging the gap between research and conservation of stream fishes. BioScience, **52**: 483–498.

Flick, W.A., and Webster, D.A. 1975. Movement, growth, and survival in a stream population of wild brook trout (*Salvelinus fontinalis*) during a period of removal of non-trout species. J. Fish. Res. Board Can. **32**: 1359–1367.

Gowan, C., and Fausch, K.D. 1996. Mobile brook trout in two high-elevation Colorado streams: re-evaluating the concept of restricted movement. Can. J. Fish. Aquat. Sci. **53**: 1370–1381.

Gowan, C., and Fausch, K.D. 2002. Why do foraging stream salmonids move during summer? Environ. Biol. Fishes, **64**: 139–153.

Gowan, C., Young, M.K., Fausch, K.D., and Riley, S.C. 1994. Restricted movement in resident stream salmonids: a paradigm lost? Can. J. Fish. Aquat. Sci. **51**: 2626–2637.

Griffith, J.S. 1972. Comparative behavior and habitat utilization of brook trout (*Salvelinus fontinalis*) and cutthroat trout (*Salmo clarki*) in small streams in northern Idaho. J. Fish. Res. Board Can. **29**: 265–273.

Griffith, J.S. 1988. Review of competition between cutthroat trout and other salmonids. Am. Fish. Soc. Symp. **4**: 134–140.

Harig, A.L., Fausch, K.D., and Young, M.K. 2000. Factors influencing success of greenback cutthroat trout translocations. N. Am. J. Fish. Manag. **20**: 994–1004.

Hilderbrand, R.H., and Kershner, J.L. 2000. Movement patterns of stream-resident cutthroat trout in Beaver Creek, Idaho–Utah. Trans. Am. Fish. Soc. **129**: 1160–1170.

Hughes, N.F. 1998. A model of habitat selection by drift-feeding stream salmonids at different scales. Ecology, **79**: 281–294.

Hughes, N.F. 1999. Population processes responsible for larger-fish-upstream distribution patterns of Arctic grayling (*Thymallus arcticus*) in interior Alaskan runoff rivers. Can. J. Fish. Aquat. Sci. **56**: 2292–2299.

Hunt, R.L. 1965. Dispersal of brook trout during their first summer of life. Trans. Am. Fish. Soc. **94**: 186–188.

Kahler, T.H., Roni, P., and Quinn, T.P. 2001. Summer movement and growth of juvenile anadromous salmonids in small western Washington streams. Can. J. Fish. Aquat. Sci. **58**: 1947–1956.

Kennedy, B.M., Peterson, D.P., and Fausch, K.D. 2003. Different life history of brook trout populations invading mid-elevation and high-elevation cutthroat trout streams in Colorado. W. N. Am. Nat. **63**: 215–223.

Kot, M., Lewis, M.A., and van den Driessche, P. 1996. Dispersal data and the spread of invading organisms. Ecology, **77**: 2027–2042.

Krueger, C.C., and May, B. 1991. Ecological and genetic effects of salmonid introductions in North America. Can. J. Fish. Aquat. Sci. **48**(Suppl. 1): 66–77.

Lewis, M.A. 1997. Variability, patchiness, and jump dispersal in the spread of an invading population. *In* Spatial ecology: the role of space in population dynamics and interspecific interactions. *Edited by* D. Tilman and P. Karieva. Princeton Monographs in Population Biology No. 30, Princeton University Press, Princeton, N.J. pp. 46–69.

Mourning, T.E., Fausch, K.D., and Gowan, C. 1994. Comparison of visual implant tags and Floy anchor tags on hatchery rainbow trout. N. Am. J. Fish. Manag. **14**: 636–642.

Moyle, P.B., and Cech, J.J., Jr. 2000. Fishes: an introduction to ichthyology. 3rd ed. Prentice Hall, Upper Saddle River, N.J.

Nakano, S. 1995. Individual differences in resource use, growth and emigration under the influence of a dominance hierarchy in fluvial red-spotted masu salmon in their natural habitat. J. Anim. Ecol. **64**: 75–84.

Neubert, M.G., and Caswell, H. 2000. Demography and dispersal: calculation and sensitivity analysis of invasion speeds for structured populations. Ecology, **81**: 1613–1628.

Northcote, T.G. 1997. Potamodromy in Salmonidae — living and moving in the fast lane. N. Am. J. Fish. Manag. **17**: 1029–1045.

Novinger, D.C. 2000. Reversals in competitive ability: do cutthroat trout have a thermal refuge from competition with brook trout? Ph.D. thesis, University of Wyoming, Laramie, Wyo.

© 2003 NRC Canada

Peterson, D.P. 2002. Population ecology of an invasion: demography, dispersal, and effects of nonnative brook trout on native cutthroat trout. Ph.D. thesis, Colorado State University, Fort Collins, Co.

Peterson, D.P., and Fausch, K.D. 2003. Testing population-level mechanisms of invasion by a mobile vertebrate: a simple conceptual framework for salmonids in streams. Biol. Invasions, **5**: 239–259.

Peterson, D.P., Fausch, K.D., and White, G.C. 2004. Population ecology of an invasion: effects of brook trout on native cutthroat trout. Ecol. Appl. In press.

Rahel, F.J. 2002. Homogenization of freshwater faunas. Annu. Rev. Ecol. Syst. **33**: 291–315.

Riley, S.C., and Fausch, K.D. 1995. Trout population response to habitat enhancement in six northern Colorado streams. Can. J. Fish. Aquat. Sci. **52**: 34–53.

Riley, S.C., Fausch, K.D., and Gowan, C. 1992. Movement of brook trout (*Salvelinus fontinalis*) in four small subalpine streams in northern Colorado. Ecol. Freshw. Fish, **1**: 112–122.

Rodríguez, M.A. 2002. Restricted movement in stream fish: the paradigm is incomplete, not lost. Ecology, **83**: 1–13.

Schmetterling, D.A. 2001. Seasonal movements of fluvial westslope cutthroat trout in the Blackfoot River drainage, Montana. N. Am. J. Fish. Manag. **21**: 507–520.

Schrank, A.J. 2002. Ecological significance of movement patterns of Bonneville cutthroat trout in a western Wyoming watershed. Ph.D. thesis, University of Wyoming, Laramie, Wyo.

Shepard, B.B., Robison-Cox, J., Ireland, S.C., and White, R.G. 1996. Factors influencing retention of visible implant tags by westslope cutthroat trout inhabiting headwater streams in Montana. N. Am. J. Fish. Manag. **16**: 913–920.

Skalski, G.T., and Gilliam, J.F. 2000. Modeling diffusive spread in a heterogeneous population: a movement study with stream fish. Ecology, **81**: 1685–1700.

Suarez, A.V., Holway, D.A., and Case, T.J. 2001. Patterns of spread in biological invasions dominated by long-distance jump dispersal: insights from Argentine ants. Proc. Natl. Acad. Sci. U.S.A. **98**: 1095–1100.

Thompson, P.D., and Rahel, F.J. 1998. Evaluation of artificial barriers in small Rocky Mountain streams for preventing the upstream movement of brook trout. N. Am. J. Fish. Manag. **18**: 206–210.

Young, M.K. 1994. Mobility of brown trout in south-central Wyoming streams. Can. J. Zool. **72**: 2078–2083.

Young, M.K. (*Editor*). 1995. Conservation assessment for inland cutthroat trout. Rocky Mountain Forest and Range Experimental Station, U.S. Department of Agriculture Forest Service, General Technical Report RM-GTR-256, Fort Collins, Co.

Young, M.K. 1996. Summer movements and habitat use by Colorado River cutthroat trout (*Oncorhynchus clarki pleuriticus*) in small, montane streams. Can. J. Fish. Aquat. Sci. **53**: 1403–1408.

© 2003 NRC Canada

Differential effects of turbidity on prey consumption of piscivorous and planktivorous fish

Alex De Robertis, Clifford H. Ryer, Adriana Veloza, and Richard D. Brodeur

Abstract: Contrast degradation theory predicts that increased turbidity decreases the visibility of objects that are visible at longer distances more than that of objects that are visible at short distances. Consequently, turbidity should disproportionately decrease feeding rates by piscivorous fish, which feed on larger and more visible prey than particle-feeding planktivorous fish. We tested this prediction in a series of laboratory feeding experiments, the results of which indicated that prey consumption by two species of planktivorous fish (juvenile chum salmon (*Oncorhynchus keta*) and walleye pollock (*Theragra chalcogramma*)) is much less sensitive to elevated turbidity than piscivorous feeding by sablefish (*Anoplopoma fimbria*). Planktivorous feeding in the turbidity range tested (0–40 nephelometric turbidity units (NTU)) was reduced at high light intensity, but not at low light intensity. Comparatively low (5–10 NTU) turbidity decreased both the rate at which sablefish pursued prey and the probability of successful prey capture. These results suggest that turbid environments may be advantageous for planktivorous fish because they will be less vulnerable to predation by piscivores, but will not experience a substantial decrease in their ability to capture zooplankton prey.

Résumé : La théorie de la dégradation des contrastes prédit qu'une turbidité accrue décroît plus la visibilité d'objets qui sont visibles à de plus grandes distances que celle d'objets visibles à de courtes distances. En conséquence, la turbidité devrait faire décroître de façon disproportionnée les taux d'alimentation des poissons piscivores qui se nourrissent de proies plus grandes et plus visibles par comparaison aux taux d'alimentation des poissons planctonophages qui se nourrissent de particules. Une série d'expériences d'alimentation en laboratoire nous a permis de vérifier cette prédiction : la consommation de proies de deux espèces de poissons planctonophages, de jeunes saumons kéta (*Oncorhynchus keta*) et des goberges de l'Alaska (*Theragra chalcogramma*), est beaucoup moins affectée par une augmentation de la turbidité que la consommation de poissons par des morues charbonnières (*Anoplopoma fimbria*). Dans la gamme des turbidités étudiées (0–40 unités néphélométriques de turbidité, NTU), l'alimentation des planctonophages est réduite aux fortes intensités de lumière, mais non aux intensités faibles. Des turbidités relativement faibles (5–10 NTU) entraînent une réduction du taux de poursuite ainsi que de la probabilité de capture des proies chez la morue charbonnière. Ces résultats semblent démontrer qu'un environnement turbide peut être avantageux pour les poissons planctonophages parce qu'ils y sont moins vulnérables à la prédation par les poissons piscivores, sans que leur capacité à capturer des proies zooplanctoniques ne soit substantiellement réduite.

[Traduit par la Rédaction]

Introduction

Scattering and absorption of light by suspended materials in turbid waters limits visibility in aquatic environments through two primary mechanisms. Under elevated turbidity, light attenuation increases (Kirk 1985), decreasing light penetration, which impairs vision. This process is of particular importance to organisms occupying deeper waters because small turbidity-induced changes in light extinction coefficients have large cumulative effects at depth (Eiane et al. 1999). In addition to reducing ambient light intensity, turbidity can impair visibility by degrading apparent contrast (Lythgoe 1979). Scattering of light by suspended materials reduces the apparent difference in brightness between an object and its background, which decreases the visibility of the object. For an object to be visible, its apparent contrast must exceed a physiological threshold value known as the contrast threshold. The contrast threshold of fish depends on factors such as object size and light intensity (Anthony 1981) but should remain constant for a given prey and illumination. In water, the scattering of light due to suspended particles influences contrast as follows (Duntley 1962):

Received 3 January 2003. Accepted 31 August 2003. Published on the NRC Research Press Web site at http://cjfas.nrc.ca on 22 December 2003.
J17264

A. De Robertis[1,2] **and R.D. Brodeur.** Estuarine and Ocean Ecology Program, Fish Ecology Division, Northwest Fisheries Science Center, NMFS, NOAA, Hatfield Marine Science Center, Newport, OR 97365, U.S.A.
C.H. Ryer. Fisheries Behavioral Ecology Program, Alaska Fisheries Science Center, NMFS, NOAA, Hatfield Marine Science Center, Newport, OR 97365, U.S.A.
A. Veloza. Biology Department, East Stroudsburg University, East Stroudsburg, PA 18301, U.S.A.

[1]Corresponding author (e-mail: Alex.DeRobertis@noaa.gov).
[2]Present address: Alaska Fisheries Science Center, NMFS, NOAA, 7600 Sand Point Way NE, Seattle, WA 98115-0070, U.S.A.

 doi: 10.1139/F03-123 © 2003 NRC Canada

$$(1) \qquad C_a = C_0 e^{-\alpha r}$$

where C_a is apparent contrast, C_0 is inherent contrast of the object, α is the beam attenuation coefficient for visible light (a measure of water clarity and the sum of the absorption (a) and scattering (b) coefficients for visible light), and r is the distance between the object and the eye. The degree of contrast degradation thus depends on the optical properties of the water and increases exponentially with the distance between the object and the eye. Thus, for a given increase in turbidity (α), contrast degradation will reduce the visibility of large prey such as fish that can be seen at great distances (i.e., large r), much more than the visibility of small prey that can only be seen at short distances (i.e., small r). Likewise, contrast degradation is likely to be an important factor in near-surface waters during the day when light intensity is relatively high and prey-sighting distances are long and likely to be less important when light intensity is relatively low and prey-sighting distances are short.

Fishes are the primary visual predators in many aquatic systems and are often functionally divided into piscivores and planktivores, based on their primary prey. The ability of visually foraging fish to detect prey depends on light intensity, water clarity, and prey characteristics such as size, pigmentation, and motion (Confer et al. 1978; O'Brien 1987; Aksnes and Utne 1997). Piscivorous and planktivorous fish consume prey of different sizes, and changes in water clarity are likely to affect them in different ways. Piscivores feed on large conspicuous fish, whereas planktivorous fish feed on small, comparatively inconspicuous zooplankton. Under high light intensity in clear water, piscivores are able to detect fish prey at distances much larger than those at which planktivorous fish are able to detect zooplankton prey (Breck 1993). Thus, for a given increase in turbidity, contrast degradation should disproportionately impair prey detection by piscivores relative to planktivores. All other things being equal, moderately turbid waters may be advantageous habitats for planktivorous fish because their encounter rates with piscivorous predators are reduced more than their encounter rates with planktonic prey.

In this study, we examine the effect of turbidity-induced light scatter on feeding rates in a series of laboratory experiments using two species of fish that are planktivorous as juveniles, chum salmon (*Oncorhynchus keta*) and walleye pollock (*Theragra chalcogramma*), and a piscivore, sablefish (*Anaplopoma fimbria*). We test the prediction that increased turbidity depresses the feeding rates of piscivores more than those of planktivores. In addition, we test the hypothesis that feeding by planktivorous fish is more likely to be impaired by increases in turbidity at high light levels when zooplankton prey are visible at longer distances.

Materials and methods

Fish collection and maintenance

Chum salmon were raised from eggs collected from wild adults returning to Whiskey Creek, Tillamook County, Oregon, in November 2001. When the chum had completely absorbed their yolk sac, they were transferred to seawater. Juvenile walleye pollock (45–60 mm) were captured in May 2002 from Puget Sound near Port Townsend, Washington, by dip-netting them as they aggregated around a light. Fish were transported to the laboratory and held in 720-L tanks provided with a continuous flow of seawater. Pollock were held in the laboratory for 4–6 weeks before experimentation, and chum were held for 6 months before beginning experiments. Sablefish used as predators in the piscivory experiments were collected as ~50-mm juveniles 32 km off the coast of Newport, Oregon, in May 2001 and were held in the laboratory for 13 months. All species were primarily fed formulated foods at rations sufficient to promote growth, but they readily consumed live prey.

Planktivory experiments

Feeding rates of juvenile chum and pollock were measured under varying levels of turbidity and light intensity in six replicate 50 cm × 50 cm × 50 cm glass tanks supplied with flow-through seawater and located inside a light-proof blind. Each tank was equipped with a feeding tube that allowed prey to be introduced from the other side of the blind with minimum disturbance of the experimental fish. The experimental system has been described in detail elsewhere (Ryer and Olla 1999) and will be described only briefly here. Visible illumination was provided by four green 555-nm light emitting diode (LED) illuminators that could be controlled to produce irradiances between 1.9×10^{-7} and 1.0×10^{-3} $\mu E \cdot m^{-2} \cdot s^{-1}$. Green LEDs were selected to mimic the predominant wavelengths of light in coastal marine waters during both day and night (McFarland 1986). Light levels above 1.0×10^{-3} $\mu E \cdot m^{-2} \cdot s^{-1}$ were achieved by supplementing the LED illuminators with additional light emitted by a rheostat-controlled 40-W incandescent light mounted above each tank and reflected from a white ceiling 150 cm above the tank.

Fish are differentially sensitive to different wavelengths of light, and it is unclear how a shift from green to white light may have affected the response of the planktivores. However, changes in spectral composition of light in the experiments are unlikely to have biased the results to a great degree as in both these and previous experiments (Ryer and Olla 1999), planktivorous feeding in the apparatus occurred well below the change from green to multispectral illumination, and there were no large changes in prey consumption when supplemental light was first used.

Light intensity was measured with a radiometer (model 1700; International Light, Inc., Newburyport, Mass.) equipped with a photosynthetically active radiation filtered, cosine response detector. Measurements were made at the water surface with the detector pointed upwards. Illumination in the six replicate tanks differed by 6–18% depending on light level, and the values reported here represent means of the six measurements. Light measurements were made at the beginning of the study and were periodically checked to confirm that light levels were consistent thought the study period.

Turbidity was controlled by adding a bentonite clay suspension to the experimental tanks. Clays are weakly absorptive of visible light, but highly scattering (Kirk 1994), and often are the primary contributor to reductions in beam attenuation coefficient in turbid environments (Vant 1990). A predetermined amount of clay was mixed into 2 L of seawater, and the suspension was slowly added to the experimental tanks through the feeding tube. In experiments in clear water, seawater without clay was added to the tanks in the same

© 2003 NRC Canada

manner. Turbidity was measured with a Hach 2100A turbidimeter (Hach, Loveland, Colo.), which quantifies the amount of light from an incandescent bulb scattered at a 90° angle in nephelometric turbidity units (NTU). Preliminary observations indicated that turbidity was reduced by ~50% within 1 h as a result of settling and that fish were agitated by the increase in turbidity for <5 min. To minimize settling during experiments, but allow the fish to acclimate to changes in turbidity, the fish were allowed 30 min to acclimate. A series of preliminary experiments ($n = 25$) established that turbidity after 35 min (i.e., at the end of trials) was reproducible to within 10% of the average level over the range of 0–40 NTU. Turbidity values reported here represent the mean of these measurements.

General planktivory protocol

All planktivory experiments followed a similar experimental protocol: groups of five fish were selected haphazardly from holding tanks and were acclimated to experimental tanks for 16–20 h. Before starting the experiments, the lights were set to the desired intensities, and the flow-through seawater was turned off. To prevent the loss of prey through the outflow drains, the water level in the tank was siphoned down to a height of 37 cm, which is 5 cm below the tank drain. This reduced the water volume in the tank to 93 L. The fish were allowed to acclimate for 60 min before prey introduction.

Live *Artemia salina* were used as a proxy for zooplankton prey in planktivory experiments. Prey cultures were initiated 3–4 days apart, and a subsample of 25 prey was measured daily to ensure that prey size (~2.5 mm) did not vary appreciably between trials. In each trial, 100 prey were counted and placed in a beaker containing 300 mL of seawater. The prey were poured into the experimental tank through a funnel at the end of the feeding tube, and the beaker was rinsed with 750 mL of seawater, which was then poured into the feeding tube. The fish were allowed to feed for 5 min, and the experiment was then terminated by entering the blind and rapidly removing the fish with a dip net. Any prey removed with the fish were quickly separated. Fish were measured and returned to holding tanks and were not reused in subsequent trials. The remaining prey were removed by methodically straining the tank with a fine-mesh dip net for 5 min. Preliminary trials in which prey were added to the tanks without fish and subsequently recovered indicated that almost all prey ($\bar{x}$ ± standard deviation (SD), 98.9 ± 0.3%, $n = 6$) added through the feeding tubes were recovered, and the number of prey missing at the end of the feeding trial was taken to be the number of prey consumed. Experimental temperatures were ~11 °C and ranged between 9.9 °C and 11.8 °C. Five replicate trials were conducted for a given treatment, and the order of trials was randomized in blocks of 2 and 3.

A series of preliminary experiments (5.02×10^{-1} $\mu E \cdot m^{-2} \cdot s^{-1}$, 0 NTU) were videotaped from above to investigate the possibility of quantifying the distance at which prey were detected by planktivores. Analysis of video records indicated that both chum and pollock began making rapid forward movements of up to 10–20 cm followed by sharp turns shortly after prey were introduced. Although prey were generally not resolved in the video records, in several cases we were able to confirm that prey were consumed as the planktivores turned. These observations suggest that prey-sighting distances by both planktivores were on the order of 20 cm at high light intensity in clear water. However, because position of individual prey could not be reliably resolved, we did not further characterize the distance at which prey were detected in the planktivory experiments.

Light threshold of chum salmon

Although the thresholds for visual feeding by sablefish and pollock have been previously established (Ryer and Olla 1999), the threshold for visual feeding by chum salmon, which was required to design the turbidity experiments, was unknown. We thus established the threshold for visual feeding by chum salmon in clear water (0.2 NTU, no added bentonite) by recording prey consumption at 1.14, 1.16×10^{-1}, 1.20×10^{-2}, 0.98×10^{-3}, 1.17×10^{-4}, and 0.91×10^{-5} $\mu E \cdot m^{-2} \cdot s^{-1}$ and in complete darkness ($<1.0 \times 10^{-8}$ $\mu E \cdot m^{-2} \cdot s^{-1}$). Mean *Artemia* length ranged from 2.2 mm to 2.6 mm. Fish length was 42.0 ± 3.3 mm ($\bar{x}$ ± SD), and the mean size of fish did not vary with illumination (analysis of variance (ANOVA), $F_{[6,168]} = 1.55$, $p = 0.17$). Prey consumption was analyzed by one-way ANOVA after a square-root transformation to homogenize variance (Bartlett's test $p = 0.21$) in order to meet ANOVA assumptions. A posteriori multiple comparisons were made using Tukey's test.

Effect of turbidity on planktivory

We investigated the effects of elevated turbidity on planktivory by chum and pollock at two light intensities. A high light intensity was selected such that additional light would not increase feeding rates, and a lower light intensity was selected such that feeding rates were below those observed at high light intensity but above those in the dark. Based on the results of the light threshold of experiment for chum salmon and previous studies of pollock in the same apparatus (Ryer and Olla 1999), trials were conducted at 5.02×10^{-1} (high light) and 4.80×10^{-4} $\mu E \cdot m^{-2} \cdot s^{-1}$ (low light). These light levels correspond approximately to illumination at the water surface during sunrise or sunset and under a half moon, respectively (Macy et al. 1998).

For each species, trials were conducted at 0.2 (no added bentonite), 5.1, 9.3, 19.6, and 39.9 NTU under both high and low light conditions. To remove the confounding effects of decreased light intensity in the turbid treatments (up to 59% reduction, measured at the bottom of the tank), illumination was increased such that the measured light level at the center of the tank was approximately constant (within 5%) over all turbidity levels.

Chum used in turbidity trials averaged 47.0 ± 5.2 mm in length, and size did not vary among treatments (ANOVA, $F_{[9,240]} = 0.87$, $p = 0.55$). Pollock averaged 71.6 ± 7.8 mm in total length, and size did not vary among treatments (ANOVA, $F_{[9,240]} = 0.345$, $p = 0.96$). Mean prey size ranged between 2.2 and 2.6 mm in chum experiments and between 2.4 and 2.9 mm in pollock experiments. Prey consumption was analyzed by two-way ANOVA after a square-root transformation to homogenize variance (Bartlett's test, $p > 0.05$ in both cases) to meet ANOVA assumptions. A posteriori multiple comparisons were made using Tukey's test.

© 2003 NRC Canada

Piscivory experiments

We investigated the effects of turbidity on piscivory by studying predation by 1-year-old sablefish on juvenile chum salmon at 0.4 ± 0.2, 5.1 ± 0.5, and 10.0 ± 0.5 ($\bar{x}$ ± SD) NTU, which correspond to the three lowest turbidity levels tested in the planktivory experiments. Before use in experiments, sablefish were fed shiner surfperch (*Cymatogaster aggregata*) for a week to habituate them to live prey, and then they were starved for 7–12 days to ensure that they would be motivated to feed. Six replicate trials at each turbidity level were conducted in three identical indoor flow-through circular tanks (1.3 m deep, 3 m diameter). To ensure that predator and prey would be visible to overhead video cameras under turbid conditions, water depth was held at 0.5 m at all times by means of an external standpipe. The experimental volume was 2700 L. One replicate at each of the three turbidity levels was tested in a single day, with the order of trials randomized within that day. The tanks were lit with overhead fluorescent lights, which produced a light intensity ranging from 1.29 to 1.45 $\mu E \cdot m^{-2} \cdot s^{-1}$ at the water surface. The highest turbidity level reduced light levels at the bottom of the tank by <15%, and no compensation was made for decreased light intensity in turbid treatments.

In each trial, two sablefish predators (mean length ± SD, 353.8 ± 17.8 mm) were haphazardly drawn from a holding tank and introduced to the arena to acclimate for 16–20 h. Before each trial, an overhead partition was lowered to confine the predators to half of the tank, and the seawater supply was turned off. A turbid suspension was prepared by adding pulverized kaolin to 120 L of seawater. Kaolin was used to produce the desired turbidity rather than bentonite because it was found that settling of kaolin was negligible over a period of 1–2 h. Half of the suspension was pumped into each side of the experimental tank, and an additional 30 L of seawater was used as a rinse. Preliminary turbidity measurements showed that the kaolin suspension mixed through small holes in the partition and dispersed evenly throughout the tank within several minutes. In the 0.4 NTU trials, water without kaolin was pumped into the tanks as a control. After introducing the suspension into the arena, six chum salmon (82.9 ± 11.5 mm) were drawn from a holding tank, measured, and added to the tank opposite the predators. The fish were then allowed to acclimate to conditions in the arena for 70 min. Trials were initiated by turning on the videotape recorders and raising the partition 50 cm above the water surface with a pulley system from a location outside of the field of view of the fish. Predator and prey were allowed to interact for a period of 15 min. After the conclusion of experiments, the lengths of the predators and remaining prey were measured, as were water temperature and turbidity. Tanks were drained and refilled before further use. Fish used in experiments were not used in subsequent trials. Predator size (ANOVA, $F_{[2,33]} = 0.24$, $p = 0.79$) and prey size (ANOVA, $F_{[2,105]} = 0.98$, $p = 0.38$) were not significantly different among turbidity treatments. Experimental temperatures ranged between 9.3 °C and 9.9 °C. Significant changes in prey consumption were identified using the Kruskal–Wallis test, followed with a posteriori multiple comparisons using the Nemenyi test.

To determine whether turbidity affected predator–prey encounter rates or capture success, the number of pursuits was quantified from the video records of experimental trials. Pursuits could be clearly distinguished from routine swimming by sudden acceleration, rapid changes in direction, and prey responses. In some of the clear-water trials, the predators consumed all of the prey in <15 min, and the number of encounters was normalized by the time until all prey were consumed. Capture success was calculated by dividing the number of pursuits by the number of prey consumed. Significant changes in pursuit rate and encounter rates were identified using the Kruskal–Wallis test, followed with a posteriori multiple comparisons using the Nemenyi test.

Effect of type of suspended material

The experiments with planktivores and piscivores differed in the material used to increase turbidity levels, which were measured in NTU. The beam attenuation coefficient of kaolin and bentonite suspensions was measured at nine turbidity levels ranging from 0 to 40 NTU with a Wetlabs C-Star 25 cm path length transmissometer (Wet Labs, Philomath, Oreg.). This instrument measures the sum of absorption and scattering coefficients at a wavelength of 660 nm.

To confirm that kaolin and bentonite had a similar effect on planktivory, the feeding rates of groups of five chum salmon on *Artemia* prey (mean length 2.7–2.9 mm) were measured at 0.3 NTU (no kaolin) and at 9.8 NTU of kaolin-induced turbidity and compared with the results of trials using bentonite (described above). Experiments were conducted at 5.02×10^{-1} $\mu E \cdot m^{-2} \cdot s^{-1}$. Experimental fish averaged 78.9 ± 12.2 mm ($\bar{x}$ ± SD) in length, and fish size did not vary between treatments (*t* test, $t_{48} = 1.40$, $p = 0.17$). Five trials were conducted at each turbidity level.

Results

Light threshold of chum salmon

The relationship between prey consumption by juvenile chum salmon and log light intensity was sigmoidal (Fig. 1). There was a significant decrease in prey consumption at low light intensities (ANOVA, $F_{[6,34]} = 33.5$, $p < 0.001$; Fig. 1). The threshold illumination at which feeding increased was between 10^{-5} $\mu E \cdot m^{-2} \cdot s^{-1}$ and 10^{-4} $\mu E \cdot m^{-2} \cdot s^{-1}$ (~5×10^{-5} $\mu E \cdot m^{-2} \cdot s^{-1}$). Prey consumption reached a maximum at ~1×10^{-1} $\mu E \cdot m^{-2} \cdot s^{-1}$ and did not increase with further illumination.

Effect of light and turbidity on planktivory

Turbidity at the tested levels of 0–40 NTU did not have a strong effect on prey consumption by juvenile chum salmon and walleye pollock except at the highest turbidity at the high illumination (Figs. 2*a*, 2*b*). Although there was a strong light effect for both species, there was a significant interaction between light and turbidity (Tables 1, 2), indicating that the effect of turbidity on prey consumption depends on light intensity. Pairwise comparisons (Tables 1, 2) identified significant turbidity effects only at the higher light intensity.

Effect of turbidity on piscivory

The number of chum salmon consumed by sablefish decreased significantly under elevated turbidity (Kruskal–Wallis test, $H = 13.0$, df = 2, $p < 0.001$). Pairwise comparisons revealed that the number of prey consumed was significantly higher at 0 than at 10 NTU, but prey consumption at these

© 2003 NRC Canada

Fig. 1. Mean number of prey (± standard error) consumed by groups of five juvenile chum salmon (*Oncorhynchus keta*) in clear (0.2 nephelometric turbidity units (NTU)) water at illuminations ranging from $<1 \times 10^{-8}$ (darkness) to 1 $\mu E \cdot m^{-2} \cdot s^{-1}$. Prey consumption at underlined light intensities does not differ significantly (Tukey's test, $p < 0.05$). Five replicate trials were conducted at each illumination, with 100 prey per trial and fish allowed 5 min to feed.

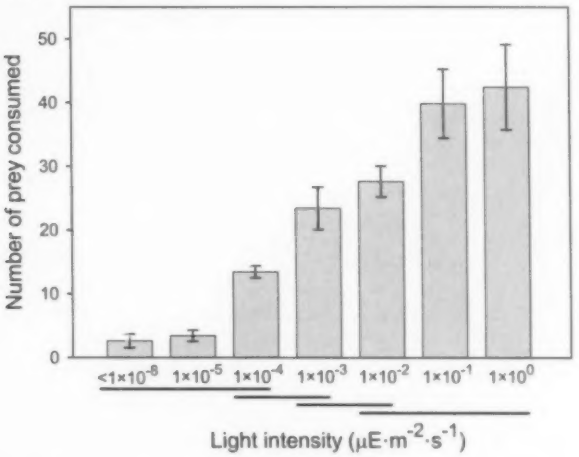

turbidities could not be distinguished from that at 5 NTU (Nemenyi test). Predation rates were about threefold lower at 5 NTU than in clear water, and no prey were consumed in the 10 NTU trials (Fig. 3).

Analysis of the video records indicated that as turbidity increased, sablefish pursued the chum prey less often (H = 9.76, df = 2, p = 0.008; Fig. 4*a*). Pairwise comparisons revealed that pursuit rates were higher at 0 than at 10 NTU, but pursuit rates at neither of these turbidities could be statistically distinguished from those at 5 NTU (Nemenyi test). In clear water, the sablefish generally responded to the chum immediately after the barrier was raised, crossing the tank and initiating pursuit. Under elevated turbidity, the sablefish did not respond as rapidly to the chum and were often observed to swim around the periphery of the tank as they typically did when no prey were present in the tank. In many cases, the prey tended to occupy the central areas of the tank while the sablefish, which appeared not to detect the prey, swam around the periphery of the tank. In addition to reducing the frequency of pursuits, elevated turbidity reduced the rate of prey capture (H = 11.92, df = 2, p = 0.003; Fig. 4*b*). Pairwise comparisons revealed that pursuit rates were significantly higher at 0 than at 10 NTU, but capture success at either turbidity could not be statistically distinguished from that at 5 NTU (Nemenyi test).

The sablefish did not exhibit stereotyped orienting responses before pursuing chum prey, making it difficult to establish when prey detection occurred. This precluded the calculation of prey-sighting distances from the video records. However, the ability of sablefish to detect prey appeared to decrease substantially as turbidity increased. At 0 NTU, the predators often crossed the 3-m-diameter tank to pursue prey, indicating that prey were visible at distances of over 3 m. At 5 NTU, pursuits were initiated at predator–prey distances of

Fig. 2. Effect of turbidity (in nephelometric turbidity units (NTU)) on planktivory by juvenile (*a*) chum salmon (*Oncorhynchus keta*) and (*b*) walleye pollock (*Theragra chalcogramma*). Bars indicate the mean number (± standard error) of prey consumed by groups of five fish at five turbidity levels and two light intensities. Open bars indicate high light conditions (5.02×10^{-1} $\mu E \cdot m^{-2} \cdot s^{-1}$) and shaded bars indicate low light conditions (4.80×10^{-4} $\mu E \cdot m^{-2} \cdot s^{-1}$). Five replicate trials were conducted at each illumination, with 100 prey per trial and fish allowed 5 min to feed.

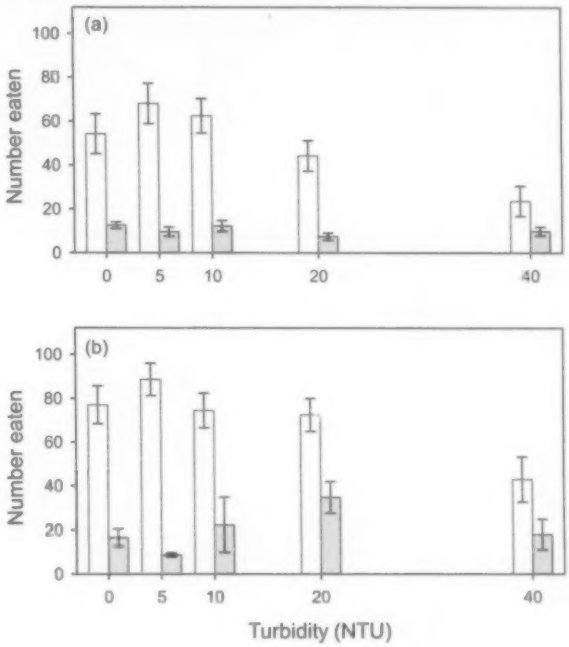

less than 1 m, and pursuit ended when predator and prey were separated by more than 1 m. Pursuits at 10 NTU were initiated when predator and prey were separated by <40 cm.

Effect of type of suspended material

The beam attenuation coefficient (α) measured at 660 nm was linearly related to turbidity in NTU for both the bentonite ($y = 1.44x$, $r^2 = 0.99$) and kaolin ($y = 0.63x$, $r^2 = 0.99$) suspensions. Given that the bentonite suspension had a higher α at a given NTU value, this indicates that bentonite is more absorptive than kaolin at this wavelength. However, the effect of elevated turbidity on the feeding rates of chum salmon was similar regardless of the material used to generate the turbidity. At high light intensity, chum salmon consumed 56.8 ± 10.0 ($\bar{x}$ ± standard error (SE)) prey in clear water compared with 75.4 ± 6.6 at a kaolin-induced turbidity of 10 NTU. Prey consumption in clear water and 10 NTU of kaolin-induced turbidity was not significantly different (t_8 = 1.52, p = 0.16). Although these fish were ~30 mm larger than the fish used in bentonite planktivory trials (see above), the observed 33% increase in prey consumption at kaolin-induced turbidity of 10 NTU relative to control fish of the same size in clear water is comparable to the 15% increase above control observed at 10 NTU generated using bentonite (Fig. 2*a*).

© 2003 NRC Canada

Table 1. Two-way analysis of variance of juvenile chum salmon prey consumption at turbidities ranging from 0 to 40 NTU (nephelometric turbidity units) at light intensities of 5×10^{-4} and 5×10^{-1} $\mu E \cdot m^{-2} \cdot s^{-1}$. Turbidity levels are listed in order of descending prey consumption. Prey consumption at the underlined turbidity levels does not differ significantly (Tukey's test, $p < 0.05$). Degrees of freedom, df.

Factor	*F* ratio	df	*p*
Light	149.1	1,49	<0.001
Turbidity	5.1	4,49	0.002
Turbidity × light	3.8	4,49	0.01

	Turbidity (NTU)				
High light	5	10	0	20	40
Low light	0	10	40	5	20

Table 2. Two-way analysis of variance of prey consumption by juvenile walleye pollock at turbidities ranging from 0 to 40 NTU (nephelometric turbidity units) at light intensities of 5×10^{-4} and 5×10^{-1} $\mu E \cdot m^{-2} \cdot s^{-1}$. Turbidity levels are listed in order of descending prey consumption. Prey consumption at the underlined turbidity levels does not differ significantly (Tukey's test, $p < 0.05$). Degrees of freedom, df; NS, not significant.

Factor	*F* ratio	df	*p*
Light	95.3	1,49	<0.001
Turbidity	2.4	4,49	NS (0.07)
Turbidity × light	3.2	4,49	0.02

	Turbidity (NTU)				
High light	5	0	10	20	40
Low light	20	10	40	0	5

Discussion

These experiments indicate that piscivorous feeding by sablefish is substantially more sensitive to elevated turbidity than planktivorous feeding by chum salmon and walleye pollock. At 10 NTU, sablefish did not successfully consume juvenile chum salmon in 15-min trials, whereas feeding by both of the planktivores was unaffected relative to clear water conditions at this turbidity level. Our behavioral observations of sablefish are consistent with the interpretation that their ability to detect and capture prey was substantially impaired at this turbidity level. Although our experiments were designed to measure prey consumption, our observations of foraging fish are similar to previous reports that at high light in clear water, piscivores are able to detect their prey at distances of metres (Breck 1993; Vogel and Beauchamp 1999), whereas planktivores are able to detect prey at distances of 10s of centimetres (O'Brien 1987; Utne 1997).

Our results are consistent with contrast degradation theory, which predicts that the visibility of objects that can be seen at a large distance in clear water will be disproportionately reduced in turbid waters compared with that of objects that are visible at a shorter distance in clear water. This effect is analogous to the familiar situation where fog has little effect on short-range vision but can greatly diminish the visibility of objects at a distance (Lythgoe 1979). These results

Fig. 3. Effect of turbidity (in nephelometric turbidity units (NTU)) on piscivory by sablefish (*Anoplopoma fimbria*). Bars indicate the mean (± standard error) number of chum salmon consumed by pairs of sablefish in 15-min trials ($n = 6$), with six prey per trial.

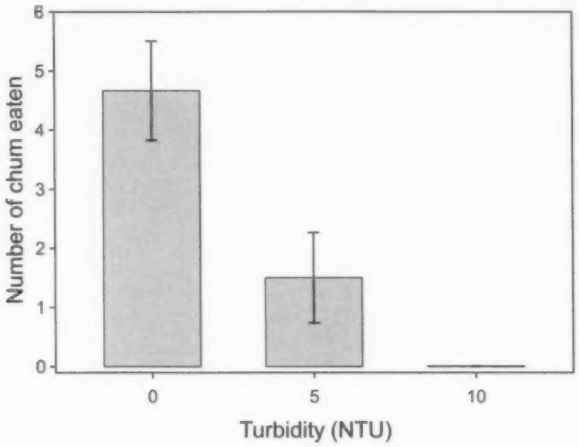

Fig. 4. Effect of turbidity (in nephelometric turbidity units (NTU)) on mean (± standard error) (*a*) pursuit frequency and (*b*) capture success of sablefish (*Anoplopoma fimbria*) feeding on chum salmon (*Oncorhynchus keta*) in 15-min trials ($n = 6$).

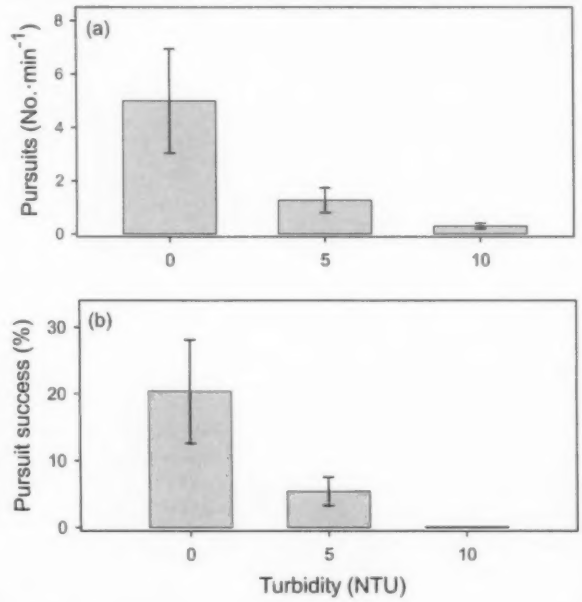

© 2003 NRC Canada

support the "turbidity as cover" hypothesis (Gregory 1993) and suggest that elevated turbidity may be advantageous for planktivorous fish because they will be less vulnerable to piscivores but will not experience a substantial decrease in feeding opportunity. Although our experiments were conducted with saltwater species, the implications of contrast degradation should be generally applicable and should also apply to freshwater species.

Increased turbidity decreased both the rate at which sablefish pursued chum prey and the probability of prey capture. The reduction in pursuits likely reflects reduced predator–prey encounter rates resulting from a decrease in visibility. Capture success averaged ~20% in clear water, and no successful pursuits were observed at 10 NTU. The generally low capture success reflects the high mobility and maneuverability of the chum prey. Reduced capture success at elevated turbidity indicates that lower prey consumption in turbid water cannot be attributed solely to a reduction in encounter rate, as has been proposed previously (Gregory and Levings 1996). Increased turbidity likely decreases capture success by increasing the probability that prey escape responses will displace the prey outside of an attacking predator's field of view. Visual encounter models based on piscivore reactive distances (e.g., Beauchamp et al. 1999), which implicitly assume constant capture success, will overestimate feeding opportunities under turbid conditions if capture success decreases in turbid environments.

Our experiment was designed to eliminate the confounding effect of decreased ambient light intensity due to light attenuation under elevated turbidities, and the effects of turbidity on planktivorous feeding observed in the experiments can be attributed primarily to increased scattering of light by suspended materials. High turbidity significantly decreased prey consumption by the two planktivores at the higher illumination, but not at the lower illumination. At lower illuminations, prey will be visible at shorter distances (Aksnes and Utne 1997), which will reduce the effects of contrast degradation relative to high illuminations resulting from a decreased path length between predator and prey. It should be noted that prey depletion over the course of planktivory experiments has the potential to result in an underestimation of prey consumption, particularly in the high light trials in which larger fractions of available prey were consumed. However, given that the trends observed in chum salmon are similar to those of pollock, which consumed more prey, the effects of prey depletion should not alter our primary conclusion that feeding by planktivores is less sensitive to turbidity than piscivores.

Although we did not observe a strong effect of turbidity on prey consumption by planktivores, lower levels of turbidity than those tested here will substantially increase light attenuation with depth. Decreased light penetration will restrict feeding by visually foraging planktivorous fish to shallower water where light levels are higher (Eiane et al. 1999). Because light attenuation increases exponentially with depth (Kirk 1985), the effects of light attenuation will be most pronounced for species that live at greater depths. As a result, the primary effect of turbidity on feeding by planktivorous fish in all but the most turbid waters may be to reduce illumination at depth and thus limit the depth at which fish are able to feed effectively.

The experiments with planktivores and piscivores differed in the material used to manipulate turbidity. The beam attenuation coefficient at 660 nm at a given turbidity (NTU) was measured to be higher for a bentonite than for a kaolin suspension. Given that NTUs are a measure of light scatter, this indicates that bentonite absorbs more light at this wavelength. This suggests that bentonite may be more disturbing to the visual system than kaolin, although this depends on light absorption at other wavelengths, the spectral distribution of ambient light, and the spectral sensitivity of the fish. If this were the case, then our interpretations would be conservative, as the experiments with planktivores were conducted with more visually disturbing suspended materials than experiments with piscivores. However, at 10 NTU, neither bentonite nor kaolin resulted in a significant change in prey consumption by chum salmon, which indicates that the use of different suspended materials does not introduce a substantial bias and cannot account for the difference in turbidity-induced prey consumption between piscivores and planktivores.

In our experiments, we used model species to simulate natural predator–prey interactions. Although all predator species are able to consume prey in complete darkness, they should be considered primarily visual predators as feeding rates in well-illuminated conditions are substantially higher than in the dark (Ryer and Olla 1999; this study). Thus, the results are primarily applicable to fish that visually search for individual prey. Although the *Artemia* used as prey were approximately the same size as natural prey consumed by juvenile chum salmon and walleye pollock (Bailey et al. 1975; Schabetsberger et al. 2000), *Artemia* have poorly developed escape responses and are less likely to escape once attacked by a planktivore. When visibility is poor, prey with more developed escape responses may decrease capture success by moving outside of the predator's reduced field of vision. Thus, although the use of *Artemia* as prey may adequately reflect encounter rates with small prey, their limited escape responses may bias our experiments as consumption of *Artemia* may be overestimated at low light intensity and high turbidity compared with consumption of more evasive prey. However, given that turbidity at the levels tested had only weak effects on planktivore feeding rate, it is unlikely that elevated turbidity greatly reduced the planktivore's visual field to the point that it would have greatly increased the ability of more evasive prey to escape. Even if *Artemia* never successfully escape planktivores and the results of the planktivory experiments can be ascribed purely to changes in encounter rate, this does not invalidate the conclusion that piscivores are more sensitive to increases in turbidity than planktivores, as significant decreases in pursuit rate by piscivorous sablefish were observed at 10 NTU, whereas no changes in prey consumption by the two planktivores were observed at this turbidity level.

A substantial body of work has demonstrated that high turbidity decreases the distance at which planktivorous fish are able to detect prey (e.g., Vinyard and O'Brien 1976; Confer et al. 1978; Utne 1997). Turbidity in many of these studies was measured based either on light absorbance or on measures of visibility to human observers, and these studies are thus not directly comparable to our experiments. Studies of particle-feeding planktivorous fish in which turbidity was

© 2003 NRC Canada

measured in a comparable manner support our conclusions, as they suggest that relatively high turbidity is required to reduce prey consumption. In a comparative study of diadromous planktivores, a significant decrease in feeding rate was observed in three species at turbidities of 20, 160, and 640 NTU, whereas three other species were unaffected by turbidities as high as 640 NTU (Rowe and Dean 1998). Feeding of juvenile chinook salmon on adult *Artemia* decreases at >150 NTU, although prey-sighting distance decreases by ~50% by 25 NTU (Gregory and Northcote 1993). Planktivory by bluegills is reduced at turbidities of 60 NTU (Gardner 1981). Overall, these studies indicate that moderately high levels of turbidity are required to impair feeding by planktivorous fish.

The distance at which fish are able to respond to other fish is known to decrease sharply with small increases in turbidity. Measurements of the reactive distance of lake trout to salmonid prey indicate that turbidities as low as 3 NTU will decrease reactive distances by ~40% under well-illuminated conditions (Vogel and Beauchamp 1999). The distance at which bluegills are able to detect largemouth bass predators is highly dependent on turbidity, decreasing from ~210 cm in clear water to ~35 cm at 5 NTU (Miner and Stein 1996). These measurements are consistent with our results and suggest that turbidity greatly impairs the ability of fish to detect large, visible objects. However, previous experimental studies of prey consumption by piscivores (Vandenbyllaardt et al. 1991; Reid et al. 1999) have demonstrated statistically significant decreases in prey consumption only at substantially higher turbidities than those tested in this study (37 NTU and 100 NTU), respectively. Gregory and Levings (1996) did not detect a significant difference in predation by cutthroat trout on juvenile salmonids at turbidities as high as 87 NTU. These results may be attributable to methodological differences. Previous studies used comparatively long experimental periods (1–162 h), which constrained highly mobile predators in fairly small volumes for extended periods, and predator satiation may have masked changes in predator–prey encounter rates (Gregory and Levings 1998). This experimental bias is consistent with previous experiments in which elevated turbidity was observed to decrease feeding by piscivores in 1-h but not 4-h trials (Vandenbyllaardt et al. 1991). In addition, the piscivores in our experiments were starved, which motivated them to feed.

Increases in turbidity alter the background against which a prey item is viewed and can lead to increases in the inherent contrast between the prey and the background. This makes the prey more visible and can compensate for turbidity-induced degradation of apparent contrast. However, this does not appear to be a primary effect in our study, as piscivory by sablefish decreased sharply at elevated turbidity, and prey consumption by both species of planktivores was not significantly elevated in turbid vs. clear water. The relative importance of turbidity in increasing prey background inherent contrast decreases sharply with the distance at which prey can be seen (Fiksen et al. 2002). Thus, turbidity-induced changes in prey inherent contrast should be most important for larval fish and least important for piscivorous fish. This prediction is consistent with studies of larval fish that have shown that under well-lit conditions, elevated turbidity either has a minor effect on feeding rate (Breitburg 1988) or leads to an increase in feeding rate (Boehlert and Morgan 1985; Miner and Stein 1993).

If, as our experiments suggest, feeding by piscivores is substantially more sensitive to elevated turbidity than feeding by planktivores, then turbid habitats may be favorable for planktivorous fish, as they will be less vulnerable to attack by piscivores. Recent studies indicating that elevated turbidity makes planktivores less susceptible to predation by piscivores (Gregory and Levings 1998; Beauchamp et al. 1999; Johnson and Hines 1999) support the notion that turbid waters may be favorable habitats for planktivores. This is consistent with the distribution of small fishes in both freshwater and marine environments, where small fish are often associated with more turbid waters (e.g., Blaber and Blaber 1980; Heege and Appenzeller 1998). For example, 16 of 20 species of juvenile fishes studied in a turbid estuary were disproportionately found in waters with turbidities exceeding 10 NTU (Cyrus and Blaber 1987). In addition, planktivorous fish may respond to turbid water by decreasing predator-avoidance behaviors (Gregory 1993; Miner and Stein 1996; Abrahams and Kattenfeld 1997). This may be advantageous, as predator-avoidance behavior often comes at the cost of decreased feeding opportunities (Gilliam and Fraser 1987; Lima and Dill 1990).

Turbidity levels sufficient to reduce the effectiveness of piscivory are more likely to occur in freshwater and estuarine environments than in marine environments. Turbidity in these habitats is often high as a result of inputs of inorganic particles from land (Kirk 1985). However, turbidity may have a locally important effect in productive coastal marine habitats during dense phytoplankton blooms (Lovvorn et al. 2001), in river plumes (Grimes and Kingsford 1996), or in areas where bottom sediments are resuspended (Churchill et al. 1994). Estuaries serve as nursery areas for many marine fishes; turbidity in these habitats may often be sufficient to reduce vulnerability to visual predators (Blaber and Blaber 1980; Miller et al. 1985; Vant 1990). For instance, turbidity has the potential to reduce the mortality of juvenile salmon, such as the chum used as both predator and prey in our experiments, which often inhabit turbid freshwater and estuarine habitats. Salmonids are often associated with river plumes in the coastal ocean during their first months in the ocean, and decreased visibility in these environments is unlikely to affect planktivorous feeding but may be sufficient to reduce vulnerability to piscivorous fish and seabirds. Focused field studies (e.g., Gregory and Levings 1998) should be conducted to evaluate if turbidity reduces predation risk for planktivorous fish exposed to natural environmental conditions and predator assemblages.

In conclusion, turbidity decreases visibility in aquatic systems by decreasing light penetration and reducing apparent contrast. Our experiments suggest that there is an asymmetry in how turbidity-induced contrast degradation affects the feeding rates of visually hunting piscivorous and planktivorous fish. This asymmetry has important ecological implications, as moderately turbid aquatic environments may provide an advantage for planktivorous fish. Increased turbidity will decrease predation risk substantially more than the ability to feed on zooplankton prey. Our inferences are limited in scope

© 2003 NRC Canada

because they are based on experiments with two species of planktivores and a single piscivore. However, we anticipate that our results are broadly relevant to these two trophic levels, as the expectation that piscivores are more sensitive to turbidity is based on fundamental optical principles.

Acknowledgements

We thank Michelle Ottmar, Mara Spencer, and Richard Titgen for assistance with aquarium facilities, prey culture, and electronics, respectively. This work would not have been possible without the support of Allan Stoner and Edmundo Casillas, which is sincerely appreciated. The comments of Robert Emmett, Thomas Hurst, Dan Kreeger, and Anne Utne Palm improved the manuscript. A.D.R. was supported by a National Research Council Postdoctoral Fellowship, and A.V. was supported by Minority Summer Internship in Fisheries Behavioral Ecology by the Equal Employment Opportunity Office of the National Marine Fisheries Service, National Oceanic and Atmospheric Administration.

References

Abrahams, M., and Kattenfeld, M. 1997. The role of turbidity as a constraint on predator–prey interactions in aquatic environments. Behav. Ecol. Sociobiol. **40**: 169–174.

Aksnes, D.L., and Utne, A.C. 1997. A revised model of visual range in fish. Sarsia, **82**: 137–147.

Anthony, P.D. 1981. Visual contrast thresholds in the cod *Gadus morhua* L. J. Fish Biol. **19**: 87–103.

Bailey, J.E., Wing, B.L., and Mattson, C.R. 1975. Zooplankton abundance and feeding habits of fry of pink salmon *Oncorhynchus gorbuscha* and chum salmon *O. keta* in Traitors Cove, Alaska, with speculations on the carrying capacity of the area. Fish. Bull. **73**: 846–861.

Beauchamp, D.A., Baldwin, C.M., Vogel, J.L., and Gubala, C.P. 1999. Estimating diel, depth-specific foraging opportunities with a visual encounter rate model for pelagic piscivores. Can. J. Fish. Aquat. Sci. **56**: 128–139.

Blaber, S.J.M., and Blaber, T.G. 1980. Factors affecting the distribution of juvenile estuarine and inshore fish. J. Fish Biol. **17**: 143–162.

Boehlert, G.W., and Morgan, J.B. 1985. Turbidity enhances feeding abilities of larval Pacific herring, *Clupea harengus pallasi*. Hydrobiologia, **123**: 161–170.

Breck, J.E. 1993. Foraging theory and piscivorous fish: are forage fish just big zooplankton? Trans. Am. Fish. Soc. **122**: 902–911.

Breitburg, D.L. 1988. Effects of turbidity on prey consumption by striped bass larvae. Trans. Am. Fish. Soc. **117**: 72–77.

Churchill, J.H., Wirick, C.D., Flagg, C.N., and Pietrafesa, L.J. 1994. Sediment resuspension over the continental shelf of the Delmarva Peninsula. Deep Sea Res. **41**: 341–363.

Confer, J.L., Howick, G.L., Corzette, M.H., Kramer, S.L. Fitzgibbon, S., and Landesberg, R. 1978. Visual predation by planktivores. Oikos, **31**: 27–37.

Cyrus, D.P., and Blaber, S.M.J. 1987. The influence of turbidity on juvenile fishes in estuaries. Part 1. Field studies at Lake St. Lucia on the southeastern coast of Africa. J. Exp. Mar. Biol. Ecol. **109**: 53–70.

Duntley, S.Q. 1962. Underwater visibility. *In* The sea. Vol. 1. Physical oceanography. *Edited by* M.N. Hill. John Wiley and Sons, Inc., London. pp. 452–455.

Eiane, K., Aksnes, D.L., Bagoien, E., and Kaartvedt, S. 1999. Fish or jellies — a question of visibility? Limnol. Oceanogr. **44**: 1352–1357.

Fiksen, Ø., Aksnes, D.L., Flyum, M.H., and Giske, J. 2002. The influence of turbidity on growth and survival of fish larvae: a numerical analysis. Hydrobiologia, **484**: 49–59

Gardner, M.B. 1981. Effects of turbidity on feeding rates and selectivity of bluegills. Trans. Am. Fish. Soc. **110**: 446–450.

Gilliam, J.F., and Fraser, D.F. 1987. Habitat selection under predation hazard: test of a model with foraging minnows. Ecology, **68**: 1856–1862.

Gregory, R.S. 1993. Effect of turbidity on the predator avoidance behaviour of juvenile chinook salmon (*Oncorhynchus tshawytscha*). Can. J. Fish. Aquat. Sci. **50**: 241–246.

Gregory, R.S., and Levings, C.D. 1996. The effects of turbidity and vegetation on the risk of juvenile salmonids, *Oncorhynchus* spp., to predation by adult cutthroat trout, *O. clarkii*. Environ. Biol. Fishes, **47**: 279–288.

Gregory, R.S., and Levings, C.D. 1998. Turbidity reduces predation on migrating juvenile Pacific salmon. Trans. Am. Fish. Soc. **127**: 275–285.

Gregory, R.S., and Northcote, T.G. 1993. Surface, planktonic, and benthic foraging by juvenile chinook salmon (*Oncorhynchus tshawytscha*) in turbid laboratory conditions. Can. J. Fish. Aquat. Sci. **50**: 233–240.

Grimes, C.B., and Kingsford, M.J. 1996. How do riverine plumes of different sizes influence fish larvae: do they enhance recruitment? Mar. Freshw. Res. **47**: 191–208.

Heege, T., and Appenzeller, A.R. 1998. Correlations of large-scale patterns of turbidity and pelagic fish biomass using satellite and acoustic methods. Adv. Limnol. **53**: 489–503.

Johnson, J.E., and Hines, R.T. 1999. Effect of suspended sediment on vulnerability of young razorback suckers to predation. Trans. Am. Fish. Soc. **128**: 648–655.

Kirk, J.T.O. 1985. Effects of suspensoids (turbidity) on penetration of solar radiation in aquatic ecosystems. Hydrobiologia, **125**: 195–208.

Kirk, J.T.O. 1994. Light and photosynthesis in aquatic ecosystems. Cambridge University Press, Cambridge.

Lima, S.L., and Dill, L.M. 1990. Behavioral decisions made under the risk of predation: a review and prospectus. Can. J. Zool. **68**: 619–640.

Lovvorn, J.R., Baduini C.I., and Hunt, G.L. 2001. Modeling underwater visual and filter feeding by planktivorous shearwaters in unusual sea conditions. Ecology, **82**: 2342–2356.

Lythgoe, J.N. 1979. The ecology of vision. Clarendon Press, Oxford.

Macy, W.K., Sutherland, S.J., and Durbin, E.G. 1998. Effects of zooplankton size and concentration and light intensity on the feeding behavior of Atlantic mackerel *Scomber scombrus*. Mar. Ecol. Prog. Ser. **172**: 89–100.

McFarland, W.N. 1986. Light in the sea — correlations with behaviors of fishes and invertebrates. Am. Zool. **26**: 389–401.

Miller, J.M., Crowder, L.B., and Moser, M.L. 1985. Migration and utilization of estuarine nurseries by juvenile fishes: an evolutionary perspective. Contrib. Mar. Sci. **27**: 338–351.

Miner, J.G., and Stein, R.A. 1993. Interactive influence of turbidity and light on larval bluegill (*Lepomis macrochirus*) foraging. Can. J. Fish. Aquat. Sci. **50**: 781–788.

Miner, J.G., and Stein, R.A. 1996. Detection of predators and habitat choice by small bluegills: effects of turbidity and alternative prey. Trans. Am. Fish. Soc. **125**: 97–103.

O'Brien, W.J. 1987. Planktivory by freshwater fish: thrust and parry in the pelagia. *In* Predation: direct and indirect impacts on aquatic

© 2003 NRC Canada

communities. *Edited by* W.C. Kerfoot and A. Sih. University Press of New England, Hanover, N.H. pp. 3–17.

Reid, S.M., Fox, M.G., and Whillans, T.H. 1999. Influence of turbidity on piscivory in largemouth bass (*Micropterus salmoides*). Can. J. Fish. Aquat. Sci. **56**: 1362–1369.

Rowe, D.K., and Dean, T.L. 1998. Effects of turbidity on the feeding ability of the juvenile migrant stage of six New Zealand freshwater fish species. N.Z. J. Mar. Freshw. Res. **32**: 21–29.

Ryer, C.H., and Olla, B.L. 1999. Light-induced changes in the prey consumption and behavior of two juvenile planktivorous fish. Mar. Ecol. Prog. Ser. **181**: 41–51.

Schabetsberger, R., Brodeur, R.D., Ciannelli, L., Napp, J.M., and Swartzman, G.L. 2000. Diel vertical migration and interaction of zooplankton and juvenile pollock (*Theragra chalcogramma*) at a frontal region near the Pribilof Islands, Bering Sea. ICES J. Mar. Sci. **57**: 1283–1295.

Utne, A.C.W. 1997. The effect of turbidity and illumination on the reaction distance and search time of the marine planktivore *Gobiusculus flavescens*. J. Fish Biol. **50**: 926–938.

Vandenbyllaardt, L., Ward, F.J., Braekevelt, C.R., and McIntyre, D.B. 1991. Relationships between turbidity, piscivory and development of the retina in juvenile walleyes. Trans. Am. Fish. Soc. **120**: 382–390.

Vant, W.N. 1990. Causes of light attenuation in nine New Zealand estuaries. Estuar. Coast Shelf Sci. **31**: 125–137.

Vinyard, G.L., and O'Brien, W.J. 1976. Effects of light and turbidity on the reactive distance of bluegill (*Lepomis macrochirus*). J. Fish. Res. Board Can. **33**: 2845–2849.

Vogel, J.L., and Beauchamp, D.A. 1999. Effects of light, prey size, and turbidity on reaction distances of lake trout (*Salvelinus namaycush*) to salmonid prey. Can. J. Fish. Aquat. Sci. **56**: 1293–1297.

© 2003 NRC Canada

Does the value of newly accessible spawning habitat for walleye (*Stizostedion vitreum*) depend on its location relative to nursery habitats?

Michael L. Jones, John K. Netto, Jason D. Stockwell, and Joseph B. Mion

Abstract: The benefit accrued from habitat restoration actions may depend not only on the quality and quantity of habitat restored, but also on its location relative to other critical habitats. For example, walleye (*Stizostedion vitreum*) larvae need to be transported by river currents from spawning to nursery habitats soon after emergence. We developed a model of river transport survival for larval walleye to evaluate potential recruitment from riverine spawning habitats to lacustrine nursery areas. Published relationships were used to model transport survival as a function of temperature and velocity. At greater distances from nursery areas, mortality risk increases, particularly as a result of starvation at relatively high river temperatures. We applied the model to the Sandusky River, a tributary to western Lake Erie, and found potential larval production from spawning habitat above an existing dam to exceed the potential of presently accessible spawning areas by a factor of 8. We used a generalized version of the model to show that for transport distances of less than 100 km, transport survival is much more sensitive to variations in river flows, whereas at greater distances, temperature becomes increasingly important.

Résumé : Les bénéfices accumulés par les actions de restauration des habitats peuvent dépendre non seulement de la qualité et de la quantité des habitats restaurés, mais aussi de leur situation par rapport à d'autres habitats critiques. Par exemple, les larves du doré jaune (*Stizostedion vitreum*) doivent être transportées par les courants de rivière de leurs sites de naissance vers leurs sites d'élevage tôt après leur émergence. Nous avons mis au point un modèle de survie des larves de doré au transport en rivière pour évaluer le recrutement potentiel depuis les sites de fraye dans les cours d'eau vers les sites d'élevage dans les lacs. Des relations tirées de la littérature ont permis d'élaborer un modèle de la survie au transport en fonction de la température et de la vitesse du courant. Le risque de mortalité augmente avec la distance des sites d'élevage, causé surtout par les risques de disette aux températures relativement élevées. Le modèle appliqué à la rivière Sandusky, un tributaire de l'ouest du lac Érié, révèle que la production potentielle de larves dans un habitat de frayère situé en amont d'un barrage dépasse le potentiel des sites de fraye actuellement accessibles par un facteur de 8. Une version généralisée du modèle montre que, pour des distances de transport de moins de 100 km, la survie au transport est affectée surtout par les variations du débit du cours d'eau, alors que, pour des distances plus grandes, c'est la température qui devient le facteur plus important.

[Traduit par la Rédaction]

Introduction

Fish habitats have been drastically altered throughout the Laurentian Great Lakes by human settlement, agriculture, and industrial development (Kelso et al. 1996). Great Lakes shorelines have been modified, leading to "hardening", structural simplification, and loss of nearshore wetland habitats. During the past 200 years, dams have been constructed on nearly every sizeable stream draining into the Great Lakes, limiting access for many Great Lakes fishes to spawning and early rearing habitats. Great Lakes fishery management agencies consider habitat restoration a top priority (Great Lakes Fishery Commission 1987, 2001), but the pervasive nature of aquatic habitat alterations implies that habitat restoration initiatives would benefit from evaluating where the greatest ecological and socioeconomic benefits are likely to accrue. Experience with habitat restoration is still limited (Kondolf and Micheli 1995; Minns et al. 1996*a*; Thompson 2002), so such evaluations are likely to depend on model-derived forecasts of the potential benefits. In this paper, we

Received 24 January 2003. Accepted 7 September 2003. Published on the NRC Research Press Web site at http://cjfas.nrc.ca on 22 December 2003.
J17305

M.L. Jones,[1] **J.K. Netto,**[2] **and J.D. Stockwell.**[3] Department of Fisheries and Wildlife, 13 Natural Resources Building, Michigan State University, East Lansing, MI 48824, U.S.A.
J.B. Mion. Inland Fisheries Research Unit, ODNR — Division of Wildlife, 10517 Canal Road SE, Hebron, OH 43025, U.S.A.

[1]Corresponding author (e-mail: jonesm30@msu.edu).
[2]Present address: U.S. Fish and Wildlife Service, Green Bay Fishery Resources Office, 2661 Scott Tower Road, New Franken, WI 54229, U.S.A.
[3]Present address: The Jackson Laboratory, 600 Main Street, Bar Harbor, ME 04609, U.S.A.

 doi: 10.1139/F03-130 © 2003 NRC Canada

Fig. 1. A map of Lake Erie showing the location of the Sandusky and Maumee rivers and details of the Sandusky River basin. River kilometre, rkm.

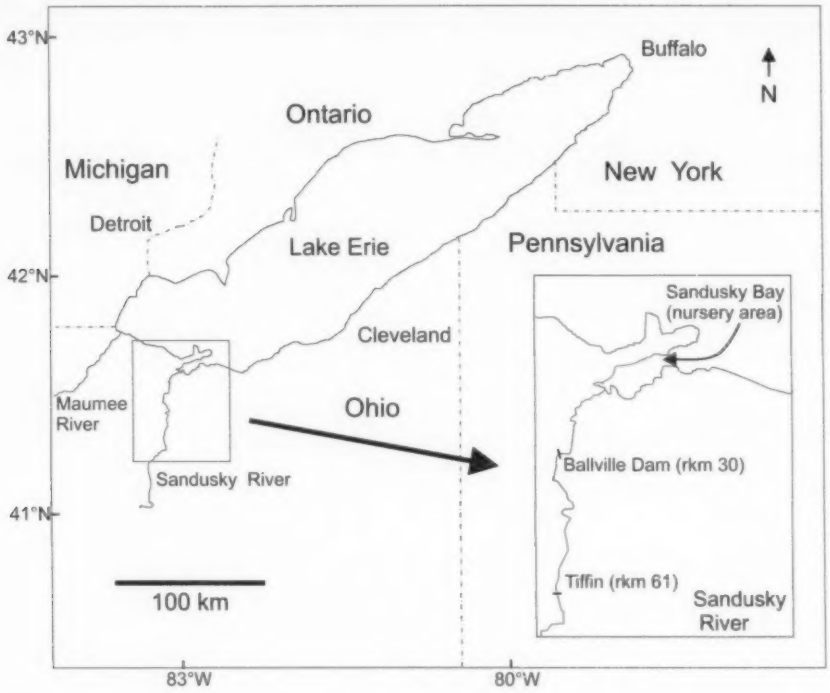

present and analyze a model to evaluate the potential benefits of dam removal as a means to increase walleye (*Stizostedion vitreum*) production and apply the model to a Lake Erie tributary stream.

The ecological effects of dams, including the interruption of migratory fish passage, have been extensively documented (Ligon et al. 1995; Ward and Stanford 1995; Bednarek 2001). There are tens of thousands of extant dams in the United States alone, and many of these dams are derelict, no longer serve their original purpose, or are of marginal economic value. As well, many are under consideration for relicensing by the Federal Energy Regulatory Commission. Because of this, state and federal management agencies are now routinely considering the removal of many dams with the objective of restoring lost ecosystem amenities (Bednarek 2001). Dam removal can be expensive, however, so it is important to have as clear an idea as possible of the potential benefits. Although dam removal has occurred on many U.S. rivers (Born et al. 1998), the ecological benefits derived from these actions have not been well-documented (Shuman 1995), with a few notable exceptions (e.g., Kanehl et al. 1997). In particular, it would be valuable to have estimates of the magnitude of the potential benefits to be derived from providing increased access to spawning habitat for migratory fish species.

Walleye are a species of considerable economic importance in the Great Lakes. They are abundant in western Lake Erie where they support important commercial and recreational fisheries (Leach and Nepszy 1976). Most of the walleye harvested in western and central Lake Erie are believed to originate from three spawning areas: a midlake reef complex, west of Port Clinton and near the Bass Islands (Baker 1971), and two Ohio rivers, the Sandusky and the Maumee (Fig. 1). Walleye spawn in the lower reaches of both of these rivers, approximately 25 km from the river mouth. They deposit adhesive eggs on a variety of substrates in moderate- to fast-flowing water. Upon emergence, the larvae are passively transported downstream to river mouths and nearshore areas where they begin feeding on zooplankton (Houde 1969; Jude 1992; Mion et al. 1998). The larvae do not typically feed while they are being transported downstream, probably because of the scarcity of zooplankton in riverine habitats at this time (Mion et al. 1998). During this period of transport, walleye larvae appear to be vulnerable to two sources of mortality: physical damage during very high flows and starvation due to slow downstream transport during low flows (Mion et al. 1998). The magnitude of these effects will depend on the amount of time that the larvae spend traveling from the spawning area to the nursery grounds and thus the duration of their exposure to these risks. This in turn depends on the distance that they have to travel.

In the Sandusky River, the upstream extent of walleye spawning is limited by the Ballville Dam at river kilometre (rkm) 30 (Fig. 1). Removal of this dam is being considered, partly as a measure to provide walleye with access to additional spawning habitat in this river. The Ohio Division of Wildlife (ODW) released adult walleye above the dam in 1997–1998, and migrating larvae were subsequently collected at rkm 51 after the spawning season (Plott 2000).

© 2003 NRC Canada

These observations demonstrate that usable spawning habitat exists in the Sandusky River above the dam. As spawning occurs at increasingly large distances from the nursery habitats, however, there will be increased risk of larval mortality caused by starvation or damaging flows (Mion et al. 1998) because the larvae will spend more time being transported. To quantify the potential additions to larval walleye recruitment that could result from removal of the Ballville Dam, it is necessary to consider not only the amount of spawning habitat that would become accessible, but also its distance from the nursery grounds.

In this paper, we present a model that includes a simple but mechanistic representation of walleye spawning, emergence, and downstream transport to lacustrine nursery habitats. We use the model to forecast the effects of spawning habitat quantity, quality, and location on potential recruitment of walleye larvae to nursery habitats. We apply the model to the Sandusky River using data from a recent survey of riverine habitat supply below and above the Ballville Dam and examine the potential additions to recruitment in this river that could be obtained if the Ballville Dam were removed. We also use the model to examine the general interaction between stream discharge, water temperature, and distance to nursery grounds as factors affecting walleye reproductive success in other streams.

Model description

Spawning

Walleye ascend rivers each spring to spawn, broadcasting negatively buoyant eggs over a variety of spawning substrates. Commencement of walleye spawning is associated with temperature, with spawning typically occurring when water temperatures are between 5 °C and 11 °C (Baker 1971; Wolfert et al. 1975). We simulate spawning using U.S. Geological Survey (USGS) daily water temperature data observations from the Sandusky River from 1968 to 1981 (observations from Fremont, Ohio). In the model, spawning begins on the first day that the 5-day running average temperature exceeds 5 °C and ends on the first day that the 5-day running average temperature exceeds 11 °C. Eggs are deposited throughout this interval according to a temporal pattern described by a normal distribution function with mean date (μ) and standard deviation (σ) according to the following equations:

$$(1) \qquad \mu = (t_s + t_e)/2 \text{ and } \sigma = (t_e - \mu)/2.58$$

where t_s and t_e are the first and last days of spawning, respectively.

Walleye are known to spawn on a variety of substrate types. There is evidence that incubation success varies depending on the coarseness of the substrate (Gibson and Hughes 1977; Corbett and Powles 1986). We divided the total area available for spawning into areas of good, average, and poor habitat quality, to reflect differences in particle sizes and embeddedness, and assumed that eggs are deposited at random over all three habitat types. Substrates of cobble, rubble, and gravel were classified as good spawning habitat, sand substrate was classified as average, and mud–silt was classified as poor spawning habitat. We assumed that walleye would not spawn on bedrock substrate. We used literature values to determine egg carrying capacities for each spawning substrate type (Table 1).

To simulate the effect of habitat location on reproductive success, we divided the river into 3-km-long habitat units. Each habitat unit is characterized by a quantity of substrate in each of the three spawning substrate types and its distance from the downstream nursery area in Sandusky Bay. We estimated the amount of spawning habitat in each habitat unit in the Sandusky River from river substrate maps generated by the Ohio Geological Survey (S. Mackey, Ohio Geological Survey, 1634 Sycamore Line, Sandusky, OH 44870, U.S.A., unpublished data). The maps record the substrate composition from rkm 27 to rkm 58, based on data collected using bottom grabs along regularly spaced line transects running perpendicular to the river flow. We scanned the maps and converted the digital images to a polygon GIS (geographical information system) coverage (Arcview ™, ESRI Ltd., Redlands, Calif.), with substrate type and distance from the nursery area as attributes of each polygon. The polygon data were then aggregated into a summary of the area of substrate of each type in each habitat unit.

Egg survival, development, and emergence

Following deposition, walleye eggs incubate for several weeks before emerging from the spawning substrate. Survival of incubating eggs is largely determined by the degree of exposure to risks such as predation, displacement, and physical disruption. Coarse, porous substrates with deep interstitial spaces provide greater protection from these risks than finer substrates. We used literature values for egg survival in the three substrate categories (Table 2) to model the probability of survival from egg deposition to emergence.

Egg development times depend on ambient temperatures. We fitted walleye egg incubation data from Smith et al. (1975) to describe a quadratic regression relationship between temperature and the daily percentage of egg development:

$$(2) \qquad Y = 0.0479T^2 - 0.2385T + 2.499$$

where Y is the predicted percent of development per day towards hatching, and T is the mean daily incubation temperature (°C). In our simulations, the model accumulated development "units" each day for the eggs currently in the substrate. When the eggs deposited on a particular date accumulated 100 units, they were assumed to have hatched. Walleye emerge into the water column immediately upon hatching (Corazza and Nickum 1981). All eggs hatching on a given day were combined into a single daily cohort for simulation of downstream movement.

Transport and transport survival

Upon emergence from riverine spawning substrates, larval walleye drift downstream to nursery grounds, typically shallow lacustrine habitats with an abundance of zooplankton. In the Sandusky River, the principal nursery area for larval walleye is believed to be in Sandusky Bay, a large shallow embayment at the mouth of the river. Larval walleye are weak swimmers, so their rate of travel is a function of river velocity (Corbett and Powles 1986). We assume that larval

© 2003 NRC Canada

Table 1. Literature values for maximum densities of walleye eggs (number·m^{-2}) held by different substrate types.

Source	Location	Waterbody type[a]	Rubble	Cobble	Gravel	Sand	Mud–detritus
Gibson and Hughes 1977	Hamilton's Creek, MB	R	588	4730	2537	1302	
Eckersley 1986	Hoople Creek, ON	R	5274				
Johnson 1961	Lake Winnibigoshish, MN	L		7050		1001	807
Eschmeyer 1950	Lake Gogebic, MI	L			6082		
Newburg 1975	Lake Osakis, MN	L	4015				
Mean					4325	1151	807

Note: Rubble, cobble, and gravel estimates are pooled for calculation of mean values across studies. MB, Manitoba; ON, Ontario; MN, Minnesota; MI, Michigan.
[a]R, river; L, lake.

Table 2. Proportion of walleye eggs surviving to hatching as a function of substrate type.

Source	Location	Waterbody type[a]	Rubble	Cobble	Gravel	Sand	Mud–detritus
Corbett and Powles 1986	Apsley Creek, ON	R			0.42	0.01	
Corbett and Powles 1986	Redmond Creek, ON	R					0.06
Gibson and Hughes 1977	Hamilton's Creek, MB	R	0.56	0.85	0.91	0.64	
Eckersley 1986	Hoople Creek, ON	R	0.33				
Johnson 1961	Lake Winnibigoshish, MN	L		0.26		0.03	0.01
Newburg 1975	Lake Osakis, MN	L	0.16				
Newburg 1975	Lake Osakis, MN	L	0.07				
Newburg 1975	Lake Osakis, MN	L	0.05				
Newburg 1975	Lake Osakis, MN	L	0.04				
Mean					0.37	0.23	0.04

Note: Rubble, cobble, and gravel estimates are pooled for calculation of the mean value across studies. ON, Ontario; MB, Manitoba; MN, Minnesota.
[a]R, river; L, lake.

Fig. 2. Estimated survival of age-0 walleye (*Stizostedion vitreum*) from spawning areas to nursery habitats in Sandusky and Maumee bays at a variety of river velocities.

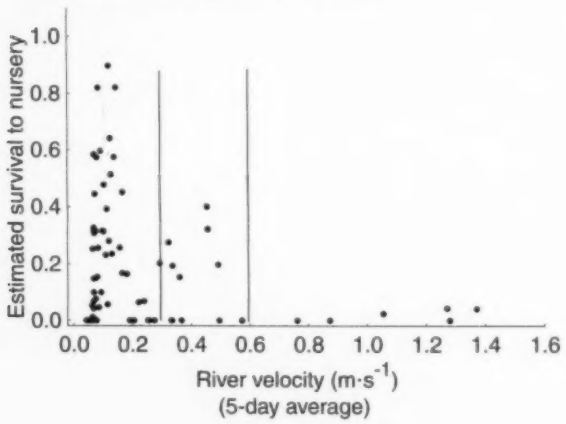

walleye remain in the water column and move downstream at the same rate as the water itself. The distance traveled each day is calculated as

$$D_j = V_j \mathrm{DL} \quad (3)$$

where j represents the day, D_j is the daily travel distance (m), V_j is the average daily river velocity for day j (m·s^{-1}), and DL is the length of a day in seconds (86 400 s). We assumed that walleye larvae drift downstream throughout the 24-h period, based on observations of Mion et al. (1998). Daily river velocity (V_j) is calculated from the daily discharge data as

$$V_j = Q_j/A \quad (4)$$

where Q_j is the mean daily discharge and A is the cross-sectional area of the river (Gordon et al. 1992). For the Sandusky River, we used the river cross-sectional area near Fremont, Ohio, together with the discharge data from the USGS gauging station near this location.

Mion et al. (1998) computed an index of larval survival for the Maumee and Sandusky rivers and found that it was consistently low when river velocity was >0.6 m·s^{-1} but can be very high when velocity was <0.3 m·s^{-1}; velocities between 0.3 m·s^{-1} and 0.6 m·s^{-1} yielded low to moderate survival values. They concluded that low river discharge was a necessary but not sufficient condition for high survival during transport from spawning to nursery grounds. At low discharge, if river transport is too slow, starvation may become a factor as larvae deplete their yolk reserves before reaching habitats with sufficient prey.

To apply the findings of Mion et al. (1998) to our model, we needed to convert the survival index that they reported to an actual survival probability. Using daily estimates of larval walleye density at the mouth of the river (J.B. Mion, unpublished data), we calculated the total number of larvae entering the nursery area each day with the larval production estimation methods of Mion et al. (1998). To determine hatch dates of surviving larvae, we used otolith-derived ages (J.B. Mion, unpublished data) of larvae subsampled from

© 2003 NRC Canada

Fig. 3. A flowchart describing the procedure used in the simulation model to select a transport survival value for each daily cohort of emerging walleye (*Stizostedion vitreum*) larvae. The bar plots represent frequency histograms of the survival rates shown in Fig. 2 for three river velocity ranges.

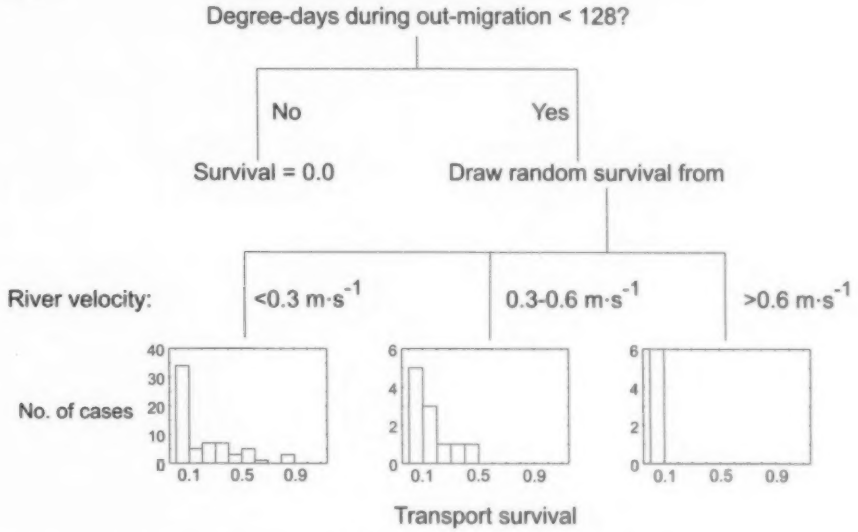

field collections for all dates that larvae were captured (Mion et al. 1998). The proportion of aged larvae represented by each hatch date was multiplied by the total number of larvae estimated to have reached the nursery area each day to give the daily number of larvae surviving for each hatch date. We calculated the total number of larvae surviving from each hatch date by summing the results of all days that had larvae from that hatch date arriving at the nursery area. Overall survival probability for each hatch date was estimated by dividing the total number of larvae from each daily cohort surviving out-migration by the estimated number of larvae produced on that date (Mion et al. 1998). Finally, we plotted the survival probability for each daily cohort versus the average river velocity experienced by that cohort during transport to the nursery area (Fig. 2).

We used the observed relationship between river velocity and survival for the Sandusky River (Fig. 2) and between temperature and yolk absorption (Krise and Meade 1986) to estimate transport survival. Yolk absorption is complete when larvae accumulate 128 thermal units, defined as degree-days above 0 °C. For example, a fish exposed to average daily temperatures of 9 °C and 12 °C on two consecutive days would accumulate 21 thermal units over those two days.

The combination of velocity and temperature conditions experienced by each daily-emerging cohort can give rise to several possible transport survival scenarios (Fig. 3). If a cohort accumulates more than 128 thermal units before reaching the nursery area, their survival is zero. If a cohort has accumulated less than 128 thermal units by the time they reach the nursery area, we draw a cohort survival rate at random from the distribution of survival probabilities observed (Fig. 2) for the velocity conditions that they experienced during downstream transport. If river velocity is low, we draw a survival rate from the distribution of survival for velocities below 0.3 $m \cdot s^{-1}$. If velocity is between 0.3 $m \cdot s^{-1}$ and 0.6 $m \cdot s^{-1}$, we draw survival from the distribution of survival for velocities in this range, and if velocity is high (>0.6 $m \cdot s^{-1}$), we draw a survival rate from the distribution of survival for velocities above 0.6 $m \cdot s^{-1}$. We use the average river velocity experienced by each cohort during transport for these calculations.

Predation is often cited as an important source of mortality in larval fishes, including walleye. We have not included predation mortality as an explicit mechanism in our model but recognize that predation may be contributing to the low observed survival of many larval walleye cohorts, even at low river velocities (e.g., more than 50% of cohorts for velocities <0.3 $m \cdot s^{-1}$ have low survival). Furthermore, longer transport times and warmer temperatures probably increase predation risk, as well as starvation risk, for larval walleye; in fact, the two risks may be directly coupled (Jonas and Wahl 1998). We view our model as implicitly incorporating the effect of predation on survival through the discharge, temperature, and travel distance effects. Our model is not designed to evaluate the effects of manipulating predation risk directly, except insofar as it is driven by variations in flow, temperature, or transport time.

Simulations

The survival of walleye from spawning to their arrival as larvae in nursery habitats depends on the effects of environmental factors (temperature, discharge) that are inherently unpredictable. To properly assess the potential recruitment of walleye larvae to nursery areas from upstream spawning habitats, it is necessary to account for this uncertainty. In our model, water temperature and discharge affect spawning, incubation, and larval transport to nursery areas. Temperature and discharge vary from year to year — our simulations need to account for the range of environmental conditions that different year classes might experience. In addition, we have modeled transport survival as a stochastic process (Fig. 3). For these reasons, we used a Monte Carlo approach

© 2003 NRC Canada

Table 3. Simulated first day (day of year) and duration (days) of egg deposition, fry emergence, and arrival at nursery habitats for walleye spawning in the existing spawning area below Ballville dam (river kilometre 27).

	Egg deposition		Emergence		Arrival at nursery	
Year	Start	Duration	Start	Duration	Start	Duration
1967	86	7	98	13	109	12
1969	78	21	98	17	107	17
1970	98	16	113	14	122	12
1971	91	13	106	15	115	17
1972	77	29	101	23	112	19
1973	66	47	88	43	105	33
1975	55	56	89	38	108	26
1976	59	30	82	27	94	23
1977	71	33	97	20	108	18
1978	91	12	106	19	119	16
1979	79	32	102	23	114	18
1980	80	32	106	21	117	13

Note: Estimates are presented for each year for which river temperature and discharge data were available.

Fig. 4. (*a*) Estimated area of good (solid bars), average (not visible), poor (lightly shaded bars), and unsuitable (darker shaded bars) spawning habitat for 3-km sections of the Sandusky River from river kilometre (rkm) 28 (below Ballville Dam) to rkm 61 (near Tiffin). (*b*) Estimated capacity for production of emerging walleye (*Stizostedion vitreum*) fry for the same sections of the Sandusky River.

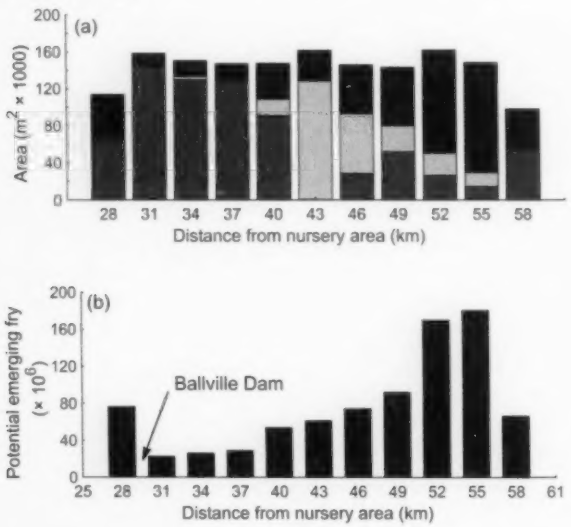

to our simulations and summarize the model results across a range of possible "realizations" of these stochastic processes.

To estimate the number of larvae that could potentially be produced from upstream spawning areas, we set the number of eggs deposited in each habitat unit at a level that would fully saturate the available spawning substrate given our egg carrying capacity estimates for each substrate type. In this way, we forecasted the potential of upstream spawning habitats without making any assumptions about the actual supply of spawning walleye that might utilize these habitats. We estimated the potential production of walleye larvae from each habitat unit, which depends only on habitat quantity and quality, and the potential recruitment of walleye larvae to the Sandusky Bay nursery area from each habitat unit, which also depends on environmental conditions during downstream transport. We forecasted larval recruitment to the nursery area for the environmental conditions observed in each of the years for which both discharge and temperature data were available (1967–1980, except 1968 and 1974). For each year, we repeated the simulations 100 times to average across uncertainty in transport survival (Fig. 3) and reported the mean survival or recruitment from the 100 simulations.

Observations of larval recruitment to the Sandusky Bay nursery area do not exist for the time period over which we have made our forecasts, so we cannot compare our predictions with commensurate observations. However, the Ohio Division of Wildlife conducted routine trawl surveys of age-0 walleye at 6–8 fixed stations along the southern shore of Lake Erie's western basin from 1969 to 1980 (R. Knight, Ohio Division of Wildlife, 306 E. Shoreline Dr., Sandusky, OH 44870, U.S.A., unpublished data). We compared our predictions of larval recruitment to Sandusky Bay from the existing spawning area, below the Ballville Dam, with the fall age-0 index for the corresponding years to see whether the environmental conditions included in our model could explain interannual variation in walleye year-class strength.

In addition to the results for the Sandusky River, we also generalized our findings by looking at the joint influence of habitat location (distance from nursery areas), temperature, and discharge on larval walleye survival to nursery habitat. We used the model described above for transport survival and predicted survival rates for temperatures ranging from 8 to 28 °C, river velocities ranging from 0.1 to 1.2 $m \cdot s^{-1}$, and transport distances ranging from 20 to 180 km.

Results

The simulated timing of egg deposition, larval emergence, and arrival at nursery habitats varied considerably among years (Table 3). Egg deposition was predicted to begin as early as 24 February (day 55) in 1975 and as late as 8 April

© 2003 NRC Canada

Fig. 5. Model predictions of the potential recruitment of walleye (*Stizostedion vitreum*) larvae to nursery areas from spawning habitats between river kilometre (rkm) 28 and rkm 61 in the Sandusky River for the 12 years for which temperature and discharge data were available.

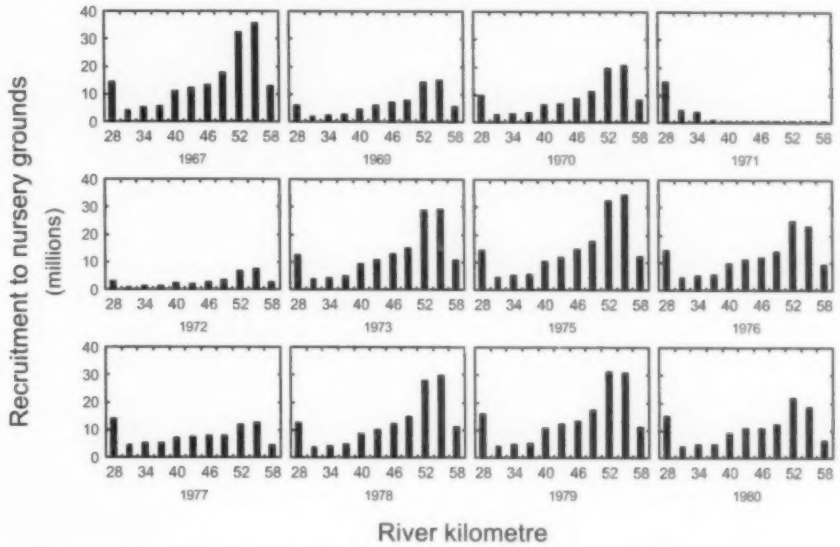

Table 4. Predicted potential recruitment of walleye (*Stizostedion vitreum*) larvae (millions) to nursery areas from spawning habitats below and above the existing dam at Ballville.

Year	Below dam	Above dam
1967	14.49	149.01
1969	5.96	66.64
1970	9.42	89.41
1971	14.71	10.90
1972	3.07	29.52
1973	12.59	128.60
1975	14.43	148.09
1976	14.37	118.25
1977	14.10	73.28
1978	12.37	126.86
1979	15.66	140.61
1980	15.19	101.99
Mean	12.20	98.60
Coefficient of variation	0.33	0.46

Fig. 6. Average river temperatures (●) and velocities (▽) during the simulated period of emergence of walleye (*Stizostedion vitreum*) fry in the Sandusky River for the 12 years for which temperature and discharge data were available. The large circle highlights the high average velocities experienced during the 3 years with generally low predicted recruitment. The vertical arrows indicate years in which a combination of low velocities and relatively high temperatures were observed; in these years, predicted recruitment was reduced from spawning habitats at relatively great distances from the nursery areas.

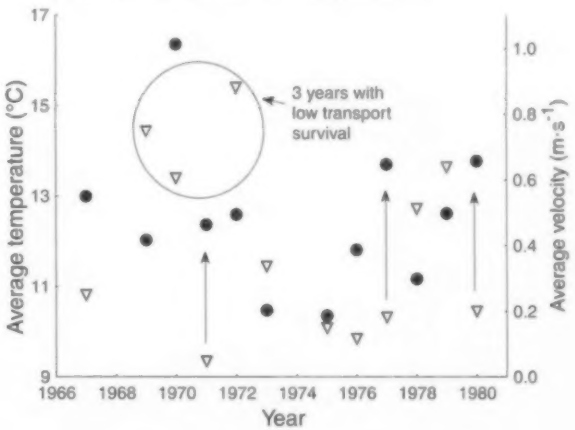

(day 98) in 1970, reflecting relatively warm or cool late winter conditions, respectively, in these two years. The duration of the spawning (deposition) and emergence periods also showed wide variation (7–56 days for deposition; 13–43 days for emergence), reflecting interannual variation in the rates of spring warming.

Spawning habitat quantity and quality varies considerably above the Ballville Dam (Fig. 4*a*). Bedrock predominates the substrate in the first 10 km above the dam (61–90% of total habitat from rkm 31 to rkm 40; Fig. 4*a*). Further upstream, the proportion of average and high quality habitat increases substantially (64–90% of total habitat from rkm 46 to rkm 55). Overall the estimated capacity of habitats above the existing dam to produce walleye fry (840 million) far exceeds the estimated capacity of the existing spawning area below the dam (76 million), with the greatest potential occurring between rkm 50 and rkm 57 (Fig. 4*b*).

Potential larval recruitment to the nursery area from upstream habitat units mirrors emerging fry production in some years but is quite different in others (Fig. 5). The magnitude

© 2003 NRC Canada

Fig. 7. A comparison of observed fall indices of age-0 walleye (*Stizostedion vitreum*) abundance for western Lake Erie with predicted larval recruitment to Sandusky Bay from the existing spawning grounds below Ballville Dam for the years 1969–1980, except 1974.

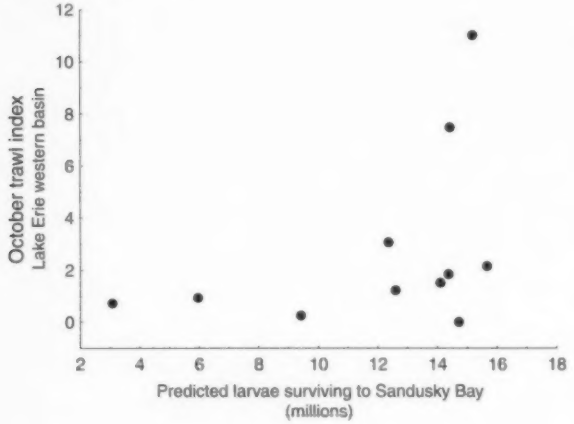

and spatial pattern of potential recruitment is very similar in five of 12 years (1967, 1973, 1975, 1978, and 1979). In three years (1969, 1970, and 1972), the spatial pattern is similar, but potential recruitment is generally lower (especially in 1972). In four years (1971, 1976, 1977, and 1980), the spatial pattern of potential recruitment also differs from that for emerging fry. This is particularly evident in 1971, when no successful recruitment was forecast to occur from spawning areas more than 40 km from the nursery area. In all years except 1971, potential larval recruitment from spawning areas above the Ballville Dam greatly exceeds that from the existing spawning area (Table 4). Averaged across all 12 years, potential recruitment was over eight times larger from currently inaccessible spawning habitats (Table 4), although the among-year variation was somewhat greater for the upstream areas (coefficient of variation is 46% above dam versus 33% below dam).

Contrasting environmental conditions during the emergence period explain the differences among years in the patterns of potential recruitment (Fig. 6). During two of the three years with generally lowered recruitment (1969, 1972), average river velocities were higher than in any other years. Velocities were above average in 1970, and this year experienced by far the highest average temperature (16.4 °C). Average velocities were relatively low in each of the four years in which potential recruitment was reduced more at greater distances from the nursery (four of the five lowest velocity years). As well, in each of these years, average temperatures were relatively high, in contrast to the other low velocity year, 1975, when temperatures remained low (10.4 °C) during the emergence and transport period.

Our predictions of larval recruitment to Sandusky Bay corresponded partially with the fall index of age-0 walleye abundance from western Lake Erie (Fig. 7). Walleye abundance in western Lake Erie was consistently low when the model predicted fewer than 10 million recruits. The two years with the highest observed abundance of age-0 walleye

Fig. 8. Isopleths of transport survival for walleye (*Stizostedion vitreum*) larvae plotted as a function of river velocity and river temperature for travel distances of (*a*) 40, (*b*) 80, (*c*) 120, and (*d*) 160 km from spawning to nursery habitats. Survival ranges between isopleths: B, 0.2–0.25; C, 0.15–0.2; D, 0.1–0.15; E, 0.05–0.1; F, <0.05. The large crosshair on each panel indicates the among-year mean ± 1 standard deviation of the average river temperatures and velocities experienced during the period of emergence for walleye on the Sandusky River.

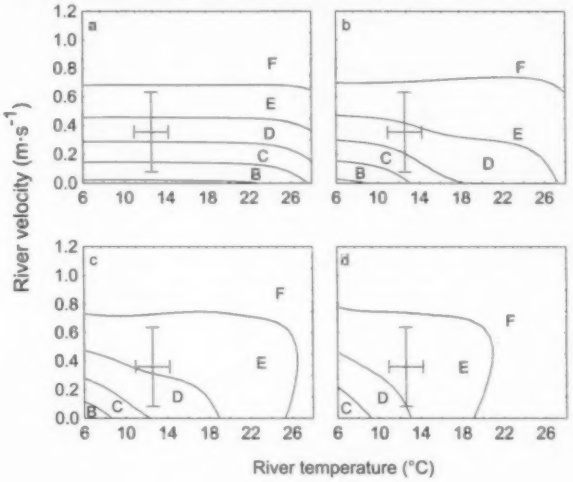

in the fall were years in which model predictions of recruitment were relatively high (>14 million recruits). On the other hand, predictions of strong recruitment to Sandusky Bay were not associated with high lake abundances of age-0 walleye in other years.

Our general model of transport survival indicates that river velocity has a greater influence than temperature on survival for transport distances of up to 80 km (Fig. 8). In general, as transport distance increases, temperature becomes a more important factor in determining survival for a wider range of river velocities. For distances greater than 80 km, survival declines rapidly with increasing temperature at velocities as high as 0.5 $m \cdot s^{-1}$. For the range of environmental conditions observed in our Sandusky River analysis, variation in stream flow was the primary factor affecting survival, particularly at the distances considered (<80 km). This may not be the case for other rivers in which walleye are able to spawn further upstream, where flows are more stable or water temperatures rise more rapidly in spring.

Discussion

Unusually warm river temperatures during late winter sometimes led to predicted spawning dates that were earlier than had been observed in Lake Erie walleye (e.g., 1975, 1976). This suggests that water temperature is not the only trigger of the onset of walleye spawning and that a model that also included photoperiod or time of year as a covariate might yield more accurate predictions. Our model forecasts of the timing of emergence overlapped with the observations of Mion et al. (1998), although the among-year variation that

© 2003 NRC Canada

we forecasted over 12 years is greater than that which they observed during 1993–1995. On average, we predicted that the emergence period would last 22 days, which is shorter than the 29 reported by Mion et al. (1998). Forney (1976; Oneida Lake, N.Y.) and Johnston et al. (1995; Valley River, Man.) observed shorter durations for the hatching and larval drift periods, respectively. The differences may reflect systematic differences among walleye populations but could also result from large among-year variation in environmental conditions, as our model suggests. In most years, the duration of the egg deposition period was longer than the period of emergence or arrival at the nursery grounds. Because water temperatures are normally rising during the egg incubation period, eggs deposited later in the spawning period will develop more rapidly than those deposited earlier. This leads to a compression of the emergence period relative to the spawning period.

Our Sandusky River simulations suggest that considerable potential exists to enhance recruitment of walleye by allowing access to upstream spawning sites. In all but one of the years that we considered, spawning at sites well upstream of the Ballville Dam resulted in successful recruitment to the nursery areas. In eight of 12 years, distance from nursery grounds had relatively little effect, and averaged across all 12 years, potential recruitment above the dam was estimated to be more than eight times as great as the estimate for the existing spawning area. Interannual variation in potential production increased further upstream, but not enough to suggest that the suitability of the upstream habitat for walleye spawning was much lower than for downstream sites. Nevertheless, the expected benefit of access to upstream spawning habitats is large on average, but the risk of poor recruitment in any given year increases with distance from the nursery grounds.

Western Lake Erie walleye stocks are thought to be a mixture of fish derived from spawning populations in the Sandusky and Maumee rivers and a lake-spawning stock. Little is known about the relative contribution of these three sources to the overall population. The partial association observed between our predictions of larval walleye recruitment to Sandusky Bay for 1969–1980 and the western basin fall index of age-0 walleye abundance could be interpreted as suggesting that good conditions for river survival of larval walleye are necessary, but not sufficient, for production of a strong year class in the lake. When conditions were poor for survival, fall age-0 abundance was consistently low. When conditions were good, fall age-0 abundance was high in two years, moderate in five years, and low in one year. Environmental conditions favoring good recruitment in the Maumee River are likely to correlate closely with those of the Sandusky River, given the geographical proximity of the two rivers and similar spawning locations relative to the river mouths. On the other hand, environmental conditions favoring high survival of lake-spawned walleye larvae may not be synchronous with ideal riverine conditions. We hypothesize that unusually high fall age-0 abundance occurs in years when environmental conditions coincidentally favor both lake- and river-spawning populations. Recent advances in walleye stock discrimination techniques (T. Johnson, Ontario Ministry of Natural Resources, R.R. 2, Wheatley, ON N0P 2P0, Canada, personal communication) may allow testing of this hypothesis by determining whether strong year classes are associated with substantial contributions from both spawning populations.

Our general model suggests that distance may pose a greater constraint to stock rehabilitation in river systems where walleye are able to spawn at greater distances from nursery grounds. Adult walleye are known to spawn in habitats greater than 50 km from nursery lakes in several systems (Priegel 1970 (Fox River, 64 km; Wolf River, 155 km); Schneider and Leach 1979 (Muskegon River, 63 km); Mrozinski et al. 1991 (Saginaw River, 110 km); Johnston et al. 1995 (Valley River, 20–70 km)). In numerous Great Lakes tributaries such as the Muskegon and Saginaw rivers in Michigan, removal of dams or placement of fish passage structures could provide access to potential spawning areas well in excess of 80 km from lacustrine nursery areas. The productive potential of these habitats will likely depend on the flow and temperature conditions in the river downstream of spawning areas. Where these data are available, the model presented here could be used to explore the potential of these systems as targets for fishery restoration.

In addition to walleye, many other fishes rely on Great Lakes tributaries for spawning and early rearing habitat. A recent survey of fish species known to occur in the Great Lakes region (Coon 1999) suggested that more than half of these species (92 of 171) exhibit some form of migratory behavior and might therefore be affected by barriers to fish movement (R.L. McLaughlin, Department of Zoology, University of Guelph, Guelph, ON N1G 2W1, Canada, unpublished data). It is difficult to assess the effects that barrier removal might have on many of these species because little is known about the importance and function of their movements. As for walleye, however, the potential benefit of dam removals will in part depend on the extent to which the dam currently operates as a barrier between important habitats that are close enough to each other to be of use to a single population.

Generally speaking, to assess the potential benefits of an action to restore fish habitat, it is important to answer three questions. First, how much new habitat is being created and what is its quality? Second, are the new habitats sufficiently close to habitats required by the species at later life stages to be useful for the population? Third, is the habitat being created actually limiting production of the species in question (Minns et al. 1996*b*)? Most habitat restoration proposals consider only the first question. In this analysis, we have considered the first two questions — answers to the third question call for a model of the entire life history of the species. We are currently developing a whole life cycle model for Lake Erie walleye similar to that presented by Minns et al. (1996*b*) for northern pike (*Esox lucius*).

The issue of habitat location has been raised in several general discussions of habitat–population linkages in riverine ecosystems (Scheimer et al. 1991; Grossman et al. 1995; Schlosser 1995) but has seen very limited application to specific problems. Kocik and Ferreri (1998) developed a model for juvenile salmonid production that explicitly considers the spatial relationship among habitat units, but their analysis was largely theoretical and was not applied to actual

© 2003 NRC Canada

salmonid-producing rivers. Marine ecologists have long recognized the importance of physical processes for transporting fish and invertebrate larvae into nursery areas (e.g., Norcross and Shaw 1984; Eggleston et al. 1998). In contrast, larval fish transport in rivers has received very little attention, and even where it has been considered (Mion et al. 1998), the effect of distance on survival was not. In at least some situations, ignoring the relative location of habitats could result in an overestimate of the potential contribution to production made by providing walleye access to upstream habitats for spawning.

There are several limitations of the simple model presented here that warrant further examination. First, allowing walleye access to upstream spawning areas does not necessarily mean that they will move beyond the current spawning location to spawn in upstream locations. Walleye that were released above the dam in 1998 produced migrating fry, but these fish were manually transported above the dam. Because walleye have a fairly high degree of fidelity to spawning grounds (Forney 1961; Crowe 1962; Spangler et al. 1977), walleye ascending the Sandusky River may stop at the current spawning site below the Ballville Dam. The tendency for walleye to migrate beyond currently used spawning habitat will likely increase as adult abundance increases but may depend on the degree to which existing habitat is perceived as overcrowded by the spawning population. Complete saturation of the potential spawning habitats above the Ballville Dam would require approximately 30 000 spawning female walleye, an estimate that is not implausible given recent estimated abundances of walleye (tens of millions of age-2+ fish) in Lake Erie.

A second, related limitation of this analysis is that there is no clear indication that the production of walleye in the Sandusky River, or in Lake Erie as a whole, is limited by the supply of spawning habitat. If other factors such as the supply of nursery habitat are limiting, increasing spawning habitat will have little effect on the recruitment of walleye to the lake, regardless of its location. Conversely, if the population is limited by spawning habitat, any increase in production from upstream sites would contribute to the growth of the Lake Erie population. Minns et al. (1996*b*) presented a modeling analysis suggesting that contrary to common assumptions, northern pike (*Esox lucius*) populations in Hamilton Harbour, Lake Ontario, were not limited by spawning habitat. Our whole life cycle modeling efforts are intended to provide insight on these questions.

A third limitation concerns our assumption that walleye larvae migrate downstream continuously after emerging from the spawning substrate. Direct observations of migrating walleye during daylight hours supports this assumption in the Sandusky and Maumee rivers (Mion et al. 1998). On the other hand, a propensity for reduced movement during daylight hours has been observed in other, less turbid rivers (Franzin and Harbicht 1992). When we repeated the simulations used to generate Fig. 8, but assuming that walleye larvae only move downstream at night, the survival isopleths are shifted to the left, especially for transport distances of 120 km or 180 km. This represents an increased mortality risk for upstream spawning habitats in rivers where walleye downstream movement is constrained by daytime predation risks. It suggests that the general model presented may overestimate the potential production from spawning habitats at large distances from nursery grounds in relatively clear streams. This effect will be countered, however, by a general tendency for stream gradients, and thus velocities, to increase at greater distances from the river mouth, which will tend to increase rates of downstream transport of larvae during those times when they are being transported. Further, it is often the low-gradient, slow-moving sections of rivers where turbidity is higher, whereas clearer water is often associated with higher-gradient, faster-moving upstream reaches.

Fourth, our assumption of complete mortality of all walleye that fail to reach the nursery grounds before accumulating 128 thermal units is clearly a simplification of the true state of nature. We view this assumption as a compromise between the likelihood that mortality risk increases as the cohort approaches 128 thermal units and that mortality risk does not increase to 100% as soon as 128 units are accumulated. The assumption seems reasonable, but the general survival patterns illustrated herein depend strongly on the temperature–starvation link; therefore, further field-based research on this linkage should be seen as a priority.

Finally, our analysis assumes that larval walleye need to reach the nursery area before they can start feeding. Mion et al. (1998) found that exogenous feeding by walleye larvae was limited during out-migration, likely due to low densities of zooplankton (typically <5 individuals·L^{-1}). However, in one year of that study, a protracted period of extremely low flow resulted in relatively high densities of zooplankton in the lower Sandusky River, which led to increased feeding, growth, and survival of larval walleye. This was an atypical condition, and given that larval walleye are particulate feeders (Mathias and Li 1982), it is reasonable to assume that their feeding success is minimal in the turbid flows typifying the period of out-migration. Hence, as noted by Priegel (1970), it is likely that timely transport of larvae to nursery areas is critical to successful recruitment of walleye in most river-spawning populations.

Acknowledgements

The research described in this paper was funded through a grant to the lead author from the Great Lakes Fishery Commission. Scudder Mackey and the Ohio Geological Survey generously provided the substrate data for the Sandusky River. Roger Knight, Ohio Division of Wildlife, provided the age-0 walleye trawl survey data for 1969–1980. The manuscript was improved by comments from two anonymous reviewers.

References

Baker, C.T. 1971. Walleye spawning area study in western Lake Erie. Ohio Department of Natural Resources, Federal Aid to Fish and Wildlife Restoration Project F-35-R-10. Ohio Department of Natural Resources, Columbus, Ohio.

Bednarek, A.T. 2001. Undamming rivers: a review of the ecological impacts of dam removal. Environ. Manag. **27**: 803–814.

Born, S.M., Genskow, K.D., Filbert, T.L., Hernandez-Mora, N., Keefer, M.L., and White, K.A. 1998. Socioeconomic and institutional dimensions of dam removals: the Wisconsin experience. Environ. Manag. **22**: 359–370.

Coon, T.G. 1999. Ichthyofauna of the Great Lakes basin. *In* Great Lakes fisheries policy and management: a binational perspec-

© 2003 NRC Canada

tive. *Edited by* W.W. Taylor and C.P. Ferreri. Michigan State University Press, East Lansing, Mich. pp. 55–71.

Corazza, L., and Nickum, J.G. 1981. Positive phototaxis during initial feeding stages of walleye larvae. Rapp. P.-V. Reun. Cons. Int. Explor. Mer, **178**: 492–494.

Corbett, B.W., and Powles, P.M. 1986. Spawning and larval drift of sympatric walleyes and white suckers in an Ontario stream. Trans. Am. Fish. Soc. **45**: 301–314.

Crowe, W.R. 1962. Homing behavior in walleyes. Trans. Am. Fish. Soc. **91**: 350–354.

Eckersley, M. 1986. Assessment of walleye spawning grounds in Hoople Creek, 1985. Report of the St. Lawrence River Subcommittee of the Lake Ontario Committee, Great Lakes Fishery Commission, Ann Arbor, Mich.

Eggleston, D.B., Armstrong, D.A., Elis, W.E., and Patton, W.S. 1998. Estuarine fronts as conduits for larval transport: hydrodynamics and spatial distribution of Dungeness crab postlarvae. Mar. Ecol. Progr. Ser. **164**: 73–82.

Eschmeyer, P.H. 1950. The life history of the walleye, *Stizostedion vitreum vitreum*, in Michigan. Bull. Inst. Fish. Res. (Michigan) No. 3, Ann Arbor, Mich.

Forney, J.L. 1961. Marking of walleyes and smallmouth bass: routine sampling of Oneida Lake fish populations. 1961. Federal Aid to Fish and Wildlife Restoration Project F-17-R-6, Job 2.

Forney, J.L. 1976. Year class formation in the walleye population of Oneida Lake, New York 1966–73. J. Fish. Res. Board Can. **33**: 783–792.

Franzin, W.G., and Harbicht, S.M. 1992. Tests of drift samplers for estimating abundance of recently hatched walleye larvae in small rivers. N. Am. J. Fish. Manag. **12**: 396–405.

Gibson, R.J., and Hughes, C.W. 1977. A walleye stream spawning study on Hamilton's Creek, 1969. Manitoba Department of Renewable Resources and Transportation Services, Research Branch, MS Rep. No. 77-31.

Gordon, N.D., McMahon, T.A., and Finlayson, B.L. 1992. Stream hydrology: an introduction for ecologists. John Wiley and Sons Ltd., Chichester, U.K.

Great Lakes Fishery Commission. 1987. Report of the Habitat Planning and Management Task Force and Habitat Advisory Board of the Great Lakes Fishery Commission. Great Lakes Fishery Commission, Spec. Publ. 87-15, Ann Arbor, Mich.

Great Lakes Fishery Commission. 2001. Strategic vision of the Great Lakes Fishery Commission for the first decade of the new millennium. Great Lakes Fishery Commission, Ann Arbor, Mich.

Grossman, G.D., Hill, J., and Petty, J.T. 1995. Observations on habitat structure, population regulation, and habitat use with respect to evolutionary significant units: a landscape perspective for lotic ecosystems. *In* Evolution and the aquatic ecosystem: defining unique units in population conservation. *Edited by* J. Nielsen. American Fisheries Society, Bethesda, Md. pp. 381–391.

Houde, E.D. 1969. Sustained swimming ability of larvae of walleye (*Stizostedion vitreum*) and yellow perch *(Perca flavecens*). J. Fish. Res. Board Can. **26**: 1647–1659.

Johnson, F.H. 1961. Walleye egg survival during incubation on several types of bottom in Lake Winnibigoshish, Minnesota, and connecting waters. Trans. Am. Fish. Soc. **90**: 312–322.

Johnston, T.A., Gaboury, M.N., Janusz, R.A., and Janusz, L.R. 1995. Larval fish drift in the Valley River, Manitoba: influence of abiotic and biotic factors, and relationships with future year-class strengths. Can. J. Fish. Aquat. Sci. **52**: 2423–2431.

Jonas, J.L., and Wahl, D.H. 1998. Relative importance of direct and indirect effects of starvation for young walleyes. Trans. Am. Fish. Soc. **127**: 192–205.

Jude, D.J. 1992. Evidence for natural reproduction by stocked walleyes in the Saginaw River tributary system. N. Am. J. Fish. Manag. **12**: 386–395.

Kanehl, P.D., Lyons, J., and Nelson, J.E. 1997. Changes in the habitat and fish community of the Milwaukee River, Wisconsin, following removal of the Woolen Mills Dam. N. Am. J. Fish. Manag. **17**: 387–400.

Kelso, J.R.M., Steedman, R.J., and Stoddart, S. 1996. Historical causes of change in Great Lakes fish stocks and the implications for ecosystem rehabilitation. Can. J. Fish. Aquat. Sci. **53**(Suppl. 1): 10–19.

Kocik, J.F., and Ferreri, P.C. 1998. Juvenile production variation in salmonids: population dynamics, habitat, and the role of spatial relationships. Can. J. Fish. Aquat. Sci. **55**(Suppl. 1): 191–200.

Kondolf, G.M., and Micheli, E.R. 1995. Evaluating stream restoration projects. Environ. Manag. **19**: 1–15.

Krise, W.F., and Meade, J.W. 1986. Review of the intensive culture of walleye fry. Progr. Fish Cult. **48**: 81–89.

Leach, J.H., and Nepszy, S.J. 1976. The fish communities of Lake Erie. J. Fish. Res. Board Can. **33**: 622–638.

Ligon, F.K., Dietrich, W.E., and Trush, W.J. 1995. Downstream ecological effects of dams. Bioscience, **45**: 183–192.

Mathias, J.A., and Li, S. 1982. Feeding habits of walleye larvae and juveniles: comparative laboratory and field studies. Trans. Am. Fish. Soc. **111**: 722–735.

Minns, C.K., Kelso, J.R.M., and Randall, R.G. 1996*a*. Detecting the response of fish to habitat alterations in freshwater ecosystems. Can. J. Fish. Aquat. Sci. **53**(Suppl. 1): 403–414.

Minns, C.K., Randall, R.G., Moore, J.E., and Cairns, V.W. 1996*b*. A model simulating the impact of habitat supply limits on northern pike, *Esox lucius*, in Hamilton Harbour, Lake Ontario. Can. J. Fish. Aquat. Sci. **53**(Suppl. 1): 20–34.

Mion, J.B., Stein, R.A., and Marschall, E.A. 1998. River discharge drives survival of larval walleye. Ecol. Appl. **8**: 88–103.

Mrozinski, L.E., Schneider, J.C., Haas, R.C., and Shepherd, R.E. 1991. Rehabilitation of walleye in Saginaw Bay, Lake Huron. *In* Status of walleye in the Great Lakes: case studies prepared for the 1989 workshop. *Edited by* P.J. Colby, C.A. Lewis, and R.L. Eshenroder. Great Lakes Fishery Commission, Spec. Publ. 91-1, Ann Arbor, Mich. pp. 63–84.

Newburg, H. 1975. Evaluation of an improved walleye (*Stizostedion vitreum*) spawning shoal with criteria for design and placement. Job completion report. Federal Aid in Fish Restoration Project F-26-R. Minnesota Department of Natural Resources, St. Paul, Minn.

Norcross, B.L., and Shaw, R.F. 1984. Oceanic and estuarine transport of fish eggs and larvae: a review. Trans. Am. Fish. Soc. **113**: 153–165.

Plott, J.R. 2000. Sandusky River walleye upstream expansion. Final performance report, Federal Aid in Sport Fish Restoration Project F-69-P5, Fish management in Ohio. Ohio Department of Natural Resources, Division of Wildlife, Columbus, Ohio.

Priegel, G.R. 1970. Reproduction and early life history of the walleye in the Lake Winnebago region. Wisconsin Department of Natural Resources, Tech. Bull. 45, Madison, Wis.

Scheimer, F., Spindler, T., Wintersberger, H., Schneider, A., and Chovanec, A. 1991. Fish fry associations: important indicators for the ecological status of large rivers. Verh. Int. Ver. Limnol. **24**: 2497–2500.

Schlosser, I.J. 1995. Critical landscape attributes that influence fish population dynamics in headwater streams. Hydrobiologia, **303**: 71–81.

Schneider, J.C., and Leach, J.H. 1979. Walleye stocks in the Great Lakes, 1800–1975: fluctuations and possible causes. Great Lakes Fishery Commission, Tech. Rep. 31, Ann Arbor, Mich.

© 2003 NRC Canada

Shuman, J.R. 1995. Environmental considerations for assessing dam removal alternatives for river restoration. Regul. Rivers Res. Manag. **11**: 249–261.

Smith, L.L., Koenst, W.M., and Hokanson, K.E.H. 1975. Temperature effects on eggs and fry of percoid fishes. U.S. E.P.A., National Environmental Research Center, Corvallis, Oreg.

Spangler, G.R., Payne, N.R., and Winterton, G.K. 1977. Percids in the Canadian waters of Lake Huron. J. Fish. Res. Board Can. **34**: 1839–1848.

Thompson, D.M. 2002. Long-term effect of instream habitat-improvement structures on channel morphology along the Blackledge and Salmon Rivers, Connecticut, U.S.A. Environ. Manag. **29**: 250–265.

Ward, J.V., and Stanford, J.A. 1995. Ecological connectivity in alluvial river ecosystems and its disuption by flow regulation. Regul. Rivers Res. Manag. **11**: 105–119.

Wolfert, D.R., Busch, W.-D.N., and Baker, C.T. 1975. Predation by fish on walleye eggs on a spawning reef in western Lake Erie, 1969–71. Ohio J. Sci. **75**: 118–125.

© 2003 NRC Canada

A two-dimensional geostatistic method to simulate the precision of abundance estimates

Alf Harbitz and Michaela Aschan

Abstract: In this paper, we outline a geostatistic method to simulate the relative precision (coefficient of variation, CV) of total abundance estimates of one species in a predetermined, stratified area when it is appropriate to treat the observations within each stratum as realizations of a second-order homogenous and ergodic random process. To model the spatial correlations, a variogram is fitted to normal-transformed values of the original observations. Based on the variogram and its corresponding covariance matrix, extensive simulations on a fine grid that includes the sample locations provide random realizations of the process. The normal values are back-transformed to original observation space by nonparametric reversed bootstrap, as well as by a parametric Weibull approach. The method is applied to a total of 1069 shrimp (*Pandalus borealis*) abundance observations from 11 annual surveys in the Barents Sea (1992–2002) where a 20 nautical mile sampling grid has been applied. On average, the CV was estimated to be 6.4% for the applied regular grid when the simulations were conditional on the observations, compared with 8.1% when the sampling locations within each of the six strata were random.

Résumé : On trouvera ici la description d'une méthode géostatistique pour simuler la précision relative (coefficient de variation, CV) des estimations d'abondance totale d'une espèce dans une aire prédéterminée et stratifiée, lorsqu'il est approprié de traiter les observations dans chacune des strates comme les résultats d'un processus aléatoire de second degré homogène et ergodique. Afin de modéliser les corrélations spatiales, nous ajustons un variogramme aux valeurs normalisées des observations originales. Des simulations répétées, basées sur le variogramme et sa matrice de covariance correspondante et faites sur une grille fine qui comprend les stations d'échantillonnage, fournissent des résultats aléatoires du processus. Les valeurs normalisées sont retransformées dans l'espace original d'observation au moyen d'un bootstrap non paramétrique inversé, ainsi qu'au moyen d'une approche paramétrique de Weibull. La méthode est utilisée sur un total de 1069 observations d'abondance de crevettes (*Pandalus borealis*) provenant de 11 inventaires dans la mer de Barents (1992–2002) qui emploient une grille d'échantillonnage de 20 milles marins. En moyenne, le CV est estimé à 6,4 % pour la grille utilisée lorsque les simulations sont dépendantes des observations, alors qu'il est de 8,1 % lorsque les sites d'échantillonnage dans chacune des six strates sont aléatoires.

[Traduit par la Rédaction]

Introduction

In classical sampling theory, random sampling locations are often advocated in order to get design-unbiased estimates of abundance (Cochran 1977). In these cases, the population of all possible sample outcomes in terms of abundance observations is considered fixed, while the randomness is included in the sampling design. In the so-called model approach (Thompson 1992; Thompson and Seber 1996) applied in this paper, the opposite is true. Using this approach, sampling sites are fixed and the sample outcomes are stochastic. If the sampled abundance observations can be considered a random sample from the population distribution of all possible sample outcomes, then an unbiased abundance estimate can be provided with respect to the population distribution.

There is no general rule saying that one of the above approaches is superior to the other. The random sampling approach is the most robust one in the sense that there is no need to model either the population distribution of possible abundance observations or spatial correlations. Another advantage is that the minimum sailing distance tends to be shorter than for regular sampling (Beardwood et al. 1959; Christofides and Eilon 1969). It is also clear that the model approach must assume some kind of randomness in the spatial distribution of the abundance to provide unbiased abundance estimates. On the other hand, when spatial correlations between observations are present and the spatial structure can be appropriately modelled, more precise abundance estimates may be obtained with a regular sampling design than by random location sampling (Cochran 1977; Rivoirard et al. 2000). Another argument in favour of regular sampling is that the tidy

Received 13 March 2002. Accepted 19 October 2003. Published on the NRC Research Press Web site at http://cjfas.nrc.ca on 22 December 2003.
J16806

A. Harbitz[1] **and M. Aschan.** Institute of Marine Research, Havforskningsinstituttet, Sykehusvegen 23, PB 9404, 9294 Tromsø, Norway.

[1]Corresponding author (e-mail: alf.harbitz@imr.no).

 doi: 10.1139/F03-134 © 2003 NRC Canada

handling of the samples could be very complicated with succeeding stations close to each other (Harbitz et al. 1998).

In this paper, the abundance observations during a survey are considered as realizations of a second-order homogenous random process, which is in accordance with the intrinsic hypothesis in geostatistics (Rivoirard et al. 2000). This means that a possible spatial correlation between two observations is dependent on the distance between their locations only. This is a situation that is realistic for many surveys but is especially true in the open sea (Harbitz and Lindstrøm 2001). The term "homogenous process" was deliberately chosen over the more traditional term "stationary process". This is partly because the focus is on the spatial properties of the process and partly because the process is a spatial–temporal process where different terms in space and time are useful. The term "stationary" is, in our opinion, a more natural term to use with respect to time.

Even if a regular grid under the homogeneity assumption provides classical unbiased abundance estimators, it is more difficult to obtain unbiased variance estimators due to the possible spatial correlations between the samples. To examine if such correlations exist and to take this into account in the variance, geostatistics has proven to be an appropriate tool. During the last decade, there has been an increased focus on spatial statistics within marine resource abundance estimation (Petitgas 1993; Rivoirard et al. 2000).

In this paper, a general two-dimensional simulation method is outlined that provides good estimates of abundance estimator precision, taking the spatial correlation appropriately into account. A major feature of this approach is that there is no need to establish a good model for the spatial correlations in original observation space. It is sufficient to have a good model in normal-transformed space, which in practice is much easier to obtain.

Though many of the different elements of the method are not new, the composition and focus differ from earlier work (e.g., Petitgas 1993; Kern and Coyle 2000). As an example, the method includes a nonparametric approach in which the empirical abundance distribution can be used in the back-transformation from normal space to abundance space (reversed bootstrap; Harbitz and Lindstrøm 2001). In addition, it is straightforward to implement irregular contours that enclose the study area.

An important element of the method is that it accounts for the fact that the expected sampling variance in cases in which density observations are positively correlated will be smaller than the variance in the process distribution that generates random realizations of the process. This difference is due to a finite study area and is important when the correlation length, i.e., the distance between two observations beyond which the spatial correlation disappears, is not negligible compared with the extension of the area.

The method can, in principle, be applied to any sampling design and so is useful for comparing different sampling designs. A major goal of the present study is to offer an easily applied and useful supplement to the geostatistic tool kit for estimating the precision of abundance estimates.

Materials and methods

Notations are given in Appendix A and a detailed chart of the simulation procedure is given in Appendix B.

The Barents Sea shrimp data

The Barents Sea is delineated by the coastline of northern Norway and Russia in the south, by Bear Island and Spitzbergen towards the west, and by Novaja Zemlja and Frans Josef Land at the east and the north (Fig. 1). It is a relatively shallow shelf sea with a mean depth of 230 m, covering approximately 1.4 million km^2. The Atlantic water from the south and the colder, less saline Arctic water from the north meet in the Polar Front. During winter, the Arctic water is covered with ice, but most of the Barents Sea is ice-free during summer (Loeng 1991). The shrimp stock is distributed throughout the area at depths deeper than 150 m. Norway has conducted annual shrimp surveys in the Barents Sea in April–May since 1982. The study area is divided into six strata (A–F) and covers approximately 50 000 nautical miles^2 (n.mi.^{2}) (Fig. 1). A Campelen 1800 survey trawl was towed at 3 knots for 20 min, resulting in a tow distance of 1 n.mi. Since 1992, a 20 n.mi. regular grid has been used to locate trawl stations (Fig. 1), and data from 1992–2002 are used in this study. The actual trawl stations in 1992 (shown as solid circles in Fig. 1) are close to the idealized nodes in the grid. In 1996, a 10 n.mi. sampling grid was used in the area where shrimp were most abundant (stratum E) to study the abundance variation on a finer scale than 20 n.mi. Stratum E had the greatest abundance of shrimp (*Pandalus borealis*), but it was also the stratum with the most difficulties caused by ice (Fig. 2). The location of the fine 2 n.mi. simulation grid nodes applied in this stratum are shown as dots, along with the actual sampling sites (solid circles) in 1996 approximated to the nearest 2 n.mi. grid node. For the other strata, a 4 n.mi. simulation grid was chosen.

A total of 1069 trawl stations with distinct sampling locations for each survey are included in the analyses of the coefficient of variation. In addition, in several surveys the same locations have been repeatedly trawled within a few hours. These observations provided a total of 115 different within-survey observation pairs. Aschan and Sunnanå (1997) gave a detailed description of the surveys.

The abundance and its estimator

Let b denote density, e.g., in tonnes·n.mi.$^{-2}$. Density, $b = b(\mathbf{x},t)$, is generally a function of time, t, and horizontal location in space, $\mathbf{x} = (x, y)$. For simplicity, the vertical component is omitted here. The abundance (biomass or number) to be estimated, B, is then

$$(1) \qquad B(t) = \mu(t)A = \int_{\Omega} b(\mathbf{x})\mathrm{d}(\mathbf{x})$$

where A is the area of the predetermined region Ω of interest. Further, μ is the average density and $\mathrm{d}\mathbf{x} = \mathrm{d}x\mathrm{d}y$. For simplicity, only one stratum is considered initially; the extension to m nonoverlapping strata will be discussed later. It is assumed that B is varying slowly in time on a time scale corresponding to the duration Δt of a survey. Because the area is assumed to be known, estimation of B is synonymous with estimation of μ.

Let $\mathbf{b}_s = (b_1, \ldots, b_n)$ denote a density sample vector consisting of n density observations at the location $\mathbf{x}_s = (\mathbf{x}_{s1}, \ldots, \mathbf{x}_{sn})$, where subscript "s" is used as an abbreviation for sample observation. The classical abundance estimator, $\hat{B}$, for the abundance is now

© 2003 NRC Canada

Fig. 1. The location of the Barents Sea shrimp (*Pandalus borealis*) study area, along with its six main strata A–E. Idealized regular 20 nautical miles (n.mi.) sampling grid nodes are indicated by plus signs (+), and the actual sampling sites in 1992 are indicated by solid circles (●).

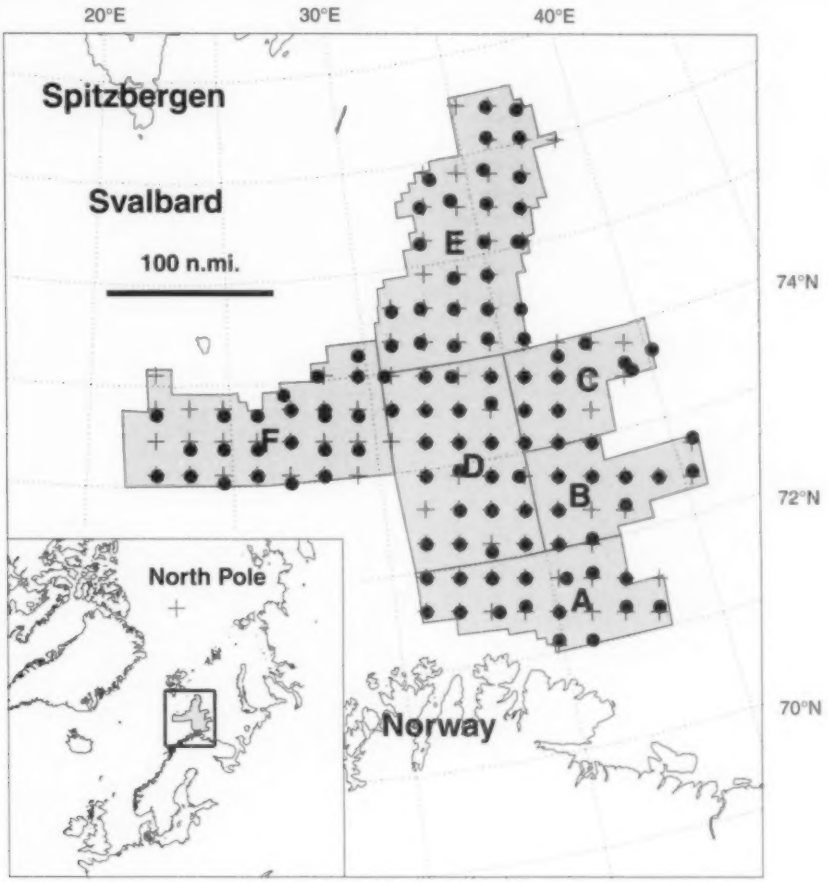

$$\hat{B} = \frac{1}{q}\left(\frac{1}{n}\sum_{j=1}^{n} b_j\right)A = \bar{b}A/q \qquad (2)$$

where a bar over a variable denotes arithmetic average and q is catchability. For simplicity, q is assumed to be constant; then q disappears from the CV expressions to follow and will from now on be set equal to one. In a fixed-population approach, the estimator above is unbiased under a randomized design, e.g., when the n observation locations are chosen randomly. Under the intrinsic geostatistic hypothesis, which is the approach used in this paper, the estimator is unbiased under any sampling design that is not dependent on the observation variable, e.g., a regular sampling grid (Petitgas 1993). The term unbiased, as used in this intrinsic geostatistic context, implies that $E(\hat{\mu}\,|\mu) = \mu$ (conditional unbiasedness), where $\hat{\mu} = \bar{b}$ and the expectation is taken with regard to the distribution of all possible realizations of the process providing μ and $\hat{\mu}$.

If all b_js are uncorrelated, the following estimator, $\hat{\sigma}^2_{\hat{B}}$, will be an unbiased variance estimator for $\sigma^2_{\hat{B}} = \mathrm{var}(\hat{B})$, independent of population distribution:

$$\hat{\sigma}^2_{\hat{B}} = S^2A^2/n \qquad (3)$$

where $S^2 = (1/(n-1))\sum_{j=1}^{n}(b_j - \bar{b})^2$ is the sample variance, which in this case is an unbiased estimator for $\sigma^2 = \mathrm{var}(b_j)$. A reasonable (though in general biased) estimator $\hat{\mathrm{CV}}_0$ for the coefficient of variation $\mathrm{CV}_0 = \sigma_{\hat{B}}/B$ is in this case

$$\hat{\mathrm{CV}}_0 = \frac{\sqrt{\hat{\sigma}^2_{\hat{B}}}}{\hat{B}} \qquad (4)$$

If spatial correlations between observations are present, the variance estimator in eq. 3 is biased (unless the sample locations are random). A key focus in this paper is to provide a CV estimator with negligible bias that takes such spatial correlations into account, assuming that it is reasonable to treat the set of possible density samples in a survey as a realization of a second-order homogenous random process. The geostatistic variogram is applied as the structural tool, and the corresponding covariance is applied for simulations of random realizations of the process.

© 2003 NRC Canada

Fig. 2. The most abundant shrimp area, Hopen area (stratum E), with the fine 2 nautical mile simulation grid nodes indicated by dots. The actual sampling sites in 1996 approximated to the nearest simulation grid nodes are indicated by solid circles (●).

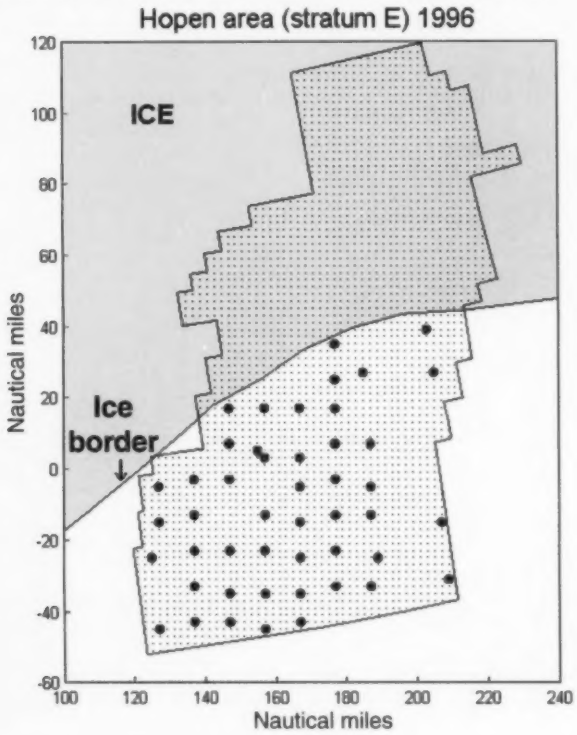

Variogram and covariance

The realization $\mathbf{b}_s = (b_1, \ldots, b_n)$ of n density observations at a particular time, t, is considered a realization of a second-order homogenous random process, b, with properties

$$(5) \quad Eb(\mathbf{x} + \mathbf{h}) = Eb(\mathbf{x})$$

$$\operatorname{cov}(b(\mathbf{x}), b(\mathbf{x} + \mathbf{h})) = \mathbf{C}_b(\mathbf{h})$$

The expectation and the covariance are with respect to all possible realizations of the process, and $\mathbf{C}_b$ denotes the covariance matrix of the process.

To get the necessary link between statistics of different realizations and the statistics in space for a given realisation (where we have data), we assume that the process is ergodic (Cressie 1993). In other words, averaging over realizations (ensemble average) at any given location in space is equivalent to averaging in space over an infinite area for any realization.

The sample and process distributions

However, because the study area is limited, the statistics of the sampled densities within the area for a given realization will differ from the infinite situation. To distinguish the finite and infinite cases, the terms sample and process (population) distributions will be distinguished. The sample distribution is the empirical distribution of the real density observations, or a fitted parametric distribution. The process distribution is the distribution of a single density observation drawn randomly at any location from the distribution of possible process realizations and is the appropriate one to be used in the density simulations (to which we return later). Because of the assumption of ergodicity, the process distribution is synonymous with the sample distribution of an infinite number of observations evenly spread over an infinite area.

The sample distribution will depend on the sampling design and will tend to be less dispersed (possess a smaller variance) than the process distribution resulting from a finite study area (Fig. 3). For a fixed area, the similarities between the two distributions will increase with a decreasing range (correlation length) and an increasing number of evenly distributed sampling locations. An important feature of the simulation method is the ability to account for the difference between the sample and process distributions with regard to the variance.

Variogram, covariance, and normal transformation

The variogram in observation space, $\gamma_b(\mathbf{h})$, and its correspondence with the covariance matrix, $\mathbf{C}_b(\mathbf{h})$, are

$$(6) \quad \gamma_b(\mathbf{h}) = \tfrac{1}{2}\operatorname{var}(b(\mathbf{x} + \mathbf{h}) - b(\mathbf{x})) = \mathbf{C}_b(\mathbf{0}) - \mathbf{C}_b(\mathbf{h})$$

where the latter equality follows from the homogeneity assumptions given by eq. 5 and $\mathbf{C}_b(\mathbf{0})$ equals the variance in the process distribution. For convenience, only isotropic variograms will be considered; in which case, the variogram becomes a one-dimensional function of the lag, $h = |\mathbf{h}|$.

There exist several theoretical models for the variogram (Rivoirard et al. 2000). To be considered, the candidate model must be consistent with a positive definite covariance matrix, $\mathbf{C}_b$. Before a model is chosen, an empirical variogram should be examined. Because of the generally skewed population distributions of abundance observations, it is recommended (Petitgas 1993) that the observations be normalized before the empirical variogram is calculated. This is partly to examine if a structure exists and, if so, to stabilize the variogram. Nonparametrically, the Φ transformation can be applied, transforming the original observations $b_1, \ldots, b_n$ to quantiles $z_1, \ldots, z_n$ in the standard normal $N(0,1)$ distribution based on the ranks of the original observations (Petitgas 1993):

$$(7) \quad z_j = k\Phi^{-1}(\operatorname{rank}(b_j)/(n + 1)), \quad j = 1, \ldots, n$$

where k is a correction factor (close to one) to obtain a sample variance of the z values equal to one and independent of n. The corresponding normalized variogram is denoted $\gamma_z(h)$, and the corresponding covariance matrix is $\mathbf{C}_z(h) = 1 - \gamma_z(h)$.

A widely used variogram model made of a nugget effect and a spherical function was chosen to fit the empirical shrimp variograms:

$$(8) \quad \gamma_Z(h) = \begin{cases} \mathrm{NU} + (\mathrm{SI} - \mathrm{NU})(1.5(h/r) - 0.5(h/r)^3), & 0 \le h \le r \\ \mathrm{SI}, & h > r \end{cases}$$

© 2003 NRC Canada

Fig. 3. Illustration of the difference between the process distribution and the less dispersed sampling distribution in a realization of a one-dimensional (1D), 2nd-order homogenous and ergodic random process with NU = 0.4 and r = 75. The broken line illustrates a more extensive part of the "infinite" process realization than the solid line, which is limited by the sampling domain.

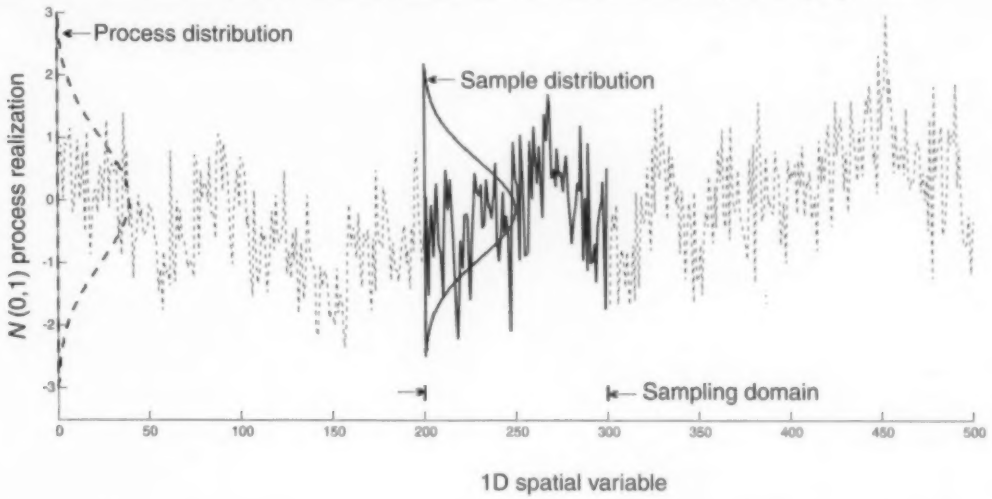

The three parameters are NU (expressing the nugget effect), SI = $\mathbf{C}_z(0)$ (the asymptotic value of the variogram (the sill)), and r, the range beyond which the spatial correlation disappears. The critical parameter is NU, which expresses the variance contribution due to random (nonstructural) variation as well as local spatial variations on a much finer spatial scale than what is possible or practical to detect at the sampling scale.

To get a first visual impression of the empirical variogram $\hat{\gamma}_Z(h)$, this is often done by averaging within equidistant distance bins:

(9)
$$\hat{\gamma}_Z(h) = \frac{1}{2n_h}\sum_{j,k}(z_j - z_k)^2, \qquad h_{jk} \in \left[h - \frac{dh}{2}, h + \frac{dh}{2}\right],$$
$$h = dh, 2dh, \ldots, n_{\text{lag}}dh$$

where the lag resolution, dh, may correspond to the average distance between two adjacent observations. The sum is over all n_h pairs of observations with distance h_{jk} within the interval given by the brackets, and h is divided into equidistant steps $dh, 2dh, \ldots, n_{\text{lag}}dh$. The shape of the empirical variogram is an important first validation check of the homogeneity assumption, where the absence of an apparent horizontal asymptote (possibly superimposed by cyclic oscillations) is an indication of nonhomogenous conditions.

Note that there is generally no trivial correspondence between the variogram γ_z in normal-transformed space and the variogram γ_b in original observation space, though transformation formulas exist for special cases (Rivoirard et al. 2000). Even if the same model applies in both cases (e.g., the nugget + spherical model), the NU-to-SI ratio (NU:SI) will, in general, differ. A great advantage of the simulation approach is that a good variogram model in normal-transformed space is sufficient, precluding the need to know the variogram in original observation space.

Estimation of variogram parameters for a regular sampling grid

For a regular sampling grid, there are a limited finite number of distinct h values with rather many observations at many of the discrete hs. By using this, the need for smoothing in eq. 9 is avoided, and a better basis is obtained for the estimation of the variogram parameters. Let h_d, γ_d and n_d denote the lag, the variogram, and the number of observations with a distance h_d apart, respectively, by this discrete approach, where $d = 1, \ldots, n_d$, and n_d denotes the number of discrete lags. The parameters NU, SI, and r can be estimated by minimizing a sum of (weighted) squares of terms that reflect the differences between the theoretical and empirical variograms at each lag. The following sum appeared to give better results for the shrimp data than the more common sums given in the theory chapter in Rivoirard et al. (2000):

(10) $$Q = \sum_{d=1}^{n_r} \ln^2(\hat{\gamma}_d(h_d)/\gamma_d(h_d))n_d$$

where $\hat{\gamma}_d$ is calculated analogous to eq. 9, and n_r is equal to the number of distinct h_d values less than or equal to r, or a slightly larger value based on a rough estimate of r from the variogram provided by eq. 9. The reason for this restriction on n_r is that NU is considered to be the most important parameter, and its estimator should not be influenced by variogram values at lags beyond the range r. The rational for using the logarithm of the variogram values is that the coefficient of variation of $(z(\mathbf{x} + \mathbf{h}) - z(\mathbf{x}))^2$ at each lag $h_d = |\mathbf{h}|$ is constant, thus each term in the sum is expected to have approximately the same variance if the variogram model is appropriate.

Studying the summation terms before they are squared as a function of h_d is considered a fair model validation check, where independence, homoscedasticity (constant variance), and absence of trends are model-supporting properties. Note, however, that many of the variables contributing to each

© 2003 NRC Canada

term in the sum are dependent, which complicates the challenge of finding an optimal construction of the square sum to be minimized. The properties (accuracy, precision, and covariation) of the estimators determined by this approach can be assessed by Monte Carlo simulation as described later.

An important validation technique (Chilès and Delfiner 1999) is to analyze scatterplots for the pairs of z values at locations providing the same lag, h. These should be elliptically shaped with a correlation coefficient similar to the covariance, $\mathbf{C}_z(h)$, in normal-transformed space calculated from the variogram model and in accordance with a binormal distribution.

The expectation of the sample variance equals the mean of the empirical variogram values for positive lags, i.e., $ES^2 = \overline{\gamma}_+$. Thus for evenly distributed sampling locations (regular or random) and a small range compared with the extension of the area, the estimated SI should be close to one under the assumptions made.

Monte Carlo simulation

The simulation procedures are first outlined for one area and for nonconditional simulations, i.e., simulations that are not dependent on the actual density observations at the sampling sites. To distinguish nonconditional from conditional simulations introduced later, the subscripts "nc" and "c" will be used, respectively. At the end of the section, how to treat a study area consisting of m adjacent strata is outlined.

The simulation grid and random N*(0,1) realizations*

A variogram model consistent with an isotropic and homogenous process of second order is synonymous with a one-to-one correspondence between the covariance of normalized variables at two different locations and the variogram

$$(11)\quad c_{jk} = \mathrm{cov}(z_j, z_k) = \begin{cases} 1 - \gamma_Z(h_{jk}), & j \neq k \\ 1, & j = k \end{cases}$$

where $h_{jk} = |\mathbf{x}_j - \mathbf{x}_k|$ denotes the distance between the locations $\mathbf{x}_j$ and $\mathbf{x}_k$.

Now define a fine, regular simulation grid, with N grid nodes at $\mathbf{x}_g = (\mathbf{x}_{g1}, \ldots, \mathbf{x}_{gN})$ located so that a minimum distance between the sampling sites and the nearest nodes in the simulation grid is obtained. These approximate sampling locations will be denoted sampling nodes. The resolution in the simulation grid (distance between adjacent nodes) should be so fine that a negligible difference between the true density μ and the average of the N densities at the grid nodes is obtained.

Let $\mathbf{C}(\mathbf{x}_g,\mathbf{x}_g) = \{c_{jk}\}$ denote the $N \times N$ grid covariance matrix found by using eq. 11 with $h_{jk} = |\mathbf{x}_{gj} - \mathbf{x}_{gk}|$, and let $\mathbf{D}$ denote a decomposition of $\mathbf{C}(\mathbf{x}_g,\mathbf{x}_g)$ so that $\mathbf{DD}^T = \mathbf{C}(\mathbf{x}_g,\mathbf{x}_g)$. A random realization vector of normalized densities at all nodes, $\mathbf{z}_{nc}(\mathbf{z}_g)$, with the appropriate spatial correlation structure can then be generated as follows:

$$(12)\quad \mathbf{z}_{nc}(\mathbf{x}_g) = \mathbf{D}\mathbf{z}_{iid},\ \mathbf{DD}^T = \mathbf{C}(\mathbf{x}_g,\mathbf{x}_g)$$

where superscript "T" denotes transpose, and $\mathbf{z}_{iid}$ is a $N \times 1$ vector of independent $N(0,1)$ variables. The simulation by eq. 12 is repeated n_{sim} times to obtain a sufficient number of random realizations. For the variogram in eq. 8, it is convenient to split the simulations into one structural part and one white-noise part as follows:

$$(13)\quad \mathbf{z}_{nc}(\mathbf{x}_g) = (1 - \mathrm{NU})^{1/2}\mathbf{D}_0\mathbf{z}_{iid,1} + (\mathrm{NU})^{1/2}\mathbf{z}_{iid,2}$$

where $\mathbf{D}_0\mathbf{D}_0^T = \mathbf{C}_0 = \mathbf{C}(\mathbf{x}_g,\mathbf{x}_g;\ \mathrm{NU} = 0,\ \mathrm{SI} = 1)$ and $\mathbf{z}_{iid,1}$ and $\mathbf{z}_{iid,2}$ are independent $N \times 1$ vectors of independent $N(0,1)$ variables. If, for example, different nugget values are to be used, $\mathbf{D}_0$ is the only decomposed matrix needed.

There are several candidates for $\mathbf{D}$, where a very fast numerical solution is to define $\mathbf{D}$ as a Cholesky decomposition of $\mathbf{C}$ (Ripley 1987). Note, however, that if the Cholesky factorization creates an upper-triangular matrix $\mathbf{D}$, not a lower-triangular matrix as defined by Ripley (1987), $\mathbf{D}$ in eq. 12 should be replaced by $\mathbf{D}^T$. This is the case in Matlab (The Mathworks, Inc., Natick, Mass.), the computer program used to provide the results in this paper. Another important precaution that should be considered with regard to a Cholesky decomposition is that a variety of numerical inaccuracies might occur if $\mathbf{D}$ is large, e.g., greater than 1000 × 1000 (Cressie 1993). An easy way to check this is to calculate $\mathbf{DD}^T$ after the decomposition and see if each element deviates from the corresponding element in the original $\mathbf{C}$ within the accuracy of the computer. In the Barents Sea application (returned to later), $\mathbf{D}$ is a 5035 × 5035 Cholesky decomposition matrix, and no numerical problems occurred. Other more robust (and slower) decomposition techniques are described by Chilès and Delfiner (1999, p. 465).

Conditional simulation

Conditional simulation in a geostatistic context is synonymous with simulations of random realizations of a process with the constraint that the simulations are conditional on the observed values at the sample locations (Cressie 1993; Chilès and Delfiner 1999). This is an appealing feature, because it intuitively takes peculiarities of the realization providing the observations into account better than nonconditional simulation. Mathematically, the multinormal distribution of $\mathbf{z}_g$, conditional on the normal-transformed observations $\mathbf{z}_s$, is the basis for the conditional simulations. This distribution, $f(\mathbf{x}_g|\mathbf{x}_s)$, was outlined based on standard multivariate calculations (Mardia et al. 1992), modelling the process as the sum of a pure spatial structure component and a white-noise (nugget) component. As a result, the following expressions were found for the conditional expectation $E(\mathbf{z}_g|\mathbf{z}_s)$ and covariance matrix $\mathbf{C}_c = E(\mathbf{z}_g\mathbf{z}_g^T|\mathbf{x}_s)$, where subscript c denotes conditional:

$$(14)\quad E(\mathbf{z}_g|\mathbf{z}_s) = (1 - \mathrm{NU})\mathbf{C}_0(\mathbf{x}_g,\mathbf{x}_s)\mathbf{C}(\mathbf{x}_s,\mathbf{x}_s)^{-1}\mathbf{z}_s$$

$$\mathbf{C}_c = E(\mathbf{z}_g\mathbf{z}_g^T|\mathbf{z}_s) = \mathbf{C}(\mathbf{x}_g,\mathbf{x}_g) - (1 - \mathrm{NU})^2 \times \mathbf{C}_0(\mathbf{x}_g,\mathbf{x}_s)\mathbf{C}(\mathbf{x}_s,\mathbf{x}_s)^{-1}\mathbf{C}_0(\mathbf{x}_s,\mathbf{x}_g)$$

Subscript 0 in the expressions above denotes, as before, that the actual matrix is calculated with NU = 0 and SI = 1. Note that the dimensions of the matrices above are given by the subscript on the xs. As an example, $\mathbf{C}_0(\mathbf{x}_g,\mathbf{x}_s)$ is an $N \times n$ matrix where the elements are calculated as follows:

$$(15)\quad \mathbf{C}_0(\mathbf{x}_g,\mathbf{x}_s) = \{\mathrm{cov}_0(|\mathbf{x}_{gj} - \mathbf{x}_{sk}|)\},\quad j = 1,\ldots,N,\ k = 1,\ldots,n$$

© 2003 NRC Canada

where cov_0 denotes the covariance with NU = 0 and SI = 1.

Based on eq. 14, the following procedure can be used to generate random realizations of the process conditional on observations, $\mathbf{z}_c(\mathbf{x}_g) = z(\mathbf{x}_g|\mathbf{z}_s)$:

$$\mathbf{z}_c(\mathbf{x}_g) = (1 - \mathrm{NU})\mathbf{C}_0(\mathbf{x}_g,\mathbf{x}_s)\mathbf{C}(\mathbf{x}_s,\mathbf{x}_s)^{-1}\mathbf{z}_s + \mathbf{D}_c\mathbf{z}_{iid} \quad (16)$$

where $\mathbf{D}_c$ is a decomposition of $\mathbf{C}_c$ (e.g., Cholesky), i.e., $\mathbf{C}_c = \mathbf{D}_c\mathbf{D}_c^T$, and $\mathbf{z}_{iid}$ is a $N \times 1$ vector of iid $N(0,1)$ variables.

Parameter uncertainties

Based on the random realizations by using eq. 12 or eq. 13, the properties of variogram parameter estimators such as the least squares estimators defined by minimizing the square sum in eq. 10 can be estimated. In these simulations, the parameter estimates based on normal-transformed real data are used as true values except that SI is set equal to one, which is the appropriate value in the process distribution. Then the covariance matrix to be used in the simulations is established with elements defined by eq. 11. Note, however, that now only the n sampling nodes are used.

For each random realization at the sampling nodes, new estimates of the involved variogram parameters are estimated. The properties of the estimators are then assessed based on the simulated estimates. To obtain reasonable estimates of bias and variance, about 1000 simulations are sufficient for most practical situations. If the absolute value of the bias is considerably less than the standard deviation, the bias is normally considered to be negligible.

Backtransformation from N(0,1) to biomass densities and estimation of scaling factor between standard deviations in sampling and process distributions

The simulated normal variates at the sampling nodes can also be used to simulate the scaling factor needed to take account of the different dispersions in the process and sampling distributions. This can be done either based on the empirical sampling distribution, which is called reversed bootstrap (Harbitz et al. 2001), or by use of a fitted parametric distribution. First the cumulative $N(0,1)$ value Φ is calculated for each generated $N(0,1)$ value z. If a parametric cumulative sampling distribution, F, is applied, each z value is then back-transformed to a density b by the equation $b = F^{-1}(\Phi(z))$, where F^{-1} denotes the inverse cumulative distribution function. In the reversed bootstrap case, the Φ values are first made discrete by the formula $R = \mathrm{int}(\Phi n) + 1$, where "int" rounds Φn to the nearest integer towards zero. The assigned observation value is then the observed density with rank equal to R. The rational for the bootstrap term in this context is that the empirical population distribution is used to mimic the true population distribution, which is a basis for bootstrap.

The sample distribution is now treated as the true process distribution, and the distribution of the back-transformed densities from the $N(0,1)$ realizations are treated as simulated sample distributions. This is analogous to the change of roles between an unknown parameter and its estimate from data when simulations are performed to examine the properties of the estimator. Because of the finite area effect, the average standard deviation, S_{MC}, of the simulated sample distributions should be less than the standard deviation, S, in the empirical sample distribution. In the CV expressions to follow, the lack of dispersion by applying the sample distribution to mimic the process distribution is taken into account by using S/S_{MC} as a scaling factor.

Estimation of precision

Let the true abundance density, μ, with estimator, $\hat{\mu}$, at the time of sampling correspond to one realization of the process. The challenge is to find an appropriate estimator for the CV of $\hat{\mu}$. Based on the previously described procedures, n_{sim} random realizations in $N(0,1)$ space are generated with one value in each simulation grid node. For each realization, the normal values are back-transformed to density values parametrically or nonparametrically as described before. The average based on simulations in each of the fine grid nodes, $\bar{b}_g$, is treated as the true density of that particular realization. The simulated density estimate is the average, $\bar{b}_s$, of the simulated values at the sampling nodes. An appropriate estimator for $\mathrm{CV}(\hat{\mu})$ is then obtained as follows:

$$\hat{\mathrm{CV}} = (S/S_{MC})\,\hat{\mathrm{std}}(\bar{b}_s/\bar{b}_g) \quad (17)$$

where $\hat{\mathrm{std}}$ is the standard deviation of the n_{sim} simulated values of the ratio within the parentheses. The estimator above applies to conditional as well as to nonconditional simulations, though the correction factor (S/S_{MC}) may vary somewhat between the two alternatives.

If the study area consists of m adjacent strata and we neglect the effect of spatial correlation between strata, the CV estimator corresponding to eq. 17 becomes

$$\hat{\mathrm{CV}}_m = \frac{\sqrt{\sum_{i=1}^{m} \bar{b}_{si}^2 \mathrm{CV}_i^2 A_i^2}}{\sum_{i=1}^{m} \bar{b}_{si} A_i} \quad (18)$$

where A_i is the area of stratum i, $\bar{b}_{si}$ is the mean of observed densities in stratum i, and CV_i is calculated for each stratum separately by applying eq. 17.

A considerable improvement of the method can be obtained if the standardized density obtained by dividing each individual density observation with the stratum expectation value follows a common distribution and the standardized variogram γ_z is independent of stratum, or even better, independent of survey (time) as well. The CV estimator in eq. 18 can then be expressed as follows:

$$\hat{\mathrm{CV}}_m = \hat{\mathrm{std}}\left(\sum_{i=1}^{m} \bar{b}_{si} A_i \Big/ \sum_{i=1}^{m} \bar{b}_{gi} A_i\right)(S/S_{MC}) \quad (19)$$

where a common correction factor (S/S_{MC}) is calculated for the entire study area, and the terms $\bar{b}_{si}$ and $\bar{b}_{gi}$ are the simulated estimates and true densities in stratum i. In this case, within-stratum spatial correlations might be taken into account, and far more observation pairs will be available for the empirical variogram. This is demonstrated in the shrimp case study to follow.

© 2003 NRC Canada

Results

Sample population model

A rather linear relationship independent of year and stratum was found between the logarithmic value of the strata means, $\ln(\bar{b}_i)$, and the strata sampling standard deviations, $\ln(S_i)$, with a slope β close to one (Fig. 4). In addition, a smooth shape of the relative frequency distribution of the 1069 standardized density values (observed density divided by empirical stratum mean) appeared where a fitted Weibull distribution gave a good fit (Fig. 5). A standard χ^2 test based on the fitted distribution (the bins from $z = 3.2$ to $z = 5$ were lumped together) resulted in an estimated significance value (p value) of $\hat{P}_W = 0.45$. In the further simulations, the Weibull distribution was therefore applied as a parametric sample distribution, along with the empirical standardized distribution when applying reversed bootstrap, as common sample distributions of standardized densities for all strata and years.

Normalized variogram

The normalized empirical variograms were based on the normal-transformed values of the standardized densities year by year, treating the entire study area as one stratum. No apparent anisotropy was seen from the directional variograms. Isotropic annual variograms were calculated applying eq. 9 with a lag resolution (dh) of 20 n.mi. At the first lag, all distances between 0 and 30 n.mi. were included, 0 exclusive. All variograms appeared to have the same concave shape with a horizontal asymptote (Fig. 6, thin lines), and their average was calculated by using weights proportional to the number of observation pairs for each year at each lag (Fig. 6, ●). In addition, the variogram parameters were estimated by applying a modified version of eq. 10, accumulating 5 × 5 succeeding discrete lags to obtain a sufficient number of pairs at each lag (Fig. 6, ○). Each sample location was approximated to the nearest simulation grid node. The results were $\hat{r}$ = 77.4 n.mi., NU = 0.406, and SI = 1.07, and the resulting variogram is shown by the broken line in Fig. 6. Based on 5000 simulations and eq. 10, the corresponding empirical standard deviations were 4.5 n.mi., 0.063, and 0.032, respectively, and considerably smaller bias estimates. For mathematical convenience, the values r = 75 n.mi and NU = 0.4 were used in the simulations of random realizations of the process, which were close to the bias corrected estimates 0.39 n.mi., and 75.1 n.mi., respectively. Further, SI = 1 was used for the sill parameter, which is the appropriate value in $N(0,1)$ space.

The summation terms (before squaring) in the weighted least square sum defined by eq. 10 appeared to be rather independent, with a constant variance independent of lag (Fig. 7) and no apparent trends. A scatter plot of the normal-transformed observations with sampling nodes 20 n.mi. apart showed no apparent deviation from a binormal distribution, with a correlation coefficient given by the model (Fig. 8). Applying the latter (ρ = 0.37), a 95% ellipse was constructed, and the number of observations outside the ellipse did not deviate significantly (5% test level) from the binormal hypothesis. The independent empirical estimate of the nugget parameter based on the normal-transformed values of the standardized 115 observation pairs with $h = 0$ was 0.37, i.e., rather close to the nugget estimate when the observations at lag $h = 0$ were excluded. Thus several model-supporting features were seen from the data.

Fig. 4. Empirical stratum means vs. stratum standard deviations on a log–log scale. The fitted curve has slope equal to one, which is equivalent to a proportional relationship.

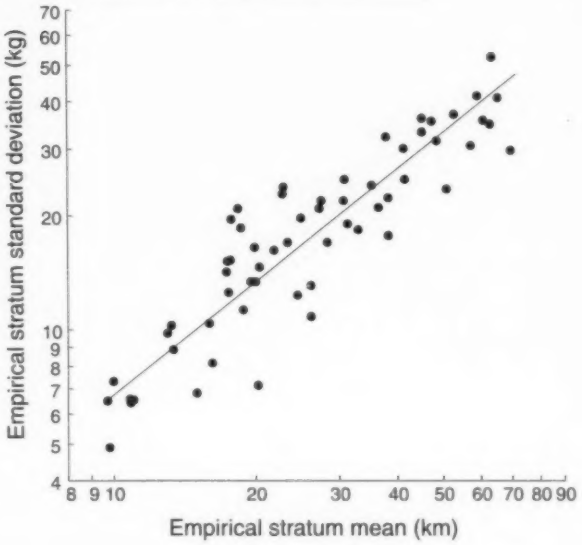

Correction factor S/S_{MC}

The correction factor S/S_{MC} based on 5000 nonconditional simulations was 1.089 when applying the Weibull distribution fit and 1.083 when applying reversed bootstrap. These close values were seen as a support to both approaches. For the conditional simulations, a slightly smaller correction factor S/S_{MC} = 1.074 was found based on reversed bootstrap.

Note that the factors do not contain the finite area effect alone, but also the finite sample size effect resulting from the use of empirical means instead of unknown expectation values in the establishment of the standardized empirical sample distribution. To separate the finite sample size effect, simulations were conducted with NU = 1 (no spatial structure), because in this case, the finite area effect disappears. The result was a scaling factor S/S_{MC} = 1.035, with a negligible difference between conditional and nonconditional simulations.

Abundance precision

A 5035 × 5035 covariance matrix $\mathbf{C}(\mathbf{x}_g,\mathbf{x}_g)$ for the process in normal-transformed space was calculated based on all of the 5035 4 and 2 n.mi. nodes in the simulation grid and the previously established variogram. The nonconditional random normal $N(0,1)$ realizations for the entire study area at each grid node were generated applying eq. 12, and the conditional simulations were generated by use of eq. 16. These were transformed to standardized biomass densities by applying the empirical distribution of standardized densities as well as the Weibull fitted distribution and then were multiplied by the empirical strata means. The simulated CV was calculated by applying eq. 17. The Cholesky decomposition

© 2003 NRC Canada

Fig. 5. Empirical sample distribution of 1069 biomass values from 1992–2002 divided by their empirical stratum mean at the year at which they were sampled, with fitted Weibull distribution.

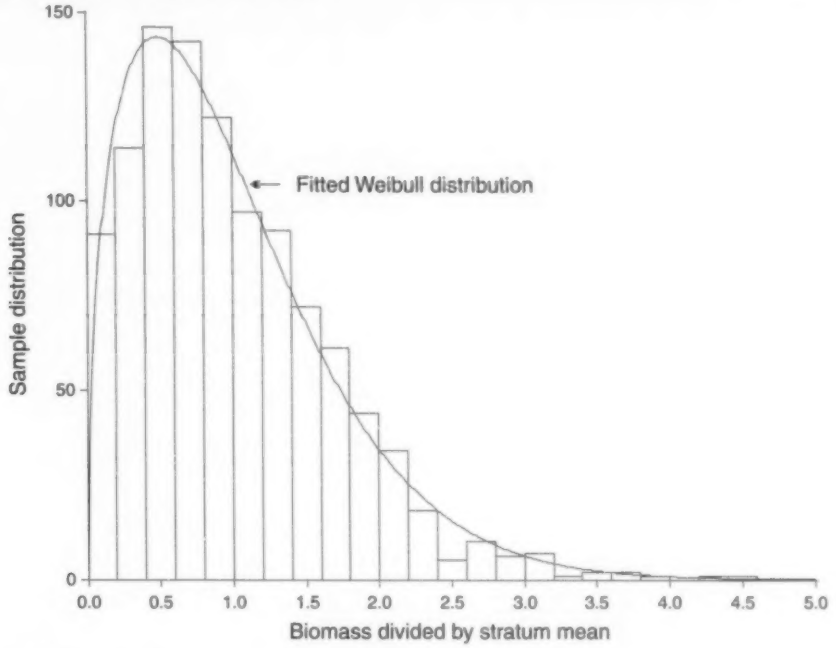

Fig. 6. Shrimp (*Pandalus borealis*) variograms based on Φ-transformed, standardized biomass values. Thin lines illustrate annual empirical variograms for each of 11 years (20 nautical mile (n.mi.) resolution), and solid circles (●) indicate average over years. Smaller, open circles (○) indicate more discrete empirical estimates, accumulating 5 × 5 succeeding distinct lags. The dotted line illustrates the fitted theoretical variogram with estimated parameters.

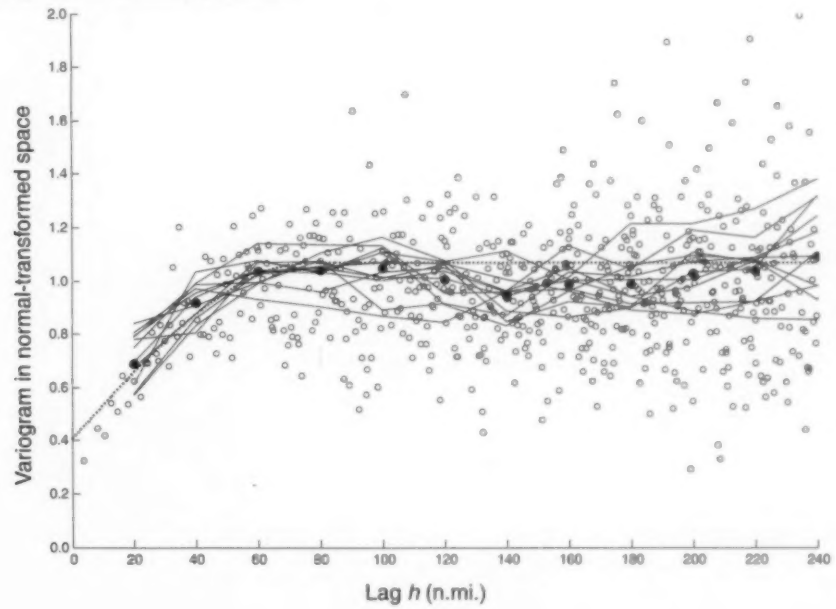

of $\mathbf{C}(\mathbf{x}_g,\mathbf{x}_g)$ with Matlab 5.3 took 36 s of CPU time on a PC with 2.2 GHz processor and 768 Mb RAM, with similar computing times required for the other analyses.

Based on 5000 reversed bootstrap simulations, the average CV value over years was 6.4%, based on regular sampling and conditional simulations (Table 1). For nonconditional

© 2003 NRC Canada

Fig. 7. (*a*) Summation terms $\ln(\hat{\gamma}_Z/\gamma_Z)n_d$ minimizing weighted square sum used to define estimates for NU, SI, and r, see eq. 10, as a function of lag, h_d. (*b*) Random normal plot of independent normal variables with mean and variance equal to series in (*a*). Nautical mile, n.mi.

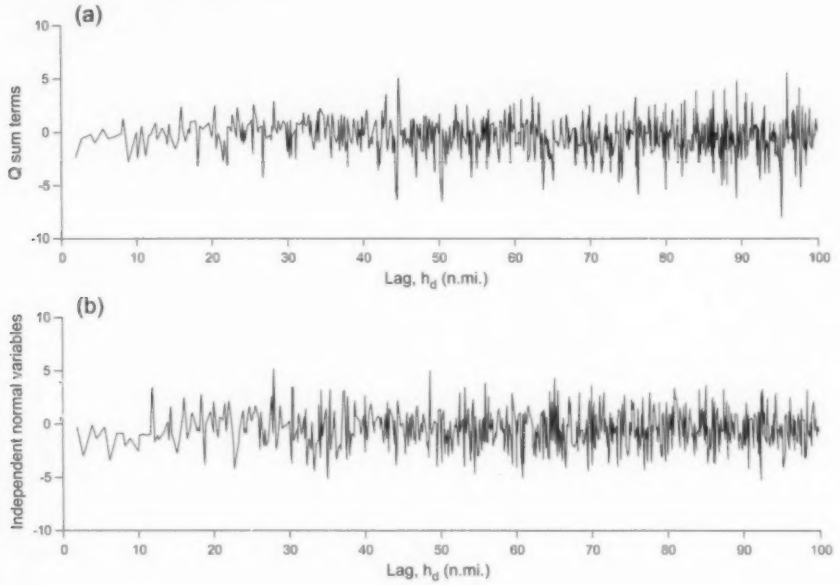

simulations, the corresponding average was 7.4% for the reversed bootstrap simulations and 7.2% for the Weibull simulations. The same marginal difference between the reversed bootstrap and Weibull approaches was seen for nonconditional simulations and random sampling, i.e., with random locations within each stratum (average CV = 8.2% and 8.0%, respectively). These results indicate that an appropriate CV estimator is found by the conditional simulation approach and that the regular design in this case is substantially better than the random design. On average, the conditional CV estimator is also considerably smaller than the wrongly calculated CV based on data alone and neglecting spatial correlations. An exception is 1996 when a rather dramatic increase in CV is seen (CV = 7.8%), whereas a rather small CV is calculated assuming uncorrelated data (CV = 6.0%). This clearly indicates the need to take spatial correlations into account in this case.

The CV was also simulated for different values of NU (n_{sim} = 2000, r = 75 n.mi.) based on perfect regular sampling by applying the 118 idealized sampling grid nodes instead of real locations and with strata means proportional to the average strata means over years ($\mu = 10k$, $15k$, $20k$, $10k$, $30k$, and $15k$ for strata A, B, C, D, E, and F, respectively, with k an arbitrary scaling constant). For NU = 0.4, the CV based on random locations was 30% larger than that based on regular sampling, i.e., comparable to the relative difference between random and regular results from the Barents Sea data. The CV dependence on NU for the idealized regular case appeared to be rather linear, with a CV value of 3.1% for NU = 0 (Fig. 9), i.e., about half of the CV obtained with random sampling. Again a negligible difference is seen between the Weibull simulations and reversed bootstrap, also regarding the CV for random sampling. More interestingly, a negligible difference between conditional (Fig. 9, heavy broken line) and nonconditional simulations is seen as well. For random locations, we also see that the results based on only the sample nodes (Fig. 9, ● and +) are similar, but more stable, than the results obtained by use of all simulation grid nodes (Fig. 9, solid and dotted lines).

Fig. 8. Scatter plot of normal-transformed values of densities with sampling node locations 20 nautical miles (n.mi.) apart. The dotted line indicates model-based 95% ellipse.

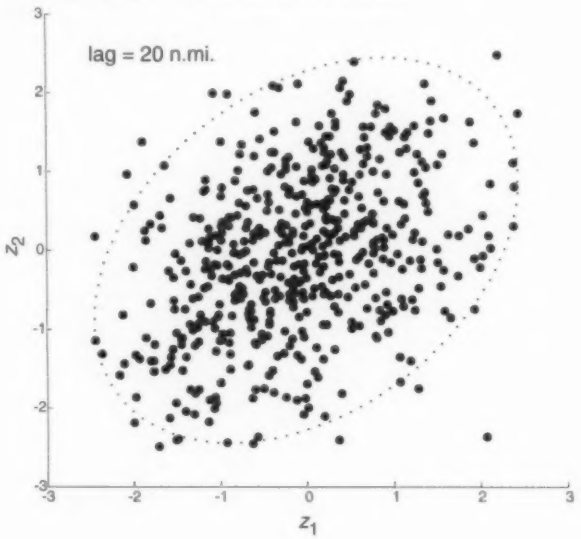

© 2003 NRC Canada

Table 1. Comparison of coefficient of variation (CV) values for the Barents Sea data by parametric (Weibull) and nonparametric (bootstrap) approach, conditional and nonconditional simulations, and by the actual sampling sites (approximately regular grid) and random sample locations.

	CV, regular sampling, nonconditional simulation (%)		CV, random sampling, nonconditional simulation (%)		CV, regular sampling, conditional simulation (%)	CV, spatial correlation neglected (%)
Year	Weibull	Bootstrap	Weibull	Bootstrap	Bootstrap	Data only
1992	5.7	5.9	7.1	7.1	5.3	5.6
1993	6.8	7.0	8.0	8.0	6.4	6.2
1994	6.8	6.8	8.1	8.5	6.3	8.6
1995	6.1	6.5	7.8	8.2	5.9	9.4
1996	10.6	10.6	9.9	9.8	7.8	6.0
1997	7.3	7.4	8.1	8.6	6.7	9.3
1998	8.4	8.5	8.0	8.1	7.7	8.0
1999	6.0	6.4	8.0	8.2	5.9	8.2
2000	6.3	6.3	7.5	8.1	5.9	7.2
2001	6.8	7.3	8.4	8.6	6.4	6.2
2002	7.9	8.3	7.3	7.5	6.3	7.9
Average	7.2	7.4	8.0	8.2	6.4	7.5

Note: The far-right column contains CV results when spatial correlation is neglected.

Fig. 9. Simulated abundance (%) coefficient of variation (CV; 2000 simulations) for different values of NU in the normalized variogram and with r = 75 nautical miles. Heavy broken line illustrates results based on conditional simulations, the others are based on nonconditional simulations. Lower curves are based on regular sampling with sampling locations at the 118 idealized 20 nautical mile sampling grid nodes. Upper curves are based on 118 random sampling locations with the same number of values within each stratum as for regular sampling. Solid lines are based on reversed bootstrap; dotted lines are based on Weibull fit. Solid circles (●; reversed bootstrap) and plus signs (+; Weibull fit) indicate random location results based only on sampling nodes.

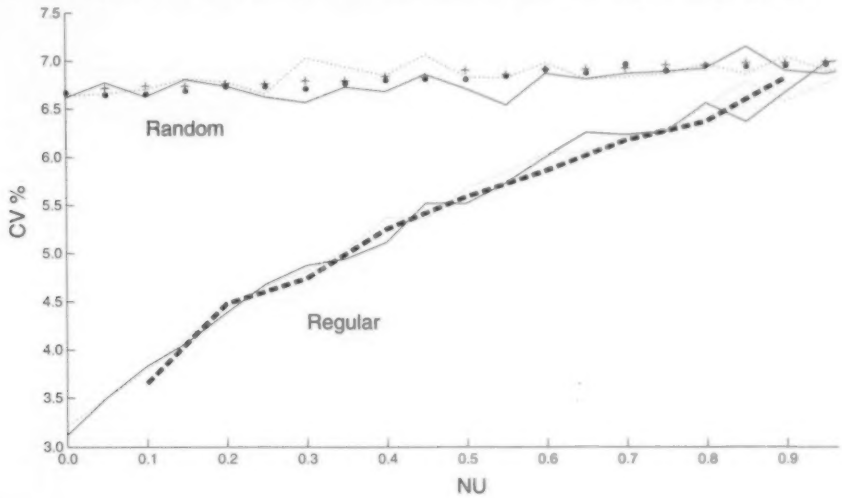

Discussion

The dramatic difference in CV between conditional and nonconditional simulations for 1996 is explained by the ice coverage in the stratum where shrimp were most abundant, preventing evenly distributed samples over the area. The extension of the sampled subarea was about the same as the extension of the noncovered subarea and comparable to the correlation length, r. Using nonconditional simulations, we expect several realizations with substantially larger abundance in the sampled subarea than in the noncovered subarea, and vice versa, which will increase the simulated CV. By conditional simulations, however, the abundance difference between the two subareas will remain more constant, as a consequence of the constraint that the simulations are conditional on the actual observations of density.

A large difference in CV between conditional and nonconditional simulations was also seen for the 2002 data. In this case, some clusters of very close sampling points (2 n.mi. grid) were chosen to study spatial correlations at a fine scale. One of these clusters consisted of nine points in a square in the most abundant stratum (Fig. 1, stratum E). Using nonconditional simulations, sometimes the mean density in a cluster will be considerably larger than the true stra-

© 2003 NRC Canada

tum average, and sometimes considerably smaller. This will increase the simulated CV. However, using conditional simulations, the difference between the cluster average and the true stratum average will remain more constant.

The CV differences between conditional and non-conditional simulation for the regular design clearly illustrate that the CV is sensitive to deviations from an idealized grid, because no apparent difference is seen in the latter case. This also provides a plausible explanation for why the change in CV among methods (regular vs. random) does not correspond well over time. The general change in CV between years is also due to annual variations in sample size and the relative importance (i.e., abundance of shrimp) of each stratum.

As expected, the CV results for random locations can be estimated by using the sampling nodes alone, ignoring the other grid nodes, as verified by the simulations. In this case, the CV can be simply estimated from data without simulations, ignoring possible spatial correlations. Similar results would come from data in a sufficiently ideal regular grid. Thus data from a regular grid can be used to estimate the CV that would be obtained by random locations, independent of a spatial structure or not, without the need for simulations. In practice, however, an idealized sampling design will often not be used, and in these cases, simulations are useful for "almost random" situations.

The assumption of a second-order homogenous process is crucial for this method to be appropriate. An objection to the homogeneity assumption in the shrimp case study is related to border effects. The irregular border of the study area is closely related to the depth contours, because the shrimp abundance is negligible in shallow areas. It is therefore natural to question if the spatial structure will be different close to the border contrary to the centre of the area. No such behaviour is apparent at first glance, probably because of slowly changing depths. The effect of the border enclosing the study area is a task for further studies.

The assumption of having homogenous conditions within each stratum with different average densities in the different strata is obviously a simplification, because this implicitly assumes a very steep gradient at the strata borders. In practice, density will vary more smoothly between strata, equivalent to the presence of local trends. These trends may influence the concave shape of the variogram at small lags. To examine this, a "nonergodic" covariance and corresponding variogram can be constructed (Isaaks and Srivastava 1988) consisting of the covariance of the "head" and "tail" observation for each observation pair at each lag. A preliminary analysis applied to the shrimp data using the northernmost location as the head location and the southernmost location as the tail location revealed that the concave shape of the variogram was modified only slightly.

The term "process distribution" was introduced as a term for the distribution of densities to be used in the simulations of random process realizations. Applying an appropriate scaling (variance adjustment) of the sampling distribution of densities provided a reasonable estimate of the process distribution. This idea could be extended to also take into account properties other than the variance, which can vary from the process to the sampling distribution. If, for example, the Weibull distribution appears to give a good fit to the sampling distribution, as well as to the simulated sampling distribution provided by applying the sampling distribution as process distribution, then the Weibull parameters in the latter can be adjusted. In this manner, not only the variance difference, but also the difference in shape between the process and sampling distributions, can be taken into account. To examine if such an approach is reasonable, an extensive and hierarchical simulation scheme could be applied, in some analogy to double bootstrap or calibration (Efron and Tibshirani 1993; Davison and Hinkley 1997).

Acknowledgements

Petter Abrahamsen at the Norwegian Computing Centre in Oslo, Professor Nils Lid Hjort at the University of Oslo, and Professor Henning Omre at the Technical University of Norway in Trondheim provided great help with clarifying discussions and encouraging comments. Peter Corceron at the Institute of Marine Research helped improve the clarity of the writing. The referees also contributed substantially to the improvement of the paper. This research was directly connected to the shrimp assessment financed by the Norwegian Fisheries Department. We thank the scientific staff and crews of R/V *Jan Mayen* for assistance with fieldwork over many years.

References

Aschan, M., and Sunnanå, K. 1997. Evaluation of the Norwegian Shrimp Surveys conducted in the Barents Sea and the Svalbard area 1980–1997. ICES CM 1997/Y:07.

Beardwood, J., Halton, J.H., and Hammersley, J.M. 1959. The shortest path through many points. Proc. Cambridge Philos. Soc. **55**: 299–327.

Chilès, J.P., and Delfiner, P. 1999. Geostatistics. Modeling spatial uncertainty. John Wiley & Sons, Inc., New York.

Christofides, N., and Eilon, S. 1969. Expected distances in distribution problems. Operations Res. Quart. **20**(4): 437–443.

Cochran, W.G. 1977. Sampling techniques. 3rd ed. John Wiley & Sons, Inc., New York.

Cressie, N.A.C. 1993. Statistics for spatial data. John Wiley & Sons, Inc., New York.

Davison, A.C., and Hinkley, D.V. 1997. Bootstrap methods and their application. Cambridge University Press, Cambridge.

Efron, B., and Tibshirani, R.J. 1993. An introduction to the bootstrap. Chapman & Hall, London.

Harbitz, A., and Lindstrøm, U. 2001. Stochastic spatial analysis of marine resources with application to minke whales (*Balaenoptera acutorosatrata*) foraging: a synoptic case study from the southern Barents Sea. Sarsia, **86**: 485–501.

Harbitz, A., Aschan, M., and Sunnanå, K. 1998. Optimal effort allocation in stratified, large area trawl surveys, with application to shrimp surveys in the Barents Sea. Fish. Res. **37**: 107–113.

Isaaks, E.H., and Srivastava, R.M. 1988. Spatial continuity measures for probabilistic and deterministic geostatistics. Math. Geol. **20**(4).

Kern, J.W., and Coyle, K.O. 2000. Global block kriging to estimate biomass from acoustic surveys for zooplankton in the western Aleutian Islands. Can. J. Fish. Aquat. Sci. **57**: 2112–2121.

Loeng, H. 1991. Features of the physical oceanographic conditions in the Barents Sea. Polar Res. **10**: 5–18.

Mardia, K.V., Kent, J.T., and Bibby, J.M. 1992. Multivariate analysis. Academic Press, London.

© 2003 NRC Canada

Petitgas, P. 1993. Geostatistics for fish stock assesments: a review and an acoustic application. ICES J. Mar. Sci. **50**: 285–98.
Ripley, B.D. 1987. Stochastic simulation. John Wiley & Sons, Inc., New York.
Rivoirard, J., Simmonds, J., Foote, K.G., Fernandes, P., and Bez, N. 2000. Geostatistics for estimating fish abundance. Blackwell Science, London.
Thompson, S.K. 1992. Sampling. John Wiley & Sons, Inc., New York.
Thompson, S.K., and Seber, G.A.F. 1996. Adaptive sampling. John Wiley & Sons, Inc., New York.

Appendix A. Notations.

- A area
- B abundance, e.g., biomass in study area
- b density, e.g., tonnes per square nautical mile
- $\bar{b}_s$ mean empirical density based on data or simulations at sample nodes
- $\bar{b}_g$ mean simulated density based on simulations in all grid nodes
- $\bar{b}_i$ empirical stratum mean
- c subscript for conditional
- $\mathbf{C}$ covariance matrix $\mathbf{C} = \{c_{jk}\}$ in $N(0,1)$ space with SI = 1
- $\mathbf{C}_0$ covariance matrix with NU = 0 and SI = 1
- c_{jk} element in $\mathbf{C}$, $c_{jk} = \text{cov}(b(\mathbf{x}_j), b(\mathbf{x}_k))$
- $\mathbf{D}$ matrix with property $\mathbf{DD}^T = \mathbf{C}$, e.g., a Cholesky decomposition of $\mathbf{C}$
- CV coefficient of variation (standard deviation divided by mean)
- F cumulative sample distribution
- g subscript for grid
- $\mathbf{h}$ vector lag, i.e., vector distance between two observation sites
- h lag, scalar distance between two observation sites, $h = |\mathbf{h}|$
- i index for stratum, $i = 1,\ldots, m$
- iid abbreviation for independent and identically distributed
- j and k index for spatial location
- il composed index for location l in stratum i
- m number of strata
- MC abbreviation for Monte Carlo
- n number of samples
- nc subscript for nonconditional
- N number of grid nodes in simulation grid
- n.mi. nautical mile
- n_{sim} number of simulations
- NU nugget parameter in variogram
- q catchability
- r correlation length, parameter in variogram
- Q weighted sum of squares to estimate variogram parameters
- s subscript for sampling
- S sample standard deviation
- S_{MC} estimated sampling standard deviation applying S as true process standard deviation
- SI sill parameter in variogram
- R rank
- rnd abbreviation for random
- $\mathbf{x}$ spatial coordinate vector in two-dimensional Cartesian coordinate system, $\mathbf{x} = (x,y)$
- x spatial coordinate in Cartesian coordinate system
- y spatial coordinate in Cartesian coordinate system
- z normal $N(0,1)$ variable
- Φ^{-1} inverse cumulative $N(0,1)$ distribution
- γ variogram
- μ expected average density in defined area
- σ standard deviation in process distribution

Appendix B. Simulation procedure for conditional simulation.

1. Transform from data, $b_1,\ldots,b_n$, to normal $N(0,1)$ variables $z_1,\ldots,z_n$, e.g.,

$$z_j = \Phi^{-1}(\text{rank}(b_j)/(n+1)), \quad j = 1,\ldots,n$$

2. Calculate empirical variogram $\hat{\gamma}_Z(h)$ based on $z_1,\ldots,z_n$ and fit theoretical variogram, e.g.,

$$\gamma_Z(h) = \begin{cases} \text{NU} + (\text{SI} - \text{NU})(1.5(h/r) - 0.5(h/r)^3), & h \le r \\ \text{SI}, & h > r \end{cases}$$

3. Calculate $N \times N$ grid correlation matrix $\mathbf{C}_g = \mathbf{C}(\mathbf{x}_g, \mathbf{x}_g) = \{c_{jk}\}$ with SI = 1:

$$c_{jk} = 1 - \gamma_z(h_{jk};\ \text{SI} = 1), \quad j \ne k,\ j,k = 1,\ldots,N$$

$$c_{jj} = 1, \quad j = 1,\ldots,N$$

$$h_{jk} = |\mathbf{x}_{gj} - \mathbf{x}_{gk}|$$

4. Calculate $n \times n$ sampling correlation matrix $\mathbf{C}_s = \mathbf{C}(\mathbf{x}_s, \mathbf{x}_s) = \{c_{jk}\}$ as in point 3, but now with $h_{jk} = |\mathbf{x}_{sj} - \mathbf{x}_{sk}|$ and with N replaced by n.
5. Calculate $N \times n$ cross covariance matrix $\mathbf{C}_0 = \mathbf{C}_0(\mathbf{x}_g, \mathbf{x}_s)$, but now with

$$c_{jk} = 1 - \gamma_z(h_{jk};\ \text{NU} = 0,\ \text{SI} = 1),$$

$$h_{jk} = |\mathbf{x}_{gj} - \mathbf{x}_{sk}|, \quad j = 1,\ldots,N,\ k = 1,\ldots,n$$

6. Calculate $N \times N$ conditional grid covariance matrix $\mathbf{C}_c$ and corresponding $N \times N$ decomposition matrix $\mathbf{D}_c$:

$$\mathbf{C}_c = \mathbf{C}_g - (1 - \text{NU})^2 \mathbf{C}_0 \mathbf{C}_s^{-1} \mathbf{C}_0^T$$

$$\mathbf{D}_c \mathbf{D}_c^T = \mathbf{C}_c$$

7. Calculate random conditional simulations $\mathbf{z}_c(\mathbf{x}_g) = (z_{c1},\ldots,z_{cN})^T$ in all grid nodes:

$$\mathbf{z}_c(\mathbf{x}_g) = (1 - \text{NU})\mathbf{C}_0 \mathbf{D}_s^{-1} \mathbf{z}_s + \mathbf{D}_c \mathbf{z}_{\text{iid}}$$

where $\mathbf{z}_{\text{iid}}$ is a $N \times 1$ vector of independent $N(0,1)$variables.
8. Backtransform to observation space by, e.g., reversed bootstrap:

$$R = \text{int}(n\Phi(z_{cj})) + 1;$$

$$b_{cj} = b_{(R_j)}, \quad j = 1,\ldots,N$$

where $b_{(R_j)}$ is the R_jth lowest observed density value.
9. Repeat steps 7–9 n_{sim} times and calculate CV = std($\bar{b}_s / \bar{b}_g$), i.e., the standard deviation of the n_{sim} values of the ratio between "observed" and "true" density.
10. Multiply CV with correction factor S/S_{MC}, where S is the empirical sample standard deviation and S_{MC} is the average sample standard deviation from the simulations.

© 2003 NRC Canada

PERSPECTIVE / PERSPECTIVE

Fish community change in Lake Superior, 1970–2000[1]

Charles R. Bronte, Mark P. Ebener, Donald R. Schreiner, David S. DeVault, Michael M. Petzold, Douglas A. Jensen, Carl Richards, and Steven J. Lozano

Abstract: Changes in Lake Superior's fish community are reviewed from 1970 to 2000. Lake trout (*Salvelinus namaycush*) and lake whitefish (*Coregonus clupeaformis*) stocks have increased substantially and may be approaching ancestral states. Lake herring (*Coregonus artedi*) have also recovered, but under sporadic recruitment. Contaminant levels have declined and are in equilibrium with inputs, but toxaphene levels are higher than in all other Great Lakes. Sea lamprey (*Petromyzon marinus*) control, harvest limits, and stocking fostered recoveries of lake trout and allowed establishment of small nonnative salmonine populations. Natural reproduction supports most salmonine populations, therefore further stocking is not required. Nonnative salmonines will likely remain minor components of the fish community. Forage biomass has shifted from exotic rainbow smelt (*Osmerus mordax*) to native species, and high predation may prevent their recovery. Introductions of exotics have increased and threaten the recovering fish community. Agencies have little influence on the abundance of forage fish or the major predator, siscowet lake trout, and must now focus on habitat protection and enhancement in nearshore areas and prevent additional species introductions to further restoration. Persistence of Lake Superior's native deepwater species is in contrast to other Great Lakes where restoration will be difficult in the absence of these ecologically important fishes.

Résumé : On trouvera ici une revue des changements survenus dans la communauté des poissons du lac Supérieur de 1970 à 2000. Les stocks de touladis (*Salvelinus namaycush*) et de grands corégones (*Coregonus clupeaformis*) se sont considérablement accrus et sont peut-être en train d'atteindre leurs densités d'antan. Les stocks de ciscos de lac (*Coregonus artedi*) ont aussi récupéré, mais le recrutement est sporadique. Les concentrations de contaminants ont diminué et sont maintenant en équilibre avec les influx; les concentrations de toxaphène sont, cependant, plus élevées que dans les autres Grands Lacs. Le contrôle de la grande lamproie marine (*Petromyzon marinus*), l'établissement de limites de récolte et l'empoissonnement ont favorisé la récupération des stocks de touladis et permis l'établissement de petites populations de salmoninés non indigènes. Comme la reproduction naturelle assure le maintien de la plupart des populations de salmoninés, il n'est plus nécessaire de procéder à des empoissonnements additionnels. Les salmoninés non indigènes demeureront vraisemblablement une composante mineure de la communauté de poissons. Les biomasses des poissons fourrage ne sont plus dominées par l'éperlan arc-en-ciel (*Osmerus mordax*), une espèce introduite, mais plutôt par des espèces indigènes et il est possible que la forte prédation empêche leur récupération. L'introduction d'espèces non indigènes s'est accrue et menace la récupération de la communauté de poissons. Les agences de gestion ont peu d'influence sur l'abondance des poissons fourrage ou sur le prédateur principal, le touladi siscowet; afin de promouvoir

Received 4 October 2002. Accepted 7 September 2003. Published on the NRC Research Press Web site at http://cjfas.nrc.ca on 23 December 2003.
J17126

C.R. Bronte.[2] U.S. Fish and Wildlife Service, Green Bay Fishery Resources Office, 2661 Scott Tower Drive, New Franken, WI 54229, U.S.A., and U.S. Geological Survey, Great Lakes Science Center, 1451 Green Road, Ann Arbor, MI 48105, U.S.A.
M.P. Ebener. Chippewa-Ottawa Resource Authority, 179 East Three Mile Road, Sault Ste. Marie, MI 49783, U.S.A.
D.R. Schreiner. Minnesota Department of Natural Resources, Lake Superior Area Fisheries Program, 5351 North Shore Drive, Duluth, MN 55804, U.S.A.
D.S. DeVault. U.S. Fish and Wildlife Service, Ecological Services, 1 Federal Drive, Bishop Henry Whipple Federal Building, Fort Snelling, MN 55111, U.S.A.
M.M. Petzold. Ontario Ministry of Natural Resources, 1235 Queen Street East, Sault Ste. Marie, ON P6A 2E5, Canada.
D.A. Jensen and C. Richards. University of Minnesota Sea Grant Program, 2305 E. 5th Street, Duluth, MN 55812, U.S.A.
S.J. Lozano. National Oceanic and Atmospheric Administration, Great Lakes Environmental Research Laboratory, 2205 Commonwealth Boulevard, Ann Arbor, MI 48105, U.S.A.

[1]This paper forms part of the proceedings of a workshop on Salmonid Communities in Oligotrophic Lakes II convened at The University of Toronto at Mississauga, 18–20 May 2000.

[2]Corresponding author (e-mail: charles_bronte@fws.gov).

 doi: 10.1139/F03-136 © 2003 NRC Canada

la récupération, les agences doivent se concentrer sur la protection des habitats et l'amélioration des zones littorales et elles doivent prévenir l'introduction de nouvelles espèces non indigènes. Le maintien des poissons indigènes d'eau profonde distingue le lac Supérieur des autres Grands Lacs dans lesquels la récupération sera difficile en l'absence de ces poissons de grande importance écologique.

[Traduit par la Rédaction]

Introduction

The objective of the first International Symposium on Salmonid Communities in Oligotrophic Lakes (SCOL-1) in 1971 was to assess the effects of cultural eutrophication, exploitation, and species introductions on the native fish communities of the Laurentian Great Lakes and other large lakes from European settlement to the late 1960s. The Lake Superior account (Lawrie and Rahrer 1972) detailed the physical description of the basin, lake, and land use, the invasion of sea lamprey (*Petromyzon marinus*), the expansion and decline of commercial fisheries, and their combined effects on native fish communities. Early degradation was attributed to depreciation of fluvial, estuarine, and shallow water environments, which affected local stocks of selected species (i.e., lake sturgeon (*Acipenser fulvescens*), brook trout (*Salvelinus fontinalis*)), but habitat degradation did not account for any lakewide declines in nearshore or offshore fish populations. Overfishing and sea lamprey predation were clearly the major causes of the decline of commercially important fishes (lake trout (*Salvelinus namaycush*), lake herring (*Coregonus artedi*)). Failure of fisheries managers to control exploitation and recognize the stock structure of these species led to the sequential exploitation of discrete stocks. Sea lamprey predation and its indirect effects would likely have completed the demise of lake trout and other species if not for the timely arrival of chemical control in the late 1950s (Smith and Tibbles 1980), which allowed for the possibility of restoration and recovery of the fish community.

Before 1970, knowledge of the biological and ecological processes of Lake Superior was limited. Physical and chemical limnology of Lake Superior was detailed in comparison to the limited study of primary and secondary production. Status of fish populations was measured mostly from analysis of commercial fishery catch and effort statistics, as no independent stock assessments, other than for lake trout, were in place. Biological study was limited to life history descriptions of commercial species and the performance of hatchery-reared lake trout for the newly implemented restoration program. Exotic fishes, other than sea lamprey, were limited to alewife (*Alosa pseudoharengus*), rainbow smelt (*Osmerus mordax*), and newly introduced Pacific salmon (*Oncorynchus* sp.), the former two implicated in the demise of native coregonines (Smith 1970) and the latter, intentionally introduced to create additional fishing opportunities. Sea lamprey control was limited to electrical weirs and chemical control. Contamination of sediments and bioaccumulation of toxic chemicals were of little concern or were unknown. The emphasis was clearly on the most obvious stressors, commercial fishing and sea lamprey predation, with minimal consideration of potential threats of less conspicuous factors.

The second International Symposium on Salmonid Communities in Oligotrophic Lakes (SCOL-2) concentrated on biological and anthropomorphic stressors that have resulted in changes to the Great Lakes since 1970. Fish community changes in Lake Superior since 1970 have been substantive and include the continued establishment of nonnative species along with the recovery of native species. Here we document the changes to Lake Superior's aquatic community from 1970 to 2000 in the face of the following potential stressors: habitat degradation, contaminants, changes in phosphorus loading, potential impacts from global warming, impacts of sea lamprey and other unintentional exotic species, impacts of intentional introductions of Pacific salmon and other nonnative salmonines, and fishery exploitation. We compare the expected outcome of the stressors to the observed changes to the fish community and offer expectations for the future of Lake Superior's fish community.

Habitat degradation

As was the case before 1970, the majority of habitat degradation in Lake Superior is limited to shoreline areas, embayments, and tributaries. These shallow-water habitats are most readily impacted by sediment and nutrient inputs from physical alterations of the watershed accompanying urban development, farming, mining, and logging. This results in sedimentation and loss of spawning habitat and local eutrophication, especially in areas draining surficial clay deposits, which predominate in western Lake Superior (Robertson 1997). Less than 5% of Lake Superior's shoreline is developed, but urban and recreational expansion will likely increase in future years. Fish species with early life histories in nearshore (<80 m; only 24% of lake surface area) and offshore (>80 m) waters do not appear to be limited by habitat loss. These include lean and siscowet lake trout (*Salvelinus namaycush*), lake herring, lake whitefish (*Coregonus clupeaformis*), deepwater ciscoes (*Coregonus* spp.), and round whitefish (*Prosopium cylindraceum*). In contrast, inshore species that have been impacted by habitat loss include brook and brown trout (*Salmo trutta*), walleye (*Stizostedion vitreum vitreum*), lake sturgeon, yellow perch (*Perca flavescens*), northern pike (*Esox lucius*), and smallmouth bass (*Micropterus dolomieui*), as well as other species that have not been monitored.

Physical and chemical degradation of spawning habitat was hypothesized to limit lake trout restoration in the Great Lakes, but there is little evidence of any significant biological impact to offshore areas in Lake Superior (Edsall and Kennedy 1995). All native species in Lake Superior proper have persisted and are reproducing, and in some cases, populations are expanding (i.e., lean and siscowet lake trout); hence, there is little evidence for habitat limitation and (or)

© 2003 NRC Canada

degradation in nearshore and offshore areas. Future habitat restoration will involve attempts to reduce erosion to curb stream and embayment sedimentation and physical improvements to streams to increase spawning habitat and cover.

Contaminants

Because of its remote location, limited industrial activity, and the large lake surface area to watershed ratio, Lake Superior receives the majority of its chemical loading via atmospheric deposition, which is the dominant source of polychlorinated biphenyls, polychlorinated dibenzodioxins, polychlorinated dibenzofurans, toxaphene, and mercury (Eisenreich and Strachan 1992). It was thought that body burdens and background contamination would persist at high levels for many years given the chemical stability of many of the pollutants. The resulting impairment to the aquatic ecosystem would include reproductive failure of fish and birds and high mortality of young fishes and adults. Over the last 30 years, concentrations of nearly all measured contaminants in fish and the water column, with the exception of toxaphene, have declined in Lake Superior and remain at low levels. Where habitat is not limiting, natural reproduction appears to be evident in all native and nonnative fishes lakewide, which may suggest that biological impacts are minimal, although undetected effects may still be present.

Since the early 1980s, toxaphene concentrations have dramatically declined in lake trout across all Great Lakes except Lake Superior (Glassmeyer et al. 2000). Unlike other hydrophobic organic contaminants, atmospheric input of toxaphene is dominated by gas exchange across the air–water interface, therefore lower water temperature, larger surface area, and water volume may have led to higher historical concentrations in Lake Superior than in the other Great Lakes. The low primary productivity in Lake Superior results in very low sedimentation rates, which reduces toxaphene transport to sediments, while lower water temperatures reduce toxaphene loss through volatilization (Swackhamer et al. 1999). High concentrations of toxaphene and polychlorinated biphenyls and mercury in large lake trout are the primary reason for fish consumption advisories in Lake Superior and are of concern and will likely persist for some time.

Effect of climate warming

A growing amount of scientific evidence suggests that global warming is occurring and will result in significant changes in some ecosystems. Global climate models have been used to quantify effects of climate warming on annual temperature and precipitation in the Great Lakes region under twice the current CO_2 loadings. Summer and winter air temperatures in the Great Lakes increased during the 1900s (Magnuson et al. 1997), but significant change to the Lake Superior fish community has not yet been attributed to this warming. It is predicted that summer precipitation would be reduced by about 5% in western Lake Superior and winter precipitation would increase by up to 20% (especially in western Lake Superior). Summer temperatures would increase by 5 °C, and winter temperatures by 7 °C (Magnuson et al. 1997). An extrapolation of mean annual air temperature projections to water temperatures for Thunder Bay, Lake Superior (Hill and Magnuson 1990), indicated an increase in epilimnion and neritic waters of 1.8 °C to 5.7 °C during July–September. The 5 °C December isotherm would encompass most of Lake Superior by 2030 (Johnson and Evans 1990). These changes from climate warming would result in decreased ice cover (Hengeveld 1990), reduced lake levels (0.23–0.47 m) and outflow volumes (–8%) (Magnuson et al. 1997), and an increase in thermal habitat volume (Christie and Regier 1988). Lotic thermal habitat would also be affected. Stream temperatures in Minnesota are projected to increase 2.4 °C to 4.7 °C (Magnuson et al. 1997) and beyond the 15.5 °C for many cool-water streams. The downstream cooling effect of cold water from Minnesota streams could be shortened by 25–50% (Sinokrot et al. 1995), and the cooling ability of groundwater is expected to decrease (Meisner et al. 1987).

Climate warming would increase thermal habitat volume for lake trout, lake whitefish, coho salmon (*Onchorynchus kisutch*), yellow perch, smallmouth bass, walleye, and northern pike (Hill and Magnuson 1990; Shuter and Post 1990; Magnuson et al. 1997). In Lake Superior, smallmouth bass and yellow perch are currently restricted to warmer bays, and yellow perch are at the margins of their preferred thermal habitat (Hokansen 1977; Bronte et al. 1993); therefore, the distribution of these species should expand in Lake Superior (Shuter and Post 1990).

Nonindigenous species would benefit from climate warming (Magnuson et al. 1990). White perch (*Morone americana*; Johnson and Evans 1990) and alewife (Henderson and Brown 1985; Bronte et al. 1991) are rare in Lake Superior because of the duration of low water temperatures. White perch distribution should expand with the 5 °C December isotherm, which is correlated with white perch distribution (Johnson and Evans 1990). Alewife populations may expand beyond trace levels if water temperatures increase to allow successful egg incubation and osmoregulation (see Bronte et al. 1991). Increased temperatures of many cold-water streams would support additional sea lamprey populations (Christie and Kolenofsky 1980). Rainbow smelt would experience increased recruitment through earlier hatching promoted by warmer spring water temperatures (Nyberg et al. 2001), hence their populations may increase. Most potential invaders that are now thermally restricted to the lower Great Lakes would quickly colonize the upper Lakes under climate warming (Mandrak 1989).

A reduction in precipitation and an increase in temperature for western Lake Superior would affect fish populations, particularly those inhabiting streams, wetlands, and estuaries. The projected increase in stream temperatures would favor rainbow trout (*Oncorhynchus mykiss*) and Pacific salmon over brook trout (Fausch and White 1986; Rose 1986). In the embayments, lower lake levels could result in an increase in aquatic vegetation and thermal habitat for warm- and cool-water species, favoring centrarchids and percids. Habitat for smallmouth bass and yellow perch, which is currently marginal in Lake Superior (Hokansen 1977; Magnuson et al. 1990; Shuter and Post 1990), would increase.

Although the rate of primary production is not expected to increase, species composition would change, annual production would increase, and diversity and biomass might also

© 2003 NRC Canada

increase (Magnuson et al. 1997). Primary production could increase by 1.6 to 2.7 times, zooplankton 1.4 to 2.1 times, and fish yield 1.4 to 2.1 times (Regier et al. 1990). Bluegreen algae would be favored in warmer epilimnion water over chrysophytes and diatoms; these climate-altered communities will have different trophic efficiencies and potentially large ecosystem effects (Magnuson et al. 1997). Because most benthic production in Lake Superior occurs in the profundal zone, an increase in benthic invertebrate production would be minor.

Changes in phosphorus loading

Cultural eutrophication, primarily from increased phosphorus inputs, has caused changes in water quality and plankton and fish communities in the Great Lakes (Beeton 1965). Phosphorus is the major nutrient that limits phytoplankton growth and, hence, primary production. Lake Superior was the only Great Lake that historically did not experience measurable increases in phosphorus. Lakewide spring concentrations of total phosphorus are consistently below the International Joint Commissions' recommended maximum of 5 $mg \cdot L^{-1}$ with no temporal trend over the last 30 years. Elevated total phosphorus concentrations still occur in the western arm of the lake and in localized areas close to shore, particularly adjacent to tributaries transporting most of the phosphorus to U.S. waters of Lake Superior (Robertson 1997). Given the apparent long-term stability of phosphorus in Lake Superior and the decline of phosphorus in the other Great Lakes (Madenjian et al. 2002), we predict that the future potential for cultural eutrophication via phosphorus loading is minimal.

Intentional species introductions

Chinook salmon (*Oncorhynchus tshawytscha*), coho salmon, rainbow trout (steelhead), Atlantic salmon (*Salmo salar*), and brown trout all have been intentionally introduced into Lake Superior by state and provincial management agencies to diversify and enhance sportfishing. Small populations developed and provided seasonal nearshore fisheries. Natural reproduction has been documented for all species, except Atlantic salmon, and wild fish represent the majority of recruitment (Peck et al. 1999).

Water temperature and life history characteristics are probably the major limiting factors for nonnative salmonine production in Lake Superior. Native predators (lean lake trout, siscowet lake trout, burbot (*Lota lota*)) are physiologically tolerant of extended periods of low water temperatures, consume large prey while expending minimal energy for predation and metabolism, grow slowly, are long-lived, and can reproduce many times throughout their lives. Most nonnative salmonines lack these life history characteristics (Kitchell et al. 2000), which puts them at a disadvantage in Lake Superior. Because of metabolic thermal requirements (Coutant 1977), most nonnative salmonines are generally restricted to the nearshore zone of Lake Superior, less than 80 m, or the top 20 m of the water column during much of the year (Wismer and Christie 1987). Only during July–October are water temperatures adequate for growth of Pacific salmon and brown trout. Rarely does any significant portion of Lake Superior reach temperatures for optimal growth for these species, therefore streams and bays are the only available warm-water refugia. Year-class strength and survival of stocked nonnative fish are highly dependent on these dynamics; hence stocking programs are of limited value. Wild stocks tend to fluctuate based on climatic conditions and appear to utilize the optimal thermal refuge when it becomes available. Though some areas may benefit from continued stocking, most agencies have realized that supplemental stocking of nonnative salmonines in Lake Superior is not cost effective and are re-examining their programs (Peck 1992).

Concern over competition between recovering lake trout and introduced salmonines arose in the early 1980s when growth of lake trout appeared to be declining (Busiahn 1985). During the 1980s, diet similarity was highest between lean lake trout and chinook salmon and lower between lake trout and coho salmon (Conner et al. 1993; Table 1). However, stable isotope analysis suggested that Pacific salmon occupy a lower trophic level than native predators (Harvey and Kitchell 2000); therefore, direct interactions are less likely. Bioenergetics modeling has been applied to determine if forage availability limits lake trout restoration in the presence of nonnative salmonines. Estimated prey consumption by lean lake trout and introduced salmonines in Minnesota waters exceeded prey standing stock and production (Negus 1995). Model simulations were limited by the assumption that predation and growth occurred in Minnesota waters only, which is unlikely given the lakewide movements of chinook salmon (Peck et al. 1999) and likely that of other predators. Ebener (1995) obtained similar results on a larger spatial scale and with the inclusion of siscowet lake trout in the simulations. Most of the predatory inertia was from the large standing stock of siscowet lake trout, which consumed more prey fish than all other predators combined (Fig 1). Because recruitment and natural mortality (as opposed to sea lamprey predation and fishing) control siscowet biomass, which accounts for most of the forage consumption, it is unlikely that the absence of nonnative salmonines would improve lean lake trout growth and survival significantly. Simulations at smaller spatial scales are needed to confirm this. Lean and siscowet lake trout life histories typified by slow growth, low natural mortality, and more diverse diet (Table 1) and habitat utilization make these species more resilient to changes in forage abundance and species composition (Kitchell et al. 2000), as previously suggested for Lake Michigan lake trout (Stewart and Ibarra 1991). The disparity between modeled consumption and available forage is likely due to errors in estimating predator and forage biomass. The general results of these simulations agree well with the perceptions of Lake Superior biologists: that introduced salmonines pose little risk to lake trout recovery, which has advanced lakewide (Hansen 1999; Wilberg et al. 2003).

Unintentional species introductions

At least 39 new nonindigenous aquatic species have entered Lake Superior since 1970 (Table 2). Of these, nine (22%) are fish, seven (17%) are aquatic invertebrates, eight (19%) are fish diseases and parasites, and 17 (41%) are wetland, submerged, or emergent aquatic plants or shoreline woody plants. Additional species likely have been intro-

© 2003 NRC Canada

Table 1. Proportional diet similarity and Shannon–Wiener (H) diet diversity among principal predators in Lake Superior, based on diet data from multiple sources and summarized in Kitchell et al. (2000).

Predator	Lake trout	Siscowet	Burbot	Chinook salmon	Coho salmon	Rainbow trout
Lake trout	1.00	0.36	0.59	0.69	0.49	0.36
Siscowet		1.00	0.53	0.29	0.24	0.17
Burbot			1.00	0.50	0.49	0.44
Chinook salmon				1.00	0.65	0.36
Coho salmon					1.00	0.66
Rainbow trout						1.00
Diet diversity	1.35	1.62	1.61	1.18	1.14	0.62

Fig. 1. (*a*) Estimated standing stocks of major salmonine predators in western Lake Superior and (*b*) estimated consumption of major prey items (from Ebener 1995).

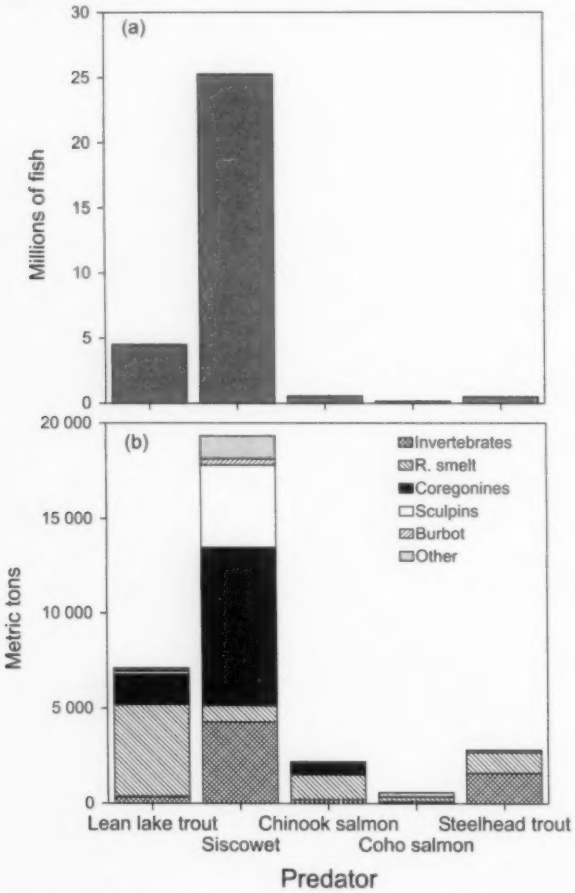

duced but failed to become conspicuous or established. Over 66% of all documented introductions have occurred since 1970, which represents an average introduction rate of 1.4 per year. Compared with other Great Lakes, Lake Superior has the least number of nonindigenous species (Mills et al. 1993).

Since 1970, transport mechanisms for most introduced species were human-mediated (Table 2). Major pathways are via ballast water (24% of introductions), cultivation of wetland and terrestrial plants (24%), release of parasites or pathogens carried by hatchery-reared fish (19%), railroads and highways, canals, and stocked fish (all at 2%), and a combination of mechanisms (multiple mechanisms, 15%). This latter category includes release by angler's bait buckets, release from aquaria, and overland transport by recreational boaters. For 10% of the nonindigenous species, methods of introduction are unknown.

The accelerated rate of unintentional introductions of nonindigenous species into Lake Superior has caused concern. Although no native aquatic species have been extirpated, the establishment of each new species has the potential to disrupt the food web and ecosystem function. Primary effects result from negative interactions with native species and secondary effects from interactions with other nonindigenous species; however, the scope and magnitude of these interactions are not well understood and such impacts to a large degree remain threats. Since 1970, many species arriving have remained localized in embayments and tributaries and are not widely distributed. Given that Lake Superior is the least species rich of all the Great Lakes, it may be the most prone to ecological and economic damage from species introductions. Interrupting the transport mechanisms is critical to preventing new infestations. The accelerated rate of new infestations combined with the increased potential of invasion from global warming is a wake-up call that the natural biodiversity of Lake Superior needs greater protection.

Sea lamprey

Sea lamprey continue to be the most detrimental exotic species in Lake Superior. Sea lamprey kill more lake trout than are harvested (Technical Fisheries Committee, Modeling Sub-Committee, unpublished data). Recent stable isotope analysis revealed that sea lamprey might have the greatest impact on nearshore coregonines (i.e., lake whitefish, lake herring) (Harvey 2001), which may be more available spatially and numerically, and continued control is required.

Lake trout that die from a sea lamprey attack have not been directly observed in Lake Superior, as in Lake Ontario (Bergstedt and Schneider 1988); therefore, attack mortality has been inferred from marking rates. Sea lamprey wounding (type-A, stages 1–3 marks; King 1980) of lean lake trout in U.S. waters of Lake Superior was stable throughout the 1970s, rose in the late 1980s and early 1990s, and has generally declined or remained stable since then (Fig. 2). Sea lamprey wounding averaged 1.2 marks·100 fish^{-1} for 432- to

© 2003 NRC Canada

Table 2. Nonindigenous species introductions, year and earliest locations detected, and method of transport or release into Lake Superior since 1970.

Common name	Scientific name	Earliest record	Earliest location	Transport or release mechanism(s)
American eel	*Anguilla rostrata*	1970	Brule River, WI	Canals
Atlantic salmon	*Salmo salar*	1972	Lake Superior, WI	Stocked fish
Eurasian ruffe	*Gymnocephalus cernuus*	1986	St. Louis River, MN	Ballast water
European flounder	*Platichthys flesus*	1981	Keweenaw Peninsula, MI	Ballast water
Fourspine stickleback	*Apeltes quadracus*	1986	Thunder Bay, ON	Ballast water or live bait
Goldfish	*Carassius auratus*	1975	St. Louis River, MN	live bait or from aquaria
Round goby	*Neogobius melanostomus*	1995	St. Louis River, MN	Ballast water
Threespine Stickleback	*Gasterosteus aculeatus*	1987	Thunder Bay, ON	Ballast water or canals
White perch	*Morone americana*	1986	St. Louis River, MN	Ballast water
Aquatic oligochaete	*Ripistes parasita*	1987	Not Available	Ballast water
Asiatic clam	*Corbicula fluminea*	1999	St. Louis River, MN	Ballast water
Bosmonid waterflea	*Eubosmina coregoni*	1970s	Unknown	Ballast water
Calanoid copepod	*Eurytemora affinis*	1960s	Unknown	Ballast water
Rusty crayfish	*Orconectes rusticus*	1985	Thunder Bay, ON	Ballast water, live bait, or from aquaria
Spiny waterflea	*Bythotrephes cederstroemi*	1987	E. Lake Superior, ON	Ballast water
Zebra mussel	*Dreissena polymorpha*	1989	St. Louis River, MN	Ballast water
Bacterial kidney disease	*Corynebacterium* ssp.	pre-1975	Unknown	Fish parasite or pathogen fish
Furunculosis	*Aeromonas salmonicida*	Unknown	Unknown	Fish parasite or pathogen fish
Whirling disease	*Myxobolus cerebralis*	Unknown	Unknown	Fish parasite or pathogen fish
Round goby parasite	*Sphaeromyxa sevastopoli*	1995	St. Louis River, MN	Fish parasite or pathogen fish
Round goby disease	*Ichthyocotylurus pileatus*	1995	St. Louis River, MN	Fish parasite or pathogen fish
Ruffe parasite	*Tryponasoma acerinae*	1986	St. Louis River, MN	Fish parasite or pathogen fish
Ruffe parasite	*Dactylogirus amphibothrium*	1986	St. Louis River, MN	Fish parasite or pathogen fish
Ruffe parasite	*Dactylogirus hemiamphibothrium*	1986	St. Louis River, MN	Fish parasite or pathogen fish
Birdsfoot trefoil	*Lotus corniculatus*	1975	Kadunce River, MN	Cultivation
Common mullein	*Verbascum thapsus*		Unknown	Unknown
Creeping yellow cress	*Rorippa sylvestris*	<1985	E. Lake Superior, MI	Unknown
Curlyleaf pondweed	*Potamogeton crispus*	1988, 1996	Knife River Marina, MN; Washburn Harbor, WI	With fish or recreational boats
Eurasian watermilfoil	*Myriophyllum spicatum*	1996	Chequamegon Bay, WI	Aquaria or recreational boats
Flowering rush	*Butomus umbellatus*	Unknown	Unknown	Cultivation
Glossy buckthorn	*Rhamnus frangula*	<1985	E. Lake Superior, MI	Cultivation
Indian balsam	*Impatiens glandulifera*	1984 1998	Grand Marais, MN Lake Superior, ON	Cultivation
Hairy willow herb	*Epilobium hirsutum*	<1998	Knife River mouth, Knife River, MN	Cultivation
	Epilobium parviflorum	<1998		Cultivation
Hawkweed	*Hieracium scabriscullum* *Hieracium scabrum*	<1996	Sugar Loaf, MN	Cultivation Cultivation
King-devil	*Hieracium piloselloides*	<1996	Sugar Loaf, MN	Cultivation
Lady's thumb	*Polygonum caespitosum*	<1985	E. Lake Superior, MI	Unknown
Lupine	*Lupinus polyphyllus*	1982	Beaver Bay, MN	Cultivation
Oak-leaved goosefoot	*Chenopodium glaucum*	<1985	E. Lake Superior, MI	Railroads and highways
Spotted knapweed	*Centaurea maculosa* (*biebersteinii*)	<1996	Sugar Loaf, MN	Unknown

532-mm fish, 5.0 marks·100 fish^{-1} for 533- to 634-mm fish, 11.3 marks·100 fish^{-1} for 635- to 736-mm fish, and 17.9 marks·100 fish^{-1} for >736 mm fish.

The sea lamprey control program has been effective at reducing mortality on smaller lean lake trout, but not on adult fish. In U.S. jurisdictions, sea lamprey marking on 432- to

© 2003 NRC Canada

Fig. 2. Spring (May–June) sea lamprey (*Petromyzon marinus*) wounding (number of type-A, stages 1–3 wounds·100 fish^{-1}) for lean lake trout (*Salvelinus namaycush*) in (*a*) Minnesota, (*b*) Wisconsin, and (*c*) Michigan waters of Lake Superior by size class and year, 1970–1999. Length classes: solid bars, 432–532 mm; open bars, 533–634 mm; cross-hatched bars, 635–736 mm; shaded bars, >736 mm.

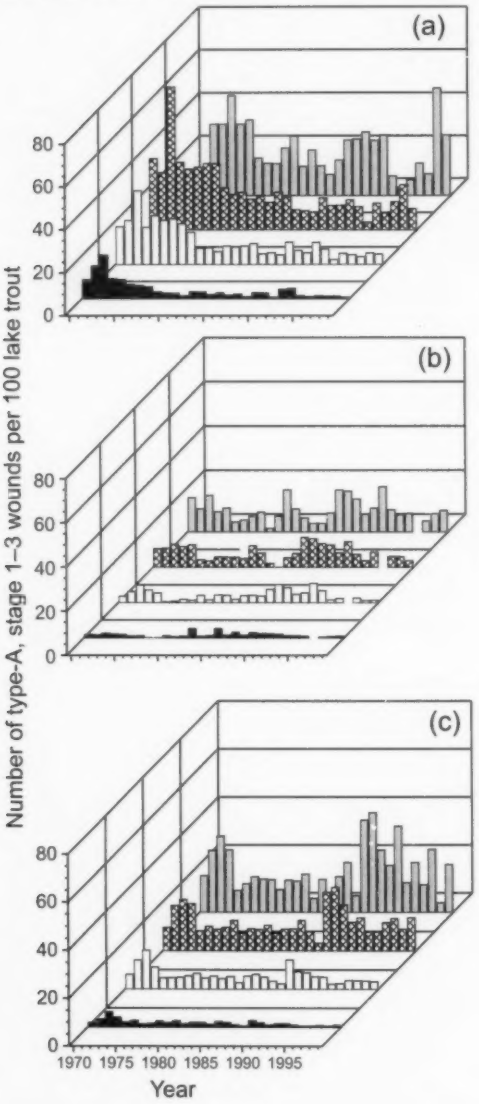

532-mm lake trout has declined to nearly zero and marking on 533- to 634-mm fish was lower during the 1990s in U.S. jurisdictions than in any other time since 1959 (Fig. 2). Unfortunately, the proportion of lake trout >634 mm with sea lamprey marks has not declined in any jurisdiction since the mid- to late 1970s. Sea lamprey marking rates on all sizes of lean lake trout were greater during 1959–1979 than after 1979, but roughly 15% of lean lake trout >634 mm still exhibited fresh wounds (type-A, stages 1–3 marks) in 1999. These trends indicate that large, adult lean lake trout may be buffering smaller fish from sea lamprey attacks, as sea lamprey prefer larger hosts (Swink 1991; Schneider et al. 1996).

The scope of the sea lamprey control program on Lake Superior has expanded to include both control and assessment activities (Heinrich et al. 2003) as initial chemical treatments dramatically reduced abundance of sea lamprey in the early 1960s (Smith and Tibbles 1980). The concept of integrated pest management has been applied to sea lamprey control to develop and use alternative techniques, which would result in a 50% reduction in lampricide used before 1990 (Great Lakes Fishery Commission (GLFC) 1992). Besides lampricides, sea lamprey control now involves releasing sterilized male sea lampreys into tributaries, placing barrier dams on tributaries, trapping and removing adult sea lampreys in tributaries (Heinrich et al. 2003), and conducting research to develop new control strategies. Stock assessments include mark–recapture studies on adult and metamorphosed sea lampreys to determine their relative abundance and to evaluate the effectiveness of control options.

Control has gradually suppressed sea lamprey adult abundance in Lake Superior from 800 000 in 1960 to less than 200 000 in 1999 (Heinrich et al. 2003). This contemporary population is greater than expectations previously established in fish community objectives for Lake Superior (Busiahn 1990). Those objectives called for a 50% reduction in parasitic sea lamprey abundance by 2000 and a 90% reduction by 2010. New objectives require that suppression continue until annual sea lamprey induced mortality is below 5% but with the realization that this will require new control methods to be implemented (Horns et al. 2003).

Further reductions in sea lamprey in Lake Superior will require increased frequency of chemical treatments, stream selection based on cost–benefit–risk analysis, and construction of low head barrier dams on streams with good habitat (Heinrich et al. 2003). Additional control options must be developed, such as use of pheromone attractants to increase trapping efficiency or disrupt spawning (see Bjerselius et al. 2000; Li et al. 2002), to further reduce sea lamprey populations.

Ruffe

The unintentional introduction of ruffe (*Gymnocephalus cernuus*) into the St. Louis River estuary has drawn considerable attention to the threat of exotic species in Lake Superior and elsewhere. These fish originated from the Elbe River drainage in northwestern Europe (C. Stepien, Cleveland State University, Cleveland, OH 44115, personal communication) and were likely transported in the ballast water of transoceanic cargo ships. Ruffe were first collected in the St. Louis River estuary in the mid-1980s but likely entered earlier and remained undetected (Bronte et al. 1998). By 1992, ruffe became the most abundant fish in the lower St. Louis River, based on bottom trawl stock assessments. An effort to control ruffe through increased predation failed (Mayo et al. 1998), and the population grew to about 6 million by 1996. Concurrent decreases in resident native fishes raised concerns over the ruffes' impact on the fish community; however, many of these declines were not correlated

© 2003 NRC Canada

with increasing ruffe abundance, and natural population dynamics could have explained some of these changes (Bronte et al. 1998). Even though ruffe have dominated the fish community numerically for many years, no species losses have occurred. Brazner et al. (1998) contends that ruffe have not been as successful in colonizing some shallow, well-vegetated areas of the Duluth–Superior harbor and that protection of nearshore vegetated habitat from degradation may help confine range expansions. Ruffe have also become abundant in several south-shore streams in Wisconsin (Czypinski et al. 2001). Although lampricides antimycin and rotenone are effective in killing ruffe (Dawson et al. 1998), field applications that target ruffe concentrations are logistically difficult and unlikely to succeed (Horns et al. 2000). Other control measures (i.e., mechanical removal) are not practical, and therefore ruffe populations will likely continue to grow and spread along the coastlines and invade other Lake Superior tributaries.

Changes in forage fishes

Rainbow smelt

Since the mid-1950s, rainbow smelt have played a major role as forage for salmonine predators in Lake Superior (Conner et al. 1993). Lakewide survey data are nonexistent before 1978, but catch-per-unit-effort data from the Minnesota commercial trap-net fishery indicate that rainbow smelt biomass averaged three times higher during 1965–1977 than during 1978–1999 (Fig. 3*a*). Peak abundance appeared to occur in 1978 followed by a steep decline into the early 1980s. This mirrors the trend observed in lakewide bottom trawl surveys (see Bronte et al. (1993) and Bronte and Hoff (1996) for survey details) in which rainbow smelt biomass significantly declined ($F = 4.63$, df = 21,1092, $P < 0.0001$) in U.S. waters by more than 90% (Fig. 2*b*). In 1982–1986, biomass recovered somewhat but declined gradually afterward. Biomass was significantly ($F = 28.06$, df = 1,10, $P < 0.0001$) higher in Canadian waters than in U.S. waters in 1989–1999, but changes in biomass have not been significant ($F = 0.97$, df = 10,357, $P = 0.47$) since 1989 (Fig. 3*b*).

Trends in rainbow smelt biomass in Lake Superior were driven by recruitment patterns and changes in total mortality. In U.S. waters, recruitment was low in 1977, 1979, 1980, and 1981 (Fig. 3*c*) and likely accounted for much of the lakewide decline in biomass during the early 1980s. The strong 1983, 1986, and 1994 year classes increased biomass of age-1 and age-2 fish and did not sustain any increase thereafter. This suggests that mortality, presumably from predation, was intense enough to preclude any recovery even with good recruitment. Fishery exploitation was not a factor as harvest has averaged less than 350 000 kg (<0.02 kg·ha^{-1}) annually in U.S. waters during the same years. Recruitment was generally higher and more stable in Canadian waters, especially for the 1993–1997 year classes, which supported higher biomass. Densities of large rainbow smelt >200 mm total length (ages 4+) declined in U.S. waters during the early 1980s (Fig. 3*d*) concurrent with biomass declines, which suggests an increase in mortality. Larger rainbow smelt (>120 mm total length), which are consumed by salmonines (Conner et al. 1993), are now scarce; hence, we concluded that predation from lean and siscowet lake trout is responsible for the high mortality and sustained low biomass. We anticipate no significant broadening of the size structure or increase in biomass future years if predation remains high.

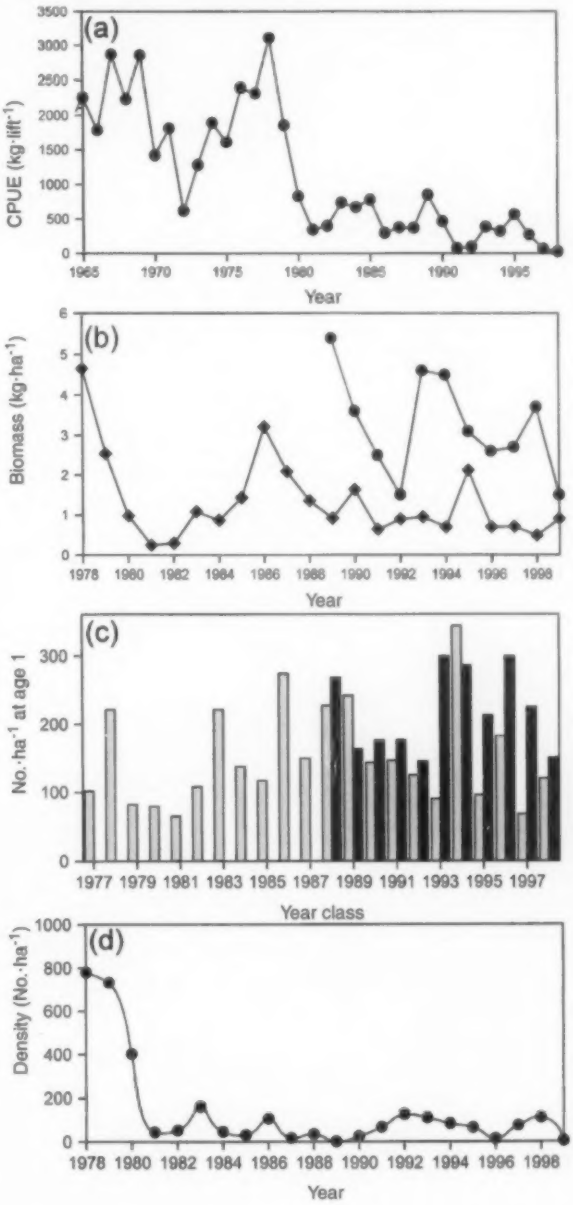

Fig. 3. (*a*) Catch-per-unit-effort (CPUE) of rainbow smelt (*Osmerus mordax*) in commercial trap-net fishery in Minnesota waters in spring 1965–1998, (*b*) 1978–1999 biomass estimates of rainbow smelt in U.S. (■) and Canadian (●) waters, (*c*) estimated strength of the 1977–1998 year classes of rainbow smelt in U.S. (shaded bars) and Canadian waters (solid bars), and (*d*) density of rainbow smelt >200 mm total length in U.S. waters of Lake Superior, 1978–1999.

© 2003 NRC Canada

The scatter plot of recruitment versus parental stock size as measured from lakewide trawl surveys (Fig. 4*a*) appears to be linear (survival is density independent), with most observations close to the origin as would be expected at lower parental stock sizes, and supports our contention for reduced rainbow smelt biomass. A lack of contrast in parental stock sizes precludes any conclusions on recruitment regulation; however, any increases in parental stock size from reduced predation could cause a potential rebound of rainbow smelt stocks.

Fig. 4. Scatter plots of age-1 recruits versus adults for (*a*) rainbow smelt (*Osmerus mordax*) and (*b*) lake herring (*Coregonus artedi*) in U.S. waters of Lake Superior, 1978–1999. Data indexed from fish captured in lakewide bottom trawl surveys by the U.S. Geological Survey.

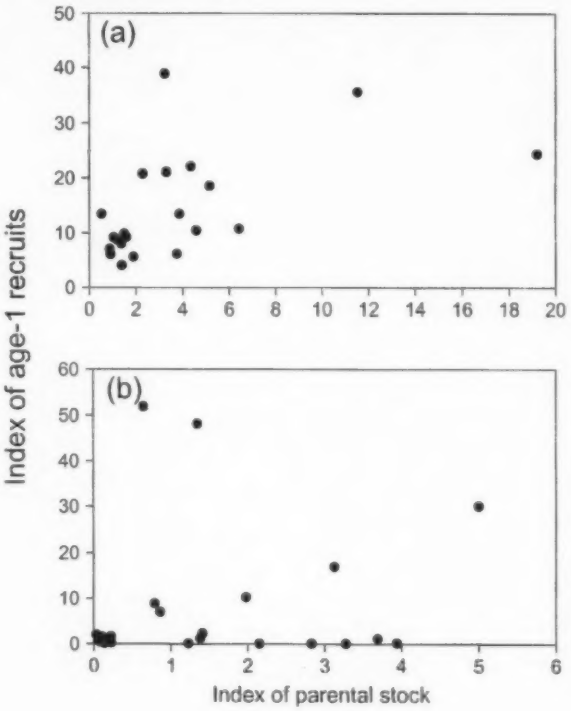

Lake herring

Before the population collapse in the 1960s, lake herring were the major component of the forage base and contributed to most of the commercial production in Lake Superior (Dryer and Beil 1964). Lake herring collapses were first attributed to interspecific competition with bloater (*Coregonus hoyi*) and introduced rainbow smelt and predation by rainbow smelt on lake herring larvae (Anderson and Smith 1971); however, more recent findings challenge these hypotheses. Selgeby et al. (1994) suggested that there was no competition for food between lake herring and rainbow smelt by virtue of spatial and temporal separation of the larvae of each species. Although predation by rainbow smelt on lake herring larvae has been documented in Black Bay, Ontario (Selgeby et al. 1978), lake herring stocks there appeared to be able to support high historical harvests (MacCallum and Selgeby 1987) up until 1990 and under higher densities of rainbow smelt than in U.S. waters (see preceding section); therefore, the effect of rainbow smelt on lake herring recruitment is unclear. Furthermore, if rainbow smelt were depressing lake herring abundance, the reductions in rainbow smelt density during 1978–1981 may have released lake herring from any predation–competition bottleneck. Rainbow smelt biomass has remained low since the late 1980s, yet lake herring recruitment failure has occurred since then, suggesting little interaction between these two species. Analysis of the lake herring fishery in Wisconsin waters strongly suggested that sequential overfishing of discrete stocks caused the collapse there (Selgeby 1982), and this likely occurred elsewhere. Recognition of this stock structure, which is apparent lakewide (Bronte et al. 1996), might have prevented collapse of the lake herring populations (Selgeby 1982).

Lake herring recruitment during the last 22 years has been sporadic. Measured as the density of age-1 fish in lakewide trawl surveys, recruitment has varied significantly from 1978 to 1999 (Fig. 5*a*), with only five significant year classes produced. Large multi-aged parental stocks have been present since the late 1980s but have produced few large year classes. Some of the weakest year classes were produced under the highest stock sizes (as measured in lakewide bottom trawl surveys) (Fig. 4*b*), which may suggest some density-dependent compensation; however, spatial correlation across U.S. and Canadian waters (Fig. 5*a*) and the contrast among levels of recruitment at any stock size also suggests that some lakewide, density-independent factor(s) (i.e., weather, water temperature) may also be important.

Inconsistent recruitment has regulated lake herring biomass over the past 22 years. Total biomass was low in U.S. waters during 1978–1984 but increased significantly (F = 11.86, df = 21,1092, $P < 0.0001$) thereafter as the large 1984 year class entered the catch (Fig. 5*b*). Biomass declined during 1987–1988, as the abundance of the 1984 year class declined and then increased in 1990 to a peak (23 kg·ha^{-1}) as the strong 1988 and 1989 year classes dominated the catch. Poor recruitment since the early 1990s has reduced lakewide biomass to below 10 kg·ha^{-1}. Lake herring biomass in Canadian waters during 1989–1999 was not statistically different (F = 0.38, df = 1,10, P = 0.54) than in U.S. waters, although means appeared lower. Similar to U.S. waters, biomass generally declined (F = 3.13, df = 10,357, P = 0.0006) during 1989–1999 because of limited recruitment, but lower total biomass may also be related to spawner-interception fisheries in Thunder and Black bays up until the mid-1990s.

Recruitment since 1978 may have increased lake herring populations to levels close to historical abundance at the time of maximum fishery removals. Maximum fishery removals were about 2.7 kg·ha^{-1} during 1941–1950 and likely exceeded maximum sustainable yield (Selgeby 1982) and were certainly lower than the level of the unfished stock. Biomass of the harvestable stock (historically fish 230–350 mm total length) (Dryer and Beil 1964) observed in contemporary populations ranged from near zero to 6.4 kg·ha^{-1} from 1978 to 1998 (Fig. 5*c*) and averaged around 3.0 kg·ha^{-1} during 1987–1998 after strong year classes became harvestable. Therefore, harvestable biomass in 1989–1995 approximated or exceeded historical levels of removal during 1941–1950, even with sporadic recruitment, but re-

© 2003 NRC Canada

Fig. 5. (*a*) Estimated strength of the 1977–1998 year classes of lake herring (*Coregonus artedi*) in U.S. (cross-hatched bars) and Canadian (solid bars) waters, (*b*) 1978–1999 biomass estimates of lake herring in U.S. (□) and Canadian (●) waters, and (*c*) biomass of harvestable lake herring (>230 mm) in U.S. waters of Lake Superior in 1978–1999 compared with average removals by the commercial fishery (vertical line) during 1941–1950. Data points near the vertical line indicate that harvestable stock sizes approximated or exceeded historical levels during the height of the fishery.

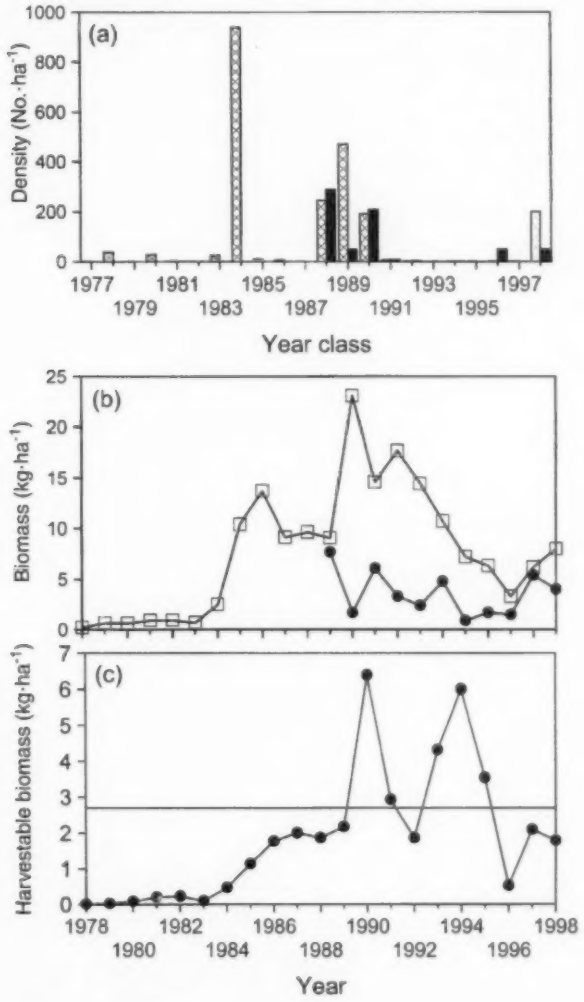

cent abundance has fallen to well below the 1941–1950 levels. Full recovery is likely impossible without more frequent recruitment events. Harvestable stock sizes are declining (Fig. 5*c*) in response to weaker recruitment, and the uncertainty in the causes of these recruitment dynamics will require diligent management to prevent overharvest.

Deepwater ciscoes

Bloater, kiyi (*Coregonus kiyi*), and shortjaw ciscoe (*Coregonus zenithicus*) became important to the commercial fisheries in all jurisdictions except Minnesota. Species delineation has and continues to be difficult because of morphological variability within and across populations and species (Todd et al. 1981), lack of readily apparent distinguishing features (Peck 1977), and lack of clear genetic differentiation (Todd 1981; Turgeon et al. 1999). Morphological differences have environmental as well as genetic origins (Todd et al. 1981). Given these problems, classifications tend to be subjective; therefore, population trends from the available data are unreliable. Species composition of the harvest in Michigan waters during the 1970s, based on morphological features, was mostly bloater (51–87%), followed by kiyi (38–40%), and shortjaw ciscoe (6–11%) (Peck 1977).

Survey data from bottom trawls indicate that bloater biomass increased ($F = 3.96$, df = 21,1097, $P < 0.0001$) in U.S. waters (Fig. 6*b*) at the same time as that of lake herring and could be an artifact of misidentification or that the same unknown factors are responsible for recruitment patterns in these closely related species. Biomass has ranged from 0.2 kg·ha^{-1} in 1978 to 12.2 kg·ha^{-1} in 1992. The lack of kiyi in trawl catches before 1989 (Fig. 6*c*) is also an artifact of identification problems, and because the nearshore trawl surveys generally do not extend into the deeper waters (>80 m) where kiyi are found, any quantifiable changes in biomass are uncertain. Shortjaw ciscoes are rarely encountered and are now being considered for listing as a threatened species. Comparisons of recent survey with historic data suggest that the decline of this species occurred before 1960 and stabilized at lower levels in the 1970s (T. Todd, U.S. Geological Survey, Great Lakes Science Center, Ann Arbor, MI 48105, personal communication).

Other forage species

Sculpins and other species that also play some role in the energy demand of predators and their dynamics may be important. In U.S. waters, ninespine stickleback (*Pungitius pungitius*) have averaged about 0.14 kg·ha^{-1} (Fig. 6*g*), but biomass was the highest in 1979, declining significantly thereafter ($F = 2.12$, df = 21,1092, $P = 0.002$) and remaining below 0.2 kg·ha^{-1} in most years. Biomass in Canadian waters averaged about 0.13 kg·ha^{-1} for 1989–1999 but has generally declined since 1996 ($F = 5.09$, df = 10,357, $P < 0.0001$). Biomass in Canadian waters has been generally higher ($F = 48.54$; df = 1, 10; $P < 0.0001$) than in U.S. waters since 1995. As with rainbow smelt, fewer large ninespine stickleback have been captured since the late 1970s, which could suggest a predation effect (Fig. 7*a*).

Total sculpin biomass in the nearshore waters is generally less than 0.10 kg·ha^{-1} and is composed mostly of slimy sculpin (*Cottus cognatus*) and to a far lesser extent of spoonhead (*Cottus ricei*) and deepwater sculpin (*Myoxocephalus thompsoni*) (Figs. 6*d*, 6*f*, 6*h*). In U. S. waters, slimy sculpin biomass was at its highest level during 1978–1981 (about 0.14 kg·ha^{-1}) but declined significantly ($F = 7.00$, df = 21,1092, $P < 0.0001$) in 1982 and has remained at less than 0.06 kg·ha^{-1} since then. Sculpin densities in Canadian waters during 1989–1998 were twice as high as in U.S. waters during the same time period. Slimy sculpin biomass was generally stable at just under 0.1 kg·ha^{-1} but in 1999 declined significantly ($F = 2.70$, df = 10,357, $P = 0.003$) to below 0.005 kg·ha^{-1}. As with rainbow smelt and ninespine stickle-

© 2003 NRC Canada

Fig. 6. Biomass of (*a*) lake whitefish (*Coregonus clupeaformis*), (*b*) burbot (*Lota lota*), (*c*) bloater (*Coregonus hoyi*), (*d*) slimy sculpin (*Cottus cognatus*), (*e*) kiyi (*Coregonus kiyi*), (*f*) spoonhead sculpin (*Cottus ricei*), (*g*) ninespine stickleback (*Pungitius pungitius*), and (*h*) deepwater sculpin (*Myoxocephalus thompsoni*) in U.S. (□) and Canadian (●) waters determined by lakewide bottom trawl surveys in nearshore waters (15–100 m), 1978–1999, conducted by the U.S. Geological Survey.

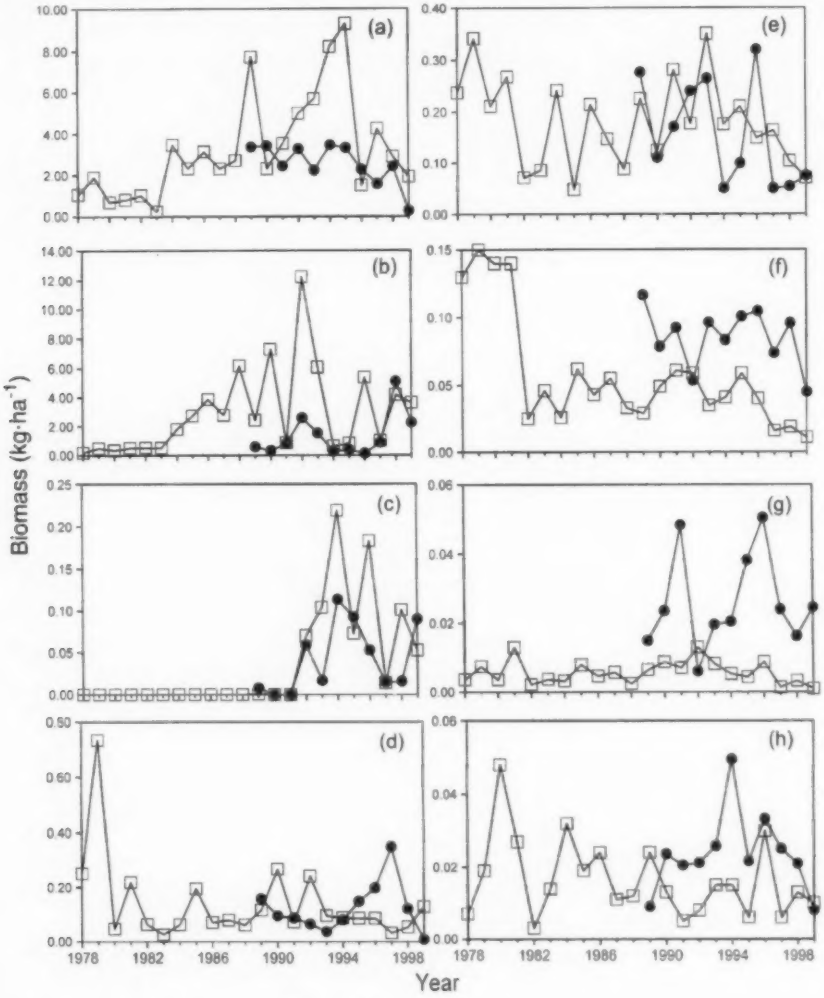

back, the maximum length range of slimy sculpins became reduced as biomass declined after 1982 (Fig. 7*b*), and this may also suggest increased predation.

Spoonhead and deepwater sculpin biomass is much lower than that of slimy sculpin in the nearshore zone and has generally declined (all $P < 0.003$) over time in both U.S. and Canadian waters (Fig. 6). Estimated deepwater sculpin density is likely not indicative of actual densities and trends as depths covered by the sampling program only reached the shallowest portions of their depth distribution.

Principal salmonine predators

Lean lake trout

The decline of lean lake trout stocks in Lake Superior in the 1950s and the success of the ensuring restoration effort have been adequately addressed elsewhere (Hansen 1999). Early efforts focused on sea lamprey control, harvest control, and stocking of lake trout. A coordinated multi-agency lake trout restoration plan was implemented, with specified stocking priorities, coordinated stock assessments, and standards of reporting and evaluating restoration progress. The recovery of wild, naturally reproducing populations of lean lake trout lakewide (Hansen 1999) has negated the need for intensive stocking since 1993 except in selected areas. The restoration program now focuses on the protection and management of wild fish through implementation of total allowable catches to limit fishing mortality.

Extremely high densities (compared with historical measures) of stocked fish and remnant, wild lake trout spurred recruitment in the 1960s and 1970s. Hansen (1999) suggested that hatchery-reared lake trout contributed to most of

© 2003 NRC Canada

Fig. 7. Total length frequency of (*a*) ninespine stickleback (*Pungitius pungitius*) and (*b*) slimy sculpin (*Cottus cognatus*) during selected years from 1979 to 1998. Smaller numbers of larger fish over time suggest a predation effect from increasing numbers of salmonine predators.

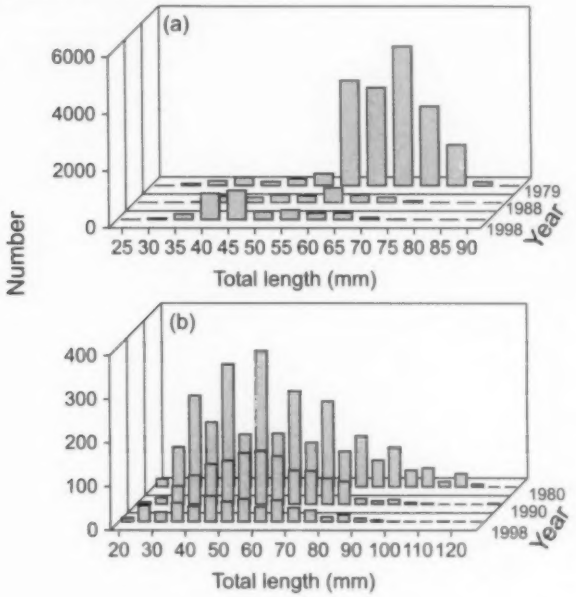

Fig. 8. (*a*) Relative abundance (geometric mean) of wild (●) and hatchery-reared (□) lean lake trout (*Salvelinus namaycush*) in 114-mm stretch measure gill nets in spring stock assessments in U.S. waters, 1970–1999, and (*b*) CPUE of an unknown mixture of lean and siscowet (▲) lake trout in nearshore commercial fisheries in Canadian waters, 1950–1999.

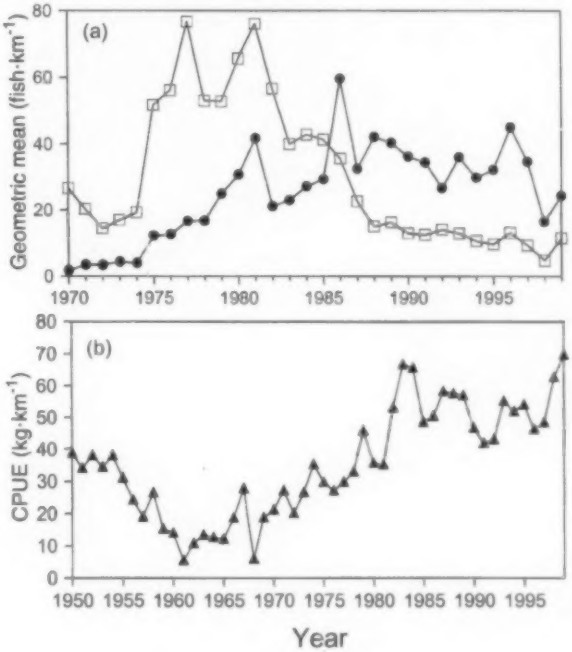

the recruitment, especially in Minnesota and Michigan waters. This is in contrast to earlier findings in which wild adult lake trout explained most of the wild recruitment at Gull Island Shoal (Schram et al. 1995); although at that location, wild fish made up most of the parental stock. A more detailed, age-structured stock–recruit analysis suggests that hatchery-reared fish may be as reproductively efficient as wild counterparts and likely played a significant role in the recovery of lake trout in Michigan waters (Richards et al. 2004).

Spring gill-net surveys indicate that densities of hatchery-reared lake trout have declined in U.S. waters (Fig. 8*a*), mostly as a result of declining survival (Hansen 1999) and reductions in stocking (Fig. 9), whereas wild fish have increased. In Ontario waters, directed stock assessments were only begun in 1997; therefore, historical trends (1950–1999) in lake trout biomass densities (kg·km^{-1} net) are only available from the commercial fishery, and these data strongly indicate that lake trout populations (an unknown combination of hatchery-reared and wild lean lake trout and siscowet lake trout) have increased significantly in Ontario waters over the last 50 years (Fig. 8*b*).

Lake trout are the principal salmonine taken by the sport fishery in Lake Superior and accounted for about 55% of the salmonine harvest in U.S. waters during 1970–1999 (Fig. 10). Landings gradually rose in the 1980s, declined throughout the 1990s, and have increased slightly in the last 5 years. Average harvest in U.S. waters from 1984 to 1999 is about 54 000 fish annually. Catch rates have gradually increased from the late 1970s and are at some of highest rates ever recorded in the last 30 years.

Recovery of lean lake trout is a milestone in the restoration of the Lake Superior ecosystem and would not have occurred without diligent sea lamprey control, limitations on fisheries, and protection of wild, remnant populations. Because of the loss of genetic diversity (Krueger and Ihssen 1995), changes in the forage and predator base, and continued sea lamprey predation, the biological potential of lake trout to reach historical stock sizes was thought to be limited (Bronte et al. 1995; Kitchell et al. 2000). Recruitment dynamics or, more specifically, the onset of density-dependent declines in survival at larger stock sizes may be an indicator of stock restoration (Bronte et al. 1995) at these new biological potentials. Richards et al. (2004) demonstrated that most wild lake trout stocks in Michigan waters underwent density-dependant declines in survival, and Wilberg et al. (2003) showed that stocks are at or higher than historical levels in most areas in Michigan waters. Both findings suggest that lake trout in these areas maybe close to restoration. The population dynamics and biology of Lake Superior's wild lake trout stocks should be used as a model to evaluate progress toward lake trout restoration in the other Great Lakes.

Siscowet lake trout

Historically, Lake Superior contained many morphotypes of lake trout occupying different depths and spawning locations (Khan and Qadri 1970; Goodier 1981; Moore and Bronte 2001). Of these, the siscowet is the most abundant morphotype in Lake Superior and is distinguished by the

© 2003 NRC Canada

Fig. 9. Total salmonine stocking in all jurisdictions of Lake Superior, 1970–2000.

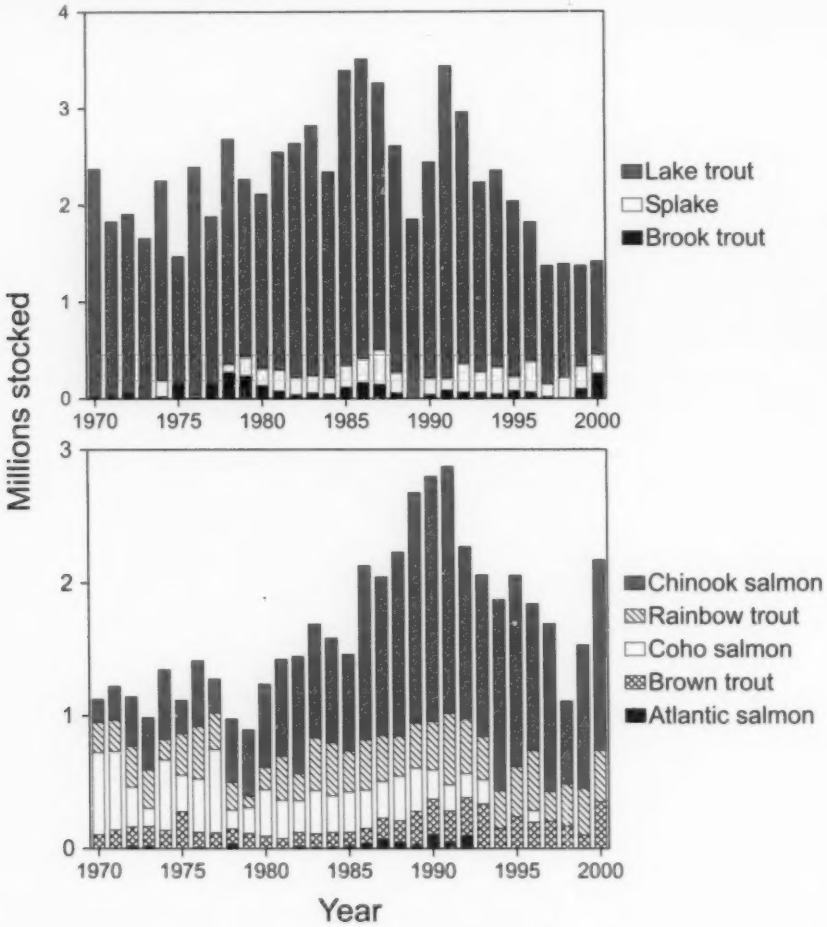

presence of excessive fat in the flesh and viscera (Eschmeyer and Phillips 1965) and its preference for waters deeper than 80 m. Of the 82 000 km^2 of surface area of Lake Superior, 76% is greater than 80 m deep, and this defines the principal habitat for siscowet, as well as suggests the potential importance of this top predator in the Lake Superior ecosystem.

Little is known about the life history of siscowets. Recent surveys indicated that densities were much higher for siscowet than for lean lake trout from the same management unit in U.S waters (Figs. 11*a*, 11*b*; see Wilberg et al. 2003 for map of management units), and siscowet outnumbered lean lake trout by about 10 to 1 in gill-net catches. Siscowet densities increased with depth, whereas lean lake trout densities decreased (Figs. 11*c*, 11*d*). Most siscowets were captured at depths greater than 150 m in June but had a shallower distribution in late August – September, with more fish captured between 70 and 150 m, suggesting seasonal nearshore movement. Unknown differences in catchability between siscowet and lean lake trout in gill nets makes it difficult to assess the ratio estimates; however, all indications suggest that siscowet lake trout significantly outnumber lean lake trout lakewide. Sagittal otoliths revealed a broad age distribution comprised of 16–30 age groups depending on area. Siscowet harvest has remained low in recent years (Fig. 12); therefore, these advanced age compositions may reflect fully restored populations in some areas. It was thought that the expanding siscowet populations would affect recovery of lean lake trout stocks but there is little trophic overlap between these two morphotypes (Harvey et al. 2003) and siscowet expansion has been concurrent with lean lake trout recovery.

Sea lamprey predation may be a significant source of mortality, as fresh wounding (type-A, stages 1–3 marks; King 1980) and scaring (healed wounds: type-A, stage 4; type-B, stages 1–4) are high, especially on large fish >736 mm long. Sea lamprey wounds averaged 5.5 marks·100 fish^{-1} and ranged from 1.3 marks·100 fish^{-1} on 432- to 532-mm fish to 167 marks·100 fish^{-1} >736 mm long during June 1996. Sea lamprey attacks on the largest fish (>736 mm) were almost 17 times higher than on lean lake trout during the same time period (Ebener 1998), which suggests that siscowets may serve as a buffer for sea lamprey predation on recovering lean lake trout stocks. Extremely high scarring rates also suggest that siscowet may be able to survive sea lamprey at-

© 2003 NRC Canada

Fig. 10. Estimated numbers of salmonines harvested in U.S. waters of Lake Superior, 1970–1999.

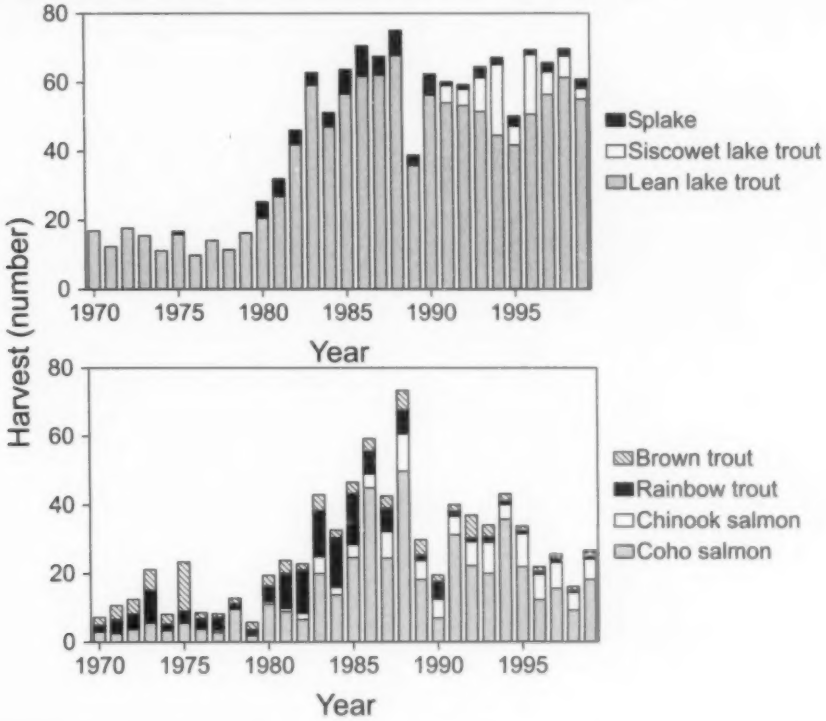

Fig. 11. Relative abundance (CPUE) and ratios of lean (solid bars) and siscowet (open bars) lake trout (*Salvelinus namaycush*) captured in graded-mesh gill-net assessments in U.S. waters of Lake Superior by (*a*, *b*) management unit and (*c*, *d*) depth during (*a*, *c*) June, 1996–1997, and (*b*, *d*) August–September, 1996–1997. See Wilberg et al. (2003) for a map of management units.

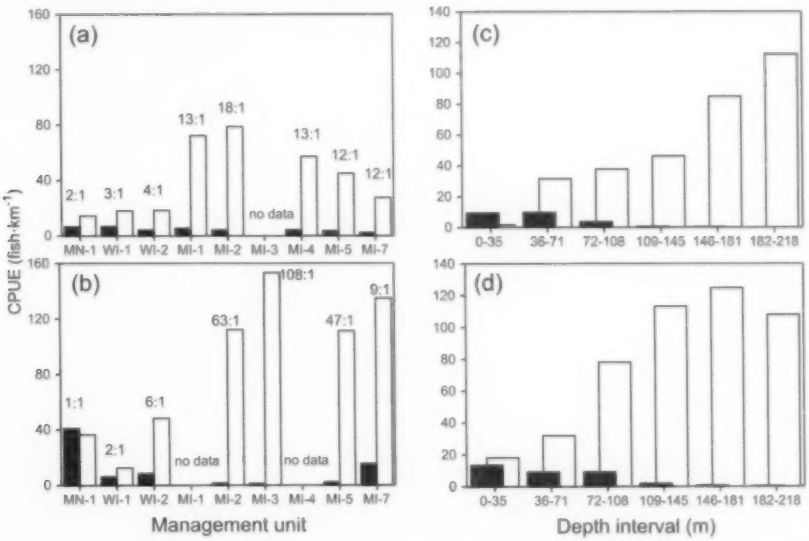

tacks better than lean lake trout. This may be related to the lower temperatures of the water that siscowets inhabit, which slows metabolic and physiologic processes associated with sea lamprey attack and feeding behavior (Schneider et al. 1996).

Siscowet abundance has increased lakewide in the past 30 years. Commercial gill-net catch and effort data from U.S. and Canadian waters indicate that densities increased steadily from >20 kg·km^{-1} net in the early 1950s to about 250 kg·km^{-1} net in the late 1990s (Fig. 13). Stock sizes have

© 2003 NRC Canada

Fig. 12. Estimated commercial landings by species and year from Lake Superior, 1970–1998.

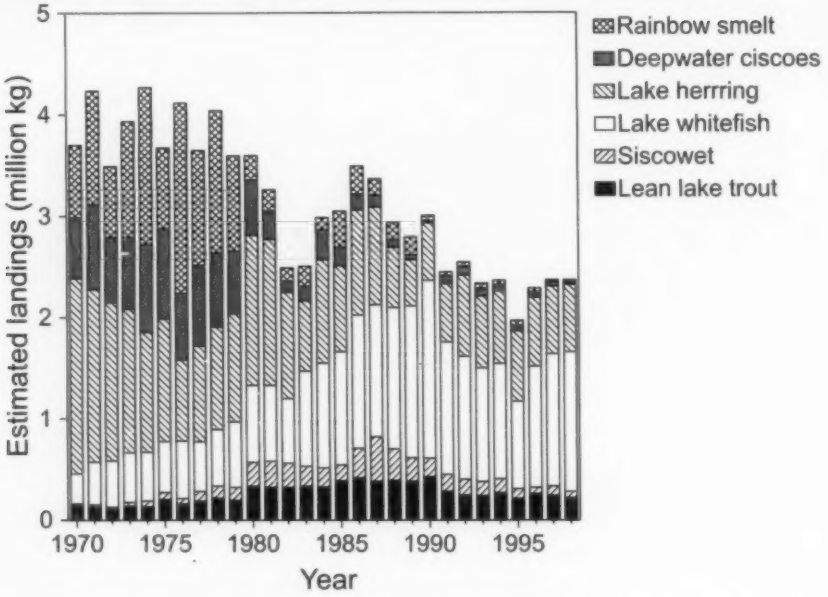

been estimated at 25 million fish of ages 1–21 years for U.S. waters west of the Keweenaw Peninsula compared with about 4.5 million for lean lake trout (Fig. 1; Ebener 1995), and this ratio (6:1) is close to that estimated from gill-net catch rates (10:1). Siscowet by-catch has increased in U.S. sport fisheries targeting lean lake trout since the early 1990s (Fig. 10), which further demonstrates the recovery and expansion of these offshore stocks.

Siscowet are the dominant predator lakewide (Harvey and Kitchell 2000) and consume mostly coregonines (lake herring, bloater, kiyi), sculpins, and burbot (Conner et al. 1993; Ebener 1998; Kitchell et al. 2000). Rainbow smelt, *Mysis*, and terrestrial insects are also consumed, as are miscellaneous items (i.e., pine needles, wood, grain, net twine, fish guts, bats, birds), suggesting extensive vertical movements to the surface and horizontal movements to nearshore areas. Nearshore species such as bullheads (*Ictalurus* sp.), unidentified shiners, and longnose dace (*Rhinichthys cataractae*) were also found in stomachs, further indicating that feeding is taking place in shallow, nearshore areas. Siscowet consume more coregonines, sculpins, and burbot and less rainbow smelt than lean lake trout (Fig. 1), which may partly explain the significant declines of bloater and burbot (F = 1.62, df = 21,1092, P = 0.04; Figs. 6*b*, 6*c*) in Lake Superior concurrent with the expansion of siscowet populations. More study of the deepwater zone of Lake Superior is needed to understand the dynamics of siscowet and their impact on the forage base.

Fig. 13. Relative abundance (CPUE) of siscowet lake trout (*Salvelinus namaycush*) in the commercial gill-net fishery, Lake Superior, 1950–1998.

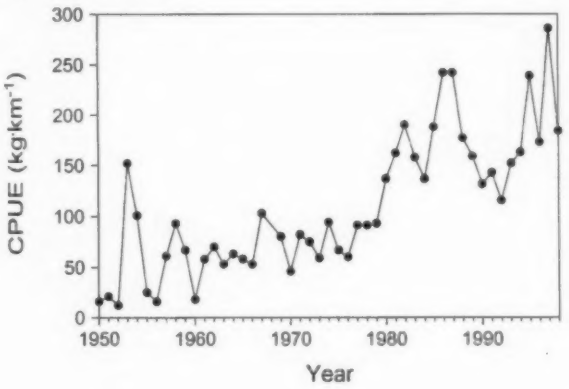

Brook trout

Over the last 10 years, interest has increased in rehabilitating native migratory brook trout in Lake Superior. These fish, also as known as "coasters", live in nearshore coastal areas, where they can attain larger sizes than stream-dwelling counterparts, but ascend rivers to spawn in the fall. Major stressors to brook trout historically were overfishing and habitat loss; currently, competition with nonnative salmonines is seen as a possible impediment to restoration. Attempts are underway to restore migratory brook trout (Newman et al. 1999); however, this may not be biologically possible for many historically important streams that have lost habitat or have stocks of nonnative salmonines. Strategies to achieve the goal include habitat protection and restoration, restrictive angling regulations, and stocking appropriate strains from remnant populations. Further research is also required on genetic profiling, general life history, and identification of remnant stocks, especially at remote sites such as those at Isle Royale.

Remnant populations of coaster brook trout still exist in a few isolated areas of Lake Superior. These include the Nipigon River system in Ontario, streams and bays around Isle Royale, and the Salmon-Trout River in Michigan (Peck

© 2003 NRC Canada

et al. 1994). Adequate genetic variability still exists among remnant brook trout stocks; hence, stocking should proceed cautiously (Burnham-Curtis 2001). Additional genetic evidence suggests that migratory brook trout in Nipigon Bay are a life history variant and are progeny of stream stocks (D'Amelio 2002).

Brook trout stocking has been continuous by most agencies since 1970 (Fig. 9), but harvest in the sport fishery has usually been less than 100 fish·year^{-1} since 1970. Only scattered harvest information on brook trout exists for Ontario waters. Most agencies have, or are in the process of implementing, restrictive harvest regulations for brook trout in Lake Superior and its tributaries. Experimental stocking of genetic strains from Lake Superior is underway in selected areas.

Splake

Splake (lake trout × brook trout) were first introduced in Michigan in 1971 and then in Wisconsin in 1973 (Fig. 9). No natural reproduction by splake has been documented, but sexually mature splake have been found in spawning lake trout aggregations (Peck et al. 1994). Harvest occurs primarily near stocking sites; hence these fish are valued for developing local and nearshore fisheries. Wisconsin has a major splake fishery during winter in Chequamegon Bay, which accounts for most of the harvest in Lake Superior (Fig. 10). Catch rates for splake have been declining since the mid-1980s in response to reduced stocking.

Rainbow trout (steelhead)

Migratory rainbow trout or steelhead became naturalized soon after initial introductions in 1895. Since about 1970, several strains have been introduced to supplement naturalized stocks in areas with intense fisheries or limited spawning habitat. In 1972, Minnesota experimented with the Kamloops, Madison, and Donaldson strains and in 1976 chose the Kamloops strain to supplement naturalized populations. Michigan has used the summer-run Siletz strain since 1984 to provide increased angling opportunities. All three U.S. states have stocked with the Skamania strain of summer steelhead (Peck et al. 1994), but returns were poor and have been discontinued lakewide. Annual stocking has ranged from 90 000 to 540 000 fish (Fig. 9), but return rates have generally averaged 1% or less and have varied widely across streams; hence steelhead populations are composed of mostly wild fish. Lakewide, naturalized rainbow trout comprise 80–90% of fish caught (Peck 1992). Continued stocking on top of wild populations may be wasteful and can also pose genetic risks (Krueger et al. 1994).

Harvest has ranged from 600 fish in 1999 to about 15 000 in 1984 in U.S waters (Fig. 10), with most of these fish taken in Wisconsin waters. Rainbow trout populations were high during the 1950s, but as lake trout recovered and Pacific salmon became established, abundance declined during the 1980s. Starting in the early 1990s, harvest restrictions have reduced exploitation and increased rainbow trout abundance as indicated by angler catch rates during the spring spawning run (Schreiner 2003; Ken Cullis, Ontario Ministry of Natural Resources, 435 James St. South, Thunder Bay, Ont., Canada, personal communication). In addition, unusually warm lake temperatures in 1998 increased both survival and growth rates of rainbow trout, which has been reflected by increasing returns to the Brule River in Wisconsin (Dennis Pratt, Wisconsin Department of Natural Resources, 1401 Tower Ave., Superior, WI 54880, personal communication). Although stocking supports a viable sport fishery for rainbow trout in a small number of Minnesota streams, it is clear that protection of naturalized spawning stocks is the best way for agencies to insure the long-term success of the rainbow trout fishery in Lake Superior.

Coho salmon

Coho salmon were first stocked by Michigan in 1966, followed by Minnesota and Ontario from 1969–1972 (Fig. 9), and quickly became naturalized throughout Lake Superior (Peck et al. 1994). These fish reproduce successfully in many tributaries that are accessible during the spawning period, have suitable substrate, and adequate winter groundwater flows. Michigan was the last agency to discontinue stocking in 1994 as stocked fish contributed less than 10% to the fishery (Peck 1992).

Coho salmon in Lake Superior have a 3-year life history, spending from 16 to 18 months in streams and the remaining 18–20 months in the lake before spawning and death. Anglers mostly exploit age-2+ fish, which results in wide harvest fluctuations, predicated by year-class strength. In most years, coho salmon are the second most harvested salmonine in the U.S. sport fishery after lake trout (Fig. 10). Total harvest in U.S. waters has ranged from 2700 fish in 1971 to 50 000 fish in 1988, with most fish taken in Michigan waters. Catch rates in the sport fishery have been slowly increasing since the early 1980s. Sport harvest regulations have become more restrictive in most jurisdictions to protect adequate numbers of parental stock, as all stocks are now supported by natural reproduction.

Chinook salmon

Chinook salmon were first introduced into Lake Superior by Michigan in 1967, followed by Minnesota in 1974, Wisconsin in 1977, and Ontario in 1988 (Peck et al. 1994). Annual stocking has ranged from 175 000 to 1.8 million fish (Fig. 9); however, the utility of continued stocking is being questioned. Lakewide, wild chinook salmon make up over 75% of all chinook salmon harvested (Peck et al. 1999). Stocked chinook salmon made up 57% of the angler harvest in Minnesota, 32% in Wisconsin, 25% in Michigan, and 9% in Ontario during the 1990–1994 fishery. Chinook salmon stocked in each jurisdiction contributed to the fisheries in all other jurisdictions, which indicates that these fish are free-ranging in Lake Superior and have little site affinity. Harvest in U.S. waters has ranged from a few fish in the early 1970s to about 11 000 fish in 1980 (Fig. 10), with most fish taken from Minnesota waters. Harvests have generally declined since then, even though catch rates in the fishery have steadily increased in the last 20 years.

Pink Salmon

In 1956, approximately 21 000 odd-year spawning pink salmon (*Oncorhynchus gorbuscha*) fry were accidentally introduced into the Current River in Ontario (Nunan 1967), became established, and are now naturalized in Lake Superior. Since 1970, abundance has fluctuated greatly but has

© 2003 NRC Canada

never approached that of other Pacific salmon. In general, pink salmon abundance increased from the 1960s through the 1970s and then declined to extremely low levels during the late 1980s (Peck et al. 1994) and may have been affected by declines in rainbow smelt (MacCullum and Selgeby 1987). However, during the mid- to late 1990s, pink salmon abundance has again started to increase as indicated by harvest (Fig. 10), angler catch rates, and number of spawning adults in tributaries. Even-year spawning stocks have also developed and it is not unusual to capture 3-year-old spawners in many streams. Harvest during 1985–1999 has averaged <250 fish·year^{-1} in U.S. waters. In Ontario, the angler catch is unknown, but a dip-net fishery in the Michipicoten River took an average of 4200 pink salmon from 1979 to 1983 (Peck et al. 1994). Minor fisheries that target strong year classes develop periodically in the tributaries during the September–October spawning period.

Brown trout

Brown trout were introduced into Lake Superior in the 1890s and established naturalized populations in some tributary streams, especially in Wisconsin. Brown trout are still stocked in Wisconsin and Michigan tributaries (Fig. 9) where they support a few localized anadromous populations. Hatchery-reared brown trout make up 50% of the angler harvest of this species in Wisconsin and 40% in Michigan (Peck et al. 1994), indicating significant natural reproduction. Sport harvest is highest in Wisconsin waters, ranging from 534 fish in 1996 to about 14 000 fish in 1975 (Fig. 10). In most years, an active winter fishery develops on Chequamegon Bay, Wisconsin, largely supported by hatchery-reared fish. Lakewide angler catch rates declined from the 1970s to the 1980s but have remained fairly consistent over the last 15 years. The Brule River supports the largest known run of migratory brown trout in Lake Superior, averaging about 3600 fish during 1987–1999 and suggesting a relatively stable population since 1987. Significant genetic variation exists among naturalized brown trout populations in Wisconsin from different drainages and between migratory and resident fish in the Brule and Sioux rivers (Krueger and May 1987).

Atlantic salmon

At present, there is no active management program for Atlantic salmon in Lake Superior. From 1972 to 1992, each state in U.S. waters experimented with stocking Atlantic salmon (Fig. 9), but naturalized populations and significant returns never developed. Minnesota had the most extensive program, but it was discontinued in 1992 because of low returns, high cost, and limited angler interest. In U.S. waters, harvest has been generally 400 fish or less each year since the early 1980s, and no fish have been detected in any creel surveys since 1997.

The commercial fishery

The effects of overexploitation by the commercial fishery were a major factor in the degradation of the fish community of Lake Superior before 1970. During the late 1960s and 1970s, state agencies began to manage primarily for recreational-based fisheries (Brown et al. 1999), which reduced the number of commercial fishing licenses, limited fishing grounds and seasons, and restricted fishing gear types (Brown et al. 1999). Further change to the commercial fishery was expedited by the re-affirmation of treaty-protected fishing rights by Native Americans in the U.S. and Canada. Reaffirmation of treaty rights in Canada came later in the 1990s through "The Sparrow Decision". No tribal fisheries were present in 1970, but in the last 10 years, tribal harvest accounted for 62% of the lake whitefish and 67% of the lake trout harvest. In 1965, there were 542 state-licensed commercial fishermen in U.S. waters of Lake Superior, but the size, scope, and effect of the fishery has declined significantly. In 1999, state, provincial, and tribal fishery agencies issued about 350 commercial licenses but very few licensees fished full-time. Total commercial harvest declined from about 4.0 million kg in 1970 to 2.4 million kg in 1996–1998 (Fig. 12). Fewer fishermen and low markets prices have reduced the fishery, and mainly those operators that control their own wholesale and retail markets fair well economically.

Lake whitefish fishery

Lake whitefish have been the primary target of the commercial fishery lakewide since the late 1980s (Fig. 12), mainly because of fishing restrictions on lake trout and lake herring, changing market conditions, and availability of large standing stocks for harvest. Lake whitefish made up only 6% of the total commercial harvest in 1970 but this increased to 40% in the 1990s. Since 1983, the annual harvest of lake whitefish has exceeded 1 million kg and has been greater than at any other time during the 20th century. Densities of young lake whitefish in bottom trawls increased lakewide during 1990–1995 (Fig. 6*a*) and recruitment of these fish to the fishery helped fuel the increased landings.

Management of lake whitefish populations is based mainly on protecting individual stocks as recommended by Lawrie and Rahrer (1972). Nine lake whitefish management units are recognized in Michigan waters (Technical Fisheries Review Committee 1992), and Ontario has about 21 units (Upper Great Lakes Management Unit 2001) where lake whitefish are managed as biological stocks. Each management unit likely contains smaller reproductively isolated stocks, but little information exists to delineate stock boundaries or structure. Rakoczy (1983) recognized six stocks of lake whitefish in Michigan waters based simply on the wide geographic distance between sampling locations and the spatial segregation of the fisheries. Large concentrations of spawning lake whitefish spatially segregated by 20–30 km have been identified along the Keweenaw Peninsula and may represent reproductively isolated stocks (Ebener 1990). Whitefish Bay has at least four discrete spawning aggregations separated by 8–40 km, but stocks intermingle during the year. At least two stocks exhibit unique growth and size differences. The Apostle Islands presumably contain many reproductively isolated populations of lake whitefish but are managed as a single stock. Lake whitefish fisheries are managed by total allowable catches in Michigan and Ontario waters and through effort limitations for gill-net fishers in Wisconsin waters, where the intent is to reduce the by-catch of nontarget lake trout. Conversion to trap nets in Michigan (Schorfhaar and Peck 1993) and Wisconsin has also reduced by-catch mortality significantly.

© 2003 NRC Canada

Age composition of the commercial harvest is similar among management areas. Except for very lightly exploited stocks, ages 5–9 make up over 80% of the commercial harvest. Lake whitefish begin recruiting to the trap-net fishery at age 4 and to the gill-net fishery at age 5, and the oldest whitefish observed in the harvest are 17–20 years old (Schorfhaar and Schneeberger 1997; Petzold 1999).

Lake whitefish stocks in Lake Superior experienced a substantial density-dependent growth response to the increase in biomass and abundance observed after 1970. In the late 1970s and early 1980s, L_∞ values from various stocks ranged from 700 to 800 mm total length and K values ranged from 0.15 to 0.25. By the mid- to late 1990s, L_∞ values had declined to 500–700 mm and K values ranged from 0.22 to 0.44 (Table 3). Declines in mean weight at age also occurred across the lake. The declines in growth affected age structure of lake whitefish caught by the commercial fishery. In Whitefish Bay, age structure of lake whitefish in the commercial gill-net fishery shifted from ages 4–7 in 1983 to ages 5–17 in 1998. Modal age of whitefish in the trap-net fishery at Munising increased from age 5 in 1983 to age 7 in 1998. In Thunder Bay, Ont., fish of ages 5–7 dominated the harvest during 1975–1982, whereas ages 8–15 made up most of the harvest in 1996–1997 and ages 5–7 barely contributed to the fishery (Petzold 1999).

Lake trout fishery

Commercial harvest is regulated by various methods, but mainly through biologically based catch quotas. Total allowable catches (TACs) are used to accommodate incidental catches of lake trout in large-mesh gill-net lake whitefish fisheries, while simultaneously permitting recovery of lean lake trout populations, except in Minnesota where lean lake trout harvest is prohibited. In Wisconsin and Michigan waters, TACs are estimated using population models based on commercial fishery and biological statistics, although more sophisticated statistical catch-at-age models are now being adopted in U.S. waters (Bence and Ebener 2002). In Ontario, individual transferable quotas are assigned to each licensee, and the quotas are calibrated to surface area ($kg \cdot ha^{-1}$) of water <136 m. Lakewide catch quotas totaled about 400 000 kg in 1998.

Contemporary commercial harvests of lean lake trout (Fig. 12) represent only a fraction of precollapse levels before 1950. The average harvest of lean lake trout was 262 000 kg during 1970–1998 and represents only 13% of the historic average harvest. The majority of the lean lake trout commercial harvest is taken with large-mesh gill nets in Ontario and Michigan. Few lake trout are killed as part of commercial trap-net fisheries (Schorfhaar and Peck 1993) in comparison to gill-net fisheries. Gill-net fisheries were implicated for declining survival of hatchery-reared lake trout (Hansen 1999), but this is unlikely given the sustained increase in wild fish subjected to the same gill-net fishery during the same period.

Although siscowets are more abundant than lean lake trout in Lake Superior, commercial harvests of this morphotype are generally less because of the high fat content of siscowets, which results in lower market demand and value. Annual harvests of siscowets ranged from a low of 23 200 kg in 1970 to a peak of 441 000 kg in 1987 and averaged 148 000 kg during 1970 through 1998 (Fig. 13). Peak catches occurred when Michigan state licensed commercial fisheries were allowed to target siscowet in water >110 m deep. In 1990, the Michigan siscowet fishery was closed because chlordane concentrations were greater than permitted by guidelines for fish consumption. Populations of siscowets increased substantially during the 1980s and, given the slow growth of siscowets, was likely the result of good reproduction and survival during the late 1960s and early 1970s.

Lake herring fishery

Since 1970, lake herring has made up most of the commercial landings from Lake Superior, but this represents only a fraction of historical removals (Fig. 12). Lake herring made up about 25% of the total lakewide commercial harvest from Lake Superior in the 1990s compared with 75% in the 1960s. Annual commercial harvests declined over the last three decades from 1.45 million kg in the 1970s, to 1.16 million kg in the 1980s, and to only 0.7 million kg in the 1990s. The peak harvest during 1970–1998 was 1.9 million kg in 1970 but represented only 22% of the peak historical harvest in 1941.

Based on commercial fishery catches, lake herring appear to be about one-half as abundant since 1980 compared with before the collapse of the fishery in the mid-1960s, although comparisons with bottom trawl survey estimates suggest higher abundance (Fig. 5*c*). Lakewide catch per unit effort (CPUE) of lake herring in the commercial small-mesh gill-net fishery declined to a low of 84 $kg \cdot km^{-1}$ in 1976, then increased rapidly thereafter, and has averaged 365 $kg \cdot ha^{-1}$ since 1981. Since 1993, lakewide CPUE of lake herring has ranged from 397 to 478 $kg \cdot km^{-1}$ compared with 719 $kg \cdot km^{-1}$ during 1953–1964, at the height of the historical fishery. These direct comparisons may not actually represent a state of recovery since the historical fishery was prosecuted with bottom-set gill nets; most of the contemporary fishery uses floating gill nets, especially in fall to target gravid females for the egg market. The increase in commercial harvest and CPUE correspond well with the increase in lakewide biomass from sporadic recruitment detected in lakewide trawl surveys.

Deepwater ciscoe fishery

Deepwater ciscoes currently make up less than 10% of the total commercial harvest from Lake Superior, and this fishery has been declining over the last two decades (Fig. 12). Deepwater ciscoes have never made up more than 25% of the total commercial harvest from Lake Superior and from 1970 to 1980 made up 12 to 25% of the lakewide commercial harvest.

Relative abundance of deepwater ciscoes in the small-mesh gill-net fishery was stable during 1973–1980 (90–100 kg per km of net) but declined thereafter to only 18 kg per km of net by 1998. The continual decline in abundance of deepwater ciscoes since 1980 corresponds to the lakewide increase in abundance of siscowets and their predation pressure. Recovery of deepwater ciscoe populations is unlikely unless siscowet populations decline substantially.

© 2003 NRC Canada

Table 3. Von Bertalanffy growth parameters for Lake Superior lake whitefish stocks estimated from length-at-age data collected from commercially harvested fish during 1978–1998.

Stock	Years	Gear	L_∞ (mm)	K	Source
Apostle Islands	1981	Gill net	704	0.170	Red Cliff Fisheries Department
	1990	Gill net	569	0.250	Red Cliff Fisheries Department
	1999	Gill net	537	0.311	Red Cliff Fisheries Department
West Keweenaw Peninsula	1983	Trap net	696	0.197	Peck (1994)
	1985	Trap net	658	0.214	Peck (1994)
	1988	Trap net	610	0.206	Peck (1994)
	1994–1995	Trap net	507	0.496	Schorfhaar and Schneeberger (1997)
East Keweenaw Peninsula	1983–1985	Trap net	783	0.156	Schorfhaar and Schneeberger (1997)
	1993–1994	Trap net	800	0.200	Schorfhaar and Schneeberger (1997)
Marquette	1983–1985	Trap net	804	0.176	Schorfhaar and Schneeberger (1997)
	1993–1995	Trap net	786	0.183	Schorfhaar and Schneeberger (1997)
	1996–1998	Trap net	719	0.219	Michigan Department of Natural Resources
Munising	1983–1985	Trap net	774	0.186	Schorfhaar and Schneeberger (1997)
	1993–1995	Trap net	733	0.219	Schorfhaar and Schneeberger (1997)
	1986–1998	Trap net	706	0.234	Michigan Department of Natural Resources
Whitefish Bay, U.S. waters	1978	Trap net	748	0.251	Chippewa-Ottawa Resource Authority
	1984	Trap net	780	0.180	Chippewa-Ottawa Resource Authority
	1992	Trap net	671	0.232	Chippewa-Ottawa Resource Authority
	1997	Trap net	629	0.237	Chippewa-Ottawa Resource Authority

Note: In general, estimates of L_∞ decreased and K increased from the late 1970s to the early 1980s to the 1990s in response to increasing densities of lake whitefish.

Overview

Since 1970, much more is known about the Lake Superior fish community than was available at the time of SCOL-1. Contaminant loadings, sources, and burdens have been identified and monitored, with promising indications of declining levels in lake trout and their prey. Independent fish stock assessments have been implemented on larger temporal and spatial scales necessary to measure fish community changes and the range of population dynamics. Attention has also turned toward native species other than salmonines (lake sturgeon, brook trout, and walleye) to further fish community restoration. Given the degree of lotic habitat alteration, the recovery of some of these species may never approach historical levels but may be confined to a few areas with good habitat.

Commercial fishery production, a major factor in the initial decline of lake trout and lake herring, is limited by the need for conservation and for allocation of resources among diverse user groups and market conditions. Harvest is only a fraction of that historically and has shifted from state-licensed fishers to Native American users under court-reaffirmed treaty rights. The initial controversy over the exercising of these rights has led to increased cooperation among tribal, state, and federal fishery agencies and has resulted in a better understanding of the biology and management of the exploited populations.

Continued introductions of plants and animals have increased, potentially threatening the recovering fish community in unknown ways, and are likely one of the most significant threats to the ecosystem. Although many new invaders have been documented and the potential for greater colonization is rising with the onset of global warming, sea lamprey still appear to be the most deleterious as their impact was and can still be lakewide if control efforts falter. Predation by sea lamprey continues to be a problem and will require continued control with an integrated combination of methods and biological and economic evaluation of control options. Restoration of native species and naturalization of nonnative salmonines would not have been possible without sea lamprey control, which should be credited as the most significant management action to affect fish community recovery in Lake Superior. Although Pacific salmon have become naturalized and support small but popular fisheries, the need for additional stocking is being questioned given the levels of wild recruitment. Their impact on the ecosystem appears relatively small on a lakewide perspective but may have some consequences at finer spatial scales.

Lean lake trout, lake herring, and siscowet lake trout have recovered and are approaching precollapse levels of abundance. The latter two species have recovered without direct intensive intervention, which may demonstrate natural ecosystem resiliency, although the effects of sea lamprey control and lower fishing mortality cannot be overlooked. Current abundance of siscowets may be approaching an ancestral state unrecognized by most whose experience with Lake Superior follows years of prolonged overharvest and high levels of sea lamprey predation. Lake whitefish stocks have also recovered to higher levels mostly without directed management and under continued exploitation and may illustrate a biological potential in the absence of severe sea lamprey predation.

The fish community of Lake Superior has remained relatively intact and may also be responsible for the progress toward restoration. Other than paddlefish (*Polyodon spathula*) and arctic grayling (*Thymallus arcticus*), which were extirpated in the early 1800s and early 1900s, respectively, from Lake Superior tributaries (G. Smith, University of Michigan,

© 2003 NRC Canada

Ann Arbor, Mich., personal communication), there have been no native species losses from Lake Superior proper. Originally, the blackfin cisco (*Coregonus nigripinnis*) and shortnose cisco (*Coregonus reighardi*; Koelz 1929) were thought to be overfished to extinction; however, these fish never existed in Lake Superior and were likely shortjaw cisco (Todd and Smith 1980). Shortjaw ciscoe predominated historical commercial and assessment landings before 1950 but now make up only <5% of the deepwater ciscoes (T. Todd, U.S. Geological Survey, Great Lakes Science Center, Ann Arbor, MI 48105, personal communication); their decline may be related to targeted overfishing but this is our speculation. The apparent persistence of the deepwater fish community of Lake Superior is in stark contrast to that in the other Great Lakes where the deepwater piscivore (siscowet lake trout), planktivore (deepwater ciscoes), and benthivore (deepwater sculpins) assemblages were lost or disrupted from overfishing, exotic introductions, and cultural eutrophication (Eshenroder and Burnham-Curtis 1999). The deepwater fish community in Lake Superior, as was the case historically in the other Great Lakes, is highly evolved structurally and composed of species across all trophic levels (*Mysis* to siscowet) that are adapted for vertical migration (Eshenroder and Burnham-Curtis 1999). Vertical migration links production in benthic and pelagic communities through predation, thereby allowing these species to successfully use the vast hypolimnetic habitat present in Lake Superior and the other Great Lakes. This historical fish community is more sustainable than the exotic counterparts that dominate the other Great Lakes (Eshenroder and Burnham-Curtis 1999). Restoration in the other Great Lakes will likely be more difficult because of the absence of these ecologically important native species. Additionally, political and economic pressures that support less stable and sustainable fish communities composed of nonnative predator–prey complexes will also hamper restoration in the other Great Lakes.

The forage base of Lake Superior is now about 50% of its peak biomass in the early 1990s and the result of the combined effects of predation (principally from large standing stocks of lean and siscowet lake trout) and irregular recruitment of lake herring. Predation pressure appears to be high, as suggested by declining prey biomass coupled with the low occurrence of large rainbow smelt, ninespine stickleback, and slimy sculpin in bottom trawl surveys. Under the current predation pressure, rainbow smelt populations would likely not recover to pre-1978 levels. Future recruitment of lake herring is uncertain; therefore prey profiles will likely continue to consist of small rainbow smelt (<180 mm) and large adult lake herring and bloater (>200 mm). Lake trout growth and production may be highest using this prey profile (Mason et al. 1998) and suggests that the current forage situation may be desirable for this principal predator. Concern over forage demand by predators will resolve itself through density-dependent reductions in growth and survival and will remain largely out of the control of fishery managers, who have little influence on recruitment dynamics of forage fish and, to some extent, the major predator, siscowet lake trout.

Lawrie and Rahrar's (1972) prognosis for the future of Lake Superior focused on the recognition of hatcheries being critical to restoration of salmonine populations. Lean lake trout rehabilitation and establishment of Pacific salmon clearly would have been impossible without hatcheries. What probably was not envisioned was the relatively short time (30 years) that hatcheries contributed to the restoration effort, as the abundance of most salmonines in Lake Superior is no longer dependent on stocking. Hatcheries, however, will still continue to play a role in restoration of brook trout and lake sturgeon and hybrids such as splake. The recoveries of lake herring, siscowet, and lake whitefish are more noteworthy and in sharp contrast to the declining populations reported by Lawrie and Rahrar (1972). This suggests that past perturbations did not completely eliminate the reproductive and genetic potential for population increase. For siscowet and lake whitefish, reductions in sea lamprey predation and excessive fishing for prolonged periods were enough to result in restoration, whereas the case for lake herring is more complex given the intermittent recruitment over the last 20 years.

The future for Lake Superior appears to be brighter when compared with the other Great Lakes as the past 30 years is highlighted by recovery rather than by continued ecological disruption. For example, although certain Lake Michigan native fishes recovered after declines in alewife densities, certain invertebrates have declined and may be linked to continued exotic species invasions (Madenjian et al. 2002). Agencies on Lake Superior must now concentrate more on habitat protection and enhancement in nearshore and lotic areas and prevention of additional species introductions to further restore the fish community of Lake Superior.

Acknowledgments

We thank J. Bonde, J. Gunderson, C. Johnson, M. Halverson, S. Hellman, T. Halpern, S. Henderson, G. Sjervan, M. Neilson, J. Peck, S. Schram, D. Swackhamer, S. Sitar, and M. Whittle for their time, effort, and data. This is Contribution No. 1261 of the U.S. Geological Survey, Great Lakes Science Center, Ann Arbor, Mich. The Salmonid Communities in Oligotrophic Lakes (SCOL) workshop was sponsored by the Great Lakes Fishery Commission to revisit Great Lakes ecosystem change three decades since the first SCOL symposium, which was convened at Geneva Park, Ont., in July 1971 and for which the proceedings were subsequently published as a special issue of the Journal of the Fisheries Research Board of Canada (Vol. 29, No. 6, June 1972). The first paper in the SCOL-2 revisited series was previously published in this journal (Madenjian et al. 2002, Vol. 59, pp. 736–753).

References

Anderson, E.D., and Smith, L.L. 1971. Factors affecting the abundance of lake herring (*Coregonus artedii* Lesueur) in western Lake Superior. Trans. Am. Fish. Soc. **100**: 691–707.

Beeton, A.M. 1965. Eutrophication of the St. Lawrence Great Lakes. Limnol. Oceanogr. **10**: 240–254.

Bence, J.R., and Ebener, M.P. 2002. Summary status of lake trout and whitefish populations in the 1836 treaty-ceded waters of Lakes Superior, Huron, and Michigan in 2000, with recommended yield and effort levels for 2001. Technical Fisheries Committee, Michigan Department of Natural Resources, Charlevoix, Mich.

© 2003 NRC Canada

Bergstedt, R.A., and Schneider, C.P. 1988. Assessment of sea lamprey (*Petromyzon marinus*) predation by recovery of dead lake trout (*Salvelinus namaycush*) from Lake Ontario, 1982–85. Can. J. Fish. Aquat. Sci. **45**: 1406–1410.

Bjerselius, R., Li, W., Teeter, J.H., Seelye, J.E., Johnson, P.B., Maniak, P.J., Grant, G.C., Polkinghorne, C.N., and Sorensen, P.W. 2000. Direct behavioral evidence that unique bile acids released by larval sea lamprey (*Petromyzon marinus*) function as a migratory pheromone. Can. J. Fish. Aquat. Sci. **57**: 557–569.

Brazner, J.C., Tanner, D.K., Jensen, D.A., and Lemke, A. 1998. Relative abundance and distribution of ruffe (*Gymnocephalus cernuus*) in a Lake Superior coastal wetland fish assemblage. J. Gt. Lakes Res. **24**: 293–303.

Bronte, C.R., and Hoff, M.H. 1996. Population status and trends for Lake Superior forage fishes, 1978–95. *In* Minutes of the 1996 Annual Meeting of the Lake Superior Committee, Great Lakes Fishery Commission. Great Lakes Fishery Commission, Ann Arbor, Mich.

Bronte, C.R., Selgeby, J.H., and Curtis, G.L. 1991. Distribution, abundance, and biology of the alewife in U.S. waters of Lake Superior. J. Gt. Lakes Res. **17**: 304–313.

Bronte, C.R., Selgeby, J.H., and Swedberg, D.V. 1993. Dynamics of yellow perch in western Lake Superior. N. Am. J. Fish. Manag. **13**: 511–523.

Bronte, C.R., Schram, S.T., Selgeby, J.H., and Swanson, B.L. 1995. Density independent survival of wild lake trout in the Apostle Islands area of Lake Superior. J. Gt. Lakes Res. **21**(Suppl. 1): 246–252.

Bronte, C.R., Hesselberg, R.J., Shoesmith, J.A., and Hoff, M.H. 1996. Discrimination among spawning concentrations of Lake Superior lake herring based on trace element profiles in sagittae. Trans. Am. Fish. Soc. **125**: 852–859.

Bronte, C.R., Evrard, L.M., Brown, W.P., Mayo, K.R., and Edwards, A.J. 1998. Fish community changes in the St. Louis River, Lake Superior, 1989–1996: is it ruffe or population dynamics? J. Gt. Lakes Res. **24**: 309–318.

Brown, R.W., Ebener, M.P., and Gorenflo, T. 1999. Great Lakes commercial fisheries: historical overview and prognosis for the future. *In* Great Lakes fisheries policy and management. *Edited by* W.W. Taylor and C.P. Ferreri. Michigan State University Press, East Lansing, Mich. pp. 307–354.

Burnham-Curtis, M.K. 2001. Genetic profiles of selected brook trout *Salvelinus fontinalis* populations from Lake Superior. Research Completion Report. U.S. Geological Survey, Great Lakes Science Center, Ann Arbor, MI 48105.

Busiahn, T.R. 1985. Predator responses to fish community changes in Lake Superior. *In* Presented papers from the Council of Lake Committees Plenary Session of Great Lakes predator prey issues, March 20, 1985. *Edited by* R.L. Eshenroder. Gt. Lakes Fish. Comm. Spec. Publ. 85-3. pp. 39–56.

Busiahn, T.R. (*Editor*). 1990. Fish community objectives for Lake Superior. Gt. Lakes Fish. Comm. Spec. Publ. 90-1.

Christie, W.J., and Kolenofsky, D.P. 1980. Parasitic phase of sea lamprey (*Petromyzon marinus*) in Lake Ontario. Can. J. Fish. Aquat. Sci. **37**: 2021–2038.

Christie, G.C., and Regier, H.A. 1988. Measures of optimal thermal habitat and their relationship to yields of four commercial fish species. Can. J. Fish. Aquat. Sci. **45**: 301–314.

Conner, D.J., Bronte, C.R., Selgeby, J.H., and Collins, H.L. 1993. Food of salmonine predators in Lake Superior. G Lakes Fish. Comm. Tech. Rep. No. 59.

Coutant, C.C. 1977. Compilation of temperature preference data. J. Fish. Res. Board Can. **34**: 739–745.

Czypinski, G.D., Hintz, A.K., Weimer, M.T., and Dextrase, A. 2001. Surveillance for ruffe in the Great Lakes, 2000. Combined report of the U.S. Fish and Wildlife Service and Ontario Ministry of Natural Resources. U.S. Fish and Wildlife Service, 2800 Lake Shore Drive East, Ashland, WI 54806.

D'Amelio, S. 2002. Conservation genetics and metapopulation structure of brook trout (*Salvelinus fontinalis*) in Nipigon Bay (Lake Superior, Ontario). M.Sc. thesis, Trent University, Peterborough, Ont.

Dawson, V.K., Bills, T.D., and Boogaard, M.A. 1998. Avoidance behavior of ruffe exposed to selected formulations of piscicides. J. Gt. Lakes Res. **24**: 343–350.

Dryer, W.R., and Beil, J. 1964. Life history of lake herring in Lake Superior. Fish. Bull. **63**: 493–529.

Ebener, M.P. 1990. Assessment and mark–recapture of lake whitefish spawning stocks around the Keweenaw Peninsula area of Lake Superior, 1987–1990. Admin. Rep. 90-10, Great Lakes Indian Fish and Wildlife Commission, Odanah, Wis.

Ebener, M.P. 1995. Bioenergetics of predator fish in western U.S. waters of Lake Superior. Report prepared for the Red Cliff Band of Lake Superior Chippewas, Red Cliff Fisheries Department, Bayfield, Wis.

Ebener, M.P. 1998. Sea lamprey marking of lake trout in Lake Superior, spring 1997. *In* Minutes of the 1998 Annual Meeting of the Lake Superior Committee, Great Lakes Fishery Commission. Great Lakes Fishery Commission, Ann Arbor, Mich.

Edsall, T.A., and Kennedy, G.W. 1995. Availability of lake trout reproductive habitat in the Great Lakes. J. Gt. Lakes Res. **21**(Suppl. 1): 290–301.

Eisenreich, S.J., and Strachan, W.M.J. 1992. Estimating atmospheric deposition of toxic contaminants to the Great Lakes: an update. Environment Canada – Great Lakes Protection Fund, Burlington, Ont.

Eschmeyer, P.H., and Phillips, A.M. 1965. Fat content of the flesh of siscowets and lake trout from Lake Superior. Trans. Am. Fish. Soc. **94**: 62–74.

Eshenroder, R.L., and Burnham-Curtis, M.K. 1999. Species succession and sustainability of the Great Lakes fish community. *In* Great Lakes fisheries policy and management. *Edited by* W.W. Taylor and C.P. Ferreri. Michigan State University Press, East Lansing, Mich. pp. 307–354.

Fausch, D.F., and White, R.J. 1986. Competition among juveniles of coho salmon, brown trout and brook trout in a laboratory stream, and implications for Great Lakes tributaries. Trans. Am. Fish. Soc. **115**: 336–381.

Glassmeyer, S.T., DeVault, D.S., and Hites, R.A. 2000. Rates at which toxaphene concentrations decrease in lake trout from the Great Lakes. Environ. Sci. Technol. **34**: 1851–1855.

Goodier, J.L. 1981. Native lake trout (*Salvelinus namaycush*) stocks in the Canadian waters of Lake Superior prior to 1955. Can. J. Fish. Aquat. Sci. **38**: 1724–1737.

Great Lakes Fishery Commission. 1992. Strategic vision of the Great Lakes Fishery Commission for the decade of the 1990s. Great Lakes Fishery Commission, Ann Arbor, Mich.

Hansen, M.J. 1999. Lake trout in the Great Lakes: basinwide stock collapse and binational restoration. *In* Great Lakes fisheries policy and management. *Edited by* W.W. Taylor and C.P. Ferreri. Michigan State University Press, East Lansing, Mich. pp. 417–454.

Harvey, C.J. 2001. A stable isotope analysis of the food web structure in Lake Superior. Ph.D. dissertation, University of Wisconsin, Madison, Wis.

Harvey, C.J., and Kitchell, J.F. 2000. A stable isotope evaluation of the structure and spatial heterogeneity of a Lake Superior food web. Can. J. Fish. Aquat. Sci. **57**: 1395–1403.

© 2003 NRC Canada

Harvey, C.J., Schram, S.T., and Kitchell, J.F. 2003. Trophic relationships among lean and siscowet lake trout in Lake Superior. Trans. Am. Fish. Soc. **132**: 219–228.

Heinrich, J.W., Mullet, K.I., Hansen, M.J., Christie, G.T., Klar, D.A., Johnson, D.A., Young, R.J., and Adams, J.V. 2003. Sea lamprey control and abundance in Lake Superior 1957–1999. J. Gt. Lakes Res. **29**(Suppl. 1): 567–584.

Henderson, B.A., and Brown, E.H., Jr. 1985. Effects of the abundance and water temperatures on recruitment and growth of alewife near South Bay, Lake Huron, 1954–82. Can. J. Fish. Aquat. Sci. **42**: 1608–1613.

Hengeveld, H.G. 1990. Global climate change: implications for air temperature and water supply in Canada. Trans. Am. Fish. Soc. **119**: 176–182.

Hill, D.K., and Magnuson, J.J. 1990. Potential effects of global climate warming on the growth and prey consumption of Great Lakes fishes. Trans. Am. Fish. Soc. **119**: 265–275.

Hokansen, K.E.F. 1977. Temperature requirements of some percids and adaptations to the seasonal temperature cycle. J. Fish. Res. Board Can. **34**: 1525–1550.

Horns, W.H., Brown, W.P., Hulse, S.R., and Bronte, C.R. 2000. Seasonal changes in ruffe abundance in two Lake Superior tributaries: implications for control. N. Am. J. Fish. Manag. **20**: 821–825.

Horns, W.H., Bronte, C.R., Busiahn, T.R., Ebener, M.P., Eshenroder, R.L., Gorenflo, T., Kmiecik, N., Mattes, W., Peck, J.W., Petzold, M., and Schreiner, D.R. 2003. Fish community objectives for Lake Superior — 2000. Gt. Lakes Fish. Comm. Spec. Publ. 03-01.

Johnson, T.B., and Evans, D.O. 1990. Size-dependent winter mortality of young-of-the-year white perch: climate warming and invasion of the Laurentian Great Lakes. Trans. Am. Fish. Soc. **119**: 301–313.

Khan, N.Y., and Qadri, S.U. 1970. Morphological differences in Lake Superior char. J. Fish. Res. Board Can. **27**: 161–167.

King, E.L., Jr. 1980. Classification of sea lamprey (*Petromyzon marinus*) attack marks on Great Lakes lake trout (*Salvelinus namaycush*). Can. J. Fish. Aquat. Sci. **37**: 1989–2006.

Kitchell, J.F., Cox, S.P., Harvey, C.J., Johnson, T.B., Mason, D.M., Schoen, K.K., Aydin, K., Bronte, C., Ebener, M., Hansen, M., Hoff, M., Schram, S., Schreiner, D., and Walters, C.J. 2000. Sustainability of the Lake Superior fish community: interactions in a food web. Ecosystems, **3**: 545–560.

Koelz, W. 1929. Coregonid fishes of the Great Lakes. Bull. U.S. Bur. Fish. **43**: 297–643.

Krueger, C.C., and Ihssen, P.E. 1995. Review of genetics of lake trout in the Great Lakes: history, molecular genetics, physiology, strain comparisons and restoration management. J. Gt. Lakes Res. **21**(Suppl. 1): 348–363.

Krueger, C.C., and May, B. 1987. Stock identification of naturalized brown trout in Lake Superior tributaries: differentiation based on allozyme data. Trans. Am. Fish. Soc. **116**: 785–794.

Krueger, C.C., Perkins, D.L., Everett, R.J., Schreiner, D.R., and May, B. 1994. Genetic variation in naturalized rainbow trout (*Oncorhynchus mykiss*) from Minnesota tributaries to Lake Superior. J. Gt. Lakes Res. **20**: 299–316.

Lawrie, A.H., and Rahrer, J.F. 1972. Lake Superior: effects of exploitation and introduction on the salmonid community. J. Fish. Res. Board Can. **29**: 765–776.

Li, W., Scott, A.P., Siefkes, M.J., Yan, H., Liu, Q., Yun, S., and Gage, D.A. 2002. Bile acid secreted by male sea lamprey that acts as a sex pheromone. Science (Wash., D.C.), **296**: 138–141.

MacCallum, W.R., and Selgeby, J.H. 1987. Lake Superior revisited 1984. Can. J. Fish. Aquat. Sci. **44**: 23–36.

Madenjian, C.P., Fahnenstiel, G.L., Johengen, T.H., Nalepa, T.F., Vanderploeg, H.A., Fleischer, G.W., Schneeberger, P.J., Benjamin, D.M., Smith, E.B., Bence, J.R., Rutherford, E.S., Lavis, D.S., Robertson, D.M., Jude, D.J., and Ebener, M.P. 2002. Dynamics of the Lake Michigan food web, 1970–2000. Can. J. Fish. Aquat. Sci. **59**: 736–753.

Magnuson, J.J., Meisner J.D., and Hill, D.K. 1990. Potential changes in thermal habitat of Great Lakes fishes due to global climate warming. Trans. Am. Fish. Soc. **119**: 254–264.

Magnuson, J.J., Webster, K.E., Assel, R.A., Bowser, C.J., Dillon, P.J., Eaton, J.G., Evans, H.E., Fee, E.J., Hall, R.I., Mortsch, L.R., Schindler, D.W., and Quinn, F.H. 1997. Potential effects of climate changes on aquatic systems: Laurentian Great Lakes and precambrian shield region. Hydrol. Process. **2**: 825–871.

Mandrak, N.E. 1989. Potential invasion of the Great Lakes by fish species associated with climate warming. J. Gt. Lakes Res. **15**: 306–316.

Mason, D.M., Johnson, T.B., and Kitchell, J.F. 1998. Consequences of prey fish community dynamics on lake trout (*Salvelinus namaycush*) foraging efficiency in Lake Superior. Can. J. Fish. Aquat. Sci. **55**: 1273–1284.

Mayo, K.R., Selgeby, J.H., and McDonald, M.E. 1998. A bioenergetics modeling evaluation of top-down control of ruffe in the St. Louis River, western Lake Superior. J. Gt. Lakes Res. **24**: 329–342.

Meisner, D., Goodier, J.L., Regier, H.A., Shuter, B.J., and Christie, J.W. 1987. An assessment of the effects of climate warming on Great Lakes basin fishes. J. Gt. Lakes Res. **15**: 340–352.

Mills, E.L., Leach, J.H., Carlton, J.T., and Secor, C.L. 1993. Exotic species in the Great Lakes: a history of biotic crises and anthropogenic introductions. J. Gt. Lakes Res. **19**: 1–54.

Moore, S.A., and Bronte, C.R. 2001. Delineation of sympatric morphotypes of lake trout in Lake Superior. Trans. Am. Fish. Soc. **130**: 1233–1240.

Negus, M.T. 1995. Bioenergetics modeling as a salmonine management tool applied to Minnesota waters of Lake Superior. N. Am. J. Fish. Manag. **15**: 60–78.

Newman, L.E., Dubois, R.B., and Halpern, T.N. 1999. A brook trout rehabilitation plan for Lake Superior. Brook Trout Subcommittee report to the Lake Superior Technical Committee, Great Lakes Fishery Commission. Great Lakes Fishery Commission, Ann Arbor, Mich.

Nunan, P.J. 1967. Pink salmon in Lake Superior. Ont. Fish Wildl. Rev. **6**: 8–13.

Nyberg, P., Bergstrand, E., Degerman, E., and Enderlein, O. 2001. Recruitment of pelagic fish in an unstable climate: studies in Sweden's four largest lakes. Ambio, **30**: 559–564.

Peck, J.W. 1977. Species composition of deep-water ciscoes (chubs) in commercial catches from Michigan waters of Lake Superior. Res. Rep. No. 1849, Michigan Department of Natural Resources, Fisheries Division, Ann Arbor, Mich.

Peck, J.W. 1992. The sport fishery and contribution of hatchery trout and salmon in Lake Superior and tributaries at Marquette, Michigan, 1984–87. Res. Rep. No. 1975, Michigan Department of Natural Resources, Fisheries Division, Ann Arbor, Mich.

Peck, J. 1994. Effects of commercial fishing on an unexploited lake whitefish population in Michigan's waters of Lake Superior, 1983–1989. Res. Rep. No. 2007, Michigan Department of Natural Resources, Fisheries Division, Ann Arbor, Mich.

Peck, J.W., MacCallum, W.R., Schram, S.T., Schreiner, D.R., and Shively, J.D. 1994. Other salmonines. *In* The state of Lake Superior in 1992. *Edited by* M.J. Hansen. Gt. Lakes Fish. Comm. Spec. Publ. 94-1. pp. 35–52.

© 2003 NRC Canada

Peck, J.W., Jones, T.S., MacCallum, W.R., and Schram, S.T. 1999. Contribution of hatchery-reared fish to chinook salmon populations and sport fisheries in Lake Superior. N. Am. J. Fish. Manag. **19**: 155–164.

Petzold, M. 1999. Recent history of lake whitefish in Ontario waters of Lake Superior. *In* Minutes of the Lake Superior Committee Annual Meeting, March 23–24, 1999. Great Lakes Fishery Commission, Ann Arbor, Mich.

Rakoczy, G.P. 1983. Harvest levels for commercial exploited stocks of lake whitefish in Michigan waters of Lake Superior. Fish. Res. Rep. No. 1912, Michigan Department of Natural Resources, Fisheries Division, Ann Arbor, Mich.

Regier, H.A., Holmes, J.A., and Pauly, D. 1990. Influence of temperature changes on aquatic ecosystems: an interpretation of empirical data. Trans. Am. Fish. Soc. **119**: 374–389.

Richards, J.M., Hansen, M.J., Bronte, C.R., and Sitar, S.P. 2004. Recruitment dynamics of the 1971–1991 year classes of lake trout in Michigan waters of Lake Superior. N. Am. J. Fish. Manag. In press.

Robertson, D.M. 1997. Regionalized loads of sediment and phosphorous to Lakes Michigan and Superior — high flow and long-term average. J. Gt. Lakes Res. **23**: 416–439.

Rose, G.A. 1986. Growth decline in sub-yearling brook trout (*Salvelinus fontinalis*) after emergence of rainbow trout (*Salmo gairdneri*). Can. J. Fish. Aquat. Sci. **55**: 1273–1284.

Schneider, C.P., Owens, R.W., Bergstedt, R.A., and O'Gorman, R. 1996. Predation by sea lamprey (*Petromyzon marinus*) on lake trout (*Salvelinus namaycush*) in southern Lake Ontario, 1982–1992. Can. J. Fish. Aquat. Sci. **53**: 1921–1932.

Schorfhaar, R.G., and Peck, J.W. 1993. Catch and mortality of non-target species in lake whitefish trap nets in Michigan waters of Lake Superior. Fish. Res. Rep. No. 1974, Michigan Department of Natural Resources, Ann Arbor, Mich.

Schorfhaar, R.G., and Schneeberger, P.J. 1997. Commercial and sport fisheries for lake whitefish in Michigan waters of Lake Superior, 1983–96. Fish. Res. Rep. No. 2034, Michigan Department of Natural Resources, Fisheries Division, Ann Arbor, Mich.

Schram, S.T., Selgeby, J.H., Bronte, C.R., and Swanson, B.L. 1995. Population recovery and natural recruitment of lake trout at Gull Island Shoal, Lake Superior, 1964–92. J. Gt. Lakes Res. **21**(Suppl. 1): 225–232.

Schreiner, D.R. (*Editor*). 2003. Rainbow trout management plan for the Minnesota waters of Lake Superior. Spec. Publ. No. 157, Minnesota Department of Natural Resources, Division of Fisheries, St. Paul, Minn.

Selgeby, J.H. 1982. Decline of lake herring (*Coregonus artedii*) in Lake Superior: an analysis of the Wisconsin herring fishery. Can. J. Fish. Aquat. Sci. **39**: 554–563.

Selgeby, J.H., MacCallum, W.R., and Swedberg, D.V. 1978. Predation by rainbow smelt (*Osmerus mordax*) on lake herring (*Coregonus artedi*) in western Lake Superior. J. Fish. Res. Board Can. **35**: 1457–1463.

Selgeby, J.H., MacCallum, W.R., and Hoff, M.H. 1994. Rainbow smelt – larval lake herring interactions: competitors or casual acquaintances? Biol. Surv. Rep. No. 25, National Biological Survey, Washington, D.C.

Shuter, B.J., and Post, J.R. 1990. Climate, population viability, and the zoogeography of temperate fishes. Trans. Am. Fish. Soc. **119**: 314–336.

Sinokrot, B.A., Stefan, H.G., McCormick, J.H., and Eaton, J.G. 1995. Modeling of climate change effects on stream temperatures and fish habitats below barrier dams and near groundwater inputs. Clim. Change, **30**: 181–200.

Smith, B.R., and Tibbles, J.J. 1980. Sea lamprey (*Petromyzon marinus*) in Lakes Huron, Michigan, and Superior: history of invasion and control, 1936–78. Can. J. Fish. Aquat. Sci. **37**: 1780–1801.

Smith, S.H. 1970. Species interactions of the alewife in the Great Lakes. Trans. Am. Fish. Soc. **99**: 754–765.

Stewart, D.J., and Ibarra, M. 1991. Predation and production by salmonine fishes in Lake Michigan, 1978–88. Can. J. Fish. Aquat. Sci. **48**: 909–922.

Swackhamer, D.L., Schottler, S., and Pearson, R.F. 1999. Air–water exchange and mass balance of toxaphene in the Great Lakes. Environ. Sci. Technol. **33**: 3864–3872.

Swink, W.D. 1991. Host-size selection by parasitic sea lampreys. Trans. Am. Fish. Soc. **120**: 637–643.

Technical Fisheries Review Committee. 1992. Status of the fishery resource — 1991. A report by the Technical Fisheries Review Committee on the assessment of lake trout and lake whitefish in treaty-ceded waters of the upper Great Lakes: State of Michigan. Mimeo. Report, Technical Fisheries Review Committee. Michigan Department of Natural Resources, Charlevoix, Mich.

Todd, T.N. 1981. Allelic variability in species and stocks of Lake Superior ciscoes (Coregonidae). Can. J. Fish. Aquat. Sci. **38**: 1808–1813.

Todd, T.N., and Smith, G.R. 1980. Differentiation in *Coregonus zenithicus* in Lake Superior. Can. J. Fish. Aquat. Sci. **37**: 2228–2235.

Todd, T.N., Smith, G.R., and Cable, L.E. 1981. Environmental and genetic contributions to morphological differentiation in ciscoes (Coregoninae) of the Great Lakes. Can. J. Fish. Aquat. Sci. **38**: 59–67.

Turgeon, J., Estoup, A., and Bernatchez, L. 1999. Species flock in the North American Great Lakes: molecular ecology of Lake Nipigon ciscoes (Teleostei: Coregonidae: *Coregonus*). Evolution, **53**: 1857–1871.

Upper Great Lakes Management Unit. 2001. Lake Superior annual report 2000. Ontario Ministry of Natural Resources, Thunder Bay, Ont.

Wilberg, M., Hansen, M.J., and Bronte, C.R. 2003. Historic and modern abundance of wild lean lake trout in Michigan waters of Lake Superior: implications for restoration goals. N. Am. J. Fish. Manag. **23**:100–108.

Wismer, C.A., and Christie, A.E. 1987. Temperature relationships of Great Lakes fishes: a data compilation. Gt. Lakes Fish. Comm. Spec. Publ. 87-3.

© 2003 NRC Canada

ERRATUM / ERRATUM

Erratum: Planktonic invaders of the St. Lawrence estuarine transition zone: environmental factors controlling the distribution of zebra mussel veligers

Christine Barnard, Jean-Jacques Frenette, and Warwick F. Vincent

Ref: Can. J. Fish. Aquat. Sci. **60**: 1245–1257 (2003).

On page 1245, on line 6 of the left-hand column, "175 000 m^{2}" should read "175 000 individuals·m^{-2}".

On page 1246, in the left-hand column in the paragraph beginning "Zebra mussel veligers...", on lines 5 and 6, "According to these authors, the size spectrum of their prey varies between 1 and 9 μm." should instead read "According to Sprung (1993), the size spectrum of their prey varies between 1 μm and 4 μm, whereas Wright et al. (1996) observed up to 6 μm."

On page 1248, under Chlorophyll *a*, on the 9th line, "(0.001 mol·m^{-3} HCl)" should read "(10 mol·m^{-3} HCl)".

On page 1256, in the 1st paragraph under Impacts of veligers on the food web, on lines 21 and 22, "... (prey size spectrum 1–9 μm)..." should read "... (prey size spectrum 1–6 μm)...".

Accepted 19 November 2003. Received at NRC 8 December 2003. Published on the NRC Research Press Web site at http://cjfas.nrc.ca on 22 December 2003.
J16978E

C. Barnard and J.-J. Frenette.[1] Département de chimie-biologie, Université du Québec à Trois-Rivières, C.P. 500, Trois-Rivières, QC G9A 5H7, Canada.
W.F. Vincent. Département de biologie, Université Laval, Sainte-Foy, QC G1K 7P4, Canada.

[1]Corresponding author (e-mail: jean-jacques_frenette@uqtr.ca).

 doi: 10.1139/F03-161 © 2003 NRC Canada

Canadian Journal of Fisheries and Aquatic Sciences

Author Index
Volume 60, 2003

Journal canadien des sciences halieutiques et aquatiques

Index des auteurs
Volume 60, 2003

Aanes, S., 259
Abrams, P.A., 1353
Aherne, J., 1095
Allan, J.D., 309
Allard, J., 1190
Allendorf, F.W., 1440
Arai, M.N., 825
Aschan, M., 1539
Audet, D., 269
Avendaño, P., 1229
Aydin, K.Y., 1161
Badalamenti, F., 222
Bailey, N., 542
Baker, E., 491
Baldwin, B.S., 1432
Ballantyne, A.P., 12
Ballarin, L., 949
Ballert, A.G., 740
Barbier, E.B., 171
Barnard, C., 1245, 1575
Bence, J.R., 55
Benfield, M.C., 759
Bengtson, D.A., 929
Bentzen, P., 433
Berejikian, B.A., 690
Bergstedt, R.A., 23
Bisson, P.A., 1007
Blanchard, J.L., 321
Boggs, C.H., 1161
Boisclair, D., 1149, 1386, 1398
Borgmann, U., 352
Bos, D.G., 1177
Botsford, L.W., 971
Boudreau, S.A., 1307
Boustead, N.C., 1
Bradford, M.J., 390
Breen, P.A., 527
Brett, M.T., 12
Brichon, G., 1281
Brodeur, R.D., 1517
Bronte, C.R., 1552
Brown, J.A., 1289
Buckley, L.J., 929
Bunnell, D.B., 1314
Butler, M.G., 721
Caouette, J.P., 309
Carney, E.C., 43
Carpenter, G., 1258
Casselman, J.M., 471
Castro-Santos, T., 986
Charette, T., 584
Chenery, S.R., 1376
Chick, J.H., 1437
Chilcote, M.W., 1057
Chow-Fraser, P., 676
Chu, C., 624
Clark, B.J., 959
Claytor, R., 1190
Coburn, M.M., 117
Colautti, R.I., 740
Collie, J.S., 1133
Collins, N., 1345
Conde Porcuna, J.M., 919
Copley, N.J., 759
Cosgriff, R.J., 1437
Couture, P., 269
Cózar, A., 411
Croteau, M.-N., 800
Cumming, B.F., 1177
Da Ros, L., 949
Dayton, J., 1432
De Meester, L., 919
De Robertis, A., 1517
Death, R.G., 603
deBruyn, A.M.H., 1332
Declerck, S., 919
Dekker, W., 787
Deriso, R.B., 1204
Dermott, R., 471
DeVault, D.S., 1552
Dillon, P.J., 203, 959, 1095
Dinmore, T.A., 1306
Drinkwater, K.F., 563
Dunham, J.B., 840
Dunsmuir, A.L., 825
Duplisea, D.E., 1306
Ebener, M.P., 1552
Ebersole, J.L., 1266
Eggleston, D.B., 873
Enders, E.C., 1149
Essington, T.E., 1161
Etherington, L.L., 873
Evans, H.E., 959
Fairgrieve, W.T., 690
Fausch, K.D., 1018, 1502
Fiedler, P.C., 1161
Findlay, C.S., 1078
Finley, C.A., 1424
Finn, R.N., 1324
Finstad, A.G., 1104
Fisher, N.S., 1369
Fisher, T.R., 1122
Fitzsimons, J.D., 471
Flanagan, K.M., 635
Fleischer, G.W., 55
Floeter, J., 140
Francis, R.C., 1161
Francis, R.I.C.C., 441
Frank, K.T., 321
Fransen, B.R., 1007
Frenette, J.-J., 1245, 1575
Friedland, K.D., 563
Friedman, C.S., 1424
Frissell, C.A., 1266, 1440
Fryer, R.J., 448
Gal, G., 471
Gálvez, J.A., 411
García, C.M., 411
Gardner, B., 344
Garvey, J.E., 938
Geenens, V., 919
Gende, S.M., 553
Girard, P., 1386
Gittanger, L.S., 1437
Goldman, C.R., 1452
González, M.J., 1314
Goto, A., 421
Gotwalt, P.S., 301
Graham, N., 448
Grant, J.W.A., 193
Greene, C.H., 759
Grigorovich, I.A., 740
Grosjean, Ph., 237
Grout, J.A., 390
Guay, J.C., 1398

© 2003 NRC Canada

Guy, C.S., 830
Haigh, R., 640
Hanson, M.A., 721
Harbitz, A., 1539
Hare, L., 800
Haro, A., 986
Hastings, A., 971
Hayes, J.W., 1462
Heino, J., 1039
Heist, E.J., 670
Henderson, B.A., 1345
Henderson, J.N., 32
Hilborn, R., 527
Hinrichsen, R.A., 864
Hirvonen, H., 1104
Hitt, N.P., 1440
Hjelm, J., 700
Holeck, K.T., 471, 740
Holland, D.S., 159
Holt, C.A., 151
Houlahan, J.E., 1078
Hoyle, J.A., 471
Hughes, N.F., 1462
Humphries, P., 773
Hutchings, J.A., 1111
Isaak, D.J., 840
Jacobs, M.C., 825
Jangoux, M., 237
Jansen, P.A., 1104
Jassby, A.D., 1452
Jennings, S., 1306
Jensen, D.A., 1552
Johannsson, O.E., 471
Johansen, J.R., 117
Jones, C.M., 361
Jones M.L., 1527
Jones, N.E., 849
Jonsson, B., 506
Jonsson, N., 506
Jordaan, A., 1289
Juanes, F., 594
Kainz, M., 888
Kanehl, P., 491
Katopodis, C., 849
Kim, S.W., 527
King, A.J., 773
Kinnison, M.T., 1
Kirlin, R.L., 1299
Kitchell, J.F., 1161
Kocik, J.F., 214
Kraft, C.E., 379
Ladouceur, A.R., 825
Lake, P.S., 773
Lantry, B.F., 471
Lapointe, M., 1398
Latterell, J.J., 1007
Lavery, A.C., 759
Leclerc, M., 1386, 1398
Legendre, P., 1301
Lembo, A.J., Jr., 344
Lesack, L.F.W., 333
Letcher, B.H., 32
Li, W., 23
Liss, W.J., 1266
Lozano, S.J., 1552
Lucotte, M., 888
Lund, M.E.A., 460
Lund, S.G., 460
Lyons, J., 491
Ma, A., 1432
MacGregor, B.W., 809
MacIsaac, H.J., 740
Magee, J.A., 214
Maguire, J.-J., 159
Makarewicz, J.C., 471
Mandrak, N.E., 624
Marcogliese, D.J., 1332
Marin, M.G., 949
Marschall, E.A., 938
Marty, G.D., 1258
Matos, L., 612
Matozzo, V., 949
Matthaei, C.D., 731
Maunder, M.N., 527, 1204
Mayer, M.S., 1432
McCann, K.S., 971
McCauley, E., 635
McClanahan, T.R., 171
McCormick, S.D., 214
McIntyre, T.M., 1111
McLaren, I.A., 1229
McLean, J.E., 433
McMenemy, J.R., 563
McNair, S.A., 676
Melo, A.S., 731
Mendillo, J., 1432
Meneghetti, F., 949
Meyers, T.R., 1258
Millard, E.S., 471
Miller, E.K., 1477
Miller, S.A., 203
Mills, E.L., 471, 740, 1432
Milton, D.A., 1376
Minns, C.K., 100, 624
Mion, J.B., 1527
Mitro, M.G., 135
Molot, L.A., 203, 959
Moore, A., 1432
Moore, J.E., 100
Moore, T.R., 612
Morgan, G.E., 1345
Morinville, G.R., 401
Morrison, W.E., 1487
Mueter, F.J., 757
Muhlfeld, C.C., 1440
Munawar, I.F., 471
Munawar, M., 471
Muotka, T., 1039
Naiman, R.J., 1007
Negishi, J.N., 247
Nelson, J.A., 301
Netto, J.K., 1527
Nicholls, K.H., 43
Nickelson, T., 1050
Niemela, S., 491
Niyogi, D.K., 731
Noonburg, E.G., 1353
O'Gorman, R., 471
Obedzinski, M., 214
Olson, R.J., 1161
Owens, R.W., 471
Paasivirta, L., 1039
Paavola, R., 1039
Pálsson, Ó.K., 1409
Parkos, J.J., III, 182
Parrish, C.C., 888
Parrish, D.L., 279
Pau, N., 1432
Paulsen, C.M., 1122
Peck, M.A., 929
Perry, R.W., 390
Peterman, R.M., 757, 809
Peterson, D.P., 1502
Petzold, M.M., 1552
Pinnegar, J.K., 222
Podoor, N., 919
Polovina, J.J., 1161
Polunin, N.V.C., 222
Pratt, T.C., 286
Prepas, E.E., 584
Preston, J.M., 1299
Price, C.S., 910
Prowse, T., 635
Prussian, A., 309
Punt, A.E., 1217
Pyper, B.J., 757, 809
Quinn, T.J., II, 1258
Quinn, T.P., 1, 433, 553
Quist, M.C., 830
Raffenberg, M.J., 279
Rasmussen, J.B., 401, 1332
Rasmussen, P., 491
Reddin, D.G., 563
Reilly, S.B., 1161
Reiss, C.S., 1229

© 2003 NRC Canada

Reuter, J.E., 1452
Reynolds, J.A., 370
Rich, B.A., 135
Richards, C., 1552
Richardson, J.S., 247
Rieman, B.E., 840
Roberts, C.M., 171
Rochet, M.-J., 67, 86
Rodgers, J., 309
Rodwell, L.D., 171
Rogers, D.E., 553
Rønnestad, I., 1324
Rosati, T.C., 117
Roulet, N.T., 612
Roy, A.G., 1149
Rudstam, L.G., 471
Ruggerone, G.T., 553
Ruttan, L.M., 1068
Ryer, C.H., 1517
Salthaug, A., 259
Santucci, V.J., Jr., 182
Schaner, T., 471
Schindler, D.E., 12
Schnute, J.T., 640
Schreck, C.B., 910
Schreiner, D.R., 1552
Schrey, A.W., 670
Scrimgeour, G.J., 849
Secor, D.H., 1487
Seelbach, P., 491
Shearer, K.A., 1462
Shertzer, K.W., 710, 1037
Shuter, B.J., 1353
Sibbing, F.A., 700
Siefkes, M.J., 23
Simon, J.E., 321
Simon, T., 491
Smokorowski, K.E., 286
Snodgrass, J.W., 301
Somers, K.M., 151
Spirlet, Ch., 237
Squires, M.M., 333
Stanton, T.K., 759
Steedman, R.J., 43
Stein, R.A., 1314
Steingrímsson, S.Ó., 193
Stemberger, R.S., 1477
Stephen, J.L., 830
Stewart, P.M., 491
Stewart, T.J., 471
Stockwell, J.D., 1527
Stoeckmann, A., 126
Sullivan, M., 1432
Sullivan, P.J., 344
Swain, D.P., 897
Swanson, P., 690
Szalai, E.B., 55
Takahashi, H., 421
Tanner, J.E., 517
Taylor, D.L., 1133
Temming, A., 140
Tessier, A., 800
Tezak, E.P., 690
Thorrold, S.R., 361
Thorsteinsson, V., 1409
Thurow, R.F., 840
Tonn, W.M., 849
Townsend, C.R., 731
Trenkel, V.M., 67, 86
Trick, C.G., 203
Tsuruta, T., 421
Tuck, I.D., 542
Tufts, B.L., 460
Twining, B.S., 1369
Twiss, M.R., 1369
Twohey, M.B., 23
Unwin, M.J., 1
Vaillancourt, A., 1345
van de Weerd, G.H., 700
Veloza, A., 1517
Vincent, W.F., 1245, 1575
Wade, E.J., 897
Wahl, D.H., 182
Walters, C.J., 1161, 1433
Wang, L., 491
Warr, K.J., 1306
Warren, D.R., 379
Watmough, S.A., 1095
Watters, G.M., 1161
Weber, E.D., 1018
Weber, J.-M., 1281
Welch, D.W., 825
Wells, B.K., 361
Wiebe, P.H., 759
Wiley, M., 491
Williams, E.H., 710, 1037
Willits, N.H., 1258
Wipfli, M.S., 309
Wrona, F., 635
Wyatt, R.J., 997
Yan, N.D., 151, 1307
Young, R.G., 1462
Zale, A.V., 135
Zimmer, K.D., 721
Zimmermann, M., 657
Zuur, A.F., 448, 542
Zwingelstein, G., 1281

© 2003 NRC Canada

The index and/or table of contents has been removed and photographed separately within this volume year.

For roll film users, this information for the current volume year is at the beginning of the microfilm. For a prior year volume, this information is at the end of the microfilm.

For microfiche users, the index and/or contents is contained on a separate fiche.

Culinary Herbs for Short-Season Gardeners

By/par Ernest Small and /et Grace Deutsch

Co-Published with/Co-édité par Ismant Peony Press

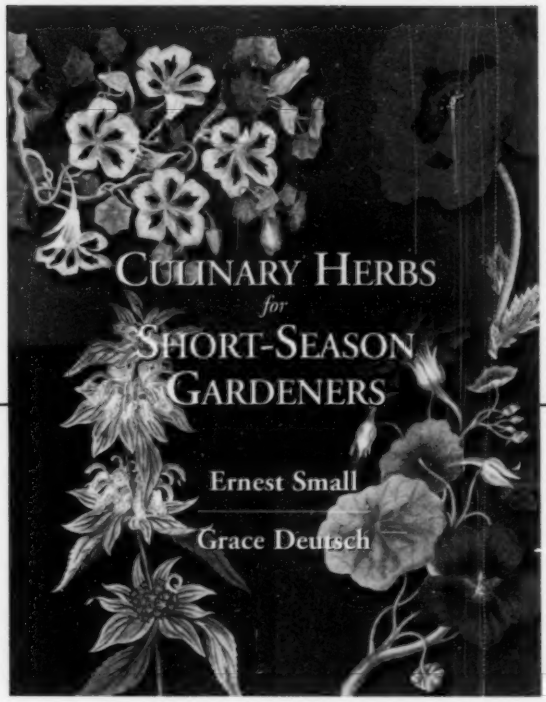

$24.95/24,95 $

Other countries $24.95 US
À l'étranger 24,95 $US

Softcover / Edition brochée
181 pages
ISBN 0-660-17785-4
NRC No./N° du CNRC 42737

Orders may be submitted by mail or fax to: Les commandes peuvent être soumises par courrier ou par télécopieur à :

Order Office/Bureau des commandes
NRC Research Press/Presses scientifique du CNRC
National Research Council/Conseil national de recherches
Ottawa, ON K1A 0R6, Canada
Telephone/Téléphone : (613) 990-2254
Fax/Télécopieur : (613) 952-7656
E-mail: research.press@nrc.ca
Courriel : presses.scientifiques@cnrc.ca
Website: http://researchpress.nrc.ca
Site web : http://pressesscientifiques.cnrc.ca

PLEASE PRINT/LETTRES MOULÉES

☐ Payment enclosed / Paiement inclus
Charge to/ Imputer à ☐ Visa ☐ MasterCard ☐ AMEX
Account no./N° de compte
Expiry date/Date d'expiration

Name/Nom

Signature

Address/Adresse

City/Ville Province

Postal code/Code postal Country/Pays

Telephone/Téléphone Fax/Télécopieur

E-mail/courriel

Prepayment required unless order is accompanied by a purchase order number. Cheques or money orders should be made payable to : "Receiver General for Canada, Credit NRC". For all orders outside Canada, rates are in U.S. Dollars. All sales are final.
Les commandes doivent être payées d'avance à moins qu'elles ne soient accompagnées d'un numéro de bon de commande. Les chèques ou mandats doivent être libellés au « Receveur général du Canada, crédit du CNRC ». Toutes les ventes sont finales.

Marine Protected Areas and Fisheries Closures in British Columbia

By/par Glen S. Jamieson and/et Joanne Lessard

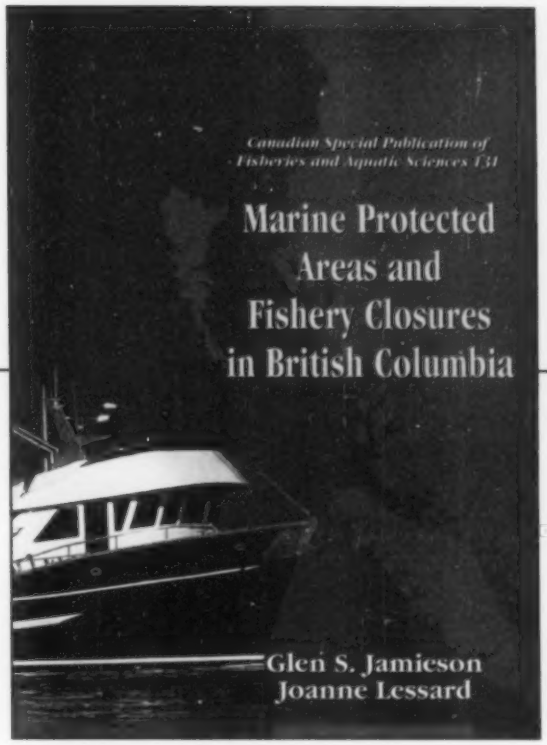
Canadian Special Publication of Fisheries and Aquatic Sciences 131
Marine Protected Areas and Fishery Closures in British Columbia
Glen S. Jamieson
Joanne Lessard

$69.95/69,95 $

Other countries $69.95 US
À l'étranger 69,95 $US

Softcover / Edition brochée
414 pages
ISBN 0-660-17788-9 ISSN 0706-6481
NRC No./N° du CNRC 42846
(Can. Spec. Publ. Fish. Aquat. Sci. No. 131)

Orders may be submitted by mail or fax to: Les commandes peuvent être soumises par courrier ou par télécopieur à :

Order Office/Bureau des commandes

NRC Research Press/Presses scientifique du CNRC
National Research Council/Conseil national de recherches
Ottawa, ON K1A 0R6, Canada
Telephone/Téléphone : (613) 990-2254
Fax/Télécopieur : (613) 952-7656
E-mail: research.press@nrc.ca
Courriel : presses.scientifiques@cnrc.ca
Website: http://researchpress.nrc.ca
Site web : http://pressesscientifiques.cnrc.ca

PLEASE PRINT/LETTRES MOULÉES

☐ Payment enclosed / Paiement inclus ☐ Charge to/Imputer à ☐ Visa ☐ MasterCard ☐ AMEX

Account no./N° de compte Expiry date/Date d'expiration

Name/Nom

Signature

Address/Adresse

City/Ville Province

Postal code/Code postal Country/Pays

Telephone/Téléphone Fax/Télécopieur

E-mail/courriel

Prepayment required unless order is accompanied by a purchase order number. Cheques or money orders should be made payable to : "Receiver General for Canada, Credit NRC". For all orders outside Canada, rates are in U.S. Dollars. All sales are final.
Les commandes doivent être payées d'avance à moins qu'elles ne soient accompagnées d'un numéro de bon de commande. Les chèques ou mandats doivent être libellés au « Receveur général du Canada, crédit du CNRC ». Toutes les ventes sont finales.

Gerhard Herzberg
An Illustrious Life in Science

by/par Boris Stoicheff

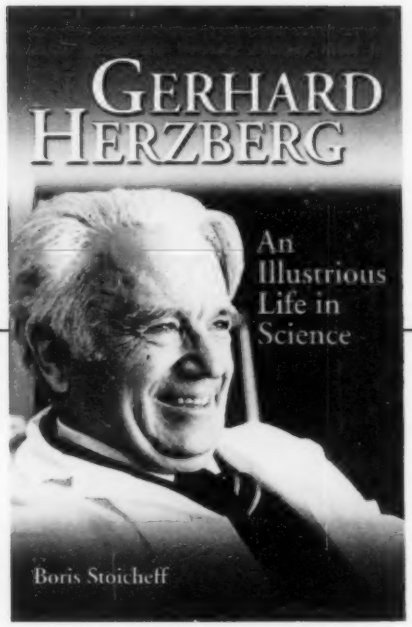

$49.95 CAN. Other countries $49.95 US
49,95 $CAN. À l'étranger 49,95 $US

Hardcover / Edition reliée
ISBN 0-660-18757-4
ISSN 1701-1833
NRC No./N° du CNRC 44462

An NRC Press Publication co-published with McGill-Queen's University Press/Une coédition des Presses du CNRC et McGill-Queen's University Press

Orders may be submitted by mail or fax to:
Les commandes peuvent être soumises par courrier ou par télécopieur à :

Order Office/Bureau des commandes
NRC Research Press/Presses scientifique du CNRC
National Research Council/Conseil national de recherches
Ottawa, ON K1A 0R6, Canada
Telephone/Téléphone : (613) 990-2254
Fax/Télécopieur : (613) 952-7656
E-mail: research.press@nrc.ca
Courriel : presses.scientifiques@cnrc.ca
Website: http://researchpress.nrc.ca
Site web : http://pressesscientifiques.cnrc.ca

PLEASE PRINT/LETTRES MOULÉES

☐ Payment enclosed / Paiement inclus ☐ Charge to/ Imputer à ☐ Visa ☐ MasterCard
Account no./N° de compte Expiry date/Date d'expiration

Name/Nom

Signature

Address/Adresse

City/Ville Province

Postal code/Code postal Country/Pays

Telephone/Téléphone Fax/Télécopieur

E-mail/Courriel

Prepayment required unless order is accompanied by a purchase order number. Cheques or money orders should be made payable to: "Receiver General for Canada, Credit NRC". For all orders outside Canada, rates are in U.S. Dollars. All sales are final.
Les commandes doivent être payées d'avance à moins qu'elles ne soient accompagnées d'un numéro de bon de commandes. Les chèques ou mandats doivent être libellés au « Receveur générale du Canada, crédit du CNRC ». Toutes les vent sont finales.

PERSPECTIVE — PERSPECTIVE

Charles R. Bronte, Mark P. Ebener, Donald R. Schreiner, David S. DeVault, Michael M. Petzold, Douglas A. Jensen, Carl Richards, and Steven J. Lozano — **1552–1574** — Fish community change in Lake Superior, 1970–2000

ERRATUM — ERRATUM

Christine Barnard, Jean-Jacques Frenette, and Warwick F. Vincent — **1575** — Erratum: Planktonic invaders of the St. Lawrence estuarine transition zone: environmental factors controlling the distribution of zebra mussel veligers

Author index for Volume 60 **A1-1**
Contents index for Volume 60 **C-1**

Index des auteurs pour le volume 60 **AI-1**
Sommaire pour le volume 60 **C-1**

National Research Council Canada
Ottawa, Canada K1A 0R6

Conseil national de recherches Canada
Ottawa, Canada K1A 0R6

Postage paid at Ottawa
Publications mail
Registration No. 40062591

Port payé à Ottawa
Poste-publication
Enregistrement n° 40062591

USPS periodical postage paid at Champlain, N.Y.

Canadian Journal of Fisheries and Aquatic Sciences

Volume 60, Number 12, 2003

Journal canadien des sciences halieutiques et aquatiques

Volume 60, numéro 12, 2003

RAPID COMMUNICATIONS		COMMUNICATIONS RAPIDES
Carl Walters	**1433–1436**	Folly and fantasy in the analysis of spatial catch rate data
John H. Chick, Robert J. Cosgriff, and Lori S. Gittinger	**1437–1439**	Fish as potential dispersal agents for floodplain plants: first evidence in North America
ARTICLES		ARTICLES
Nathaniel P. Hitt, Christopher A. Frissell, Clint C. Muhlfeld, and Fred W. Allendorf	**1440–1451**	Spread of hybridization between native westslope cutthroat trout, *Oncorhynchus clarki lewisi*, and nonnative rainbow trout, *Oncorhynchus mykiss*
Alan D. Jassby, John E. Reuter, and Charles R. Goldman	**1452–1461**	Determining long-term water quality change in the presence of climate variability: Lake Tahoe (U.S.A.)
Nicholas F. Hughes, John W. Hayes, Karen A. Shearer, and Roger G. Young	**1462–1476**	Testing a model of drift-feeding using three-dimensional videography of wild brown trout, *Salmo trutta*, in a New Zealand river
Richard S. Stemberger and Eric K. Miller	**1477–1486**	Cladoceran body length and Secchi disk transparency in northeastern U.S. lakes
Wendy E. Morrison and David H. Secor	**1487–1501**	Demographic attributes of yellow-phase American eels (*Anguilla rostrata*) in the Hudson River estuary
Douglas P. Peterson and Kurt D. Fausch	**1502–1516**	Upstream movement by nonnative brook trout (*Salvelinus fontinalis*) promotes invasion of native cutthroat trout (*Oncorhynchus clarki*) habitat
Alex De Robertis, Clifford H. Ryer, Adriana Veloza, and Richard D. Brodeur	**1517–1526**	Differential effects of turbidity on prey consumption of piscivorous and planktivorous fish
Michael L. Jones, John K. Netto, Jason D. Stockwell, and Joseph B. Mion	**1527–1538**	Does the value of newly accessible spawning habitat for walleye (*Stizostedion vitreum*) depend on its location relative to nursery habitats?
Alf Harbitz and Michaela Aschan	**1539–1551**	A two-dimensional geostatistic method to simulate the precision of abundance estimates

Continued on inside back cover / Suite au verso

Canada

Printed in Canada by / Imprimé au Canada par
University of Toronto Press Inc.
Page production by / Mise en page par
NRC Research Press / Presses scientifiques du CNRC

0706-652X(200312)60:12;1-1

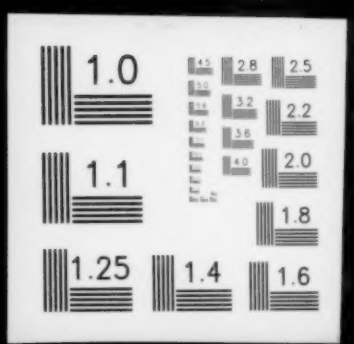
1.0
1.1
1.25
1.4
1.6
1.8
2.0
2.2
2.5
2.8
3.2
3.6
4.0